

# University of Southampton Research Repository ePrints Soton

Copyright © and Moral Rights for this thesis are retained by the author and/or other copyright owners. A copy can be downloaded for personal non-commercial research or study, without prior permission or charge. This thesis cannot be reproduced or quoted extensively from without first obtaining permission in writing from the copyright holder/s. The content must not be changed in any way or sold commercially in any format or medium without the formal permission of the copyright holders.

When referring to this work, full bibliographic details including the author, title, awarding institution and date of the thesis must be given e.g.

AUTHOR (year of submission) "Full thesis title", University of Southampton, name of the University School or Department, PhD Thesis, pagination

# UNIVERSITY OF SOUTHAMPTON FACULTY OF MEDICINE

Investigation of Adult Corneal Limbal Neurosphere cells: a Potential Autologous Cell Resource for Retinal Repair

By

Xiaoli Chen

Thesis for the degree of Doctor of Philosophy

March 2012

#### UNIVERSITY OF SOUTHAMPTON

#### **ABSTRACT**

#### **FACULTY OF MEDICINE**

#### **Doctor of philosophy**

# INVESTIGATION OF ADULT CORNEAL LIMBAL NEUROSPHERE CELLS: A POTENTIAL AUTOLOGOUS CELL RESOURCE FOR RETINAL REPAIR

#### By Xiaoli Chen

Degenerative retinal diseases are the leading cause of blindness in developed countries. Currently, there is no effective therapy available to restore vision. Recent studies have demonstrated that transplanted photoreceptor precursor cells can form synaptic connections with host retina and improve visual function in retinal degenerative animal models. However, the ability to obtain sufficient suitable cells for transplantation remains a key challenge. Stem/progenitor cells residing in the corneal limbus are easily accessible and can be readily expanded *in vitro*. Adult stem cells also demonstrate plasticity and have the ability to transdifferentiate which affords the opportunity to produce heterologous stem cell resources for the generation of retinal neurons.

The studies presented in this thesis aims to characterize the neural colonies (neurospheres) derived from adult mouse/human corneal limbus, and subsequently explore the potential of using these cells as a candidate cell resource for generation of retinal neurons. Initial investigations characterised the self-renewal, neural potential, ultrastructure and origin of limbal neurosphere (LNS). Subsequent investigations were performed using a retinal developing microenvironment to promote the differentiation of these cells along retinal lineages. The derived LNS cells displayed both photoreceptor and RPE specific characteristics. Functionally, differentiated cells also demonstrated electrical excitability. Further investigation was performed on human LNS derived from aged donor and adult live patients. Transcript retinal markers were observed when cultured in conducive conditions. Finally, a preliminary investigation introducing exogenous Crx, the key fate regulation transcription factor, was conducted and showed upregulation of downstream photoreceptor gene expression.

The results presented here provide detailed information on the characteristics of LNS cells, and for the first time, demonstrated that limbal stromal originated LNS cells are a potential valuable cell resource for autologous cell therapy in degenerative retinal diseases.

# **Contents**

1	Chapter O	ne – Introduction	19
	1.1 Ove	rview	19
	1.2 The	Mammalian eye	20
	1.3 Stru	icture of the eye	20
	1.3.1	Structure of the cornea and corneal limbus	21
	1.3.2	Structure of the retina	24
	1.4 Deg	enerative Retinal Diseases	29
	1.4.1	Age Related Macular Degeneration (AMD)	29
	1.4.2	Retinitis Pigmentosa (RP)	30
	1.4.3	Current treatments	30
	1.5 Dev	elopment of the eye	34
	1.5.1	Transcription factors for eye development	35
	1.5.2	Development of cornea	36
	1.5.3	Development of neural retina and retinal pigment epithelium	37
	1.5.4	Development of Photoreceptors	39
	1.6 Ster	n cell therapy	41
	1.6.1	Stem cells	41
	1.6.2	Immune response in the subretinal space (SRS)	41
	1.6.3	Strategy of stem cells therapy	43
	1.7 Allo	geneic cell resources	43
	1.7.1	Embryonic stem cells	43
	1.7.2	Retinal progenitor cells from developing retinas	45
	1.8 Aut	ologous cell resources	47
	1.8.1	Induced pluripotent cells	47
	1.8.2	Stem-like cells from the ciliary epithelium	47
	1.8.3	Adult iris epithelium cells (IPE)	49
	1.8.4	Retinal Müller glial cells	49
	1.8.5	Adult bone marrow stem cells	50
	1.8.6	Adult stem cells from the corneal limbus	51
	1.9 Met	hods for retinal lineage direction	5 5
	1.9.1	Retinal developing environment	5 5
	1.9.2	Stepwise defined condition	5 5
	1.9.3	Genetic transformation	58
	1 1 0 Aim	as and Objectives	60

2	Cha	ipter Tw	o- Materials and Methods	63
	2.1	Limb	al Cell Isolation and Culture	63
		2.1.1	Animals	63
		2.1.2	Cell dissociation	63
		2.1.3	Culture condition optimization	65
		2.1.4	Culture medium optimization	65
		2.1.5	Sphere generation efficiency	67
		2.1.6	Effect of growth factors on sphere formation	67
		2.1.7	Secondary sphere formation	67
		2.1.8	Viability of sphere cells	68
	2.2	Immu	unocytochemistry	69
		2.2.1	Mouse corneal limbus staining	69
		2.2.2	Neurosphere and monolayer cell analysis	69
	2.3	Flow	Cytometry	72
	2.4	Rever	rse Transcription- Polymerase Chain Reaction (RT-PCR)	73
		2.4.1	RNA extraction	73
		2.4.2	DNase treatment	74
		2.4.3	Quality assessment and quantitation of RNA	75
		2.4.4	cDNA synthesis	75
		2.4.5	Primer design and specificity checking	76
		2.4.6	Polymerase chain reaction (PCR)	78
		2.4.7	Detection of PCR products by electrophoresis	79
	2.5	Trans	smission Electron Microscopy (TEM)	80
	2.6	Retin	al cell co-culture assay	81
		2.6.1	Plate coating	81
		2.6.2	Preparation PN1 retinal cells	81
		2.6.3	Co-culture with PN1 retinal cells	82
	2.7	Calcii	um influx imaging for functional assessment	83
		2.7.1	Calcium indicator: Fluo-4 AM	83
		2.7.2	Cell preparation	83
		2.7.3	Calcium indicator loading	83
		2.7.4	Data Acquisition	84
		2.7.5	Cell excitation	85
		2.7.6	Cell viability assessment after calcium influx imaging	85
	2.8	Cell i	ntegration assessment <i>in vitro</i>	86
		2.8.1	Qdot® nanocrystals	86
		2.8.2	Cell labelling with Qdots	87
		2.8.3	Direct co-culture system for integration assessment	88
		2.8.4	Fixation and sectioning for integration assessment	89
			2	

	2.9	Statist	ical analysis	90
		2.9.1	Sphere generation analysis	90
		2.9.2	Measurement of Sphere Diameter	90
		2.9.3	Cell enumeration for phenotype analysis	90
		2.9.4	Statistical Methods	90
3	Cha	pter Thr	ee - Derivation of Neural Stem / Progenitor Cells from Adult	
Μοι	ıse (	Corneal L	imbus	91
	3.1	Backg	round	91
	3.2	Metho	ds	93
		3.2.1	Cell culture	93
		3.2.2	Reverse transcription polymerase chain reaction	94
		3.2.3	Immunocytochemistry	94
		3.2.4	Transmission Electron Microscopy (TEM)	95
	3.3	Clona	growth of adult mouse corneal limbus derived cells	96
		3.3.1	Structure of adult corneal limbus	96
		3.3.2	Sphere-cluster formation	97
		3.3.3	Optimal culture condition for sphere generation	97
		3.3.4	Cell viability within sphere	101
		3.3.5	Effect of growth factors on clonal growth	101
		3.3.6	Cells from adult corneal limbus display self-renewal capacity	103
		3.3.7	Ultrastructure of sphere cells derived from adult corneal limbus .	108
	3.4	Chara	cteristics of corneal limbal cells	110
		3.4.1	Expression of side population determinant ABCG2	110
		3.4.2	Expression of neural stem cell marker Nestin	113
		3.4.3	Expression of neural stem cells marker Sox2, Musashi1	115
		3.4.4	Expression of early differentiation neuron marker beta III tubulin	.118
		3.4.5	Lack of expression of epithelial lineage markers	118
		3.4.6	Clonal growth corneal limbal cells are neural crest derived stem/	,
		progenit	or cells	122
		3.4.7	Effect of Noggin on gene expression of LNS cells	.124
		3.4.8	Lack of expression of retinal markers on limbal cells	126
				127
	3.5	Differ	entiation of LNS cells along neural lineage	128
	3.6	Discus	ssion	129
		3.6.1	Overview	129
		3.6.2	Corneal limbal stem/progenitor cells display self-renewal and	
		prolifora	tive canability	120

	may be	Limbal spheres have a similar ultrastructure to neurospheres, b generated through a different signaling pathway	
	3.6.4	Origin of corneal limbus derived progenitor cells	13
	3.6.5	Neural potential of adult mouse corneal stem/ progenitor cells.	
	3.6.6	Characteristics of progenitor cells from adult mouse corneal lin	bus
			13
Cha	apter Fo	ur - Transdifferentiation of LNS cells towards Retinal-like Cells	s 13
4.1		duction	
4.2	Meth	ods	
	4.2.1	Neonatal retinal cell dissociation and culture	
	4.2.2	Indirect co-culture assay	14
	4.2.3	Reverse transcription polymerase chain reaction	14
	4.2.4	Immunocytochemistry	14
	4.2.5	Transmission Electron Microscopy (TEM)	14
4.3	Resu	lts	14
	4.3.1	Cell morphology change following differentiation	
	4.3.2	Ultrastructural changes following differentiation	14
	4.3.3	Expression of retinal progenitor cell markers	
	4.3.4	Detection of photoreceptor specific markers by RT-PCR	14
	4.3.5	Detection of photoreceptor, neural and synaptic markers by	
	immund	ocytochemistry	15
	4.3.6	Expression RPE specific markers	15
	4.3.7	Cell populations of LNS in co-culture with neonatal retinal cells.	15
4.4	Discu	ussion	16
Cha	apter Fiv	e – Investigation of LNS cell functionality and integration <i>in v</i>	
5.1	Intro	duction	
5.2	Meth	ods	16
	5.2.1	Cell dissociation and culture	16
	5.2.2	Calcium influx imaging	16
	5.2.3	Live Cell tracking	
	5.2.4	Cell integration assessment <i>in vitro</i>	16
5.3	Resu	lts (1) electrical excitability of induced LNS cells	16
	5.3.1	Intracellular free calcium was labeled by a calcium indicator in i	etina
	cells an	d LNS cells in neural differentiation conditions	
	5.3.2	Voltage stimulus evoked a Ca2+ influx in induced LNS cells and	

		5.3.3	Light response was not detected on developing retinal cells t	ısing
		calcium	influx/efflux assay	175
	5.4	Resu	lts (2) integration into retinal tissues in vitro	178
		5.4.1	Optimization of Qdot labeling for integration studies	178
		5.4.2	Qdot labeled cells rapidly decreased in co-culture system	178
		5.4.3	LNS cells rarely integrated into developing retinal tissue in vi	tro181
	5.5	Disc	ussion	183
		5.5.1	Functionality of induced LNS cells	183
		5.5.2	Integration of LNS cells in direct co-culture system	185
6	Cha	apter Six	c – Human LNS cell culture and transdifferentiation	189
	6.1	Intro	duction	189
	6.2	Meth	ods	191
		6.2.1	Sample collection	191
		6.2.2	Human limbal cells dissociation form donor eyes	191
		6.2.3	Human limbal cells dissociation from pterygium samples	193
		6.2.4	Co-culture with human and mouse developing retinal	193
		6.2.5	Immunocytochemistry	194
		6.2.6	Reverse transcription polymerase chain reaction	195
	6.3	Resu	lts	196
		6.3.1	Effective generation human LNS from donor limbal tissues	196
		6.3.2	Secondary LNS were generation from Primary human LNS, alt	hough a
		small n	umber of samples lost clonal growth features	199
		6.3.3	Human LNS culture from Pterygium surgery	201
		6.3.4	Expression of retinal progenitor markers were detected on h	uman
			rived cells by RT-PCR	
		6.3.5	Absence of mature retinal lineage markers in human LNS der	ived
		cells		
		6.3.6	Human Foetal retinal cells	206
		6.3.7	Absence of photoreceptor markers on human LNS cells by	
			ocytochemistry	
	6.4	Discı	ussion	210
7	Cha	apter Se	ven - Introduction of Crx gene into LNS cells by Lentiviral V	ector
	7.1		duction	
	7.2		ods	
		7.2.1	Cell culture	
		722	Cell transfection	

		7.2.3	RT-PCR	216
		7.2.4	Immunocytochemistry	217
	7.3	Resul	ts	218
		7.3.1	Expression of GFP on LNS cells following transfection with LN	/V-CRX-
		GFP and	LVV-GFP vectors	218
		7.3.2	Validation the Crx expression by RT-PCR	220
		7.3.3	Expression of rod photoreceptor markers at a transcript leve	l, but
		not at a	protein level following LVV-Crx-GFP transfection	222
		7.3.4	Upregulation of cone photoreceptor markers at a protein leve	el
		followin	g LVV-CRX-GFP transfection	226
	7.4	Discu	ssion	228
8	Cha	apter Eig	ht – Final Discussion	231
	8.1	Thesi	s summary	231
	8.2	Impli	cations for stem cell therapy for retinal disease	232
		8.2.1	A new candidate autologous cell resource for degenerative re	etinal
		diseases	5	233
		8.2.2	Derivation of excitable retinal-like cells from adult LNS cells.	234
		8.2.3	Transdifferentiation potential of human LNS cells towards a 1	etinal
		lineage		235
		8.2.4	Genetic modification of LNS cells	236
	8.3	Futur	e Plans	238
		8.3.1	Functional assessment - light responsiveness in vitro	238
		8.3.2	Investigation of Nrl-activation using gene reporter mice	238
		8.3.3	To enhance the efficiency of photoreceptor-like cell generation	on 239
		8.3.4	Functionality and integration assessment following transplar	ıtation
				240
		8.3.5	Studies on human LNS cells	241

# **List of Figures**

Figure 1-1 A diagram illustrating the structure of the human eye	21
Figure 1-2 Structure of the human cornea	22
igure 1-3 Human corneal limbus	23
igure 1-4 Structure and connections in the mammalian retinas	26
igure 1-5 Normal human retina	26
Figure 1-6 Structure of rod and cone photoreceptors	28
gure 1-7 The phototransduction cascade	28
gure 1-8 Integration of photoreceptor precursor into wild-type recipient retina	.s 33
gure 1-9 Summary of embryonic ocular development	35
gure 1-10 Development of mammalian retinal cells	38
Figure 1-11 Plasticity of bone marrow derived cells	51
gigure 1-12 Multi-stepwise photoreceptor induction from mouse and primate ES	cells57
igure 2-1 Corneal limbus dissection overview	64
rigure 2-2 RNA extraction procedure using an RNeasy Plus Micro Kit (Qiagen)	74
Figure 2-3 DNA amplification by PCR	78
rigure 2-4 Limbal neurospheres co-cultured with PN1 retinal cells	82
igure 2-5 Character of calcium indicator Fluo-4	83
igure 2-6 Structure and their intracellular distribution of Qdot nanocrystals	86
igure 2-7 The excitation and emission spectra of Qdot®655	87
igure 2-8 Direct co-culture System	88
igure 3-1 Structure of peripheral cornea and corneal limbus	96
igure 3-2 Homogenous adult mouse iris pigment epithelium and corneal limbu	s cells.
	97
igure 3-3 Sphere generation efficiency at low cell density in different media rec	ipes.99
igure 3-4 Sphere generation efficiency at high cell density in different media re	cipes.
	100
igure 3-5 Limbal cells in non-optimal culture medium	100
igure 3-6 Sphere cell viability assessment	101
igure 3-7 Effect of extrinsic factors on adult mouse LNS generation	102
Figure 3-8 Growth features of mouse LNS cells	104
igure 3-9 Limbal spheres expressed the proliferative marker PCNA	105
igure 3-10 Sphere generation efficiency	106
igure 3-11 Secondary sphere generation at extreme low cell density following	serial
dilution assay	107
igure 3-12 Transmission electron micrographs of adult mouse corneal limbal s	pheres
	109

Figure 3-13 Stem cells marker ABCG2 expressed on adult mouse limbal s	
Figure 3-14 Flow cytometric analysis of cells derived from adult mouse co	
Figure 3-15 Expression of Nestin in adult corneal limbus derived spheres	
Figure 3-16 Expression of neural stem cells markers in adult mouse LNS	
Figure 3-17 Expression of beta-III tubulin in adult corneal limbus derived	
Figure 3-18 Expression of epithelial lineage markers during sphere formi	-
Figure 3-19 Neural-crest and mesenchymal markers were detected in liml	•
cells	
Figure 3-20 Effect of Noggin on gene expression during LNS generation.	
Figure 3-21 Lack of retinal markers on limbal cells	127
Figure 3-22 Differentiation along neuronal and glial lineages	128
Figure 4-1 Human eye development	138
Figure 4-2 Co-culture System for Retinal Lineage Differentiation	
Figure 4-3 Differentiation of LNS cells cultured in neural differentiation m	edia 146
Figure 4-4 TEM images of differentiated limbal spheres	147
Figure 4-5 Expression of retinal progenitor cell markers in LNS derived ce	lls149
Figure 4-6 Expression of photoreceptor specific genes in derived LNS cell	s 151
Figure 4-7 Absence of photoreceptor specific markers in freshly isolated	limbal cells
	152
Figure 4-8 Immunocytochemistry of LNS cells in co-culture condition	154
Figure 4-9 The percentage of Rhodopsin and NF 200 positive cells from a	dult LNS cells
following 7-10 days differentiation in co-culture and control conditions	155
Figure 4-10 Expression of RPE specific markers at a transcript level	157
Figure 4-11 Expression of RPE specific markers at a protein level	158
Figure 4-12 Cell populations observed from LNS co-cultured with neonata	ıl retinal cells
	159
Figure 5-1 Intracellular Ca <sup>2+</sup> concentration in developing retinal cells and	
LNS cells.	
Figure 5-2 Differences in intracellular fluo-4 intensity due to culture cond	
Figure 5-3 Co-cultured LNS cells exhibit calcium influx following a depola	_
stimulus	
Figure 5-4 P1 retinal cells exhibit calcium influx following a depolarizing	
Figure 5-5 Effect of depolarizing stimulus on non co-cultured LNS cells	
Figure 5-6 light response of <i>in vitro</i> cultured developing retinal cells usin	_
calcium assay.	
Figure 5-7 Labelling of mouse and human LNS derived cells using Qdot n	-
	179

Figure 5-8 Qdot labeled LNS cells in neurosphere culture and co-culture system	180
Figure 5-9 Integration of Qtracker labeled LNS cells <i>in vitro</i>	182
Figure 6-1 Human corneal–scleral rims (residual tissue) from grafting surgery	192
Figure 6-2 Co-culture system for human LNS cells differentiation towards retinal	
lineage	194
Figure 6-3 Human LNS cells from a 79 years old male using Protocol 2	197
Figure 6-4 Human LNS cells from 74 - 80 years old donor eyes using Protocol 3	198
Figure 6-5 Optimal cell dissociation protocol for LNS cell culture	199
Figure 6-6 Neural potential of subcultured human LNS cells	200
Figure 6-7 Culture of limbal cells from live patients	202
Figure 6-8 Expression of retinal development transcription factors in induced hur	nan
LNS	204
Figure 6-9 Absence of mature retinal lineage markers in human LNS derived cells	205
Figure 6-10 Rhodopsin was not expressed in human foetal retinal cells (post	
conception 49-56 days)	207
Figure 6-11 Absence of photoreceptor markers in human LNS cells by	
immunocytochemistry	209
Figure 7-1 Schematic representation of a Crx and GFP lentiviral vector	214
Figure 7-2 Crx transduction plan	216
Figure 7-3 Bright field and GFP images of LNS cells transduced with LVV-GFP or no	on-
transfected cells	218
Figure 7-4 Bright field and fluorescent microscopy images of LNS cells transduced	d with
LVV-CRX-GFP	219
Figure 7-5 Validation of Crx transfection by RT-PCR	220
Figure 7-6 Expression of endogenous Crx in LNS cells following transduction	221
Figure 7-7 Rod specific markers detected on LVV-Crx-GFP transduced LNS cells by	/ RT-
PCR	223
Figure 7-8 Absence of rhodopsin expression on transduced LNS cells by	
immunocytochemistry	224
Figure 7-9 Expression of blue opsin on transduced LNS cells detected by	
immunocytochemistry	227

# **List of Tables**

Table 1-1 Transcription regulators for photoreceptor gene expression, development	
and/or maintenance	40
Table 2-1 Basal culture medium supplements and growth factors	66
Table 2-2 Primary antibodies used for immunocytochemical analysis	71
Table 2-3 Primer sequences used for phenotypic analysis and expected product sizes	;
	76
Table 3-1 Characteristics of mouse limbal stem/progenitor cells compared with	
neurospheres from CNS and neonatal retina1	36
Table 4-1 Primer sequences used for phenotypic analysis and expected product size	S
in co-culture study1	43
Table 4-2 Primary antibodies for immunocytochemical analysis in co-culture study 1	44
Table 6-1 Primary antibodies used for human LNS cell immunocytochemical analysis.	
1	94
Table 6-2 Gene specific primers used for human LNS cell RT-PCR analysis1	95
Table 7-1 Primer sequences used for phenotypic analysis on transduced LNS2	16

## **DECLARATION OF AUTHORSHIP**

I, Xiaoli Chen, declare that the thesis entitled

"Investigation of Adult Corneal Limbal Neurosphere cells: a Potential Autologous Cell Resource for Retinal Repair"

and the work presented in the thesis are both my own, and have been generated by me as the result of my own original research. I confirm that:

- this work was done wholly or mainly while in candidature for a research degree at this University;
- where any part of this thesis has previously been submitted for a degree or any other qualification at this University or any other institution, this has been clearly stated:
- where I have consulted the published work of others, this is always clearly attributed;
- where I have quoted from the work of others, the source is always given. With the exception of such quotations, this thesis is entirely my own work;
- I have acknowledged all main sources of help;
- where the thesis is based on work done by myself jointly with others, I have made clear exactly what was done by others and what I have contributed myself;
- parts of this work have been published as:

Chen X, Thomson HA, Hossain P, Lotery AL, Characterisation of mouse limbal neurosphere cells: a potential cell source of functional neurons. Br J Ophthalmol 2012 Nov;96(11):1431-7.

signed:	 	 	 	
Date:				

# Acknowledgments

I would firstly like to express my deepest gratitude to my supervisor, Prof. Andrew Lotery who has offered invaluable support, guidance and encouragement since I started my MPhil/PhD study.

Gratitude is also due to Dr. Heather Thomson who has been tremendously helpful in experimental design, technical supports and thesis revision; Mr. Parwez Hossain who has offered valuable guidance. I would like to thank members of vision group, in particular Mrs. Angela Cree, Miss Jenny Scott, Miss Helen Griffiths and Mr. Sam Khandhadia for help, advice and support throughout the course of my work, particularly during my pregnancy. Thanks also go to Dr. David Johnston for helping with confocal microscopy imaging; Dr. Carolann McGuire and Dr. Richard Jewell for flow cytometry training. In addition I would also like to thank all members of clinical neurosciences division for their comments and advice during discussions of this work.

All work presented in this thesis was performed by me except in the following instances. I am very grateful to these colleagues and collaborators and wish to thank them formally for their time and support.

- Dr. Anton Page processed TEM samples and assisted with analysis detailed in Chapters 3 and 4;
- Miss Helen Griffiths conducted PCR and electrophoresis detailed in section 4.3.3,
   Chapter 4;
- Mr. Parwez Hossain, Mr. Michael Tsatsos and Dr. Valerie Smith provided human limbal samples detailed in Chapter 6;
- Sister Marie Nelson and Sister Georgiana Matei completed the consent forms for participants detailed in Chapter 6;
- Prof. David Wilson, Miss Kelly Wilkinson and Miss Kate Wright provided developing human retinal tissue detailed in Section 6.3.6, Chapter 6;
- Dr. Jessica Cooke and Prof. Andrew Dick provided the Crx lentiviral vector detailed in Chapter 7;
- Dr. Heather Thomson and Miss Jenifer Scott performed the viral transfection and subsequent cell characterization detailed in Chapter 7.

Finally, I would like to thank my son Ruichen for bringing happiness into my life. I enjoy every day of being a mom. Thanks to my parents and my husband for their continued support and encouragement. Thanks to my friends for their encouragement and help.

#### **List of Common Used Abbreviations**

+ve Positive

ABCG2 ATP-binding cassette superfamily transmembrane protein 2

AM Acetoxymethyl ester

AMD Age-related macular degeneration

ANOVA Analysis of Variance B27 B27 supplement

B27- B27 supplement minus Vitamin A
BDNF Brain-Derived Neurotrophic Factor
bHLH basic helix-loop-helix (bHLH) genes

BM Bruch's membrane

BMP Bone Morphogenetic Protein
BMP4 Bone Morphogenetic Protein 4

C1 Complement C1
C3 Complement C3

Ca2<sup>+</sup> Calcium

CaCl2 Calcium chloride

CB Ciliary Body

cDNA complementary DNA

CD34 molecule/ antigen
CD45 CD45 molecule/ antigen
CD90 CD90 molecule/ antigen
CD133 CD133 molecule/ antigen

CE Ciliary Epithelium

CES Corneal epithelium stem cells

CFH Complement factor H

cGMP cyclic Guanosine monophosphate

Chx10 Ceh-10 homeodomain containing homolog

CMV Cytomegalovirus

CNS Central Nervous System

CNV Choroidal Neo-Vascularisation

CRALBP Cellular Retinylaldehyde-Binding Protein

Crx Cone-rod homeobox

DAPI 4'-6-diamidino-2-phenylindole

DIV Days In Vitro

DKK1 Dickkopf-related protein 1

DMEM: F12 Dulbecco's Modified Eagle's Medium with F12 media supplement

DMSO Dimethyl sulfoxide

DNA Deoxyribonucleic acid

EDTA Ethylene Diamine Tetra Acetic acid eGFP Enhanced Green Fluorescent Protein

EB Embryoid Body

EGF Epidermal Growth Factor

ERG Electroretinography
ESC Embryonic Stem Cells
FBS Foetal Bovine Serum

FGF2 Fibroblast Growth Factor 2

Fig. Figure Gravity

GABA  $\gamma$  -Aminobutyric acid

GAPDH Glyceraldehyde 3-phosphate dehydrogenase

GFP Green Fluorescence Protein

HBSS Hank's Buffered Salt Solution

hESC Human Embryonic Stem Cells

Hr Hour

HSC Hematopoietic stem cells ICC Immunocytochemistry

ICM Inner Cell Mass
IgG Immunoglobulin G
IPE Iris Epithelium Cells

iPSCs Induced pluripotent Stem Cells

IRBP Interphotoreceptor Retinoid-Binding Protein

IRES Internal ribosome entry site

K12 Cytokeratin 12

kDa kiloDalton L-Glut L-Glutamine

Lhx2 LIM homeobox 2

LNS Limbal neurosphere

LSC Limbal Stem Cell

LVV Lentiviral vector

Mg2<sup>+</sup> Magnesium Mag Magnification MG Müller glial

Mitf Microphthalmia-associated transcription factor

mg milligram

MgCl, Magnesium Chloride

Min Minute

ml Millilitre

µl Microlitre

mm Millimeter

µm Micrometer

mM Millimolar

mnd retinal/CNS degeneration mouse model

mRNA message RNA

MSC the bone marrow mesenchymal stromal cells

N Noggin

N2 N2 supplements NB/NBA Neurobasal™ Media

NC-CS Neural-crest derived cornea stroma cells

NeuroD Neurogenic differentiation 1

NF Neurofilament ng nanogram nMole nanomolar

Nrl Neural retina leucine zipper protein

NS Neural stem cells

NSA Neurosphere Assay

ONL Outer Nuclear Layer

OS Outer Segments

Otx2 Orthodenticle Homeobox 2

P63 Tumor protein p63

PA6 Mouse stromal cell line PA6

Pax6 Paired Box gene 6

PBS Phosphate Buffered Saline
PCR Polymerase Chain Reaction

P-D-L Poly-D-Lysine

PDT PhotoDynamic Therapy

PEDF Pigment Epithelium-Derived Factor

PFA Paraformaldehyde PI Propidium Iodide

PKC-α Protein Kinase C- alpha

P-L-L Poly-L-Lysine PN PostNatal

PTP Protein Tyrosine Phosphatase

qPCR quantitative PCR RA Retinoic Acid

RCS Royal College of Surgeons rats

rd retinal degeneration fast rds retinal degeneration slow

RER Rough Endoplasmic Reticulum

rho2/2 Rhodopsin knockout mice

RNA RiboNucleic Acid

RP Retinitis Pigmentosa
RPC Retinal Progenitor Cells
RPE Retinal Pigment Epithelium

RPE-65 Retinal Pigment Epithelium-specific 65 kDa protein

RPM Revolutions Per Minute

rt room temperature

RT Reverse Transcriptase

RT-PCR Reverse Transcription Polymerase Chain Reaction

Rx Retinal homeobox
SD Standard Deviation

Sec Second

SEM standard error of the mean

SFEB Serum-free floating culture of embryoid body-like aggregates

Shh Sonic hedgehog

Six3 Sex determining region Y-box 3
Six6 Sex determining region Y-box 6
Sox2 Sex determining region Y-box 2
Sox9 Sex determining region Y-box 9

SP Side Populations
SRS Subretinal Space
SSC Side-Scattered

SVZ SubVentricular Zone
TAC Transit Amplifying Cells

Transmission Floring Cens

TEM Transmission Electronic Microscopy
TuJ1 Neuron-specific β-Tubulin III antibody

U unit

UV Ultra Violet

VEGF Vascular Endothelial Growth Factor

# 1 Chapter One - Introduction

#### 1.1 Overview

Degenerative retinal conditions, such as Age-related Macular Degeneration (AMD) and Retinitis Pigmentosa (RP), are characterized by loss of the special photosensory cells in the retina and subsequent visual loss [1,2]. As part of the central nervous system, the retina has very limited regeneration capacity after damage. Therefore degenerative retinal diseases, which affect over 8 million people worldwide, remain untreatable [3].

In the last two decades, cell replacement has demonstrated a potential solution to restore visual function in degenerative retinal diseases [4,5]. The development of stem cell technologies provides an opportunity to generate sufficient and appropriate cells to utilize for cell therapy. Photoreceptor like cells have been generated from various stem/progenitor cells resources, including embryonic stem cells (ESCs), stem like cells from the ciliary epithelium, retinal glial cells, induced pluripotent stem cells (iPSCs), adult iris epithelium cells (IPE), bone marrow stem cells and progenitor cells from the corneal limbus [6-13]. Besides the ability to generate sufficient functional retinal neurons, other factors need take into account for a cell resource to be clinically applicable. These include accessibility, immune response, ethical concerns and risks such as tumor formation [14].

The literature reviewed here, introduces the relevant basic eye knowledge, candidature stem cell resources used for photoreceptor generation and the reasons why corneal limbus stem cells were chosen for this study.

### 1.2 The Mammalian eye

The eye, so called "window of the world", is the most essential and important sensory organs for a vast array of species. From unicellular organisms to mammals, the "eye" is capable of detecting light, which affords the ability to anticipate and prepare for environmental changes. The function and location of the eyes are adapted to different species' own environment and lifestyle. Eyes play an even more important role for humans. Light energy from the environment goes through the cornea, anterior chamber, pupil, lens, vitreous and is perceived by photoreceptors in the retina. The latter produces nerve action potentials that are relayed to the optic nerve, and then along the visual pathway, to the visual cortex of the brain. This is the place where the electrical signals are interpreted as images [15]. By these processes, eyes provide information for high precision vision as well as colour and depth perception.

## 1.3 Structure of the eye

The mammalian eye is a highly sophisticated spherical organ. The longitudinal diameter of the human eyeball is about 0.9 inches (20-24 mm). It consists of three layers: the external fibrous layer (sclera and cornea), the intermediate uveal layer (iris, ciliary body and choroid) and the internal nervous layer (retina) as shown in Figure 1-1 The cornea is the outermost transparent layer of the eye. It accounts for over 70% of the eye's total refractive power. The white sclera is continuous with the transparent cornea and together they form a tough protective fibrous layer. From anterior to posterior, the middle layer is composed of the densely pigmented iris, ciliary body and choroid. The iris is a circular diaphragm sited in front of the lens. Muscles in the iris constrict or dilate the pupil to control the amount of light moving towards the back of the eye. The ciliary body is the posterior extension of the iris; it is connected to the lens via suspensory ligaments. Contraction of the ciliary body controls the shape of the lens, which adjusts the focus of light onto the retina to form a clear image. The choroid is a thin membrane lying between the retina and sclera. The choroid acts to avoid confusing visual images by providing a light-tight environment, preventing stray light entering the eye. In addition, the choroid supplies nutrients and oxygen to the retina. A semitransparent neural layer, named the retina, is sited at the back of the inner eye. The vertebrate retina is a distinctly multilayered structure with complex neural circuitry [15]. The structural details of which will be discussed later.

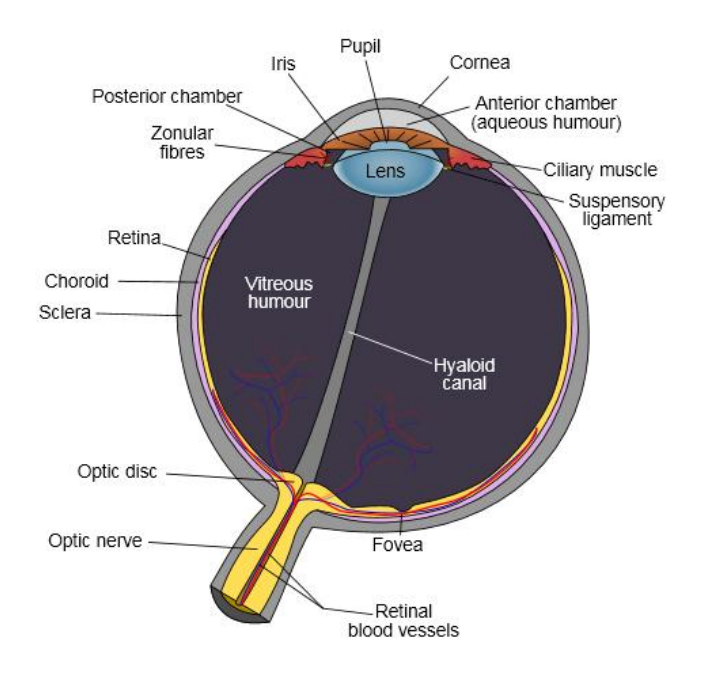


Figure 1-1 A diagram illustrating the structure of the human eye Reprinted from Wikipedia (Http://www.wikipedia.org)

#### 1.3.1 Structure of the cornea and corneal limbus

The cornea and the sclera constitute the outer fibrous layer which encases and protects the eyeball. Because transparency is of prime importance for the cornea, it does not have blood vessels and therefore receives nutrients through diffusion from tear fluid and aqueous humour. The average thickness of adult human cornea is 0.52 mm in the centre to 0.65 mm at the periphery. From anterior to posterior, the mammalian cornea is composed of five distinct tissue layers namely the corneal epithelium, Bowman's layer, stroma, Descemet's membrane and corneal endothelium as shown in Figure 1-2. The epithelium layer is the foremost protective layer. It is composed of 5-6 layers of stratified squamous epithelium which is constantly renewed throughout life. The stroma, accounting for 90 percent of corneal thickness, is comprised of intertwining lamellae of collagen fibrils and scattered keratocytes. The most posterior boundary of the cornea is the endothelium. It is only a single layer of cells, but is responsible for maintenance of the essential deturgescence of the corneal stroma. These three major layers are separated by Bowman's membrane (15µm) to the front and Descemet's membrane (10-15µm) to the back [15].

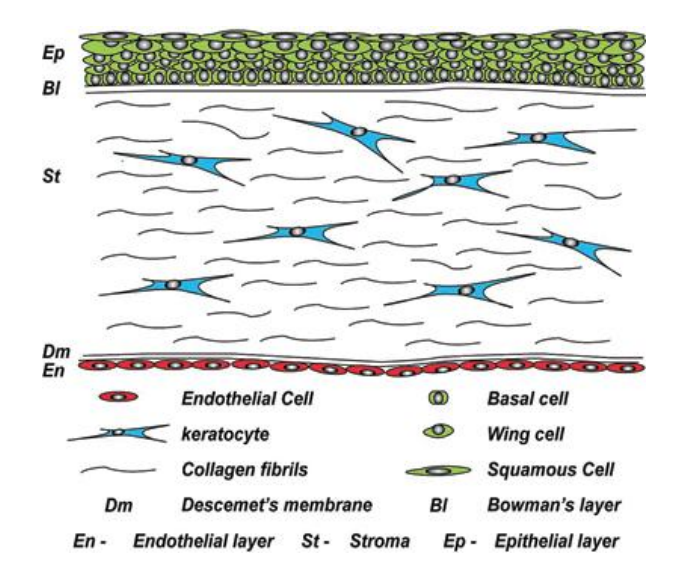


Figure 1-2 Structure of the human cornea.

The schematic diagram illustrates the layers and cell phenotype within human cornea. Reprinted from Secker *et al.* 2009, with the creative commons attribution license.

Mitotic and self-renewal abilities are remarkably distinguished between the three cellular layers of the cornea [16-18]. The cornea epithelium layer is constantly renewed throughout life. It plays an essential role in maintaining the integrity of ocular surface as well as visual function. Between the collagen rich lamellaes of the stromal layer, there are extremely flattened stellate cells with thin cytoplasmic extension, the keratocytes. They are responsible for secretion of the unique stromal extracellular matrix. The number of keratocyte cells usually remains stable after birth; hardly any mitotic activity is detected throughout a lifetime. However in the presence of inflammation or following wounding, stromal keratocytes become activated and begin to divide with a subsequent change in phenotype to fibroblasts and myofibroblasts like cells. These cells secrete connective tissue matrix, which eventually forms opaque scars within the corneal stroma. In contrast to the corneal epithelium, the number of corneal endothelial cells decreases with age from over 3000 cells/mm<sup>2</sup> at birth to approximate 2000 cells/mm<sup>2</sup> by old age [16]. The loss of endothelial cells is compensated by neighboring cells becoming flattened and enlarged [19]. In vitro, human corneal endothelial cells show only limited ability to divide after infancy [18].

The "Limbus" is the transitional region where the cornea structurally continues with the sclera (Figure 1-3). It contains a radially oriented structure known as the "palisades of Vogt" which may harbor epithelium stem cells. The palisades of Vogt present as an undulated epithelium basal layer. In 1989, Cotsarelis and colleagues [20], were the

first to identify slow cycling cells (label-retaining cells) at the limbal epithelial basal layer, this provided strong evidence that the putative stem cells, which are responsible for long term renewal of the cornea epithelium, reside in the basal layer of limbus. Corneal SCs are activated on demand for tissue regeneration and give rise to transiently amplifying cells (TACs). These are corneal progenitor cells which have the capacity for rapid division, but only a limited number of cells divisions. TACs then mature and repopulate the surface of the cornea effectively (Figure 1-3) [1,21,22]. Transplantation of cultivated human corneal limbal stem cell (LSC) has been used clinically, and has proven to be a safe and effective treatment for reconstructing the corneal surface [23-27]. Long-term follow-up has demonstrated the stability of the regenerated corneal epithelium [24]. However, a full understanding of putative corneal stem cells hasn't yet been achieved due to the lack of specific and definitive corneal stem cell markers.

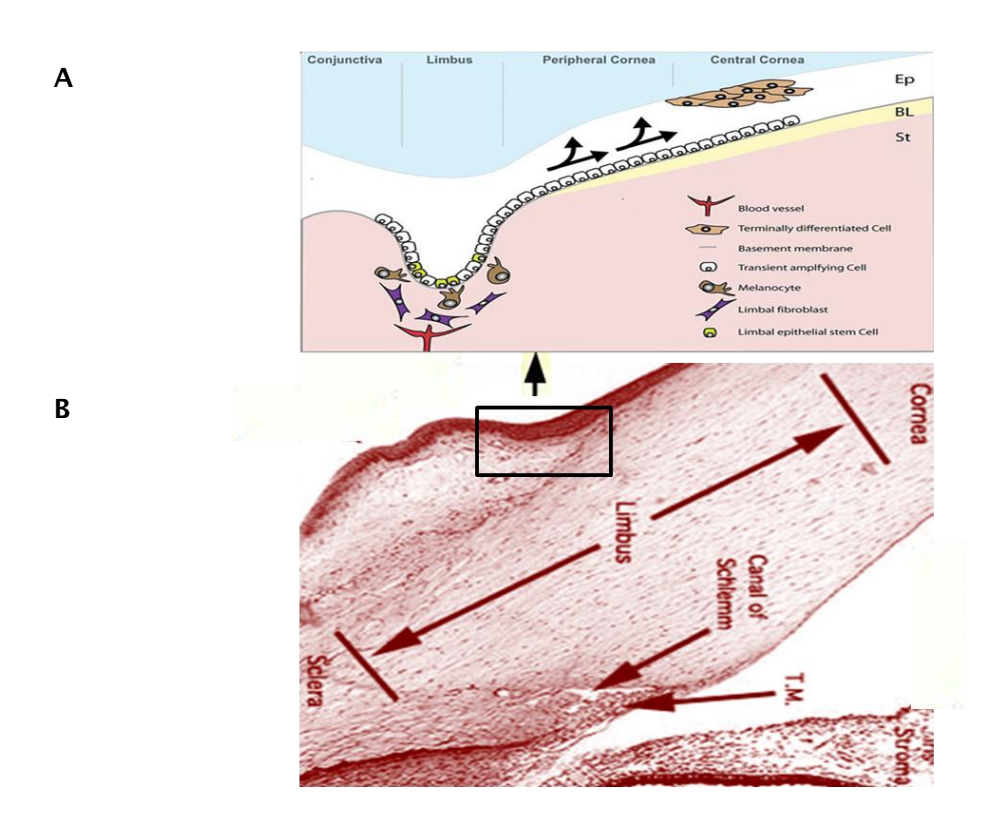


Figure 1-3 Human corneal limbus

(A) Schematic diagram illustrates the location of putative limbal epithelial stem cell and the corneal epithelial regeneration pathway (Secker *et al.* 2008 [28], reprinted with permission from Springer) (B) shows the structure of human limbus (adapted from resource http://faculty.une.edu/com/abell/histo/histolab3b.htm). T.M.: trabecular meshwork.

The limbal stroma is highly cellular and vascularised. Recent studies have identified multipotent stem cells in the adult corneal stroma from mice, rabbits and humans [29-33]. These cells have the ability to divide extensively and generate neurons, adipocytes, osteoblasts and adult keratocytes in vitro [29-32]. In humans, keratocyte stem/progenitor cells mainly reside in the anterior corneal stroma close to the limbus. They express the ocular development marker Pax6 and demonstrate a side population (SP) phenotype [30]. A SP is characterized by the ability to efflux Hoechst 33342, a DNA-binding dye. It represents a quiescent, immature and conserved feature of stem cell populations [34,35]. SP discrimination assay has been used to identify stem cells from various tissues. Further investigations of these potential stem cells in the corneal stroma may have important implications for cell based therapies in degenerative eye disease. Interestingly, corneal endothelium precursors can also be isolated and expanded in vitro from mammals, including human, though they are rarely detected in vivo [36,37]. Their proliferation in vitro is achieved through a sphere forming assays. The sphere colonies express neural stem cell marker nestin. They also produce neuronal and mesenchymal cell proteins [36,37]. This may imply a new source of cells for treating corneal endothelium deficiency diseases.

#### 1.3.2 Structure of the retina

The human retina is a highly organized laminated tissue. In the early 1900's, Ramon y Cajal first identified the structure and individual cell types of the retina based on morphological Golgi silver staining [38] (Figure 1-4A). Retina is comprised of five types of neurons: photoreceptors (rods and cones), bipolar cells, ganglion cells, horizontal cells and amacrine cells. With their processes and synaptic connections, those neurons form ten layers in tissue which is approximately 0.5 mm in thickness. From innermost to outermost, the retina is composed of: inner limiting membrane, nerve fiber layer, ganglion cell layer, inner plexiform layer, inner nuclear layer (bipolar, horizontal and amacrine cell bodies), outer plexiform layer, outer nuclear layer (rod and cone), external limiting membrane, photoreceptor layer and retinal pigment epithelium as shown in Figure 1-4B [39].

Rods and cones are light sensitive photoreceptor cells. Visual pigments in rods and cones initiate a cascade of phototransduction following light stimulation, which alters cell membrane potential. Neurotransmitters are subsequently released at the synapses between photoreceptor terminals and bipolar cells in the outer plexiform layer. The next synaptic contacts occur between the processes of the bipolar cells and ganglion cells in the inner plexiform layer. This three- neuron chain is the major transmission route from photoreceptors to the optic nerve [39,40]. Other neural cells types such as

the horizontal and amacrine cell have lateral interactions and regulate the visual system's sensitivity to luminance contrast. The overall retinal structure layers, individual cell types and signal transmitted routes are illustrated in Figure 1-4 B.

In humans and primates, cones are found in the central part of the retina termed the "macula" (Figure 1-5), which is responsible for fine resolution and color vision. The center of the macula is known as the fovea, which is comprised of only cones. There are three different types of cones, detecting short- (blue), medium- (green) and long-wave (yellow-red) light to form trichromatic color vision. Rods, on the other hand, are adapted for sensing contrast, low light vision and motion. They are mainly distributed at the periphery of human retina. The ratio of rods to cones in the retina is approximately 20:1, with a total of 120 million rods and 6 million cones. The type of photoreceptors and their distribution differ between primates and other mammals. Most mammal don't have a macular region, are referred to as dichromats as their retinas only accept long- wavelength (L-) and Short- wavelength (s-) cone signals. Interestingly, some mammals have numerous dual cones which are immunopositive for both S- and L- cone markers [41].

#### 1.3.2.1 Photoreceptors

Rod and cone photoreceptors are highly specialized for light perception. They have the same basic structure comprised of outer segments, inner segments, cells bodies and processes. Cones are shorter with conical outer segments and a wider base compared with that of rods (Figure 1-6). The membranous disks of the outer segments in both photoreceptor subtypes contain photopigments which are involved in the initiation of phototransduction and conversion of light to neural impulses.

As shown in Figure 1-7, when a photon of light arrives at the photoreceptors, opsin molecules which are manufactured at the inner segments, bind a derivative of vitamin A named "retinol" to form Rhodopsin. Rhodopsin undergoes a conformational change from the 11-cis form to an all-trans form and subsequently forms activated transducin. The latter activates cGMP phosphodiesterase which breaks down cGMP into 5'-GMP. This reduction of cGMP allows cGMP-gated cation channels to be closed, preventing the influx of positive ions, which hyperpolarize the cell membrane, thereby stopping the release of neurotransmitters. Phototransduction is also characterized by its amplification a process. A single photon of light leads to isomerisation of rhodopsin molecules in the rod cells, which subsequently activates numerous transducin and phosphodiesterase molecules in the cascade. Thus, only a few photons of light are required to hyperpolarise a rod cell [42].

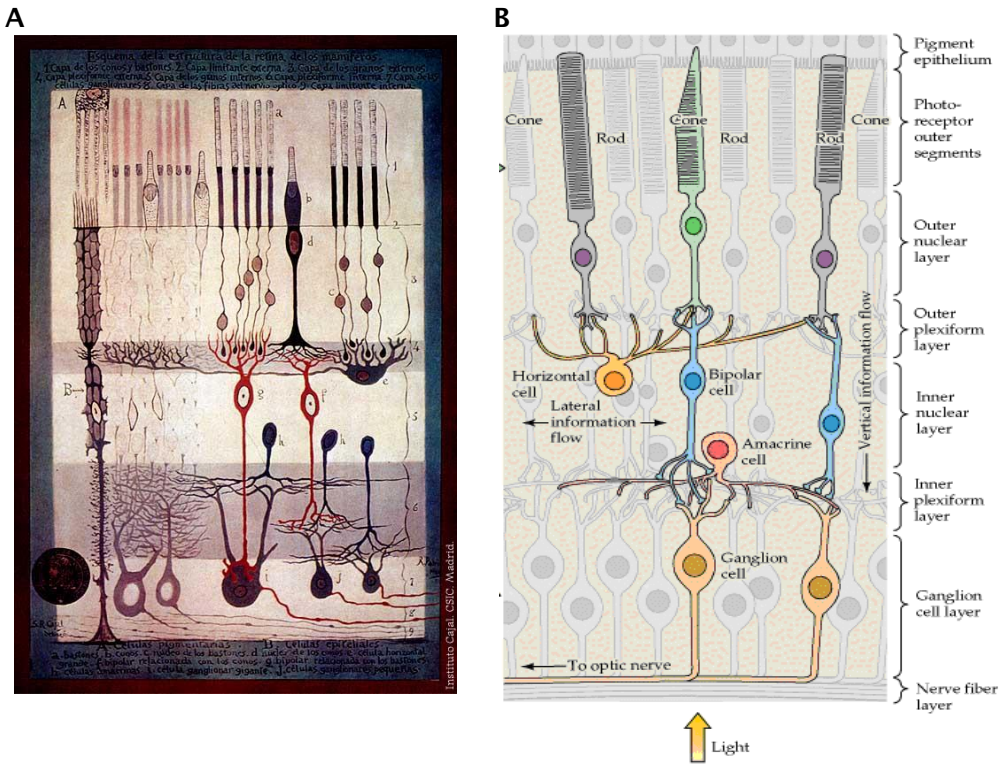


Figure 1-4 Structure and connections in the mammalian retinas (A) The structure and individual cell types of the mammalian retina identified by Ramón y Cajal using Golgi silver staining (Cajal S. 1900); (B) A schematic diagram illustrates the retinal connection (Purves *et al.* 2001 [43]. Diagram was reproduced with permission from Sinauer Associates)

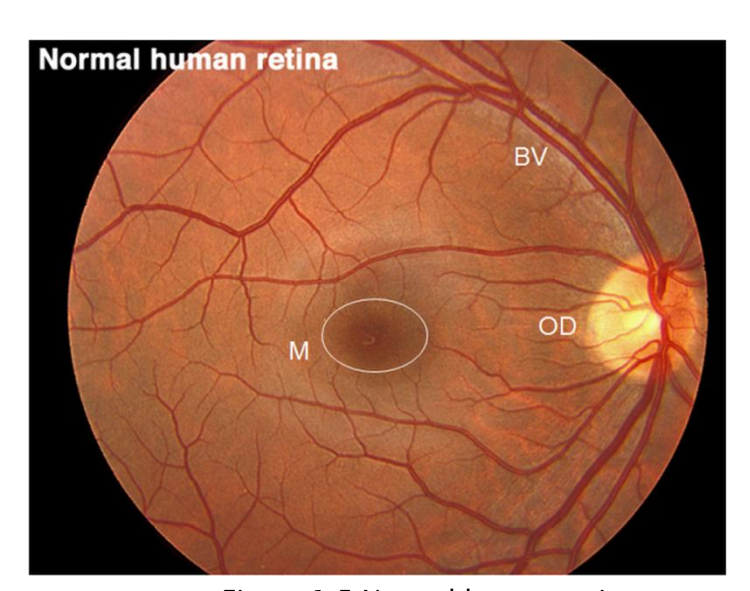


Figure 1-5 Normal human retina

Normal human retina viewed through an ophthalmoscope. The macula (M) is the oval avascular area at the center of the optic axis. Optic disc (OD, white area), where ganglion cell axons exit the eyeball to form the optic nerve, radiate the major blood vessels (BV) of the retina. Image was adapted from resource http://webvision.med.utah.edu/

#### 1.3.2.2 The Retinal Pigment Epithelium

The retinal pigment epithelium (RPE), which develops from the outer layer of the optic cup during embryogenesis, is a monolayer of cuboidal cells that are densely packed with pigment granules. The RPE is tightly attached to Bruch's membrane (BM) on top of the choroid, with it apical surface connected to photoreceptors. The RPE layer plays an essential role in supporting and maintaining general visual processes [44]. Photoreceptor excitability and the visual cycle rely on reisomerization of all-transretinal to 11-cis-retinal by the RPE. Without cis-trans isomerases, photoreceptors are not able to conduct this conformational change following phototransduction. Several proteins found in RPE cells are involved in this important process, including RDH5 (Retinol DeHydrogenase 5), CRALBP (Cellular Retinylaldehyde-Binding Protein) and RPE-65 (Retinal Pigment Epithelium-specific 65 kDa protein). In addition, RPE cells are continuously phagocytosing shed-membrane discs from the outer segments (OS) of photoreceptors. OS are constantly renewing, and replaced every 12 days. Phagocytosis functions not only to recycle and return essential substances such as retinal to photoreceptors to rebuild new photoreceptor OS, but also to eliminate potential toxic debris. Failure of or defect in phagocytosis leads to degenerative retinal diseases, such as RP, Usher type 1B Syndrome and AMD. Other important functions of the RPE include maintenance of the immune privilege of the eye, nutrition supply, homeostasis and neuronal protection. The latter is accomplished through secretion of neuroprotective factors including pigment epithelium-derived factor (PEDF), which act to decrease glutamate-induced or hypoxia-induced retinal ganglion cell apoptosis and also inhibition of endothelial cell proliferation [44]. Thus, RPE cell transplantation can in principle be used to treat degenerative retinal diseases, through support of retinal cell function and homeostasis [45].

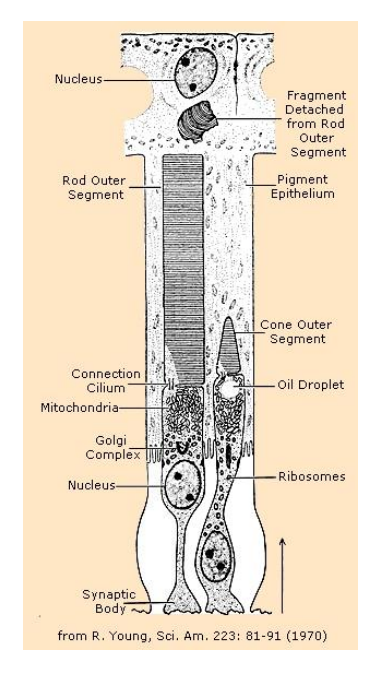


Figure 1-6 Structure of rod and cone photoreceptors.

A schematic diagram illustrating the structural comparison of rod and cone photoreceptors (Young, 1970 [46], the diagram was reprinted from Wikipedia Http://www.wikipedia.org)

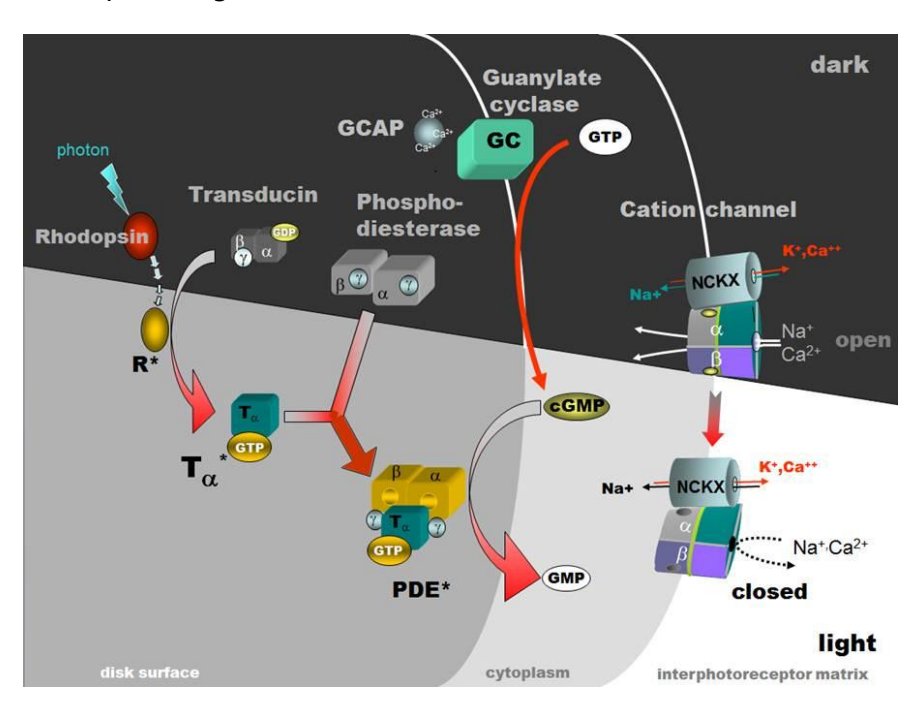


Figure 1-7 The phototransduction cascade.

A schematic diagram illustrates activation of Rhodopsin by light and the subsequent phototransduction cascade (From the source http://webvision.med.utah.edu/. Image was reproduced under Attribution, Noncommercial, No Derivative Works Creative Commons license)

### 1.4 Degenerative Retinal Diseases

There are a wide spectrum of degenerative retinal diseases, including Macular Degeneration, Retinitis Pigmentosa, Usher Syndrome, Stargardt Disease, Best Disease, Cone-Rod Dystrophy and Leber's Amaurosis. They are characterized by apoptosis of photoreceptor and/or RPE cells with subsequent visual loss. Currently, there is no effective therapy available to restore the cellular loss which accompanies these diverse diseases [1,2].

#### 1.4.1 Age Related Macular Degeneration (AMD)

AMD is the primary cause of visual disabilities in industrialized societies, especially in patients over 50 years of age. Its prevalence increases with age, and affects up to 25% of the population aged 75 and over [2,47]. AMD not only leads to considerable loss of quality of life, but also represents a formidable clinical and socio-economic burden [48].

AMD is characterized by loss of photoreceptor cells in the macula, due to progressive deterioration of the RPE, bruch's membrane (BM), and the choriocapillary-choroid complex [45,49,50]. This deterioration ultimately leads to loss of central vision. AMD presents as two distinct clinic phenotypes: "wet" and "dry". The wet form, referred to as exudative-neovascular AMD, accounts for approximately 10% of all cases. The growth of new abnormal blood vessels under the macula, choroidal neo-vascularisation (CNV), leads to accumulation of exudative fluid and hemorrhages on the retina, thereby causing damage to the photoreceptor cells. Wet AMD progresses rapidly and can cause severe damage, with the loss of central vision which may occur within a few months. The remaining approximately 90% of AMD cases are of the "dry" form, known as nonexudative AMD. It is characterized by geographic atrophy of the RPE and accumulation of drusen, the metabolic debris from dysfunctional RPE cells at BM in the macular area. Loss of RPE cells also leads to apoptosis of photoreceptors, with subsequent loss of central vision. The pathogenesis of AMD has yet to be fully understood. The disease progression is associated with environmental as well as genetic factors. Age and smoking are the proven main epigenetic risk factors [51]. Genetic risks include variants in complement genes including CFH, C3, CFB and C1 inhibitor, as well as HTRA1 [52-55].

#### 1.4.2 Retinitis Pigmentosa (RP)

Many degenerative retinal diseases are inherited. The most common of which, Retinitis Pigmentosa (RP) leads to progressive loss of photoreceptors and RPE by apoptosis. The prevalence of RP is approximately 1 in 5000, affecting over a million people worldwide [56]. Affected individuals may first suffer from night blindness, which progresses to loss of the peripheral visual field, leading in turn to tunnel vision. Patients with RP may eventually become blind in later life.

RP has been associated with molecular defects in more than 100 different genes which are related to the structure, function, survival and maintenance of photoreceptors and RPE. Among those, rhodopsin gene defects are the most common, accounting for approximately 30% of autosomal dominant forms of PR. RP has extraordinary genetic heterogeneity, and can be inherited as an autosomal dominant, autosomal recessive or X-linked trait [56]. Meanwhile, the phenotypes of diseases can be diverse and discordant with their genotypes. Currently, there is no effective treatment available to prevent loss of rod photoreceptors or restore their visual function.

#### 1.4.3 Current treatments

Current therapies are focused on the treatment of CNV (wet AMD). For the majority of cases of AMD (dry AMD) and other inherited degenerative retinal diseases; there is no effective treatment available. Cell replacement and gene therapy may provide an opportunity for restoration of visual function.

#### 1.4.3.1 Generation of thrombosis within CNV

Laser (photocoagulation), thermo-energy (transpupillary thermotherapy TTT) and photochemical reaction (photodynamic therapy, PDT) generate thrombosis within CNV, which may cause the CNV to perish. The first two methods are destructive as they also damage normal retinal tissue; thereby, they cannot be used for sub-foveal CNV. PDT has the advantage of not affecting normal retinal vasculature, and offering a potential treatment for sub-foveal CNV. However, a two-year randomized PDT clinical trial showed disappointing results. PDT was only effective for a minority subtype of CNV patients that would account for less than 25 percent of the total cases of CNV, while the majority of sub-foveal CNV patients did not show a better result compared to the untreated group [57]. Moreover, 4.4% of eyes treated with PDT had a severe decrease in vision (over 20 letters compared with visual acuity prior to PDT). Another similar trial also confirmed this lack of efficacy in the same subtypes of CNV [58]. Thus a large

proportion of patients with neovascular AMD have very limited treatment options and the underlying pathophysiology of CNV still remains, which may lead to re-occurrence.

#### 1.4.3.2 Anti-VEGF

More recently treatment which targets the central signaling molecule in ocular neovascularisation, vascular endothelial growth factor (VEGF), has been investigated. VEGF is highly selective for endothelial cells, affecting their proliferation, survival and migration, which eventually leads to angiogenesis. The synthesis of VEGF can be upregulated by many pathologic states such as hypoxia, ischemia or inflammation, with subsequent diffusion of VEGF to its target tissue [57]. VEGF exists in 4 different isoforms. Among them, VEGF is found to be largely responsible for pathological ocular neovascularization. It consists of a receptor-binding domain, which binds to the VEGF receptor. The formed binding complex induces signal transduction and vascular endothelium migration and proliferation.  $VEGF_{165}$  also has a heparin-binding site, which assists the association of  $VEGF_{165}$  with the cell membrane and enhances the effect of VEGF<sub>165</sub> [59]. Blocking of VEGF can be achieved through VEGF inhibitors such as pegaptanib or VEGF antibodies including ranibizumab. Pegaptanib is a pegylated aptamer produced by chemical synthesized of oligonucleotide sequences. It targets the heparin-binding site of VEGF<sub>165</sub> to inhibit the amplification of VEGF receptor signaling. The advantages of pegaptanib include lack of immunogenicity, stability together with high affinity and specificity [57]. Ranibizumab is a monoclonal anti-VEGF antibody fragment which can bind all isoforms of VEGF in humans. It directly targets the receptor-binding domain of VEGF to inhibit VEGF receptor signaling itself. Intravitreal injection of pegaptanib or ranibizumab both demonstrate effectiveness in reducing the risk of visual acuity loss, however visual gain was much higher using ranibizumab [57].

Although great progress has been made with anti-VEGF treatments, certain issues remain which have yet to be addressed. Firstly, the visual acuity improvements demonstrated are very limited. Improvement for most cases is 1-2 line in the standard visual acuity test chart (ERDRs) [57]. Secondly, frequent intravitreal injection are required, with the potential risk of endophthalmitis [58].

#### 1.4.3.3 Gene therapy

The pathophysiology of AMD is yet to be fully understood. Certain complement genes have been shown to be associated with AMD, but the role of specific genes and their mechanism in the development of AMD is largely under discovered. It is more likely that genetic susceptibility is multifactorial and a combination of environmental factors including smoking, contribute to the development of AMD. Therefore, direct gene therapy to repair defective genes will not be sufficient to eliminate development of

AMD. One form of gene therapy targets prolonging the survival of the RPE and retinal photoreceptors by the introduction of growth factors into RPE cells [58]. These include transfer of basic fibroblast growth factor (FGF2) and pigment epithelium derived factor (PEDF) to RPE cells to enhance their function or inhibitor angiogenesis. There are also reports on using genetically modified iris pigment epithelium cell, which are able to secret PEDF [60]. In addition, anti-angiogenic gene therapy potentially could be a good solution to overcome the disadvantages of current anti-VEGF treatments such as short term effectiveness, frequent intravitreal injection and subsequent risk of endophthalmitis.

However, sufficient consideration need be given to gene therapy in terms of safety, In particular use of retroviral vectors *in vivo*, may lead to integration of new sequence into the genome or replication of competent virus. Other adverse effects include inflammation due to administration of vectors. Overall, gene therapy can only be used to delay the progress of AMD, and as yet cannot be used to prevent the occurrence of AMD. Also gene therapy will not restore visual acuity in patients who have severe pre-existing cell loss for instance in patients with advanced "dry" AMD.

### 1.4.3.4 Subretinal surgery

CNV may be removed through submacular surgery, which is based on the three port pars plana vitrectomy. To determine the effectiveness of submacular surgery, a number of randomized multicenter clinical trials, were carried out at the end of the last century. The results showed no benefit or limited effect for subfoveal CNV removal, with a high rate of reoccurrence [61]. Some retrospective studies have also demonstrated minimal improvements in visual acuity, together with up to 50 percent recurrence of CNV [58]. Considering the high recurrence, and risks of intraocular surgery such as hemorrhage and endophthalmitis, CNV excision should not be considered as the first choice for treatment of neovascular AMD.

# 1.4.3.5 Cell therapy

Cell therapy is one of the most promising treatments for degenerative diseases of the retina, as cellular replacement may lead to long term restoration of visual acuity. An important phenotypic abnormality of degenerative retinal diseases is the loss of functional photoreceptors, however the inner most layers of the retina remain intact and functional for a comparatively long time. Cell therapy appears promising in this instance [5,62], as transplanted photoreceptors need only make a single short synaptic connection with the inner retinal circuitry for light signal transduction to be reinstated [62]. When sufficient functional photoreceptors successfully integrate into the retina, and build functional synaptic connections with the inner retina, vision loss may be

effectively delayed or reversed [63]. In addition, modern intraocular micro surgical techniques and the anatomical existence of the subretinal space allow photoreceptor transplantation to be a realistic prospect.

Encouraging outcomes following transplantation have been observed in various wildtype [62,64] and degenerative animal models including rds mice (retinal degeneration slow) [62], rd mice (retinal degeneration fast) [62], rho2/2 mice (rhodopsin knockout) [62], mnd mice (retinal/CNS degeneration) [65] and Royal College of Surgeons rats (RCS) [65,66]. Photoreceptor precursors derived from the retina of postnatal (PN) mice have been shown to successfully integrate into the outer nuclear layer (ONL) of host mice and can differentiate into mature photoreceptors as illustrated in Figure 1-8 [62]. Moreover, functional synaptic connections which contribute to visual function were formed in rds, rd and rho2/2 mice. Neuralized ESCs were also found to migrate into the host retinal tissue and prevent retinal degeneration in RCS rats and mnd mice [65,66] Preliminary clinical studies have shown that in patients with RP and dry AMD, visual acuity (VA) and light sensitivity improved following transplantation of human neural retinal progenitor cell layers (sheets) with RPE [67] or fetal retinal sheets with RPE [67].

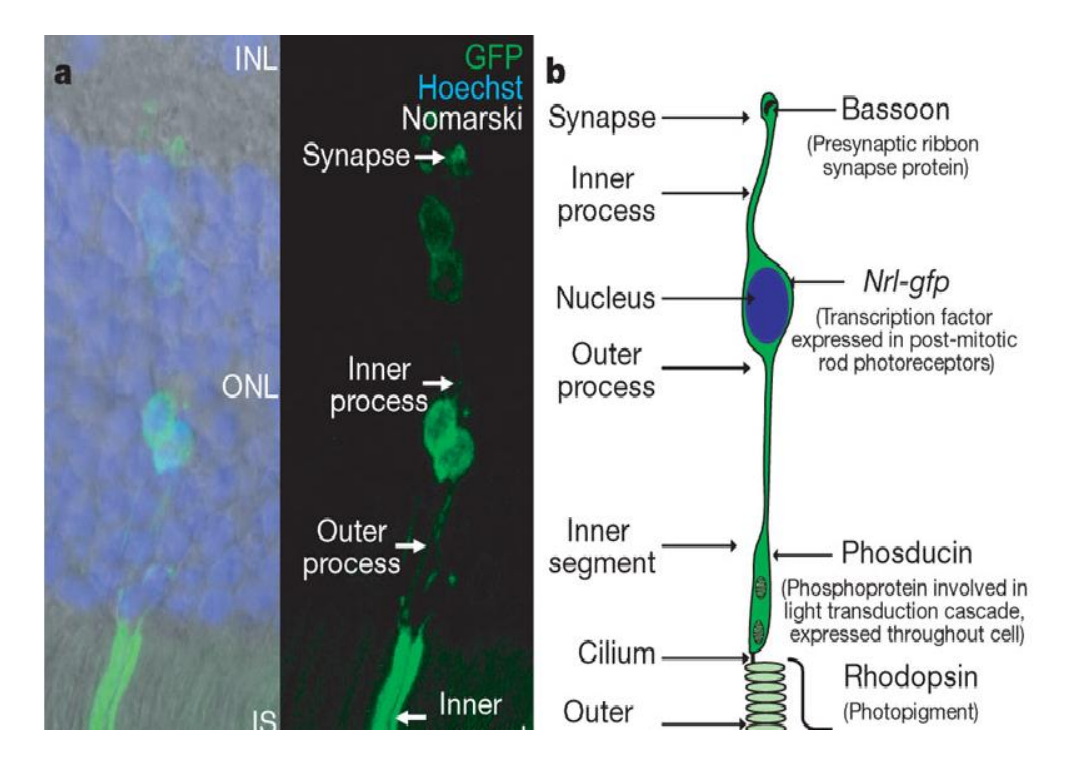


Figure 1-8 Integration of photoreceptor precursor into wild-type recipient retinas.

The image demonstrates that allograft retinal cells from P1 mice can integrate into ONL of the wild-type recipient retinas (MacLaren *et al.* 2006, Image was reprinted with permission from Nature publishing Group).

# 1.5 Development of the eye

Eye formation commences approximately 22 days after fertilization. As shown in Figure 1-9, the optic sulci of the neural plate gradually change shape from a shallow groove to a hollow cavity to form the optic vesicle. The apex of the vesicle remains closed to the surface ectoderm and connects to the forebrain by a stalk, termed the optic stalk. The optic vesicle then invaginates forming a two layer optic cup, with the top layer forming the future neural retina and bottom layer the RPE. Together with formation of the optic cup, the surface ectoderm (lens placode) also folds into the optic cup and forms the lens vesicle. The latter then separates from the rest of the surface ectoderm for mature lens development. The margin of optic cup goes on to form the pigmented epithelium layer of the ciliary body and iris. The rest of the surface ectoderm including migrated neural-crest mesenchyme forms the cornea.

The specification of eye in the anterior neural plate is synchronized with the coordinated expression of a group of eye field transcription factors, which will be explained in detail in the following section.

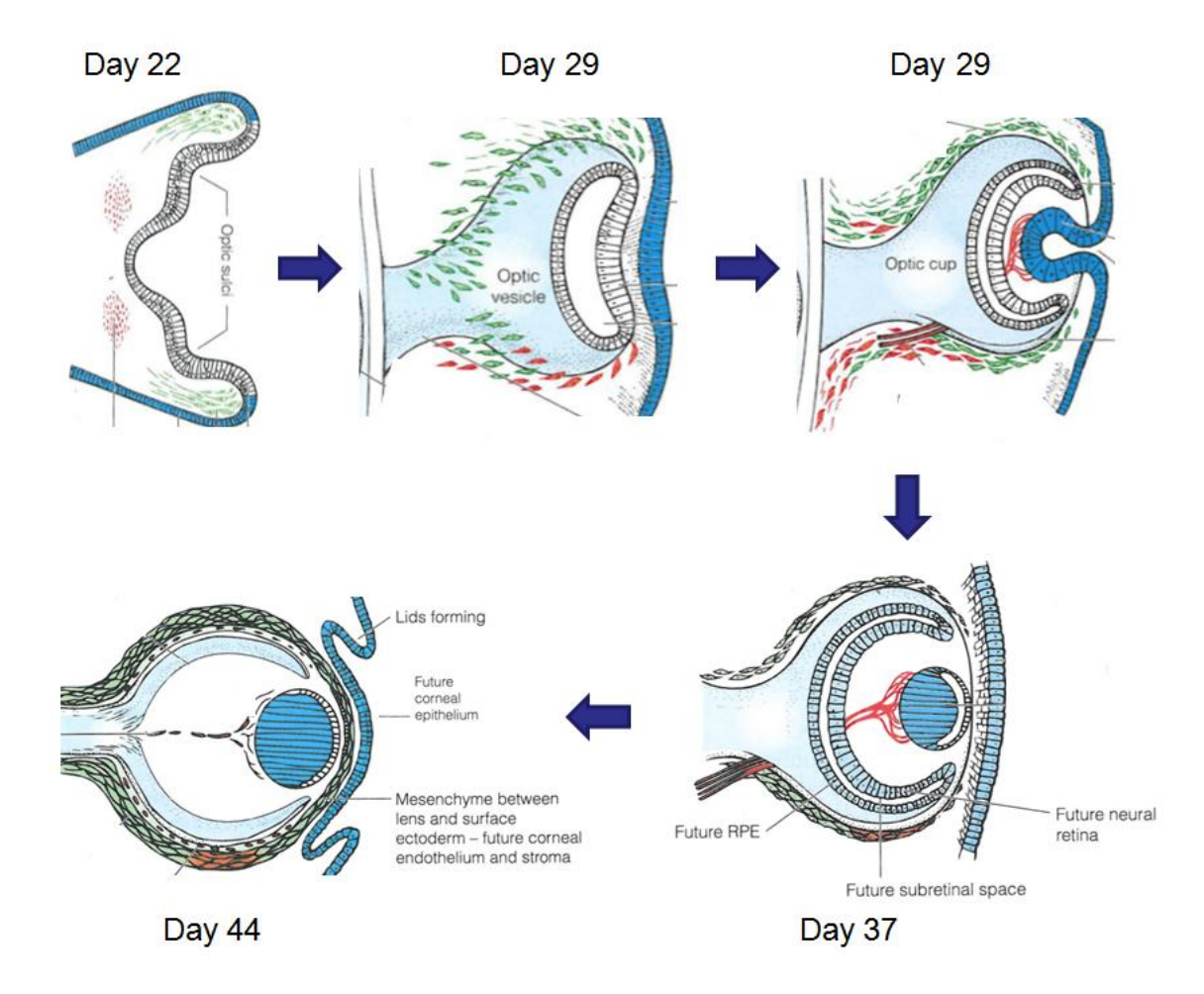


Figure 1-9 Summary of embryonic ocular development

A schematic diagram illustrating development of the human embryonic eye from day 22 to 44. Various germ layers were colour coded. Red: Mesoderm; Black: Neural Ectoderm; Green Neural Crest; Blue: Surface Ectoderm. Images were adapted from Forrester *et al.* 2002 [15].

# 1.5.1 Transcription factors for eye development

Several homeobox transcription factors have been reported to play a critical role in eye formation in both vertebrate and invertebrate. Co-ordinated expression of transcription factors including: Pax6 (paired box gene 6), Rx (retinal homeobox), Six3 (homeobox protein SIX3) and Otx2 (orthodenticle homeobox 2) have been observed in the early optic vesicle [15].

Pax6 is regarded as a universal "master control gene" for eye development [68]. The evidence for Pax6 being a "master control gene" includes expression in the developing eye of a broad range of species from insects to mammals. Pax6 is also a highly

conserved protein sequence in most species[69]. Mutations or silence in Pax6 homologs can lead to anophthalmia causing absence of eye in flies, mice and humans, while ectopic eyes can be created by targeted expression of Pax6 [68,70]. Halder *et al.* induced the formation of ectopic eyes on the antennae, wings and legs of flies, which showed functional photoreceptor activity when tested by electroretinography (ERG) [68]. Pax6 is also indispensable for the formation of almost all vertebrate retinal cell types [71].

The retinal homeobox (Rx) gene plays a critical role in regulating initial specification of retinal cells as well as eye formation [72]. The presence of Rx protein correlates with the location of retinal stem cells during the development process. Consistently, over expression of Rx mRNA induces formation of ectopic retinal tissue and hyper-proliferation of the neural retina in lower vertebrates [72]. In mammals, targeted knockout of Rx prevents formation of the optic vesicle and optic cup. Rx serves as a top level regulator for optic vesicle formation, as silence of Rx leads to inactivation of other homeobox transcription factors such as Pax6, Six3 and Otx2 [72,73].

The Orthodenticle homeobox 2 (Otx2) [74] is widely involved in optic vesicle formation and subsequent neural retina and RPE differentiation. It also regulates photoreceptor specification through regulation of the Cone-rod homeobox (Crx) gene. The last important eye development transcription factor is Sine oculis homeobox homolog 3 (Six3), which is specific to the whole region of the anterior brain, including the eye. It is also important for proliferation of retinal precursor cells [75].

### 1.5.2 Development of cornea

The cornea develops mainly from both the surface ectoderm and neural crest. At approximately 5 to 6 weeks after fertilization, corneal development begins. The corneal epithelium layer forms first when the lens placode separates from the surface ectoderm. The rest of which forms a layer of cuboidal epithelium (future corneal epithelium). After one week, neural-crest derived mesenchymal cells sited at the margin of the optic cup migrate into the space between the lens placode and epithelium, and form the corneal endothelium layer. On day 49, there is secondary migration of neural-crest derived mesenchymal cells, from the optic cup margin to the space between the epithelium and endothelium commences. In this final stage, the corneal stroma forms [15].

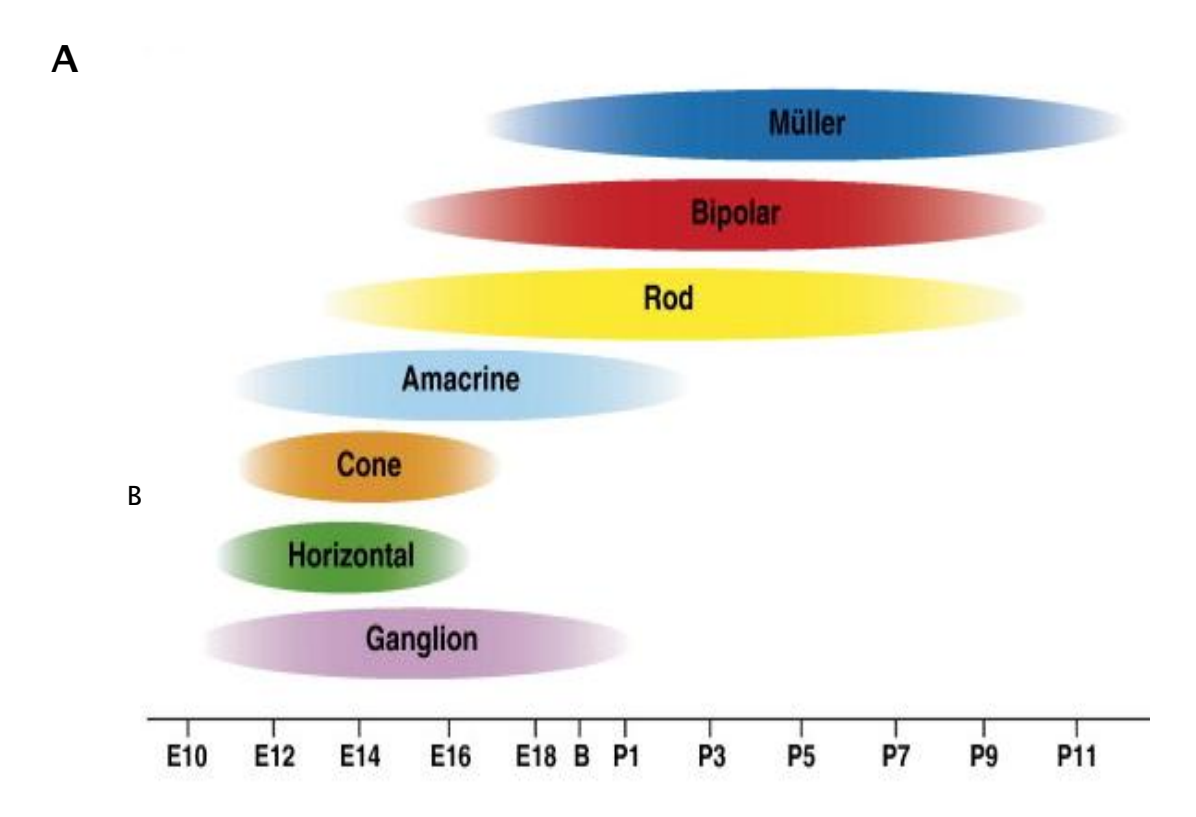
The neural crest is a discrete structure that exists transiently in the vertebrate embryo. Its component cells yield an extraordinary variety of cell types, from peripheral

neurons and satellite cells to bones, tendons, connective and adipose tissues, dermis, melanocytes and endocrine cells [76]. Neural crest cells become specified in a rostrocaudal fashion along the body axis. Subsequently, they are released from the neuroepithelium as mesenchymal cells that follow definite migratory routes, finally reaching target embryonic sites where they settle and differentiate. The whole process, including ontogeny, specification, delamination as well as later differentiation processes are regulated by Bone Morphogenetic protein 4 (BMP4) and it inhibitor Noggin [77].

# 1.5.3 Development of neural retina and retinal pigment epithelium

During embryonic development, the retina is derived from optic vesicles sited from two sides of the developing neural tube. Initially, the optic vesicles invaginate to form the optic cup, with the inner layer forming the future neural retina and the outer layer developing into the RPE layer. With further neuroblastic layer division and migration, the sensory retina forms a distinct lamellae structure. Differentiation of seven retinal cell types can be divided into two stages as shown in Figure 1-10. The first stage leads to the development of ganglion cells, cone photoreceptors, horizontal cells and amacrine cells; whilst the second wave includes rod photoreceptors, bipolar cells and finally the Müller glia [78].

Development of the retina relies on precise regulation of transcription factors on both temporal and spatial ranges. A combination of homeobox genes and basic helix-loophelix (bHLH) genes are required for retinal neuron fate determination. The network of transcription factors which direct cell differentiation, and any self-regulatory systems, are yet to be fully understood. Through targeted knockout and misexpression functional studies, genes which are essential for each type of retinal cell specification have been summarized as illustrated in Figure 1-10 B. Besides these intrinsic factors, extrinsic factors such as Ciliary Neurotrophic Factor (CNTF), Fibroblast Growth Factor (FGF) and Bone Morphogenetic Protein (BMP) may also play roles in the regulation of retinal cell differentiation as well as proliferation [79].



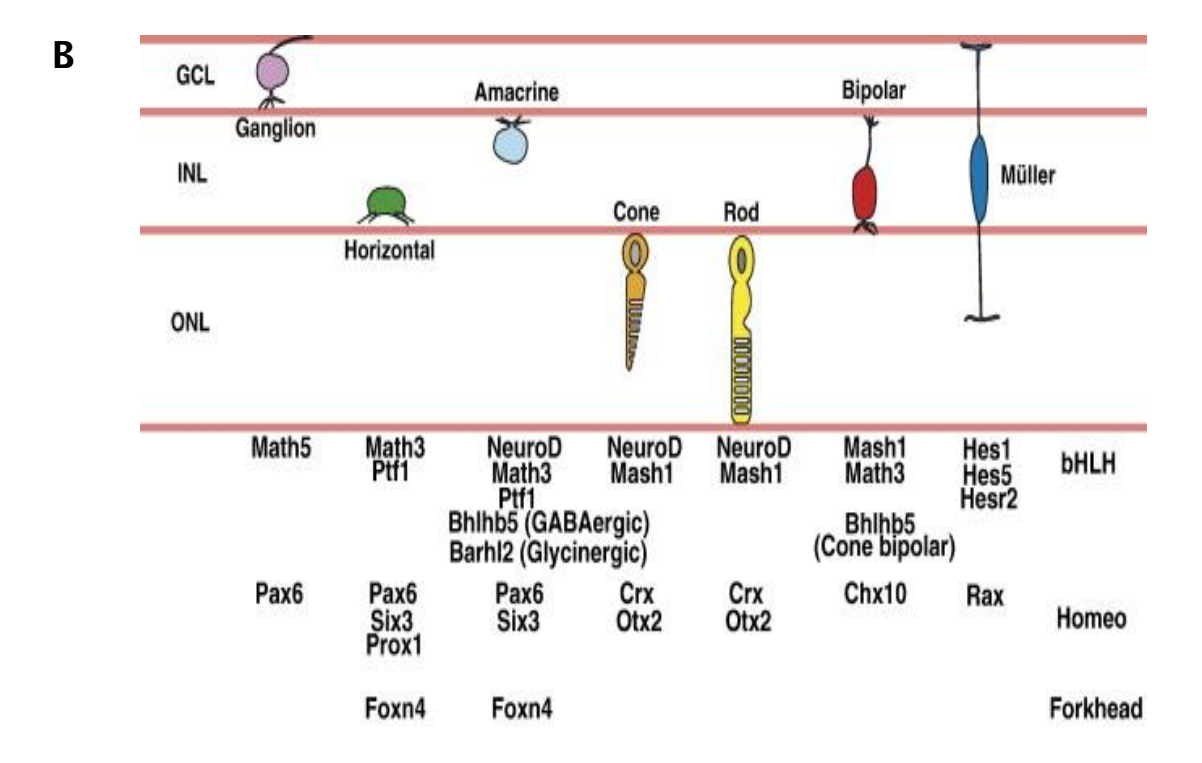


Figure 1-10 Development of mammalian retinal cells (A) illustrates the temporal order of generation of mammalian (mouse) retinal cell types; (B) demonstrates the transcription factors for retinal cell fate specification (Ohsawa, 2008 [80], the images were reprinted with permission from Elsevier).

Compared to the neural retina, regulation of RPE cell specification involves significantly less transcription factors. A network composed of Mitf, Otx2 and Pax6 is crucial for RPE cell specification [81]. Otx2 is essential for initial eye development in vertebrates. When eye development is specified, expression of Otx2 is only maintained in presumptive RPE cells to adulthood. In the adult retina, loss of Otx2 protein causes disruption of photoreceptor-RPE cell adhesion and in impaired melanogenesis in RPE cells and subsequent slow degeneration of photoreceptor cells [82]. Over expression Otx2 can also be detrimental leading to induction of pigmentation in vertebrate neural retina cells *in vitro* [83]. Similarly, loss of Mitf function cause impairs the development of the RPE in mice, and generation of a laminated second neural retina [84]. OTX2 and Mitf have been found co-localized in the nuclei of RPE cells. They can physically interact with each other. Their co-expression results in a cooperative activation of downstream regulator such as tyrosinase [83,85].

#### 1.5.4 Development of Photoreceptors

The rods and cones are the cells within the mammalian retina which are responsible for light perception. The regulation of photoreceptor development and maintenance is controlled by a network of transcription factors from four classes: Homeodomain, bZIP, bHLH and Nuclear Receptors as illustrated in Table 1-1 [73].

Homeodomain factors Otx2 and Crx (cone rod homeobox) play crucial roles in specifying the photoreceptor lineage. Otx2 acts at the highest level, through direct regulation of Crx and its target genes. The function of Crx is crucial as it acts as a trans-activator directly regulating the expression of many photoreceptor genes. Photoreceptor-like cells have been produced by introduction of either or both Otx2 and Crx into IPE and CE derived cells [8,13,86-88]. Neural retina leucine zipper protein (Nrl) and the orphan nuclear receptor (NR2E3) are found to determine rod fate. The former is also important for maintaining rod function and homeostasis; and the latter may act as cone fate suppressor. Mutation in human NR2E3 cause enhanced S-cone syndrome, an autosomal recessive inherited disease with hyperfunction of blue cones and dysfunction of rods. Cone fate determination is largely regulated by nuclear receptor family members, including thyroid hormone receptor  $\beta 2$  (Tr $\beta 2$ ), retinoid related orphan receptor Ror $\beta$ 2, and retinoid X receptor Rxr $\gamma$ . Subtypes of cones are negatively or positively regulated by each and are also influenced by extrinsic factors such as thyroid hormone [73]. This comprehensive regulatory network, with interaction and regulation between transcription factors as well as other signaling pathways, is essential for specialized photoreceptor development and functional maintenance (Review see Hennig et al.) [73].

Table 1-1 Transcription regulators for photoreceptor gene expression, development and/or maintenance

Transcription	Transcription	Expression	Function	
classes	factors		Targets	
Homeodomain	Otx2	development photoreceptor	Activator	
		precursors	Crx, Rbp3, etc.	
Homeodomain	Crx	development/adult	Activator & Regulator	
		rods/cones	Opsins	
Homeodomain	Rax	development/adult	Activator	
		photoreceptor	Rho, Arr, Rbp3	
Homeodomain	Qrx/RaxL	development/adult	Activator	
		photoreceptor	Rho	
bZIP	Nrl	development/adult rods	Activator	
			Rho, Nr2e3, Pde6b, etc.	
bHLH	NeuroD1	development rods	Survival	
			Photoreceptors	
bHLH	Mash1	development rods	Activator	
			Rho	
bHLH	Math5	development precursors	Repressor	
			NeuroD1, Neurog2	
bHLH	Neurog2	development precursors	Activator?	
			NeuroD1	
Nuclear	Trβ2	development cones	Activator & Repressor	
Receptors			S-, M-opsin	
Nuclear	Rxrγ	development cones	Repressor	
Receptors			S-opsin	
Nuclear	Rorβ	development cones	Activator	
Receptors			S-opsin	
Nuclear	Nr1d1	development photoreceptor	Activator & Repressor?	
Receptors			circadian genes	
Nuclear	Nr2e1(Tlx)	development cones	Activator & Repressor	
Receptors			S-opsin, Pax2, Rar	
Nuclear	Nr2e3	development/adult rods	Activator & repressor	
Receptors			All opsins	

Abbreviations: Arr-rod arrestin; Neurog2-neurogenin 2. Rho- Rhodopsin; RBP3-Retinol-binding protein 3 (also known as IRBP); Pde6b- Rod cGMP-specific 3', 5'-cyclic phosphodiesterase subunit beta; Crx , cone rod homeobox; Rax(Rx), retinal homeobox; S/M-opsin, Short/middle Wavelength Sensitive opsin; Nrl, Neural retina-specific leucine zipper; Qrx/RaxL: Rx like homobox; MASH, Mammalian achaete-scute homolog; Tr $\beta$ 2, Transient expression of thyroid hormone nuclear receptor; Nr2e3/ Nr2e1, retinoic X receptor-like nuclear receptor3/1; Nr1d1, nuclear receptor subfamily 1, group D; Rxry, Retinoid X receptor- $\gamma$ . Adapted from Hennig *et al.* 2008 [73].

# 1.6 Stem cell therapy

#### 1.6.1 Stem cells

Stem cells possess two unique properties: 1) Self-renewal: the ability to undergo unlimited proliferation and maintain the undifferentiated state and 2) potency: the capability to differentiate into specialized cells [14,18].

Because of these unique characteristics, stem cells provide an opportunity for producing numerous specialized cells for transplantation. Pluripotent stem cells, such as ESCs and reprogrammed iPSCs can differentiate into almost all specific cell types from the three germ layers- mesoderm, ectoderm and endoderm. Adult stem cells have been identified in the tissue of adult mammals. They were previously considered to be multipotent, with limited specialization potential to a cell lineage or specific tissue in which they reside. However, recent studies show that certain adult stem cell types have "plasticity", the ability to generate a variety of cell types, even across the boundary of germ layer [89-91]. For example, bone marrow mesenchymal stromal cells can differentiate into a variety of different cell types including hepatocytes, endothelium, myocardial, neuronal and glial cells as well as different types of epithelium [92]. The adult stem cells derived from corneal stroma can give rise to adipocytes, neurons and chondrocytes [30,93]. These "multipotent" adult stem cells would therefore be advantageous for autologous cell replacement [6,89,91].

#### 1.6.2 Immune response in the subretinal space (SRS)

The RPE layer and photoreceptors are derived from the outer and inner layers of the optic cup respectively during embryonic development; thereby producing a potential space for transplantation and surgical intervention, referred to as the SRS. Advanced intraocular surgical techniques have also been developed and established over the last century. These include comprehensive SRS surgeries such as CNV incision and cell/tissue transplantation [61,94,95].

The SRS is considered as one of the immune privileged sites in the human body [96]. Immune privilege was first discovered by Sir Peter Medawar, describing the lack of an immune response when allografts were placed into one of the ocular microenvironments, the anterior chamber [96]. Immune privileged sites generally display prolonged acceptance of foreign tissue, including solid tissue or tumor, whereas conventional sites readily prompt rejection to similar grafts. Mechanisms involved include the unique blood ocular barrier, a lack of direct lymphatic drainage,

and the presence of various immunosuppressive molecules, as well as immunomodulators [97]. The blood-retinal barrier forms part of the blood ocular barrier, and contributes to the SRS immune privilege. It is composed of non-fenestrated retinal vascular structure and tight-junctions between retinal pigment epithelial cells, preventing passage of large molecules or pathogens from choriocapillaris into the retina.

However, immune responses have been detected in animal models and humans following cell transplantation into the SRS. Following xenogeneic transplantation of mouse RPCs into pigs [98], large numbers of mononuclear inflammatory cells were observed in the choroid near the transplantation site within a few weeks. Allografts appeared to manifest a mild cell-mediated chronic immune response in the absence of typical histological inflammation [4,96,99,100]. Mild rejection in the RCS rats was observed following RPE allograft to the SRS, presenting as an increased loss of photoreceptor cells [100]. In human studies of wet AMD, RPE cell transplantation following CNV excision led to obvious rejection after three months. Most of the patients (4 of 5) lost graft fixation and showed macular edema and fluorescein leakage [94]. It was also found that RPE cells lead to more rejection compared to photoreceptors/ retinal progenitor cells. The extent of immune response was related to the amount of RPE cell grafted, the integrity of the blood retinal barrier and the time following transplantation [58,101].

The mechanism of the immune response in the SRS is unclear. It seems different from the mechanism of immune response which occurs in the brain, where local microglia could serve as potent antigen present cells to prime T cells [102]. Gregerson and Yang collected fresh adult retinal microglia and demonstrated that retinal microglia were neither efficient in priming naive T cells nor responsive to treatment with interferon-r or anti-CD40 [103]. This suggests that retinal microglia possess different immune properties.

Nevertheless, the immune-privileged status of the SRS is not absolute. It may merely help to prolong survival of allografts [104]. If the recipient and donor do not have matched histocompatibility loci, rejection will eventually occur [96]. A functional, intact RPE monolayer plays an important role in maintaining the blood retinal barrier as well as the SRS immune privilege [99]. In both AMD and RP, RPE cells suffer either deterioration or complete loss. Therefore, autologous cell sources have significant advantage as they can avoid immune responses between the host and donor, and maintain long-term functionality of grafted cells or tissues [45].

## 1.6.3 Strategy of stem cells therapy

Generation of sufficient photoreceptors or photoreceptor precursor cells remains the goal for the treatment of various degenerative retinal diseases. Cell replacement may not only delay disease progression but may actually lead to an improvement in visual function. Currently the key challenge is to identify and obtain a suitable/plentiful source of progenitor or stem cells (SCs) which could be utilized for photoreceptor repair.

Stem cells provide hope for an unlimited cell source for photoreceptor and/or RPE cell generation, based on their two main characteristics of self-renewal and multipotency. True stem cells, including totipotent and pluripotent stem cells, fulfill the above criteria. They are capable of unlimited cell divisions and can differentiate into cells of all three germ layers. There is controversy over whether multipotent and unipotent cells can be defined as stem cells since they are more restricted to their related germ layer or cell lineage. However, recent studies have proven the plasticity of these cell types. By various inducing and regulating means, cells have been transdifferentiated toward lineages other than that of their origin [91,105,106].

To generate photoreceptor or RPE cells for cell transplantation strategies, a number of candidate stem cell resources have been investigated as described below. Based on whether immune response can be avoided following transplantation, they were classified as allogeneic or autologous stem cells in this chapter.

# 1.7 Allogeneic cell resources

### 1.7.1 Embryonic stem cells

Derived from the inner cell mass (ICM) of the blastocysts (4 to 5 days post fertilization), embryonic stem cells (ESCs) can be maintained undifferentiated *in vitro* and have the potential to provide an unlimited source for cell therapy. ESCs have the most infinite proliferative capacity to generate sufficient cells of all three germ layers.

For mammalian ESC differentiation, the following approaches may be used: feeder cells, growth factors, chemical compounds and genetic modification [107]. The differentiation of ESCs into neural progenitors has been well established. The differentiation is based on a feeder free and serum free sphere-forming culture system in the presence of epidermal growth factor (EGF) and basic fibroblast growth factor

(FGF2) [108]. In addition, direct differentiation towards specific mature neural types has also been achieved based on this system. Although this highlights the possibility that specific retinal cell types may be achievable, this process has turned out to be more difficult for the generation of photoreceptor cells. Through co-culture with PN or embryonic (E6) cells, a subset of ESCs can differentiate into both retinal progenitors and mature neurons. However, the use of animal tissue in directing cell differentiation is not appropriate for clinical application. In the last decade, a few groups have made progress towards identifying safe and defined factors for differentiation of ESCs into retinal progenitor cells and/or subsequently into mature photoreceptors [7,10,109].

Based on the classic sphere forming neuronal differentiation assay, in combination with several regulatory signaling pathways including BMP and Wnt together with defined extrinsic factors, highly efficient differentiation of ESCs towards RPCs has been achieved [7,109,110]. The progenitor cells produced had a genetic profile similar to progenitors derived from human fetal retina, including expression of Pax6, Chx10, Sox2, Crx, Nrl, recoverin, S-opsin, and rhodopsin. These progenitor cells however rarely spontaneously differentiate into photoreceptor cells [109,110]. A further comprehensive stepwise defined condition has been developed to obtain photoreceptors from mouse, monkey and human ESCs [109]. Rod specific markers were found in 17% and 8% of cells derived from mouse and human ESCs respectively. Approximately 10% of the cells expressed S-cone marker, which was equivalent to the number of M/L cones after differentiation from both mouse and human ESCs. Although photoreceptor specific opsins and phototransduction components were detected at both a protein and transcription levels, the function of these cells requires further confirmation.

Generation of RPE cells from ESCs is much less complicated when compared to production of photoreceptor cells. Using feeder layers such as mouse embryonic fibroblasts or PA6 stromal cells and in the presence of animal serum, ESCs from mice and primates will differentiate towards RPE cells. The derived RPE cells display a similar transcription profile in terms of RPE specification. These cells also demonstrated phagocytic activity [111,112]. Osakada *et al.* also identified defined conditions for RPE cell differentiation to avoid the use of animal derived materials [109].

Despite this success in the generation of photoreceptors/RPE cells from ESCs, several barriers remain to limit their application in cell therapy. Firstly, *in vitro* proliferation and maintenance of undifferentiated human embryonic stem cells (hESCs) largely relies on feeder layers which are derived from animal embryonic fibroblasts. Other reagents such as serum and supplements derived from an animal origin are also required.

Thereby, the risk of diseases and immune reaction caused by nonhuman sialic acid (Neu5Gc) cannot be eliminated [113]. Secondly, tumor formation is a major risk which should be emphasized. Teratomas which contain cells from all three germ layers can be developed in vivo following ESC implantation. Arnhold et al. [114] investigated transplantation of mouse ESC derived precursors to the SRS. They found no tumor formation up to 4 weeks post transplantation. However, at 8 weeks post grafting, half of the animals exhibited neoplasias, composed of cells from different germ layers [114]. It should be noted that the embryoid body (EB) cells used in this study had underwent a selection procedure to obtain a highly purified population of neural precursor cells. Therefore, for future clinical application, more stringent selection is essential. However, currently there is no suitable surface marker for neural precursor cell sorting, and pure cell selection has yet to be achieved. Thirdly, hESC lines are allogenic. Immune response following transplantation would be a major issue. To limit the risk of rejection, it would require matching the donor and recipient's genetic makeup and the use of immunosuppressive treatments following transplantation. Finally, the use of ESCs also raises significant challenges for clinical application due to ethical concerns with the use of cells derived from embryonic tissue.

#### 1.7.2 Retinal progenitor cells from developing retinas

Developing retinal cells/tissues have been extensively investigated in the prospective treatment for retinal diseases [62,115,116]. Early studies on transplantation of mammalian retina showed survival of grafted tissues/cells in the SRS [116]. However cellular rosettes, a morphological barrier preventing retinal repair, were present at the engrafting site following transplantation into adult rodent retina [116]. Further studies using in vitro expanded embryonic (E17) rat retinal stem cells generated sufficient progenitor cells for transplantation. The grafted cells were viable in the SRS without forming rosette barriers [115]. These studies showed limited levels of grafthost integration and photoreceptor differentiation. By optimizing the isolation, expansion, and transplantation procedures, Qiu et al. engrafted E17 rat retinal stem cells into the SRS of PN 17 S334ter-3 and S334ter-5 transgenic rats, which possess mutations in the rhodopsin gene. Over 80% of the grafted RPCs demonstrated rhodopsin expression and the presence of synapsin1 processes at the interface of the graft and host retina [117]. Despite the extensive rhodopsin expression in the grafted cells, morphological incorporation was not convincing. Synapsin1 staining was mainly localised to the ganglion layer, inner nuclear layer or horizontal cells in the outer plexiform layer, while photoreceptor cells never exhibited synapsin I mRNA or synapsin I protein throughout development [118].

The developing retina contains a mix of RPCs including photoreceptor precursor cells. These precursor cells are an ideal cell resource for transplantation in terms of appropriate developmental stage and definite commitment to the photoreceptor lineage. Nrl is an early rod photoreceptor lineage-specific marker [62]. By using Nrl-GFP transgenic mouse model, a comprehensive study was conducted to investigate the integration ability and functional incorporation of mouse retinal cells from embryonic day (E) 11.5 to adulthood [62]. This study showed that retinal cells from the peak of photoreceptor genesis stage (PN1-3 mouse retinas) are the optimal donor cell resource for integration and synaptic connection following transplantation [62]. The selected postmitotic photoreceptor precursor cells displayed synaptic integration into various types of retina *in vivo*, including wildtype and mouse models of retinal degeneration. Promisingly, the visual function of receipt animals improved following cell replacement. On the contrary, proliferating RPCs from earlier stages of development were unable to integrate into the retina despite differentiation into rhodopsin positive cells and survival in the SRS [62].

For practical clinical application, a safer and more convenient cell selection process is necessary compared to genetic NrI-GFP labeling. By using fluorochrome-conjugated antibodies which recognize cell surface antigens CD24 and CD73 for sorting donor cells, integration was 18 times more efficient than unsorted RPCs and 2.3-fold higher than transgenic marker, NrI-GFP sorted cells. The cells displayed the ability to migrate into the outer nuclear layer of the retina and presented the morphology of mature photoreceptors following transplantation into wildtype and degenerative mouse models [119].

Despite the success of using developing retinal cells in mouse model, the use of the same congenic stage human cells would not be practicable. In humans, rod genesis begins at foetal week 10 and continues into the first 8 months of life. Although progenitor cells derived from developing retina do not have the risks such as tumor formation, ethical implications and limited resources remain the barriers to practical application. Again, the transplantation of allogenic resource into the SRS would potentially lead to severe cell loss due to rejection [120]. Therefore, alternative sources of autologous cells have been investigated.

# 1.8 Autologous cell resources

# 1.8.1 Induced pluripotent cells

Induced pluripotent stem cells (iPSCs) can be generated from adult human somatic cells (fibroblasts) through ectopic expression of a combination of embryonic transcription factors including: Oct3/4, Sox2, Klf4, c-Myc / LIN28 and NANOG [121,122]. iPSCs have demonstrable similarities to ESCs in most respects, and can differentiate into a variety of cell lineages. Thereby, they provide hope for an unlimited autologous cell source for both cell therapy and disease modeling for a wide range of diseases [121,122]. Recently there have been a number of reports detailing direction of iPSCs along a retinal lineage with the production of photoreceptors and RPE cells. These iPSCs derived cells have been transplanted into animal models of retinal degeneration and have shown promising results [123,124].

However, barriers for further clinical applications remain. The use of viral-transduction may cause multiple random incorporations of transgene into the recipients genomic DNA; thereby posing a high risk of oncogenesis [125]. Recent studies have discovered non-viral vectors which can be used to generate iPS cells from adult stem cells [126]. However, risk of tumor formation due to contamination with undifferentiated cells remains unresolved. Buchholz *et al.* found that at least 0.6% of mouse iPSCs remained undifferentiated in their culture system up to 15 days after differentiation [127]. These potential adverse effects need be carefully controlled prior to clinical application.

Therefore, adult stem cells/progenitor cells still remain attractive. Various adult stemlike cell resources have been extensively investigated in respects of generation new photoreceptor cells and retinal repair.

#### 1.8.2 Stem-like cells from the ciliary epithelium

Development of the retina demonstrates a central to peripheral gradient in mammals and lower vertebrates. In lower vertebrates, a special region named the ciliary marginal zone (CMZ), which is capable of regenerating the retina, is located at the peripheral margin of the retina. Evidence of slow cycling cells in the human ciliary epithelium (CE) leads to the assumption that human retinal stem cells may reside within this region [128,129]. These cells show extensive proliferation and are capable of neurosphere (NS) generation when cultured in a serum free culture system, in the presence of mitogens such as EGF and FGF2. Besides clonal growth, these cells exhibit neural stem cell and retinal progenitor specific markers. They can also be differentiated along

neuronal and glial lineages [130]. Exposure to a retinal induction environment or transfection with retinal homeobox and bHLH genes can lead cells to differentiate towards photoreceptors [87,131-133].

However, it remains controversial as to whether these stem like cells derived from the CE are true adult retinal stem cells. Although these "stem like cells" express stem cell markers such as Nestin and display clonogenic characteristics, they still retain similarities with differentiated CE cells in a number of respects including molecular profile, cellular components, and morphological features as well as the presence of melanosomes [3]. Some studies have demonstrated a limited capacity for self-renewal using CE cells [134]. In differentiation culture medium, spontaneous production of retinal cells was rarely detected [3]. A recent comprehensive study used Nrl.gfp transgenic mice to investigate definitively the ability of CE cells to produce photoreceptor cells. Despite expression of a subset of eye field and RPC markers when cultured in vitro, these cells remained characteristic of differentiated CE. Various previously reported conditions to promote photoreceptor differentiation did not effectively activate Nrl-regulated photoreceptor differentiation program [135]. To date, there is lack of in situ evidence that CB cells can migrate into retinal tissue and generate photoreceptors for retinal repair in mammals [136]. In addition, the CB area is also too high risk for a surgical approach. Thereby, CE cells are not a practical autologous cell resource for transplantation.

#### 1.8.3 Adult iris epithelium cells (IPE)

Iris pigment epithelium cells (IPE) are an excellent source of autologous cells for transplantation as this iris is relatively accessible surgically. IPE cells have the same embryonic origin as the retina and RPE cells. Like the stem like cells derived from the adult CE, in a conducive *in vitro* environment, IPE cells express the neural stem cell marker nestin, and can be expanded readily [88,137]. IPE cells also possess the ability to transdifferentiate [138]. Following transfection with Crx and/or Otx2 [86], most cells express photoreceptor specific markers such as rhodopsin. Freshly isolated and cultured IPE cells have been successfully used for clinical transplantation to replace damaged RPE cells [139]. However, it has yet to be proven that IPE have the capacity to generate sufficient cells from small amounts of tissue. There is also a lack of evidence that IPE constitute a true population of SCs [140].

#### 1.8.4 Retinal Müller glial cells

In lower vertebrates, such as teleost fish, Müller glial (MG) cells can actively repair damaged retina by re-entering the cell cycle, proliferation, and migration into the photoreceptor layer [136,141]. In mammals, this process is absent. Evidence shows that PAX6-positive MG cells were unable to proliferate following photoreceptor injury in mammals [141]. Further study demonstrated that Notch and Wnt signaling can stimulate *in vivo* MG cell proliferation and regeneration of photoreceptors[142]. However, there is still a lack of convincing evidence of functional integration of newly generated cells [136].

In vitro expanded MG cells showed promising results for generation of photoreceptor like cells. MG cells from adult mammals, including humans, displayed stem cells like properties [12,143]. They can form neurospheres, and be induced to express protein markers of various mature retinal neurons via cultured in sphere aggregates. Recently, Giannelli et al. demonstrated in vitro culture conditions that can induce over 50% of adult human MG cells to adopt a rod photoreceptor like phenotype [12]. MG derived photoreceptor-like cells also possessed membrane potential and other electrophysiological characteristics similar to adult rod photoreceptor cells. Following subretinal transplantation, a small population of cells migrated into the retina including the ONL. Nevertheless, in vitro expanded and differentiated MG cells are not a desirable autologous cells resource due to the surgical challenge to harvest them.

#### 1.8.5 Adult bone marrow stem cells

Adult bone marrow stem cells include hematopoietic stem cells (HSCs) and the marrow mesenchymal stromal cells (MSCs) [92]. The former can give rise to all blood cell types, while the latter have demonstrated a remarkable plasticity for differentiation towards various tissue specific cells including hepatocytes, endothelium, myocardial, neuronal and glial cells as well as different types of epithelium as shown in Figure 1-11 [92]. In addition, MSCs of the bone marrow can generate functional neuronal cells *in vitro* through regulation by extrinsic factors [89]. This transdifferentiation is not limited within the same germ layer of origin, but can cross the boundary to mesoderm and ectoderm. This plasticity has also been seen from other sources of adult stem cells, for instance adult mouse skeletal muscle cells and adult neural stem cells can give rise to blood cells [91].

The mechanisms that may be involved in adult stem cell plasticity include transdifferentiation (direct lineage conversion), dedifferentiation (indirect lineage conversion through the recapitulation of developmental stages) and cell fusion. Adult stem cell plasticity often occurs after local tissue injury [89,91], indicating that microenvironmental exposure (extrinsic factors) plays a crucial role.

Given the advantages of plasticity, self-renewal, accessibility and the potential for autologous transplantation to avoid immune-rejection, bone marrow cells have also been considered as a candidate stem cell resource for the treatment of degenerative retinal diseases. Kicic *et al.* have investigated the potential of MSCs for differentiate along retinal lineages [144]. By the use of extrinsic factors including activin A, taurine, EGF and CD90+ MSCs were differentiated *in vitro* into cells expressing photoreceptor specific markers (20-32%), including rhodopsin, opsin, and recoverin. Results were confirmed with immuno-blotting and reverse transcription-polymerase chain reaction (RT-PCR). Induced cells also demonstrated integration into the SRS [144]. Bone marrow stem cells have also been considered as a resource for the production of RPE cells. Arnhold *et al.* reported a promising result [145], by forced expression of pigment epithelial-derived factor (PEDF), MSCs were transduced into RPE like cells. These cells showed close contact with photoreceptor outer segments, with phagocytosis of rod outer segments following transplantation into the SRS of RCS rats. Functional improvement as determined by electroretinography was also detected.

Further studies have compared MSCs derived cells and retinal progenitor cells on both neural differentiation and potential of retinal integration. Both cell types integrated into retinal explants from rhodopsin knockout mice, and expressed neuronal and

retinal specific markers such as neurofilament, protein kinase C-alpha and recoverin *in vitro*. However, majority MSCs cells which integrated into retina expressed microglial cell markers. Compared to retinal progenitor cells which integrated, no rhodopsin expression was detected in MSCs derived cells [146]. Due to limited studies of MSCs differentiation towards RPE cells, further investigation is necessary in terms of functional visual rescue. Bone marrow stem cells are an attractive autologous source of stem cell for therapeutic application, however manipulation towards a photoreceptors lineage may be challenging as their origins are from different germ layers.

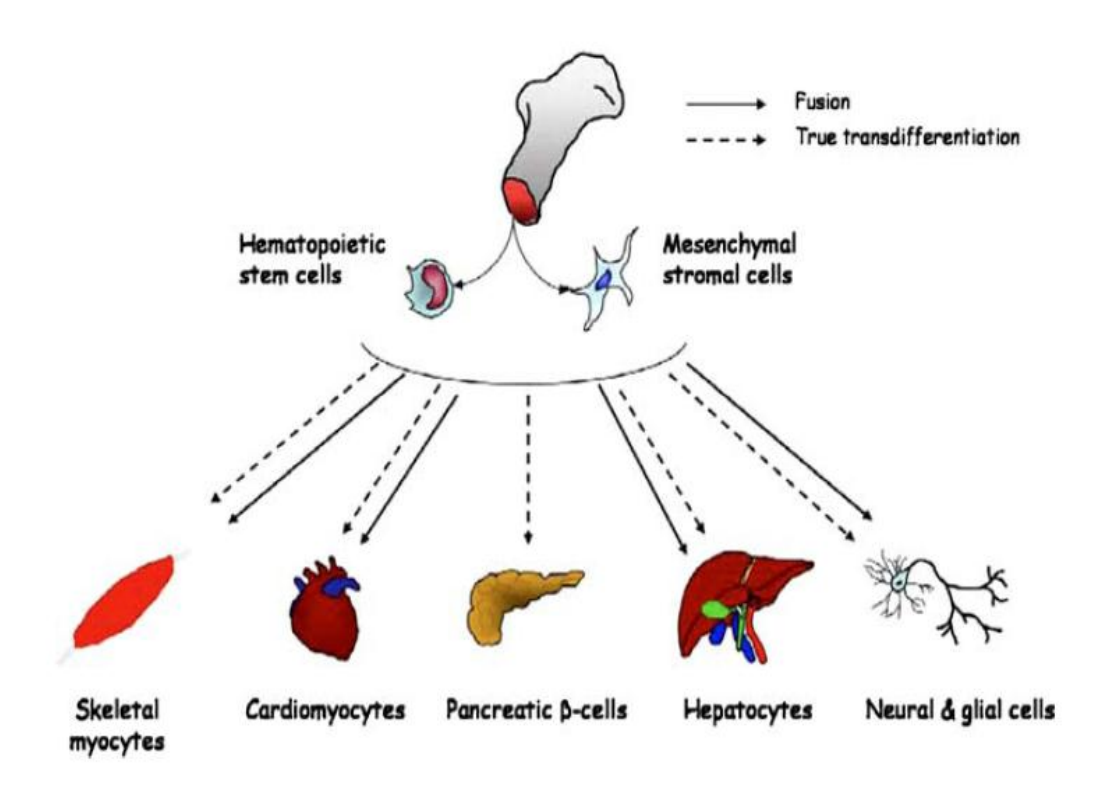


Figure 1-11 Plasticity of bone marrow derived cells

A diagram illustrating various cell types that can be derived from bone marrow stem cells via transdifferentiation or fusion (Hombach-Klonisch, 2008 [92], reproduced with permission from Springer).

#### 1.8.6 Adult stem cells from the corneal limbus

There are two stem/progenitor cell populations which reside within the superficial layers of the corneal limbus namely corneal epithelium stem cells and neural-crest derived stromal stem cells [1,20,22,30,90,147,148]. The former, which reside in the basal layer of the limbal epithelium, are responsible for the long term renewal of corneal epithelium [1,20,22,147]. The number of cells in the stromal layer usually

remains stable after birth. However, recent studies showed the derivation and expansion of multipotential stem/progenitor cells from corneal/limbal stroma *in vitro* [30,90,148]. They also can be generated from 2-3 mm of the superficial layers of human limbus [149]. These two populations of stem/progenitor cells are an ideal autologous cell resource for a number of reasons. Firstly, these cells are accessible. Unlike CE, RPE and IPE cells, intraocular surgery is not required; thereby avoiding risks such as endophthalmitis. Secondly, they are capable of generation of large number of cells for transplantation purposes. Thirdly, expression of Pax6, the master gene for oculogenesis, has been detected both from progenitors in the epithelium basal layer and the corneal stroma *in vivo* [17,33], which is indicative of an intrinsic ability for eye field generation. Therefore, limbal cells may require less manipulation to generate retinal neurons compared to other heterologous sources.

Plasticity and the ability to transdifferentiation are broadly present in adult stem cells and even the boundaries of germ layers can be crossed [89,91,105,145,150], which also provide the possibility for generation of retinal neurons from corneal limbal stem cells. In addition, the cornea and the retina both develop from the ectoderm. Ectodermal cells have a 'default' neural fate in the early embryo [151,152]. If they do not receive other inducing signals directing them to form epidermis, mesoderm, or endoderm, they will automatically differentiate towards neurons. In normal development, bone morphogenetic proteins (BMPs) inhibit this fate and specify epidermal specific development [151]. The absence of BMP signaling [153], accomplished by BMP antagonists leads to the formation of neural tissue in vertebrates [154,155]. Therefore, corneal limbal stem cells should be more suitable for generation of neurons compared to stem cells derived from other germ layers. The evidence for the neural potential of corneal limbal cells is summarized below.

#### 1.8.6.1 Corneal epithelium stem cells (CES)

The epithelium layer of the cornea is regenerated throughout life. Autologous CESC therapy for corneal diseases has been successfully used clinically [156]. *In vitro* cultured CES cells have been proven to be a safe cell resource. Also a healthy eye can tolerate a partial limbal excision of 1-2 mm which is enough to provide sufficient SCs [157].

Seigel *et al.* demonstrated that in a small proportion of cultured human corneal stem cells, there was co-localization of the epithelium stem cell marker (P63) and the neural stem cell marker (nestin) [21]. Certain neurotransmitter receptors (GABA, glycine and serotonin receptors) were also detected in P63 positive cells. Furthermore, the neurotransmitter (GABA) and the non-NMDA glutamate receptor agonist (Kainic acid)

induced a current change, indicating that these cells are capable of functional neurophysiological responses [21]. A further study by Zhao et al. demonstrated the comprehensive neural properties of neurons derived from adult rodent CES cells [6,158]. Using a neural stem cell culture system together with a BMP4 inhibitor, neural stem/ progenitor like cells which were nestin positive were harvested from CES cells. These cells had the ability to differentiate into both neuronal and glia cells. The differentiated neurons demonstrated voltage- and ligand-gated currents by electrophysiology. Other functional aspects including the presence of functional ionotropic glutamate receptors, specific synaptic vesicle protein (synaptophysin) and axo-somatic synapse-like structure as shown by a Ca2+ imaging study, immunocytochemistry and transmission electron microscopy respectively, were also demonstrable. When exposed to retinal development environments, CES derived stem like cells differentiated along a rod photoreceptor lineage both in vitro and in vivo, with expression of photoreceptor regulation genes Crx, Nrl as well as rod specific markers such as opsin, rhodopsin kinase, arrestin and interphotoreceptor retinoidbinding protein (IRBP) [6,6,158]. Although the functionality of these photoreceptors needs further investigation, this result highlights the possibility that limbal cells may become a candidate resource for cell therapy for retinal disease.

### 1.8.6.2 Neural-crest derived cornea stroma cells (NC-CS)

Corneal stroma stem/progenitor like cells are neural-crest derived mesenchymal cells, which migrate from the neuroepithelial layer at early stages of development. They are rich in the peripheral cornea and are located just under the basal layer of the epithelium in humans [30,149]. In mammals and humans, NC-CS cells form NS-like clusters in serum free suspension culture conditions in the presence of EGF and FGF2. Besides demonstration of a SP phenotype, NC-CS cells express neural stem cell markers such as Nestin, Musashi1, Sox2 and Vimentin and can differentiate toward neurons, adipocytes and chondrocytes both *in vitro* and *in vivo*, demonstrating evidence of their multipotency [29-33].

NC-CS cells may even be pluripotent. Dravida *et al.* found that cells derived from adult human corneal-limbal stroma cells not only possess the capacity to self-renew, but also express specific markers for ectoderm, mesoderm and endoderm lineages as well as some ESC markers *in vitro* [149]. A variety of cell types including corneal cells, neurons, osteoblasts, chondrocytes, adipocytes, hepatocytes, cardiomyocytes and pancreatic islet cells can be derived from these NC-CS cells [149]. Also from a 2–3 mm<sup>2</sup> limbal

biopsy, up to 60 doubling expansions can be induced, which would produce more than sufficient cells for clinical transplantation [149].

# 1.9 Methods for retinal lineage direction

### 1.9.1 Retinal developing environment

A proven differentiation method towards retinal lineage specification is provided by co-culture with embryonic or PN retinal tissue/cells [159-161]. This method is reliant on short distance diffusible signals which are released by developing retinal cells. It can efficiently direct ESC differentiation towards retinal and photoreceptor lineages, with approximately 20% of cells expressing rhodopsin, a rod photoreceptor specific photopigment [161]. This rod promoting activity is temporally correlated with the timing of rod generation in vivo in different species [159]. The ideal development stage when using murine tissue is between PN day 1 and day 3 (PN1-PN3). At this stage rod differentiation is effectively promoted, without induction of an amacrine cell phenotype [159,160]. The promoting effect varies between ESCs and retinal progenitor cells, this method can also direct heterologous stem cells to a photoreceptor lineage. Zhao et al. found the rod specific markers opsin and rhodopsin kinase were expressed in cells derived from rodent corneal limbus following co-culture with PN1 retinal cells [6]. Other developmental and functional transcription factors associated with the retina including Otx2, Crx, NeuroD, Arrestin and Opsin were confirmed through RT-PCR [6]. Although the functionality of these differentiated cells is unknown, the approach used is considered as an effective way to investigate the potential for differentiation of heterologous stem/ progenitor cells. This method however has an obvious limitation for any clinical application as this approach involves using animal tissue. Thereby, significant research has been devoted to the development of safe and defined conditions for retinal lineage development which do not rely on animal based products.

#### 1.9.2 Stepwise defined condition

It was not until recently that stepwise differentiation of ESCs into photoreceptors, using defined culture conditions, has been achieved [162]. The whole process can be divided into two steps. The first is the generation of multipotent retinal progenitor cells from ESCs. A number of groups have confirmed the veracity of this method. Lamba *et al.* cultured human ESCs as embryoid body-like aggregates in a serum-free culture system (SFEB culture) combined with extrinsic factors including Noggin/ Dkk1/LeftyA/ IGF-1 which regulate BMP, Wnt or Nodal pathway signaling [7]. An efficiency of 80% was achieved for the generation of retinal progenitor cells, with a similar gene expression profile to human fetal retina. Ikeda *et al.* also generated lineage restricted mouse neural retinal precursor cells which expressed both Rx and

Pax6, but not Nestin, following sequentially treated ESCs with SFEB/Dkk1/LeftyA/serum/activin [10].

The second step, which involves generation of photoreceptors from derived retinal progenitors, has proven to be difficult unless the cells were cultured with embryonic retinal tissues [7,10,109]. More recently, Osakada et al. further identified stepwise defined conditions which promoted ESC derived retinal progenitor cell differentiation into mature photoreceptors and RPE cells [109]. Figure 1-12 shows the detailed factors and steps required. For generation of photoreceptors, a combination of retinoic acid and taurine was required for human cells. Notch signaling inhibition combined with FGF2, Shh, taurine and retinoic acid were needed for murine cells following retinal progenitor cell (Rx+ or Mitf+) derivation. These finding highlight the use of ESCs for the treatment of degenerative retinal diseases and for further application in clinical transplantation.

However, it should be noted that the function of these induced photoreceptor cells, their capacity to integrate into host retina and ability to form synaptic connections following transplantation remain to be investigated. To eliminate the risk of tumor formation from highly undifferentiated ESC resources, purification of post-mitotic specialized cells is essential, but remains challenging.

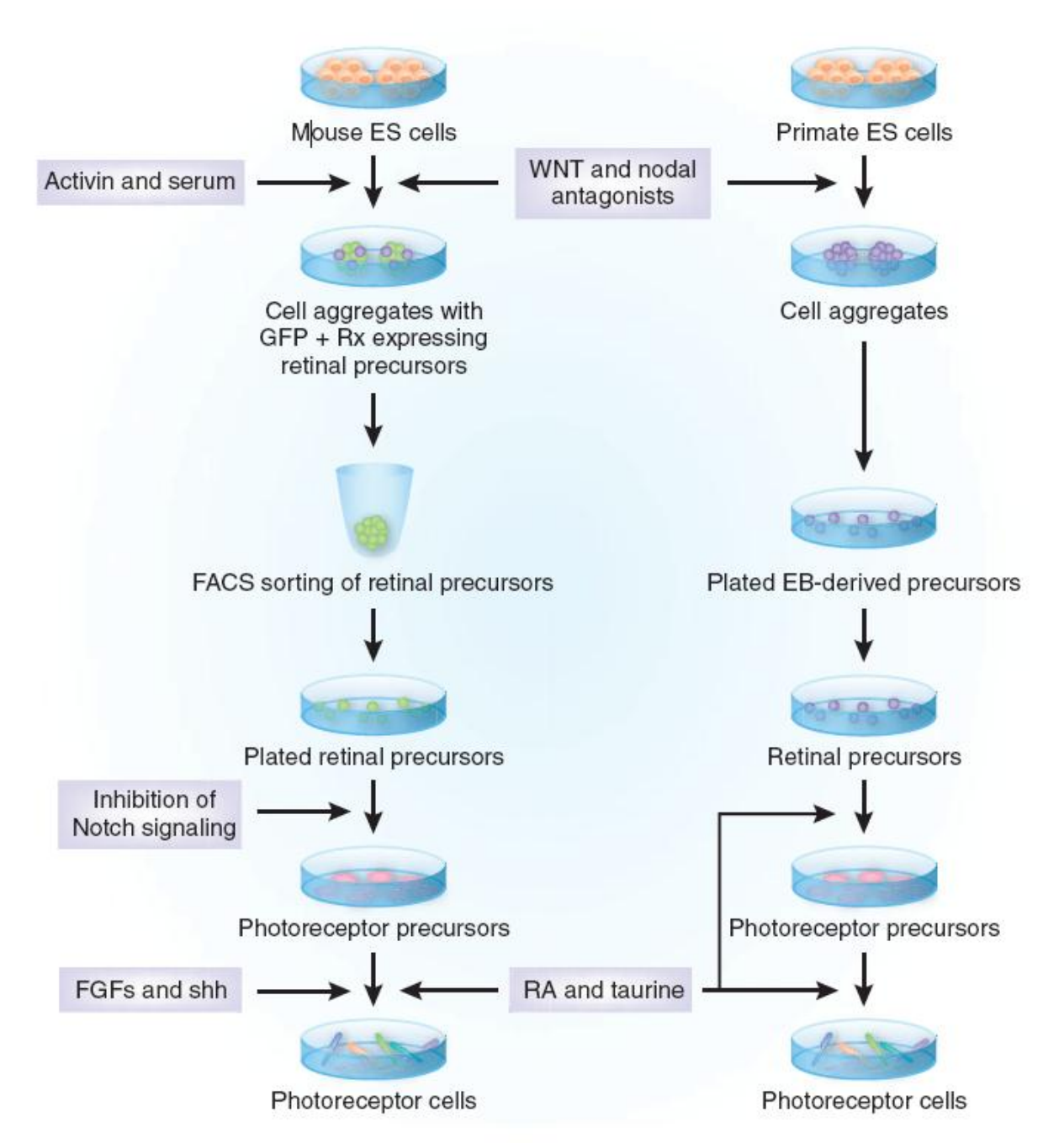


Figure 1-12 Multi-stepwise photoreceptor induction from mouse and primate ES cells This schematic diagram illustrates extrinsic factors and the stepwise induction for mouse and primate ES cells differentiation into photoreceptors *in vitro*. EB, embryoid body; FACS, fluorescence-activated cell sorting; GFP, green fluorescent protein; RA, retinoic acid; Rx, retinal homeobox; FGFs: fibroblast factors; Shh, sonic hedgehog; Wnt, Wnt Pathway; Nodal, nodal pathway (Klassen, 2008 [163], with permission from Nature Publishing Group.)

#### 1.9.3 Genetic transformation

Genetic modification of cells using transcription factors which are specific for photoreceptor generation have been investigated using adult stem / progenitor like cells derived from iris [13,60,86,88], CB [86,87] and hippocampus [13,86]. Development and maintenance of photoreceptors requires precise and comprehensive regulation of gene expression, which is mediated via a network of photoreceptor transcription factors. Crx and Otx-like homeodomain transcription factors play a central and essential role in this specification and maintenance [73]. Thereby, most gene transformations have used Crx, Otx2 and bHLH transcription factors.

### 1.9.3.1 Cone-rod homeobox (Crx)

Crx is one of the homeobox genes specifically expressed in photoreceptors. Evidence from loss-of-function studies and direct target studies (based on protein-DNA binding assays) support the hypothesis that Crx is the central transcription factor in the network for photoreceptor determination and regulation [73]. The effect of Crx induction on stem cells or progenitor cell derived from the iris, CB and adult hippocampus was investigated by several groups [13,87,88]. This research demonstrated the effectiveness of photoreceptor generation from iris and CB derived cells, but not from adult hippocampus neural stem cells following induction [13]. Photoreceptor specific markers and light stimulation tests indicate that reprogrammed cells not only have a photoreceptor specific antigen profile, but similar electrophysiological responses, however very limited integration to the host retina was detected [88]. Crx gene induction is sufficient to drive murine iris cells [13,88] and CB stem-like cells [87] to a photoreceptor phenotype *in vitro*; however additional induction with another transcription factor (NeuroD) was also required for human iris cells [88].

#### 1.9.3.2 Orthodenticle homeobox 2 (Otx2)

Although expression of Otx2 is not limited to photoreceptors, it is a homeobox gene which plays a key role in photoreceptor cell fate determination. In the Otx2 selective knockout mouse model, in which the Otx2 gene is inactivated under control of a Crx promoter, differentiating photoreceptor cells were converted to amacrine-like neurons [74]. Other evidence for the importance of Otx2 in photoreceptor cell determination includes the fact that over expression of Otx2 directs retinal progenitor cells towards photoreceptors [74,164]. Otx2 transfection can induce photoreceptor-specific phenotypes from rodent iris and CB derived cells in a similar manner to Crx. Ectopic expression of Otx2 was also effective in hippocampal stem cells, however only a small proportion  $(7.0\% \pm 4.76\%)$  of cells were found to be rhodopsin positive [86].

#### 1.9.3.3 NeuroD

Basic helix-loop-helix (bHLH) transcription factors including Mash1, Math3, Math5, Ngn2, and NeuroD are expressed in retinal precursor cells in the mammalian eye. They play an essential role in neuronal/glial cell fate determination as well as in the neuronal subtype [165]. However, the mechanism of bHLH gene specification for photoreceptor cells fate determination is poorly understood. NeuroD presents one of the central steps for two transcriptional pathways: ngn2-->neuroD-->raxL and ath5-->neuroD-->raxL in photoreceptor cell specification [166]. In certain vertebrates the retina has the ability to regenerate. NeuroD plays an important role in proliferation of photoreceptor progenitors [167]. In a Mash1/Ngn2/Math3 triple compound mutant mouse model where the NeuroD gene is active, photoreceptors generation is equivalent to wildtype, indicating that NeuroD is the most important bHLH factor for the survival of photoreceptors [165]. NeuroD alone can transform bird (chick) embryonic RPE cells to a photoreceptor phenotype with light responsive functionality [168]. In mammals however, NeuroD alone is not sufficient for acquisition of a photoreceptor phenotype. A combination of homeobox transcription factors such as Crx and/or Otx2 are also required [88].

#### 1.9.3.4 Combination of transcription factors

As described above combined photoreceptor transcription factor delivery can improve the effectiveness of reprogramming, especially in primates, more precise regulation of both temporal and spatial aspects is required. For example, Crx alone is sufficient for generation of photoreceptors from rodent iris cells, but not for human iris cells. Combination with NeuroD is required in this case. Inoue *et al.* [169] used combined transduction with Otx2 and Crx together with Chx10 in human CB derived cells and obtained robust output of photoreceptors. Although directing of heterologous stem cells towards a photoreceptor lineage has not yet been highly successful, a small proportion (7%) of adult neural stem cells do express photoreceptor specific antigens following induction with Otx2. Therefore, a combination of photoreceptor lineage transcription factors may be the most efficient method to maximize the induction effect.

# 1.10 Aims and Objectives

The overall aim of stem cell therapy for degenerative retinal diseases is to harvest sufficient retinal/photoreceptor progenitor cells from a practical and accessible source. The derived photoreceptor precursor cells could then be transplanted to repair and rescue the degenerating retina, leading to a subsequent improvement in visual function. The accessibility and persistent self-renewal capacity of limbal stem/progenitor cells are qualities which are ideal for autologous cell resources, to resolve the problem of shortage of cell resources. Additionally, using a patient's own cells will avoid any detrimental immune responses and improve graft survival long-term. The key challenge is the feasibility of directing stem /progenitor cells derived from adult limbus towards retinal like cells. Based on their plasticity and neuronal potential, it is hoped that limbal cells will be a practical new candidate resource for photoreceptor and/or RPE generation and subsequent transplantation.

Within the corneal limbus there are two populations of stem-like cells. These are putative epithelial stem cells [1,20,147] and multipotent stromal stem cells [30,90]. Neural potential has been reported in both populations of stem/progenitor cells in vitro [6] [30,90]. Dravida reported a cell population derived from the human limbal region, showing robust cell proliferation, with multilineage differentiation potential. The cells could also differentiate into neuronal cells in vitro [149]. However, these cells were cultured on Matrigel, a solubilised basement membrane derived from mouse sarcomas, which contains undefined xenogenic growth factors. The neurosphere assay (NSA), a well-defined suspension culture system, is more appropriate for the derivation of cells for clinical application. Several groups have reported generation of neural colonies (neurospheres) from cornea/ limbus by NSA [30,90]. Zhao et al. recently showed the potential of using adult rat LNS to generate photoreceptor-like cells. Under the influence of co-culture with neonatal retinal cells, rat LNS cells expressed photoreceptor specific markers [6]. However, a comprehensive characterization of LNS, including their self-renewal capacity, origin and ultrastructure, is still lacking. It remains unknown whether LNS from other species, particularly from humans and mice, can give rise to retinal like cells. In addition, the functionality of LNS derived photoreceptor-like cells is yet to be proven. Here, I investigate limbal cells from mice and humans to extend the knowledge of limbal cells to other species. Mice were chosen as there are a wide range of retinal degeneration models available, providing researchers with an opportunity to assess cell functionality in vivo in the future. Human limbal cells were also investigated here to provide an experimental basis for their potential clinical application.

Therefore, the purpose of this study can be divided into two main aims. The first is to generate neurospheres from the adult murine corneal limbus, and subsequently characterize them in respect of self-renewal, neural potential, ultrastructure and origin. This will enable us to define which cells are suitable for further transdifferentiation and generation of sufficient cells for transplantation studies.

The second aim is to determine whether adult limbal NS (LNS) cells have the potential to transdifferentiate along retinal lineages. In order to do this, various means will be investigated, including stimulation in an *in vitro* environment with developing retina (co-culture), defined culture conditions and finally genetic modification with transcription factors. For characterization of retinal lineage, transcription factors and photoreceptor specific proteins will be examined in differentiated cells. Through investigation of the response of differentiated cells to voltage stimulus and/or light induced signals, it is hoped that the functionality of derived photoreceptors will be determined. In addition, to assess the cell integration capability, LNS cells will be co-culture with developing retinal explants *in vitro*.

Furthermore, preliminary experiments will be conducted to determine whether human LNS can be derived from aged donor eyes or tissue from live patients. By further co-culture with developing retinal cells, we hope to explore whether human LNS's have the potential for differentiation towards retinal like cells.

# 2 Chapter Two- Materials and Methods

This section details the methods and techniques used for cell dissociation, culture, characterisation and functional assessment throughout this work. This chapter describes the standard techniques used in multiple experiments. Details of the specific conditions and protocols for each experiment can be found in the relevant subsequent chapters.

# 2.1 Limbal Cell Isolation and Culture

#### 2.1.1 Animals

Male C57BL/6 mice were maintained in the animal facility of the University of Southampton. Mice were housed individually in an air-conditioned room at  $21 \pm 2^{\circ}$ C with a lighting schedule of 12 hours (hrs) light (08:00-20:00) and 12hrs dark. Animals had free access to a standard rodent maintenance pellet diet and tap water. All animal studies were performed in accordance with the regulations set down by the UK Animals (Scientific Procedures) Act 1986. PN (PN) day 7-11 mice were used for initial optimization of limbal cell culture conditions. Subsequently adult mice (8 weeks old) were used for corneal limbal cell culture, characterization, and differentiation studies. PN day 1 mice were used for isolation of retina to provide a conditioned retinal development environment *in vitro*.

#### 2.1.2 Cell dissociation

Following cervical dislocation, eyes were immediately enucleated and kept in cold tissue culture medium comprising a 1:1 (vol/vol) mixture of Dulbecco's Modified Eagle's Medium with F12 media supplement (DMEM:F12) (Gibco-Invitrogen, Paisley, UK). Ophthalmological (toothed) forceps were used to hold the central cornea following puncture of the eyeball with a 30 Gauge needle (BD Plastipak, Oxford, UK). Approximately 1mm² of central cornea was removed using straight microsurgical scissors. A circular incision was made below the limbus, using curved microsurgical scissors, in order to isolate the corneal limbal region (Figure 2-1). Any pigmented tissue from the iris and ciliary body was carefully dissected away under microscopy. This dissection method ensured that the limbal tissue obtained was not contaminated with stem/ progenitor cells from the ciliary epithelium or peripheral retina. To ensure that cells isolated were not derived from the iris pigment epithelium, which can also be

expanded *in vitro*, the same tissue dissociation process and culture conditions were tested using adult mouse IPE cells.

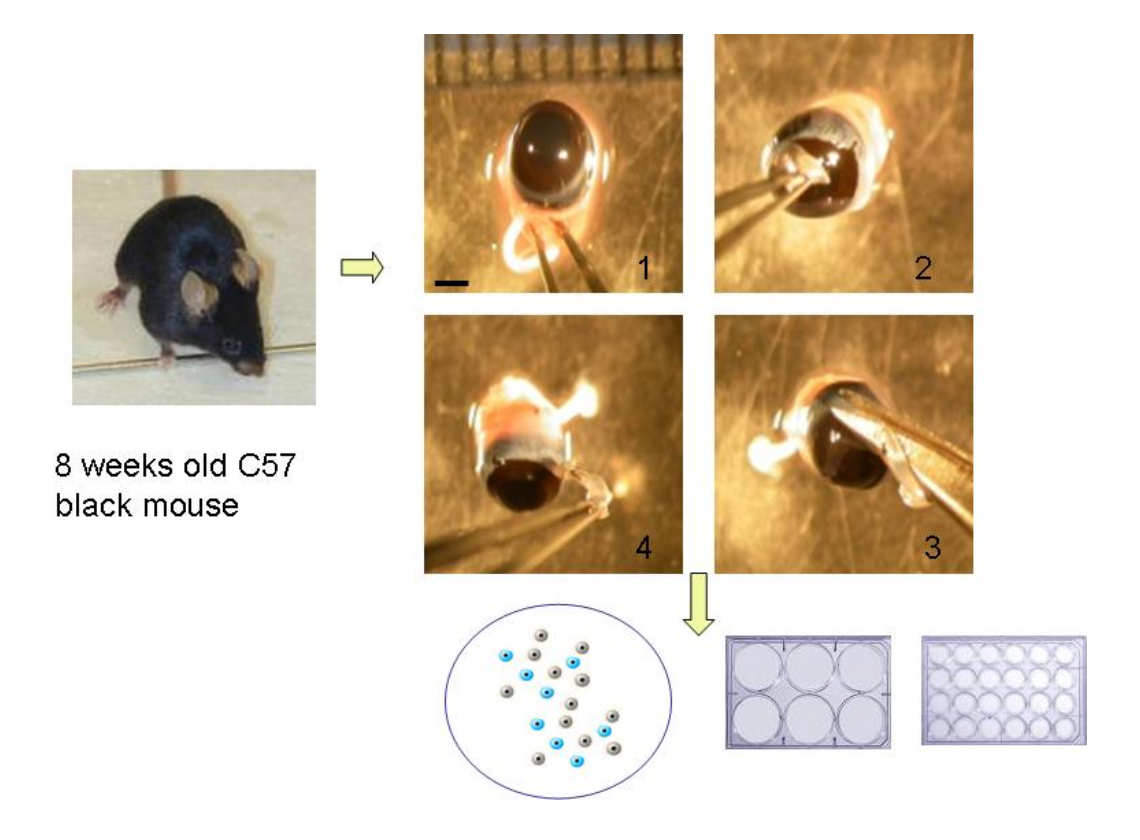


Figure 2-1 Corneal limbus dissection overview

Adult mice (8 weeks) were used in this study. Following enucleation of the eyes and removal of the central cornea, a circular incision was made below the limbus to isolate the corneal limbal region, as shown in step 1-4 under microscopy. Cells were then dissociated by enzymatic means and cultured. Scale bar: 1.0 mm

The dissociation process was carried out by a modified version of a previously described method [137,170]. The enzymatic digestion protocol was optimized according to preliminary results using PN11 mice. After washing with Ca²+, Mg²+ free Hanks Buffered Salt solutions (HBSS, Invitrogen), isolated limbal tissue was cut into small pieces and then incubated in 0.025% (w/v) trypsin/EDTA (Sigma-Aldrich, Ayrshire, UK) at 37°C for 10-12 minutes (min). To stop digestion, one volume of DMEM: F12 with 10% Fetal Bovine Serum (FBS, PAA, Somerset, UK) was added. Cells and tissues were then washed with HBSS. The secondary enzyme mixture was prepared by addition of 78 U/ml of collagenase (Sigma-Aldrich) and 38 U/ml of hyaluronidase (Sigma-Aldrich) to M2 medium (Sigma-Aldrich). Cells and tissues were incubated at 37°C for 30 min until most of the tissue had been digested. Cell strainers (70 nm, BD Falcon™) were used to remove undigested tissue; any remaining cell clumps were then triturated to a

single cell suspension using a 1 ml pipette. Following centrifugation at 100G for 5 min, cell pellets were re-suspended in a known volume of tissue culture media, either DMEM:F12GlutaMAX<sup>TM</sup> (Invitrogen) or Neurobasal<sup>TM</sup>- A (Invitrogen). For cell enumeration 50µl of cell suspension was mixed with an equal volume of 0.25% Trypan blue (Sigma-Aldrich) and counted using a Neubauer haemocytometer (Scientific Supplies Co., UK).

### 2.1.3 Culture condition optimization

Dissociated cells were plated at a density of 1×10<sup>4</sup> cells per ml and cultured at 37°C in a humidified atmosphere containing 5% CO<sub>2</sub>. A number of different culture medium recipes were investigated. Half of the tissue culture medium was replaced every 2-3 days. Fresh epidermal growth factor (EGF, Sigma-Aldrich) and basic fibroblast growth factor (FGF2, Sigma-Aldrich) were added every other day. The basal culture media and supplements used are listed below Table 2-1.

### 2.1.4 Culture medium optimization

DMEM:F12GlutaMAX<sup>™</sup> and Neurobasal<sup>™</sup>-A were chosen as basal culture mediums as the former is a classic base medium for various tissue specific SC culture techniques[6,158], and the latter is a defined and optimized neuronal/neuronal SC selective medium [6,170-172]. To find the optimal culture system for limbal stem/progenitor cell growth a number of different recipes of culture media were tested.

Neuronal Differentiation medium:

NB + B27 + 0.5mM L-Glut + 0-1% FBS + antibiotics

Serum Free medium:

Medium 1: DMEM:F12GlutaMAX<sup>™</sup> + N2 + EGF + FGF2 + antibiotics

Medium 2: DMEM:F12GlutaMAX<sup>™</sup> + B27- + EGF + FGF2 + antibiotics

Medium 3: DMEM:F12GlutaMAX<sup>™</sup> + B27 + EGF + FGF2 + antibiotics

Medium 4: Neurobasal™-A + N2 + EGF + FGF2 + antibiotics

Medium 5: Neurobasal™-A + B27- +L-Glut + EGF + FGF2 + antibiotics

Medium 6: Neurobasal™-A + B27 + L-Glut + EGF + FGF2 + antibiotics

Table 2-1 Basal culture medium supplements and growth factors

Abbreviation	Name	Company	Conc.
	DMEM:F12-GlutaMAX™	Invitrogen	
	Neurobasal™-A	Invitrogen	
N2	N2 Supplement	Invitrogen	1%
B27	B27 Supplement (standard)	Invitrogen	2%
B27-	B27 Supplement	Invitrogen	2%
	(minus Vitamin A)		
L-Glu	L-Glutamine	Sigma-Aldrich	0.5-2 mM
RA	Retinoic Acid		1 μΜ
Antibiotics	Antibiotic Antimycotic Solution	Sigma-Aldrich	1%
	(10,000 units penicillin, 10 mg		
	streptomycin, 25 µg amphotericin B		
	per ml)		
FBS	Fetal Bovine Serum	PAA	0-1%
EGF	Epidermal Growth Factor	Sigma-Aldrich	20 ng/ml
FGF2	Basic Fibroblast Growth factor	Sigma-Aldrich	20 ng/ml
Nog	Noggin	R&D systems	100 ng/ml
BDNF	Brain-Derived Neurotrophic Factor	R&D systems	1 ng/ml
Heparin		Sigma-Aldrich	5 μg/ml

## 2.1.5 Sphere generation efficiency

Single dissociated cells can clump together to form aggregates that resemble neurospheres. High cell density increases the likelihood of forming no-clonal spheres. Cell suspensions from dissociated adult mouse corneal limbus were plated in a 24-well culture plate (Nunc<sup>TM</sup> Brand, Denmark) at a density of  $1 \times 10^4$ /ml in culture medium recipes 1 to 4. At this low density, sphere generation is considered mainly due to cell clonal growth rather than cell aggregation [3,173]. After 7 days in culture, the numbers of spheres with a diameter of greater than 50µm were counted. Sphere generation efficiency was repeated four times with four replicates each time.

### 2.1.6 Effect of growth factors on sphere formation

Culture Medium 4 (DMEM:F12-GlutaMAX<sup>TM</sup> + B27- + EGF + FGF2) produced the optimal sphere generation efficiency and was therefore chosen for further study. In the presence of different extrinsic growth factors including EGF, FGF2, Noggin and their combination in DMEM +B27-, cell suspensions from dissociated adult mouse corneal limbus were plated into 24-well culture plates at a density of 1 x  $10^4$  /ml. The numbers of sphere with a diameter over  $50\mu m$  were counted for analysis. Experiments were repeated at least three times with 4 replicates each time.

#### 2.1.7 Secondary sphere formation

After 7 DIV primary spheres which were over 100µm in diameter were manually picked under a dissection microscope (Wild Heerbrugg, Micro instruments LTD, Oxford, UK). Spheres were then subjected to redissociation by enzymatic digestion with 200µl of Accutase\* solution (Sigma-Aldrich) at 37°C for 5 min, any remaining cell clumps were then triturated to a single cell suspension. Following centrifugation at 100x G for 5 min, the cell pellets obtained were resuspended in DMEM:F12-GlutaMAX™ or Neurobasal™-A. Cell suspensions were diluted in a known volume of tissue culture medium at an extremely low density of less than 100 cells per ml and plated in to 96 well plates (Nunc™ Brand, Denmark). Each well contained 5-10 cells in 100µl of medium. At this low density, the possibility of cell aggregation can be eliminated and spheres generation can be considered from single cells. The number of spheres formed was enumerated after 14 DIV to calculate secondary sphere formation efficiency.

For cell enumeration and passaging, primary spheres generated at DIV 7 were collected into 15ml sterile tubes. Following centrifugation at 100x G for 5 min, the cell pellets

obtained were resuspended into  $500\text{-}1000\mu\text{l}$  of Accutase® solution (Sigma-Aldrich), and incubated at  $37^{\circ}\text{C}$  for 5 min. By gentle trituration, spheres were dissociated into single cells. After centrifugation at 100x G for 5 min, the cell pellets were resuspended in a known volume of tissue culture medium. For cell enumeration  $50\mu\text{l}$  of cell suspension was mixed with an equal volume of 0.25% Trypan blue (Sigma-Aldrich) and counted using a Neubauer haemocytometer (Scientific Supplies). Cells were then plated at the same density ( $10^4$  or  $5\times10^4/\text{ml}$ ) as primary cultures for subculture.

# 2.1.8 Viability of sphere cells

Propidium iodide (PI, Sigma-Aldrich) staining was used to evaluate the viability of cells within the spheres. PI is generally excluded from viable cells; however it can penetrate the cell membrane of dying or dead cells [37]. PI buffer was prepared by adding 2µl of stock PI solution (1 mg/ml) (Sigma-Aldrich) to 2ml of sterile 0.1M Phosphate buffered saline pH7.4 (PBS, Sigma-Aldrich) to obtain the final concentration of 1µg/ml. NS were washed with PBS and then incubated in PI buffer for 15-20 min at 37°C; sphere viability was then analysed by fluorescence microscopy. Samples were imaged using a Leica DM IRB microscope (Leica Microsystems UK Ltd, Milton Keynes, UK). PI positive cell numbers were evaluated using Improvision Volocity software (Improvision, Coventry Lexington, UK).

# 2.2 Immunocytochemistry

Immunocytochemical labeling experiments were performed using intact limbal tissue, whole NS, NS derived monolayer cells and cells co-cultured with retinal tissue.

# 2.2.1 Mouse corneal limbus staining

Following cervical dislocation, eyes were immediately enucleated and washed with HBSS (Invitrogen). Whole eyeballs or dissected anterior eye portions which contained whole cornea, iris and ciliary body, were fixed in 4% paraformaldehyde (PFA, Sigma-Aldrich) for 2 hrs at 4°C. After which, tissues were washed 3 times with cold PBS, 5 min per wash. Tissues were then sequentially infiltrated with sucrose (Sigma-Aldrich) (10%, 20%) for 30 min at rt, followed by 30% sucrose overnight at 4°C. Whole eye balls/ anterior eye segments were then embedded in OCT embedding matrix (RA Lamb, Eastbourne, UK), prior to being sectioned at 10-20 μm thickness using a cryostat (OTF 5030, Bright Instrument Company, Cambridge, UK). Tissue sections were transferred on to Poly-L-Lysine (P-L-L) coated glass slides (Thermo Scientific, Loughborough, UK) and subsequently air dried at rt before immediate staining or storage at -80°C. To view the cell distribution, sections of corneal limbus and peripheral cornea were stained with 4'-6-diamidino-2-phenylindole (DAPI, Sigma-Aldrich). After being rinsed with PBS, sections were incubated with 10ng/ml DAPI in H<sub>2</sub>O for 6 min at rt in the absence of light. Slides were then washed with PBS twice, followed by a final wash with H<sub>2</sub>0. Images were captured and analyzed using a Leica DM IRB microscope (Leica Microsystems UK Ltd, Milton Keynes, UK).

### 2.2.2 Neurosphere and monolayer cell analysis

Neurospheres were either directly subject to immunocytochemistry or dissociated by enzymatic digestion and seeded onto Poly-D/L-Lysine (P-L-L or P-D-L, Sigma-Aldrich) and laminin (Sigma-Aldrich) coated plates, chamber slides or coverslips (see section 2.6.1) for 24 hrs prior to immunocytochemical analysis.

Cells were fixed with 4% PFA (pH 7.4) for 15-20 min at 4°C. After 3×5 min washes with PBS, PFA fixed cells were permeabilized and blocked with 0.1mM PBS supplemented with 0.1% Triton X-100 (Sigma-Aldrich) and 5% donkey block serum (Sigma-Aldrich) for 0.5-1 hrs at rt, prior to addition of primary antibodies. For ABCG2 (Abcam, Cambridge, UK) staining, cells were seeded on to coated glass chamber slides (VWR, Leicestershire, UK) for 24 hrs, and subsequently fixed with cold acetone for 10-15 min, and then blocked with PBS supplemented with 5% donkey blocking serum for 0.5-1 hr

at rt. The primary antibodies listed in Table 2-2 were diluted in blocking serum and incubate for either 2 hrs at rt or overnight at 4°C. Following gentle washing, specific IgG secondary antibodies, conjugated to an Alexa Fluor 488 or Alexa Fluor 555 (Invitrogen) at a concentration of 1:500 in PBS, were incubated at rt for 1-2 hrs. Negative controls omitted the primary antibody. Nuclei were counterstained with 10ng/ml DAPI. Images were captured by a CCD cameral under fluorescence microscope (Leica DM IRB), and analysed using Improvision Volocity software. For confocal imaging, nuclei were stained with Sytox Orange (1:20,000 Invitrogen). Samples were imaged using a Leica SP5 confocal laser scanning microscope (Leica Microsystems (UK) Ltd, Milton Keynes, UK).

Table 2-2 Primary antibodies used for immunocytochemical analysis.

Antibody	Species	Specificity	Company	Conc.
Nestin	Mouse (M) <sup>a</sup>	Neural stem cells	Chemicon	1:100
ABCG2 <sup>b</sup>	Rat (M)	Side population	Abcam	1:50
SOX2	Mouse (M)	Embryonic germ cells Neurogenesis stem cells	Millipore	1:100
SOX2	Donkey (M)	Embryonic germ cells Neurogenesis stem cells	Santa Cluz	1:250
Pax6	Rabbit (P) <sup>c</sup>	Eye field stem cells	Covance	1:100
beta-III tubulin	Rabbit (M)	Early differentiated neurons	Covance	1:500
beta-III tubulin	Mouse (M)	Early differentiated neurons	Covance	1:500
Opsin, Blue	Rabbit (P)	S-Cone	Abcam	1:200
PKC-alpha	Rabbit (P)	Bipolar cells	Abcam	1:250
GFAP	Rabbit (P)	Glia cells	DAKO	1:500
NF 200	Rabbit (P)	Neurons	Sigma-Aldrich	1:250
PCNA	Mouse (M)	Proliferating cells	Sigma-Aldrich	1:1000
P63	Mouse (M)	Epithelial stem cells	Millipore	1:100

<sup>&</sup>lt;sup>a</sup> Monoclonal antibody

 $<sup>^{\</sup>text{b}}$  Fixation in acetone for 10 min at -20  $^{\circ}$ C, air dry for 1 hr at rt , without permeabilization.

<sup>&</sup>lt;sup>c</sup> Polyclonal antibody

# 2.3 Flow Cytometry

Flow cytometry uses the principle of light scattering, fluorescent probe excitation and emission to generate specific multi-parameter data for individual cells that are suspended in a fluid stream flowing through the laser beam [172]. Cell profiles regarding the size, granularity and specific fluorochrome probe can be easily detected and quantified in real time. Side-scattered light (SSC) is proportional to cell granularity or internal complexity, which is collected at approximately 90 degrees to the laser beam. Another parameter forward-scattered light (FSC) reflects theo cell-surface area or size. This parameter is good for detection of size independent fluorescence, and so is often used in immunophenotyping.

Neurosphere cells were dissociated to single cells by enzymatic digestion. ABCG2 antibody staining for flow cytometric analysis was performed as per manufacturer's instructions (Abcam protocol). Briefly, 50,000 cells were fixed in 4% PFA at 4°C for 30 min, followed by permeabilization with 70% ethanol for 30 min at -20 °C and blocking with 10% normal mouse serum (Sigma-Aldrich) for 30 min at rt. Cells were subsequently washed with PBS and then incubated with ABCG2 antibody at rt for 30 min. Serial dilution of primary antibody (1:2, 1:5, 1:10 and 1:20 in blocking serum) was used to investigate the optimal assay concentration. Following incubation with an Alexa Fluor 488 conjugated anti-rat IgG secondary antibody (1:500, Invitrogen) at rt for 30 min, cells were washed with PBS and analyzed by FACSAria flow cytometry (Becton, Dickinson USA). Blue laser (488nm) was selected for fluorophore excitation and a 505nm for detection. Cells which had not been incubated with primary and secondary antibodies and cells in the presence of secondary antibody alone were used as negative controls.

# 2.4 Reverse Transcription- Polymerase Chain Reaction (RT-PCR)

#### 2.4.1 RNA extraction

Cell cultures were prepared for RNA extraction using an RNeasy Plus Micro Kit (Qiagen, West Sussex, UK) as shown in Figure 2-2. Cells grown in suspension or as monolayer cultures were dissociated by enzymatic digestion to single cells and the cell number determined.

Less than 5 x 10<sup>5</sup> cells were used for each RNA extraction. After centrifugation for 5 min at 300 x G, all of the supernatant was carefully aspirated. Samples were then stored at -80°C until required or subjected to further steps immediately. Further stages of RNA extraction and processing were performed in a specifically designated desktop RNA hood (PCR work station, Bigneat, Farmborough, UK) within the Gift of Sight research laboratory. The RNA work bench was irradiated by UV light for 10 min prior to use and subsequently cleaned with 'RNAseAWAY' (Invitrogen) in order to prevent RNA degradation and DNA contamination. To prevent contamination from pipettes filtered tips (Fisher Scientific) were used for all experiments.

Fresh or thawed cell pellets were flicked to loosen and resuspended in 350µl RLT Buffer Plus was added. After vortexing and pipetting for 1 min to allow for complete cell lysis, homogenized lysates were transferred to gDNA Eliminator spin columns and placed in 2 ml collection tubes. This allowed genomic DNA from the lysate to bind to the spin column, thereby eliminating genomic DNA contamination. After centrifugation for 30 sec at ≥10,000 rpm, the flow through which contained RNA was collected and mixed with 70% ethanol by pipetting. Samples were then transferred to RNeasy MinElute spin columns and placed in 2 ml collection tubes. These columns contain a specially designed membrane which binds RNA. The columns together with collection tubes were subjected to centrifugation for 15sec at ≥10,000 rpm. The flow-through was then discarded. Further RNA clean up steps were carried out by addition of 700µl Buffer RW1, 500µl Buffer RPE and 500µl of 80% ethanol with associated centrifugation steps between. Centrifugation at ≥10,000 rpm for 2 min was carried out following addition of 80% ethanol. The MinElute spin columns were then placed into new collection tubes and centrifuged for a further 5 min with the lids opened to allow complete evaporation of the ethanol. Columns were then placed into clean 1.5 ml tubes, 14µl of RNase-free water was then pipetted directly into the centre of each spin

column membrane, and columns were then centrifuged for 1 min at full speed to elute the RNA.

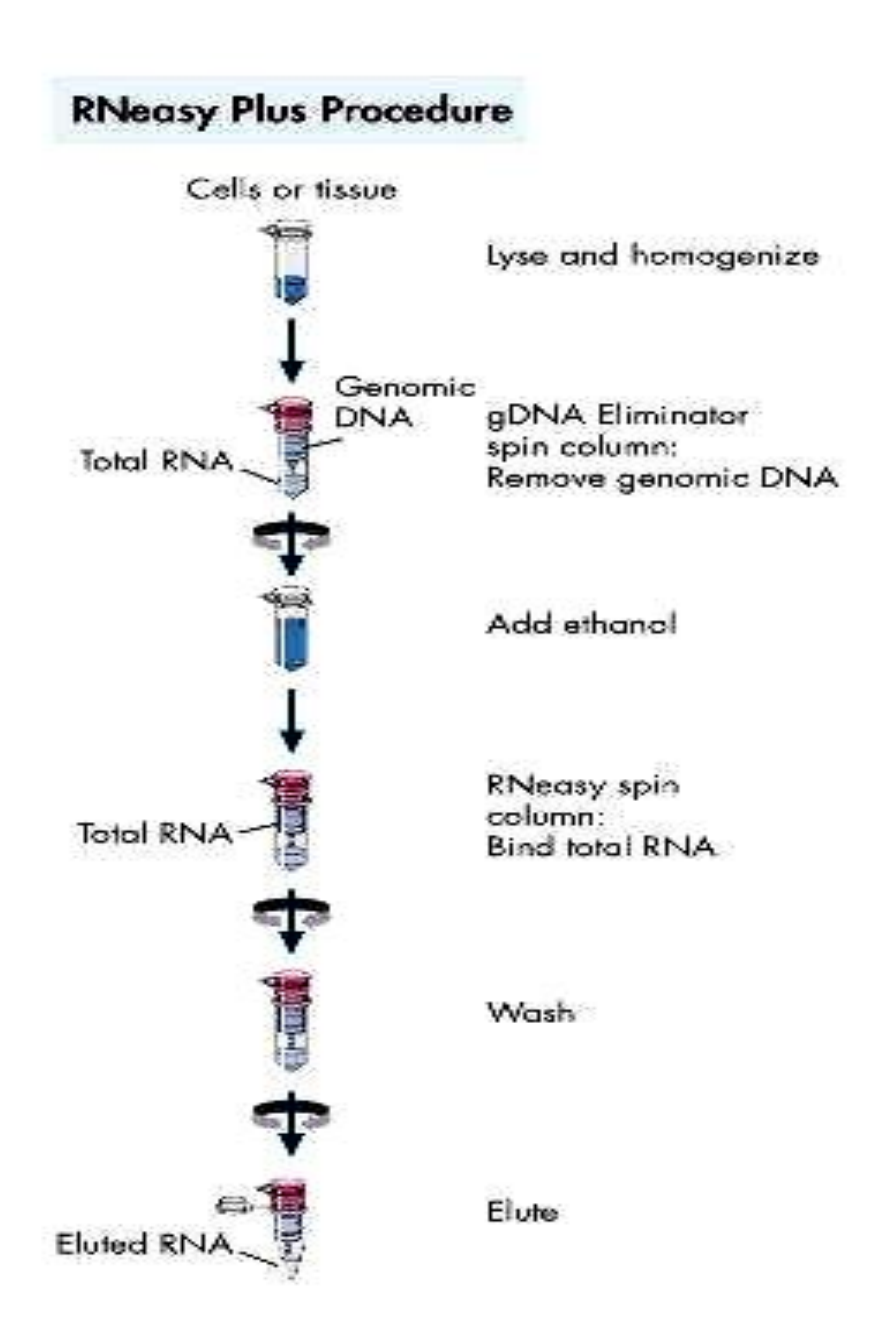


Figure 2-2 RNA extraction procedure using an RNeasy Plus Micro Kit (Qiagen)

# 2.4.2 DNase treatment

The gDNA Eliminator spin columns contained within the RNeasy Plus Micro Kits were used to remove most of the genomic DNA. However to ensure there was no trace contamination by genomic DNA, samples were subjected to DNase treatment using

DNA-free<sup>TM</sup> (AM1906, Ambion, UK). 10µl of RNA was mixed with 10µl of DNAse digestion reagents which contained 2µl 10x DNase I buffer (100mM Tris-HCl pH 7.5, 25mM MgCl<sub>2</sub>, 5mM CaCl<sub>2</sub>) and 1µl ml of recombinant DNase I (2 Units/µl) and 8µl of H<sub>3</sub>O.

The samples were incubated at  $37^{\circ}\text{C}$  for 60 min, after which the DNase was inactivated by addition of  $5\mu\text{I}$  ml of DNase Inactivation Reagent. Samples were then incubated for a further 2 min at rt with occasional mixing, following which samples were spun at 12,000rpm for 2 min at  $4^{\circ}\text{C}$ . The RNA was kept on ice and used immediately for quantification and subsequent reverse transcription.

# 2.4.3 Quality assessment and quantitation of RNA

RNA quantity was measured by spectrophotometry using a Nanodrop ND 1000 (Nanodrop Technologies, Wilmington, DE, USA). Briefly,  $1.2\mu l$  of sample was placed on to the pedestal of the machine, which forms a column by surface tension when the apparatus is closed. Absorbance was measured at 260nm and 280nm by a 10mm light path equivalent. When compared to the blank, the concentration of RNA was determined (Pure RNA: A260/A280 ratio: 1.8 to 2.1). Samples with A260/A280 ratio of approximately 2.0 were considered good quality.

### 2.4.4 cDNA synthesis

Following quantitation of RNA, cDNA synthesis was performed using a High-Capacity cDNA Reverse Transcription kit (Applied Biosystems, Warrington, UK). The reverse transcription (RT) master mix was prepared on ice, the mix contained 2µl 10×RT buffer, 0.8µl of 25×d NTP mix, 2.0µl of RT random primers, 1µl of multiScribe ™ reverse transcriptase and 3.2µl of nuclease-free H₂O for each sample. After gentle mixing, the RT final reaction mix was made by pipetting 10µl of prepared master mix and 10µl of RNA sample (100-500ng) into a 200µl thin wall tube. For future quantitative PCR (qPCR), RNA samples were normalised to 100ng in each reaction to ensure the equivalent reverse transcription efficiency. For non-qPCR, variation of DNA quantity was allowed. Following brief centrifugation of the reaction tube to spin down the contents and eliminate any air bubbles, samples were incubated on a thermocycler at 25°C for 10 min, then subsequently at 37°C for 120 min, finally samples were incubated at 85°C for 5 min. Samples were then routinely diluted 1:20 with RNA/DNase free water and stored at -20°C or 4°C prior to use. Negative controls were performed by replacement of transcriptase in the reaction mix with H₃O.

# 2.4.5 Primer design and specificity checking

Mouse specific primers were chosen from published literature or designed using webbased software Primer 3, which is provided by the Whitehead/ MIT centre for genome research (http://frodo.wi.mit.edu/primer3/). Mouse specific cDNA sequences were obtained from the online database of the National Centre for Biotechnology Information (ncbi.nlm.nih.gov). Following importation of the target cDNA sequence, several candidate primers pairs were chosen, and subjected to further specificity checking using In-Silico PCR. This is a virtual PCR tool provided by UCSC Bioinformatics (http://genome.ucsc.edu) to help eliminate the possibility of unspecific amplification due to similar fragments between different genes. The primer pairs which produced single sequences were chosen for RT-PCR. Primers which spanned exon-exon junction were preferentially chosen as any amplification products detected could only be from cDNA, thereby eliminating the effects of possible traces of genomic DNA. All primers were checked for specificity and location, and purchased from Invitrogen Custom Primers at desalted purity (25nm: 10-100, 50nm+: 5-100) with 25-50 nmole scale (https://www.invitrogen.com). The primers sequences and PCR amplicon sizes are shown Table 2-3.

Table 2-3 Primer sequences used for phenotypic analysis and expected product sizes

Primers Name	Sequence	Amplicon Size (bp) <sup>a</sup>
Mouse_ABCG2_F	GCCTTGGAGTACTTTGCATCA	62
Mouse_ABCG2_R	AAATCCGCAGGGTTGTTGTA	
Mouse_Nestin_F	AACTGGCACACCTCAAGATGT	235
Mouse_Nestin_R	TCAAGGGTATTAGGCAAGGGG	
Mouse_Musashil_F	GGCTTCGTCACTTTCATGGACC	542
Mouse_Musashil_R	GGGAACTGGTAGGTGTAACCAG	
Mouse_Sox2_F*	ATGGGCTCTGTGGTCAAGTC	300
Mouse_Sox2_R*	CCCTCCCAATTCCCTTGTAT	
Mouse_ beta-III tubulin _F	TGAGGCCTCCTCTCACAAGT	207
Mouse_ beta-III tubulin _R	CGCACGACATCTAGGACTGA	
Mouse_Oct4_F	CCAATCAGCTTGGGCTAGAG	129
Mouse_Oct4_R	CTGGGAAAGGTGTCCCTGTA	
Mouse_Pax6_F	AACAACCTGCCTATGCAACC	206
Mouse_Pax6_R	ACTTGGACGGGAACTGACAC	
Mouse_P63_F	GTCAGCCACCTGGACGTATT	321
Mouse_P63_R	ACCTGTGGTGGCTCATAAGG	
Mouse_K12_F*	CTGTGGAGGCCTCTTTTCTG	153

Mouse_K12_R*	CCAGCTATCCCCATCCCTAT	
Mouse_Slug_F	CACACACACACACACACACACAC	596
Mouse_Slug_R	TGTCTTTCCCTCCTCTTCCAAGG	
Mouse_Twist_Fb*	CCAGAGAAGGAGAAAATGGACAGTC	259
Mouse_Twist_Rb*	AAAAAGTGGGGTGGGGGACACAAA	
Mouse_CD34_Fb*	CCTTATTACACGGAGAATGGTGGAG	477
Mouse_CD34_Rb*	AAGAGGCGAGAGAGAAATGGG	
Mouse_CD45_F <sup>b</sup>	CCTGCTCCTCAAACTTCGAC	194
Mouse_CD45_R <sup>b</sup>	GACACCTCTGTCGCCTTAGC	
Mouse_CD133_Fb	GAAAAGTTGCTCTGCGAACC	195
Mouse_CD133_R <sup>b</sup>	TCTCAAGCTGAAAAGCAGCA	
Mouse_Vimentin_F <sup>b</sup>	ATGCTTCTCTGGCACGTCTT	206
Mouse_Vimentin_R <sup>b</sup>	AGCCACGCTTTCATACTGCT	
Mouse_Sca1_Fb*	ACCTCCACCCTTGTCCTTTT	250
Mouse_Sca1_Rb*	CTTCACTGTGCTGGCTGTGT	
Mouse_Snail_Fb*	CCCACTCGGATGTGAAGAGATACC	534
Mouse_Snail_R <sup>b*</sup>	ATGTGTCCAGTAACCACCCTGCTG	
Mouse_Sox9_Fb*	CGCCCATCACCCGCTCGCAATACG	545
Mouse_Sox9_R⁵*	AAGCCCCTCCTCGCTGATACTGG	
Mouse_Recoverin_F	GATCTGGGCATTCTTTGGAA	341
Mouse_Recoverin_R	GATGGGGAGGACACTGAAGA	
Mouse_GADPH_F	GGGTGTGAACCACGAGAAAT	323
Mouse_GADPH_R	ACACATTGGGGGTAGGAACA	
Mouse_β-Actin_F	TGTTACCAACTGGGACGACA	392
Mouse_β-Actin_R	TCTCAGCTGTGGTGGAAG	
Mouse_CHX10_F*	CAATGCTGTGGCTTGCTTTA	382
Mouse_CHX10_R*	AACCAATGGGCTACAACAGC	
Mouse_NeuroD_F*	CAAAGCCACGGATCAATCTT	168
Mouse_NeuroD_R*	CCCGGGAATAGTGAAACTGA	
Mouse_CRX_F	CCCATACTCAAGTGCCCCTA	122
Mouse_CRX_R	CCTCACGTGCATACACATCC	
Mouse_CRLBP_F	CGGGACAAGTATGGTCGAGT	129
Mouse_CRLBP_R	GGTTTCCTCATTTTCCAGCA	
Mouse_RPE65_F	CGGACTTGGGTTGAATCACT	282
Mouse_RPE65_R	AGTCCATGGAAGGTCACAGG	

<sup>&</sup>lt;sup>a</sup> Base Pairs

<sup>&</sup>lt;sup>b</sup> From Brandl et al [182]

<sup>\*</sup> Non-intron-spanning primers

# 2.4.6 Polymerase chain reaction (PCR)

PCRs were performed using synthesized cDNA as a template followed by a standard PCR protocol (Invitrogen). Each reaction mix contained  $1\mu l$  of cDNA per sample,  $1\mu l$  of 10X buffer, mixed nucleotides (dATP, dCTP, dGTP, dTTP), forward and reverse gene specific primers,  $MgCl_2$ ,  $0.4\mu l$  of Taq DNA polymerase (Invitrogen) and made up to a final volume of  $10\mu l$ . The steps of the PCR cycles carried out are shown in Figure 2-3.

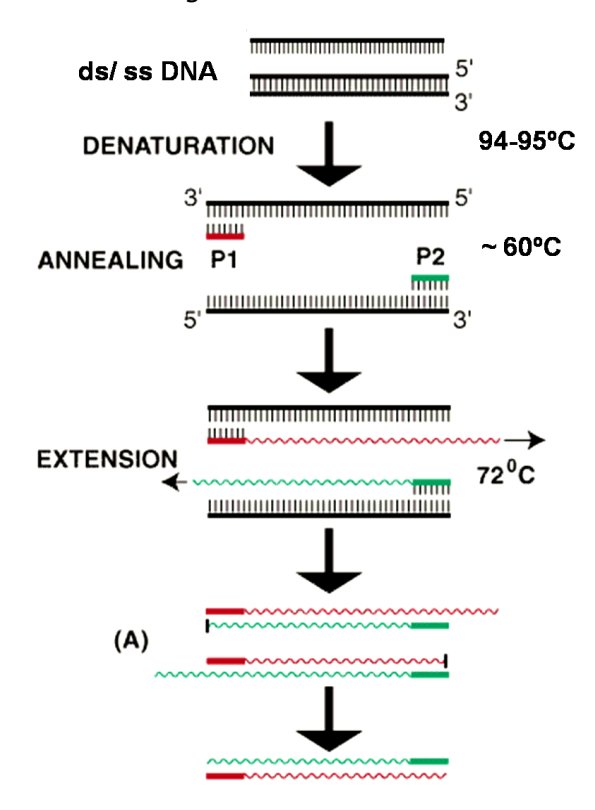


Figure 2-3 DNA amplification by PCR

Schematic diagram illustrates the DNA amplification by PCR. Cycles contain denature, annealing and extension. P1: Forward primer; P2, reverse primer. (Adopted from http://www.flmnh.ufl.edu/cowries/amplify.html)

- 1) Denaturing for 30 sec at 94°C. This produced single strands of DNA by disrupting the hydrogen bonds between complementary bases of double stranded DNA.
- 2) Annealing for 30 sec at primer-specific annealing temperature. During this process, stable DNA-DNA hydrogen bonds were formed between gene specific primers and templates. The DNA polymerase then bonded primer-template hybrid for further synthesis.

3) Extension for 30 sec at 72°C for 30 cycles. By adding dNTPs which were complementary to the template in 5' to 3' direction, the DNA polymerase synthesized a new DNA strand complementary to the DNA template strand.

All PCRs were performed at 30 repeated cycles, with each step doubling the amount of DNA and causing exponential amplification of the specific DNA fragments. Final extension was carried after 30 cycles at 72°C for 2 min to ensure any remaining single-stranded DNA was fully extended.

# 2.4.7 Detection of PCR products by electrophoresis

Agarose gels (1.5%) were used to check for the presence of DNA fragments. In brief, 7.5g of Agarose powder (Fisher Scientific) was mixed with 500ml of  $1 \times TBE$  buffer (Fisher-Scientific) and melted by heating in a microwave oven. After cooling the solution to approximately  $60^{\circ}C$ , it was poured into a casting tray containing sample combs and allowed to solidify at rt. After the gels were set, the sealers at the end of tray and the combs were removed carefully. The whole tray with the solidified gel was then placed horizontally into an electrophoresis tank (Scie-Plas, Cambridge, UK) and submerged in 2 L of  $1 \times TBE$  buffer containing  $30\mu$ l of ethidium bromide (Sigma Aldrich) for at least 2 hrs in the dark. Ethidium bromide is a fluorescent dye which incorporates into the agarose gel readily. It intercalates between bases of DNA, thereby allowing DNA to visualized following electrophoresis.

For electrophoresis, PCR products were mixed with loading buffer containing bromophenol blue (Sigma Aldrich), and xylene cyanol dyes (Sigma Aldrich), and then loaded into the sample wells of the agarose gels. A 1000 base pair (bp) DNA ladder (Axtgene, Biosciences, Cambridge, UK) was used as the molecular weight control. Electrophoresis apparatus (Bio-rad Power Pac, Hemel Hempstead, UK) was run at 180 volts for 50-60 min. To visualize DNA, gels were placed on an ultraviolet transilluminator (UVP High Performance, Cambridge, UK). Photos were captured by a CCD camera, using Doc-It®LS Image software (UVP High Performance, Cambridge, UK).

# 2.5 Transmission Electron Microscopy (TEM)

TEM is a microscopy technique involving a beam of electrons transmitting and interacting with an ultra-thin specimen to produce a higher resolution imagine. Spheres (DIV 10) derived from adult mouse corneal limbus and their culture medium were transferred into a 15 ml tube and left at 37°C for 10-15min to allow spheres to settle to the bottom of the tube and form a loose cell pellet. Culture medium was aspirated carefully. Spheres were fixed in 100 µl of primary fixative containing 0.1 M sodium cacodylate buffer, 3% glutaraldehyde, 4% PFA and 0.1 M PIPES buffer, pH 7.4 for 15 min at rt. Following fixation, spheres settled to the bottom of the tube and no further centrifugation was required during the subsequent TEM processing. Further processing was performed in the Biomedical Image Unit, University of Southampton. In brief, following initial fixation specimens were rinsed in 0.1M PIPES buffer, post-fixed in 1% buffered osmium tetroxide (1 hr), rinsed in PIPES buffer, block stained in 2% aqueous uranyl acetate (20 min), followed by dehydration in a graded series of ethanols up to 100% and embedded in TAAB resin (TAAB Laboratories, Aldermaston, UK). Gold sections were cut on a Leica OMU 3 ultramicrotome (Leica UK) Ltd, Milton Keynes, Bucks, UK), stained with Reynolds lead stain and viewed on a Hitachi H7000 transmission electron microscope equipped with a SIS megaview III digital camera (Hitachi High-Technologies Corporation, Maidenhead, Berkshire, UK).

# 2.6 Retinal cell co-culture assay

# 2.6.1 Plate coating

Plates were coated with P-D-L and laminin for monolayer culture. To reconstitute P-D-L, 100 ml of sterile tissue culture grade  $H_2O$  were added to 5 mg P-D-L (Sigma-Aldrich) to obtain a final concentration of  $50\mu g/ml$ . Laminin (Sigma-Aldrich) was diluted with sterile PBS to a final concentration of  $10\mu g/ml$ . For plate coating, sufficient P-D-L solution was added to cover the surface of culture area and incubated at  $37^{\circ}C$  incubator for 2 hrs. Following rinsing with sterile  $H_2O$  for 5 min  $\times$  3 times, plates were dried at rt. An equal volume of laminin solution was then added to the culture area and incubated at  $37^{\circ}C$  overnight. Plates were ready for use following 3 washes with sterile  $H_3O$ .

# 2.6.2 Preparation PN1 retinal cells

Whole mouse retinas were dissected from 4 PN1 mice. To dissect retinal tissues. eyeballs were enucleated immediately following sacrifice. The sclera was punctured along the ora serrata using a 30G needle (BD Plastipak), and the anterior portion of the eye was removed using microsurgical scissors. The retina was then detached from the optic nerve following removal of the lens. A drop of DMEM:F12 medium was used to assist removal of the retina from the eye cup. Retinas were then collected with a 100 μl pipette. Enzymatic digestion, using a commercially available papain dissociation kit (Worthington-Biochemical, Berkshire, UK), was used for retinal cell dissociation as per manufacturer's instructions. In brief, minced retinal tissue was incubated with a mixture of papain (20 units/ml) and DNase (0.005%) for approximately 40 min at 37°C. After gentle trituration, an equal volume of papain inhibitor containing 10% ovomucoid and 0.005% DNase in Earle's balanced saline solution was added. Cell suspensions were then filtered using 100µm cell strainers (BD Falcon) to eliminate large cell clumps. Following centrifugation at 150G for 5 min, cell pellets were resuspended and gently triturated in inhibitor solution. After a second centrifugation at 150G for 5 min, cell pellets were resuspended into 3ml of neural differentiation medium for co-culture.

#### 2.6.3 Co-culture with PN1 retinal cells

To promote cell differentiation towards photoreceptors, sphere cells derived from adult corneal limbus were co-cultured with dissociated PN1 mouse retinal cells [174]. Retinal cells were cultured on Millicel CM inserts (pore size, 0.4 µm; Millipore UK Ltd, Watford, Hertfordshire, UK) for 1 to 2 weeks in differentiation medium (NB, 2% B27, 0.5mM L-Glut, 0.5-1% FBS, 1µM retinoic acid (RA, Sigma-Aldrich) and 1ng/ml brain-derived neurotrophic factor (BDNF, R&D system). Spheres generated from adult mouse corneal limbus were collected and transferred into a sterile 15 ml tube (Corning Lifesciences, London, UK). Following centrifugation at 1000rpm for 5 min, the supernatant was removed and spheres were resuspended in neural differentiation medium and plated onto P-D-L and laminin coated wells. Millicell inserts were then carefully placed into wells containing sphere cells. The retinal cell suspensions from four PN1 mice were divided into three equal portions and carefully transferred onto Millicell inserts as demonstrated in Figure 2-4. Half of the differentiation medium was changed every other day. To test whether cell contamination occurred in the co-culture system, PN1 retinal cells were cultured on Millicell inserts in identical condition, but with the omission of LNS in the bottom of wells. No cells were detected to have crossed the Millicell inserts during 2 weeks of culture. This confirms that the Millicell insert membranes used in this study can prevent retinal cell contamination.

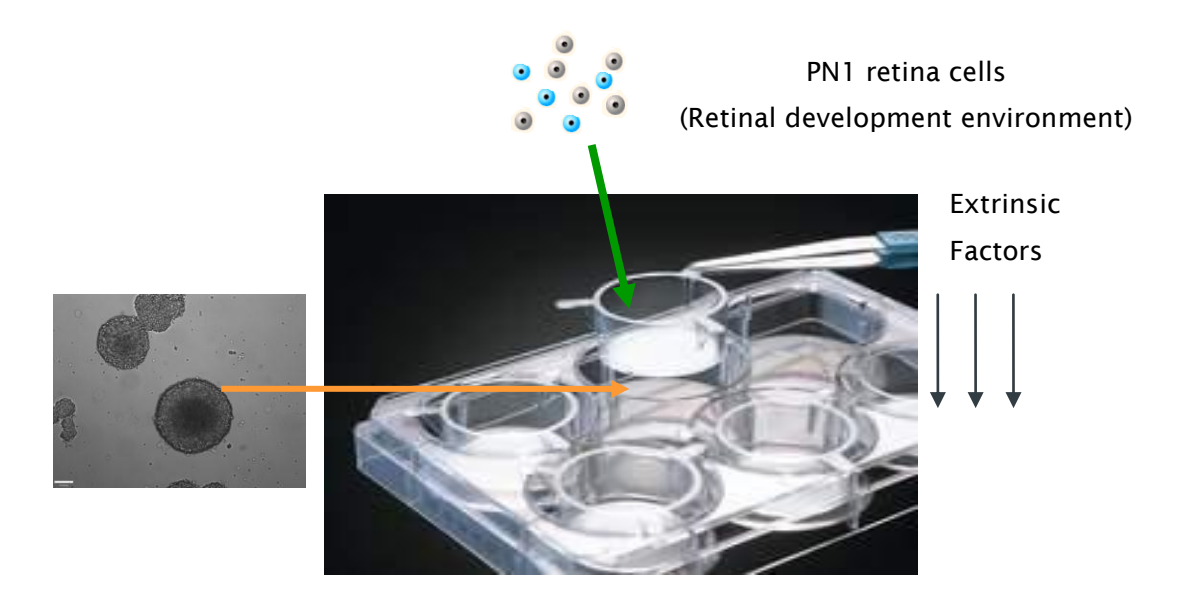


Figure 2-4 Limbal neurospheres co-cultured with PN1 retinal cells

After 7-14 DIV co-cultured, limbal cells were collected for RT-PCR analysis or fixed with

4% PFA for immunocytochemical analysis. Control cells were plated in identical
conditions with the omission of retinal cells.

# 2.7 Calcium influx imaging for functional assessment

# 2.7.1 Calcium indicator: Fluo-4 AM

Fluo-4 calcium Indicator (Invitrogen) was used for calcium influx imaging in this study. It is in the form of a non-fluorescent format, Fluo-4 acetoxymethyl ester (AM). However, when fluo-4 AM is cleaved inside the cell, it produces free fluorescent Fluo-4. The latter can be readily excited by a 488 nm Argon-ion laser, and exhibits a strong fluorescence intensity which increases upon binding to Ca<sup>2+</sup>. Unlike other ultra-violet light excited indicators, there is no accompanying spectral shift with Fluo-4. The chemical structure of fluo-4 (C51H50F2N2O23) and its excitation and emission spectrum are depicted below (Figure 2-5)

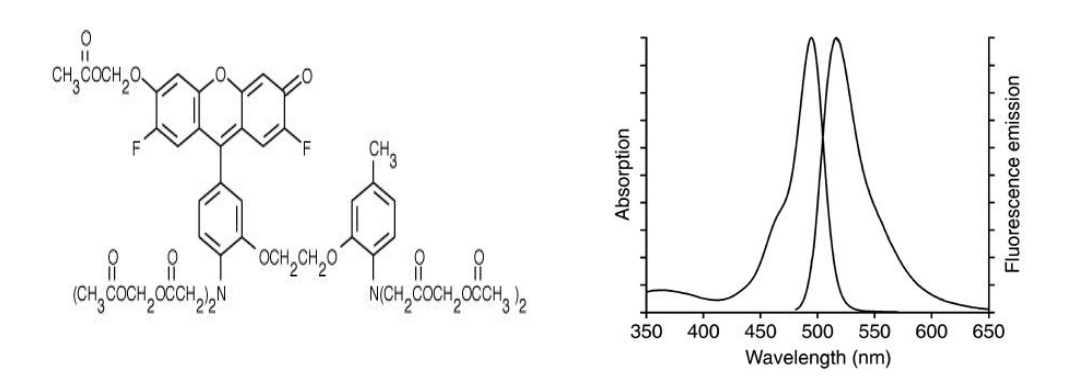


Figure 2-5 Character of calcium indicator Fluo-4. Images show the molecular form (left) and excitation and emission spectra (right) of Fluo-4. (http://products.invitrogen.com/ivgn/product/F14201)

# 2.7.2 Cell preparation

Following differentiation for 7-14 days in P-D-L and Laminin coated 6 well plates or petri dishes in the presence or absence of co-culture conditions, adult mouse limbus derived cells were subjected to functionality assessment using calcium influx imaging. Neonatal mouse retinal cells were used as a positive control. The dissociated mouse retinal cells were cultured as a monolayer for 2-4 days in differentiation medium.

# 2.7.3 Calcium indicator loading

The calcium indicator Fluo-4 AM (Invitrogen, Paisley, UK) was loaded as previously described [6]. Fluo-4 AM was freshly reconstituted in Dimethyl sulfoxide (DMSO, Sigma-

Aldrich) and vortex thoroughly before each experiment. Pluronic® F-127 (Invitrogen, Paisley, UK), a facilitator for cell loading was reconstructed in DMSO at a concentration of 20% (w/v). Working loading solution consisted of 4µM fluo-4 AM and 0.1% Pluronic® F-127 in Hanks' Balanced Salt Solution (HBSS, with Ca²+ Mg²+, without phenol red, Invitrogen, Paisley, UK) with 5mM HEPES (Invitrogen, Paisley, UK). Working loading solution composition:

Fluo-4AM	50	μg
DMSO	22	μl
Pluronic® F-127 (20%)	9	μl
HBSS	10	ml
1 M HEPES	50	μl

Following removal of culture media from each well, cells were washed with HBSS (37°C) twice for 3 min. 1ml of working loading solution was then applied per well of a 6 well plate, or 250  $\mu$ l if coverslips were used. The cells were then incubated in the dark at 37°C for 30-45min. Prior to imaging, excess dye was removed by washing and equilibrated in HBSS to allow the AM to be cleaved by cytoplasmic esterase. Plates or petri dish were maintained at rt in the dark for approximate 10 min prior to data acquisition.

### 2.7.4 Data Acquisition

An inverted Leica fluorescence microscope was utilized for visualisation and imaging of the fluo-4 AM loaded cells. Images were captured using Volocity software. Cells were checked under the microscope, and most cells displayed a typical neuronal morphology with dendritic and axonal processes. A random region of cells was chosen for imaging. Cells were excited with 488 nm light source and collected at 520nm emission. Images were acquired every 10-30 sec, with 500ms acquisition times by a cooled camera and analysed using Volocity software. Intracellular calcium concentration was presented as fluorescence intensity (raw pixel intensities). Five random background areas were chosen to obtain the average background florescence intensity. Mean background intensity was subtracted from each cellular region to minimise the noise and vibration due to staining or fluorescence fading (F = cellular average-background average). All cells were then normalized by their initial intensity respectively F/F0, then plotted against time [175].

#### 2.7.5 Cell excitation

KCl excitation buffer was prepared as follows using HBSS and Hepes buffered saline solution.

KCl	0.745 g
HBSS	10 ml
HEPES (1 M)	50 μl

After being vortexed thoroughly, the KCl solution was sterilised through a  $0.22\mu m$  filter prior to use. For a typical calcium influx imaging experiment, images were acquired every 30 sec for 5 min without any stimulation. Stimulation and control were applied under microscopy without moving the imaging plate. KCl solution ( $120\mu l$ , 1M) was added into each well containing 1ml HBSS-HEPES; and a final concentration of 100mM KCl stimulation was achieved. Imaging continued for approximately 30 min. Equivalent volume of HBSS-HEPES ( $120\mu l$ ) was added to non-stimulation control conditions. Cells cultured in different conditions were used, including: 1) Co-cultured adult limbal cells (test cells); 2) Non co-cultured adult limbal cells (control cells); 3) P1 mouse retinal cells (positive control cells)

# 2.7.6 Cell viability assessment after calcium influx imaging

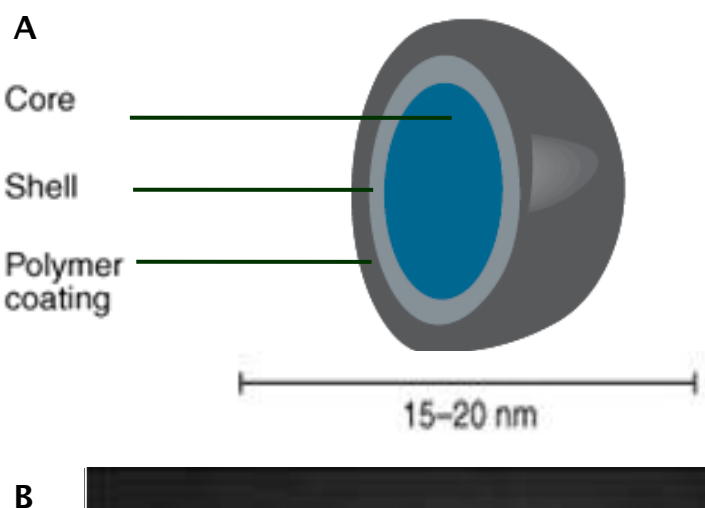
A Trypan blue exclusion assay was used to determine the cell viability following calcium influx imaging [168,175]. It is based on the principle that live cells possess an intact cell membrane which Trypan blue cannot penetrate, whereas dead cells do not. 0.5ml of Trypan blue PBS solution (0.4 %, Sigma Aldrich) was added into each well following washing the cells with HBSS-Hepes twice for 5 min. Viable cells showed a clear cytoplasm when viewed under an inverted light microscope, whereas the cytoplasm of non-viable cells was stained blue. The imaging area and another 5 random fields were chosen. The percentage of viable cells was calculated as follows:

Viable cells (%) =  $\frac{\text{total number of viable cells per field}}{\text{total number of cells per field}} \times 100$ 

# 2.8 Cell integration assessment in vitro

# 2.8.1 Qdot® nanocrystals

Qdot® nanocrystals (Qtracker 655) were used for cell tracking in the cell integration experiments. They are nanometre-scale atom clusters, coated with zinc sulphide (Figure 2-6). Both core and shell are semiconductor materials. Due to the optical features of Qdots', very bright fluorescence can be generated upon absorption of a photon of light. The intrinsic brightness and photostability of Qdot® fluoresce more strongly than traditional organic fluorophores. Qdots don't have cell-type specificity on labelling. The distribution of Qdot® nanocrystals in cytoplasmic vesicles is shown in Figure 2-6.



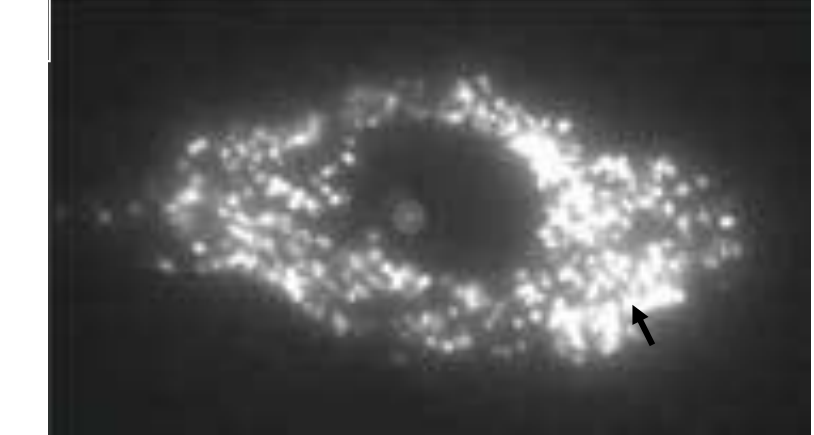


Figure 2-6 Structure and their intracellular distribution of Qdot nanocrystals (A) represents the structural elements of Qdot® nanocrystal in scale.

(B) demonstrates Qdot® nanocrystals distribution in vesicles throughout the cytoplasm (black arrow). (Adapted from http://www.invitrogen.com)

To track cells which are double or triple labelled using DAPI (excitation, emission) and Alexa 488 secondary antibody (excitation, emission), Qdot®655 were used in this study (Figure 2-7). Qdot labelled cells were visualised under a Leica DM IRB microscope (Leica Microsystems UK Ltd, Milton Keynes, UK) with Improvision Volocity software, with an excitation filter at 535 +/- 20 nm and an emission filter at 565nm long pass.

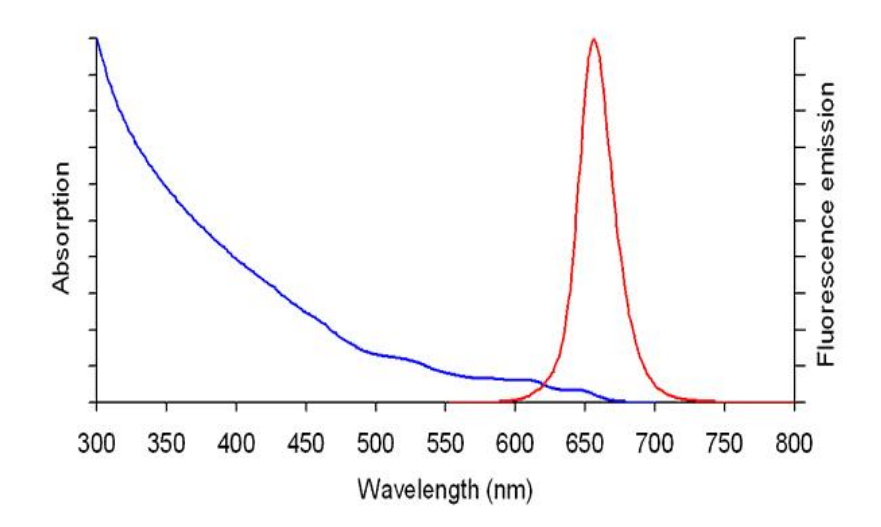


Figure 2-7 The excitation and emission spectra of Qdot®655. Diagram shows that Qdot®655 has broad excitation spectra. (From http://www.invitrogen.com)

### 2.8.2 Cell labelling with Qdots

Cells labelling was conducted as per manufacturer's instructions (Invitrogen). Adult limbal cells and media were transferred into a fresh 15ml falcon tube. Cells were collected following centrifugation for 5 min at 100G. Cells were then incubated with 1ml Accutase at 37°C for 10-15 min. After trituration using a1ml pipette, LNS were dissociated into single cells. Cells were resuspended into 1ml of fresh serum free media for counting and adjusted to a concentration of  $1 \times 10^7$  cells/ml.

The preparation of 10nM Qdot loading solution was conducted as per manufacture protocol.  $1\mu l$  of Qdot Component A and Component B were mixed in a sterile 1.5 ml microcentrifuge tube. Following incubation for 5 min at rt, 0.2 ml of fresh complete growth medium was added to the tube and vortexed for 30 sec.  $1\times10^6$  cells ( $100\mu l$  cell suspension from  $1\times10^7$  cells/ml in growth medium) were added to the tube containing the labelling solution. After incubation at  $37^{\circ}$ C for 60 min, cells were washed with full media twice and visualised under a fluorescence microscope to

estimate the labelling efficiency. Qdot labelled cells were visualised using a by-pass excitation filter at 535 + /- 20 nm and emission filter at 565nm long pass (Leica). Approximately 40-60 % cells were labelled with Qdots. Cells were the subjected to further culturing or integration experiments.

# 2.8.3 Direct co-culture system for integration assessment

In vitro cell integration was assessed using direct co-culture of Qdot labelled cells with neonatal mouse retinal explants. Dissociated Qdot labelled cells were collected into a 15ml of sterile falcon tubes. Cells (1 x10<sup>7</sup> cells/ml) were centrifuged at 120G for 5 min and re-suspended in DMEM:F12-GlutaMAX<sup>TM</sup>/B27 media containing 1% FBS. 200-200μl of cell solution was added to each Transwell® membrane (pore size 0.4 μm, Corning®, New York, USA), with 500μl of the same medium below the membrane prior to co-culture with retinal explants. Retinal tissues were dissected from PN Day 1 to Day 3 mouse eyes (Section 2.6.2). Before transferring retinal tissues to the top of Cell insert or Transwell membranes, the orientation of retina needed to be confirmed. The attachment of small numbers of RPE cells was used as an indicator of the outer retinal layer. Retinal tissues were then transferred to the cell seeded membranes with the outer retinal layer adjacent to Qdot labelled cells, as demonstrated in Figure 2-8. An additional 500μl of differentiation medium was added underneath the membrane to provide nutrition for tissues and cells.

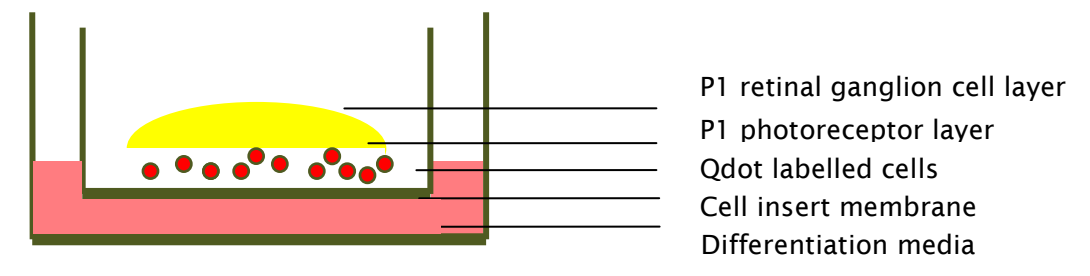


Figure 2-8 Direct co-culture System

A schematic diagram illustrates the direct co-culture system for cell integration study *in vitro*. Retinal explants were placed on top of Qdot labeled LNS cell (red) on Cell insert membrane. The photoreceptor layers of the retinal explants were adjacent to the Qdot labeled cells.

# 2.8.4 Fixation and sectioning for integration assessment

To prepare frozen tissue sections, the co-cultured tissues and cells were fixed on the cells Insert /Transwell membranes with 4% PFA fixative for 30-60 min. After removal of the fixative, samples were washed in 0.1M PBS and equilibrated in 30% Sucrose in 0.1M PBS overnight at 4°C. The cell insert membranes together with tissues/ cells were then excised and embedded with OCT in a cryo-mold block. All air bubbles were removed by lifting them to the surface of the OCT and moving them to the corners using micro pipette tips. The frozen tissue blocks were stored at -20°C or -80°C if long term storage was required prior to sectioning.

Before sectioning samples were equilibrated for a minimum of two hrs if stored at -80°C. Samples were sectioned using a cryostat (Leica CM1850 Cryostat, Leica Microsystems, Milton Keynes, UK). Sample were cut at a thickness of 15µm, and affixed to poly-L-lysine coated glass microscope slides. Following drying at 37°C for 2 hrs or rt for 24 hrs, slides were subjected to immunostaining or stored at -80°C until ready for use.

# 2.9 Statistical analysis

# 2.9.1 Sphere generation analysis

For quantification of the number of NS-like cell aggregates, total number of spheres with a diameter of 50  $\mu$ m and over was quantified using a 10 ×10 glass grid which was inserted into the eye piece of an inverted light microscope (Laborert FS Leitz, Wetzlar, Germany). Each culture condition was repeated at least three times with four replicates per experiment.

# 2.9.2 Measurement of Sphere Diameter

For quantification of the size of NS-like cell aggregates, images of spheres were taken at 7<sup>th</sup> days of culture at 4-6 random fields per culture plate. The diameters of spheres were subsequently measured at the longest and shortest dimensions using Improvision Volocity software (Improvision, Coventry Lexington, UK). A total number of 50-100 spheres were measured at each condition.

# 2.9.3 Cell enumeration for phenotype analysis

To quantify the percentage of cells expressing a particular phenotypic marker, the number of positive cells was determined relative to the total number cells (DAPI labelled nuclei) [175]. A total of 500-1000 cells were counted per marker.

## 2.9.4 Statistical Methods

All results are presented as mean ± SEM (standard error of the mean), unless otherwise stated, n represents the number of replicates. For normally distributed data, statistical comparisons were made using an unpaired student's t-test, with a significance threshold of p< 0.05. For comparison of more than two groups a one way analysis of variance (ANOVA) was used with a Bonferroni multiple comparisons test, with a significance threshold of p< 0.05. GraphPad Prism Software (GraphPad San Diego, USA) was used for statistical analysis. Excel and GraphPad Prism were used for graph production.

# 3 Chapter Three - Derivation of Neural Stem / Progenitor Cells from Adult Mouse Corneal Limbus

# 3.1 Background

Adult neural stem (NS) cells isolated from areas adjacent to the subventricular zone (SVZ) grow as floating cell aggregates in serum free culture medium in the presence of EGF and FGF2. These cell aggregates comprised of neural stem cells are referred as to "Neurospheres" [176]. This defined culture system can also be used to induce ESC differentiation into NS cells *in vitro*. Both adult and embryonic NS isolated and expanded through Neurosphere Assays (NSA) have displayed the ability to self-renew and differentiate into all neural cell types including neurons, astrocytes and oligodendrocytes [172].

Besides from the SVZ, neurospheres-like cell aggregates which express neural stem/progenitor markers such as nestin, have also been generated from a variety of tissues including brain, bone marrow, skin and retinal cells. Therefore, the NSA has been shown to be as a valuable tool for isolating stem/ progenitor cells with neural potential. Under these conditions, only NSCs and highly undifferentiated progenitor cells survive and proliferate, while committed precursors and mature cells are gradually eliminated from the culture system [177,178].

The formation of neurosphere is an ideal approach for isolation and propagation of NS cells *in vitro*. It not only avoids the use of animal substances such as serum, but also represents the "bona fide" methodology for therapeutic application. It has been reported that the NSA enables adult NS cells to maintain a stable profile with respect to self-renewal, differentiation, karyotype and molecular profile for over one year *in vitro* [179]. Furthermore, it did not cause tumor formation *in vivo* even when cells are transduced with oncogenes such as Myc and Ras [180]. Although the NSA has become the most widely used technique for the culture of adult NS cells, the cell population within neurosphere is not homogeneous. Neurospheres are composed of an ultrastructurally and morphologically heterogeneous population of cells, with expression of different neural lineage-specific markers as well as certain extraneural markers [180].

In this study, a clonogenic sphere forming assay was used to expand stem/progenitor cells from adult mouse corneal limbus. Cells were characterized in respect of self-renewal ability and neural potential. In addition, the origin of the derived adult mouse LNS was identified.

# 3.2 Methods

#### 3.2.1 Cell culture

### 3.2.1.1 Primary cell culture

Limbal cells were dissected from 8 week old mice and enzymatically dissociated using Trypsin, collagenase and hyaluronidase. For neurosphere generation and optimisation, limbal cells were maintained in DMEM: F12-GlutaMAX™ or Neurobasal™A with N2, 0.5mM L-Glutamine or B27 supplements in the presence of 20ng/ml EGF and 20ng/ml FGF2 at 37°C. The details for the six different media recipes used are listed in section 2.1.4 of Chapter 2. To investigate the effect of extrinsic factors on LNS generation, freshly isolated limbal cells were cultured with different extrinsic growth factors including EGF (20ng/ml), FGF2 (20ng/ml), Noggin (100ng/ml) or their combination in DMEM:F12 GlutaMAX™ with 2% B27 (minus VitA). Cells were plated at a density of 1 x 10⁴/ml. The numbers of spheres with a diameter over 50µm was counted for analysis. Experiments were repeated at least three times with four replicates each time.

# 3.2.1.2 Secondary sphere formation

To evaluate the self-renewal ability, secondary sphere generation was evaluated using serial dilution assays [172]. Individual spheres were picked under microscopy and dissociated to single cells by enzymatic digestion (Accutase) and mechanical trituration. Cells were seeded at extremely low densities by serial dilution 12, 25, 50, 100, 200 and 400 cells per ml, thus 1, 2, 5, 9, 18, and 36 cells in 90 µl of medium were plated into a 96 well plate (8 wells per concentration). A further 5-10 cells in100µl of medium were plated into four 96 well plates. At this low density, the possibility of cell aggregation can be eliminated and sphere generation can be considered from single cells. The number of spheres formed was enumerated after 14 DIV.

# 3.2.1.3 Cell differentiation

For differentiation, LNS cells were seeded on P-D-L and Laminin coated plate or chamber slides and cultured in neuronal differentiation medium containing

Neurobasal™A with 2% B27, 0.5mM L-Glutamine + 0-1% FBS, 1µM RA and 1ng/ml BDNF.

# 3.2.1.4 Viability of sphere cells

PI (Sigma-Aldrich) staining was used to evaluate the viability of cells within the spheres. Neurospheres were washed with PBS and then incubated in PI buffer ( $1\mu g/ml$ ) in PBS for 15-20 min at rt; sphere viability was then analysed by fluorescent microscopy.

# 3.2.2 Reverse transcription polymerase chain reaction

Investigation of the expression of neural lineage markers, epithelial lineage markers, neural crest markers and stem cell markers were conducted on adult mouse limbal cells during sphere formation by RT-PCR. Cells were cultured in DMEM: F12 GlutaMAX™ with 2% B27 (minus Vit A), 20ng/ml EGF and 20ng/FGF2 in the presence or absence of 100ng/ml Noggin. Cells from various time points 0, 3, 5 and 10 DIV were collected and subjected for RT-PCR analysis. Total RNA was isolated and cDNA synthesized as per manufactures protocols using RNeasy Plus (Qiagen) and High Capacity cDNA Reverse Transcription Kit (Applied Biosystems). Negative controls omitted reverse transcriptase. cDNA was amplified using gene specific primers. Cycles used were denaturing for 30 sec at 94°C, annealing for 30 sec at 60°C, extension for 30 sec at 72°C for 35 cycles. Electrophoresis was performed on a 1.5% agarose gel. The primer sequences used for LNS cell gene expression analysis during NSA culture are listed in Chapter 2, Table 2-1.

# 3.2.3 Immunocytochemistry

LNS cells were re-dissociated by Accutase and cultured on P-D-L and Laminin coated plate/ chamber slides for 24 hrs before immunocytochemistry. To investigate the distribution of nestin positive cells within LNSs, immunostaining was also conducted on intact LNSs. Cells/ spheres were fixed with 4% PFA for 15-20 min at 4°C. Following permeabilization and blocking with 0.1 mM PBS supplemented with 0.3% Triton X-100 and 5% DBS for 0.5-1 hr at rt, cells were incubated with primary antibodies (See Table 2-2, Chapter 2) overnight at 4°C. For ABCG2 staining, cells were fixed with cold acetone for 10-15 min, and then blocked with 5% DBS in PBS for 0.5-1 hr at rt before incubation with anti-ABCG2. Specific IgG secondary antibodies (1:500 Alexa Fluor 488 or 555) were incubated at rt for 1-2 hrs. Negative controls omitted the primary antibody. Nuclei were counterstained with10 ng/ml DAPI. To quantify the percentage of cells expressing a particular phenotypic marker, the number of positive cells was determined relative to the total number cells (DAPI labeled nuclei) [181]. A total of 500-1000 cells were counted per marker.

For phenotypic analysis of ABCG2 positive cells by flow cytometry, neurosphere cells were dissociated to single cells using Accutase. 50,000 cells were fixed in 4% PFA at 4°C for 30 min, followed by permeabilization with 70% ethanol for 30 min at -20°C and blocking with 10% normal mouse serum (Sigma-Aldrich) for 30 min at rt. Cells were subsequently washed with PBS and then incubated with ABCG2 antibody at rt for

30 min. Serial dilution of primary antibody (1:2, 1:5, 1:10 and 1:20 in blocking serum) was used to investigate the optimal assay concentration. Following incubation with an Alexa Fluor 488 conjugated anti-rat IgG secondary antibody (1:500, Invitrogen) at rt for 30 min, cells were analyzed by FACSAria flow cytometry (Becton). Blue laser (488nm) was selected for fluorophore excitation and a 505nm for detection. Cells which had not been incubated with primary and secondary antibodies and cells in the presence of secondary antibody alone were used as negative controls.

To view the structure of mouse limbus, anterior half eyeballs were dissected and fixed using 4% PFA for 30-60 minutes at 4°C. Following incubation in 30% Sucrose in 0.1M PBS overnight at 4°C, samples were embedded in OCT and sectioned at 20  $\mu$ m using a cryostat. Slides were dried at 37°C for 2 hrs before DAPI staining.

# 3.2.4 Transmission Electron Microscopy (TEM)

To investigate the ultrastructure of adult mouse LNSs, LNS were washed with PBS, then fixed in 100 µl of primary fixative containing 0.1 M sodium cacodylate buffer, 3% glutaraldehyde, 4% PFA and 0.1 M PIPES buffer, pH 7.4 for 15 min at rt. Further processing was performed in the Biomedical Image Unit, University of Southampton. In brief, following initial fixation the specimens were rinsed in 0.1M PIPES buffer, postfixed in 1% buffered osmium tetroxide (1 hr), rinsed in PIPES buffer, block stained in 2% aqueous uranyl acetate (20 min) followed by dehydration in a graded series of ethanols up to 100% and embedded in TAAB resin (TAAB Laboratories). Gold sections were cut on a Leica OMU 3 ultramicrotome (Leica), stained with Reynolds lead stain and viewed on a Hitachi H7000 transmission electron microscope equipped with a SIS megaview III digital camera (Hitachi).

# 3.3 Clonal growth of adult mouse corneal limbus derived cells

#### 3.3.1 Structure of adult corneal limbus

The structure of the adult mouse corneal limbus and peripheral cornea is similar to that seen in humans. The whole thickness of the mouse cornea is less than 100µm, it is comprised of three major layers namely the epithelium, stroma and endothelium layer (Figure 3-1). A large number of stratified squamous epithelium cells are present accounting for 10-20 percent of the thickness of the mouse cornea and limbus. The epithelial cells reside in the stroma and the proportion of endothelium cells is much less compared to corneal epithelium. The "palisades of Vogt", a distinctive feature of the human corneal limbus, are present as an undulating epithelium basal layer [22]. The palisades of Vogt are not apparent in mouse corneal limbus. Dissociated corneal limbal cells are heterogeneous, composed of all three types of cells from the corneal limbus and possibly pigmented iris epithelial cells.

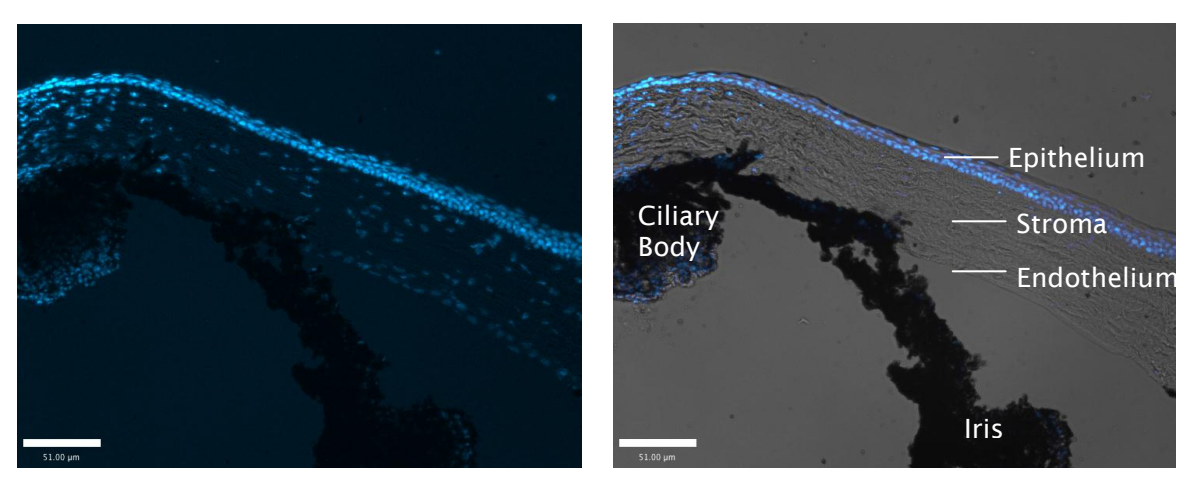


Figure 3-1 Structure of peripheral cornea and corneal limbus.

Representative images of DAPI stained adult mouse peripheral cornea and limbus in cross-section (blue, left). Stratified cells are present in the epithelial layer, while fewer cells are distributed in the cornea stroma and endothelium. The pigmented layer is the iris. It is continuous with ciliary body at its periphery. (Right) shows bright-field and DAPI merged image of peripheral cornea and limbus in cross-section. Scale Bar: 50µm.

# 3.3.2 Sphere-cluster formation

Primary cultured cells were prepared from the corneal limbus of 8 week old mice as described in Chapter 2 (Section 2.1.2). Approximately 3 x 10<sup>4</sup> corneal limbal cells were harvested from each individual adult mouse eye. Neurosphere-like cell aggregates were generated from both PN and adult murine corneal limbus in the presence of mitogens (EGF, FGF2). Small sphere-clusters ( $<50 \mu m$ ) were detected after 3 DIV from PN day 11 mice or following 5 DIV when adult mice were used. After 7 days, sphere sizes ranged from 50  $\mu m$  to 150 $\mu m$  in diameter, with defined edges and a smooth surface (Figure 3-2). In the presence of EGF and FGF2, the average sizes of spheres after 7 days in culture with DMEM:F12GlutaMAX<sup>TM</sup>/B27- and NB/B27 was 61.1  $\pm$  17.1  $\mu m$  and 66.7  $\pm$  16.4 $\mu m$  (mean  $\pm$  SD) respectively. To eliminate the possibility of iris pigment epithelium cell contamination, the same dissociation and culture condition were applied to homogenous iris derived cells. No sphere-cluster formation was detected following sphere culture for over two weeks' observation (Figure 3-2).

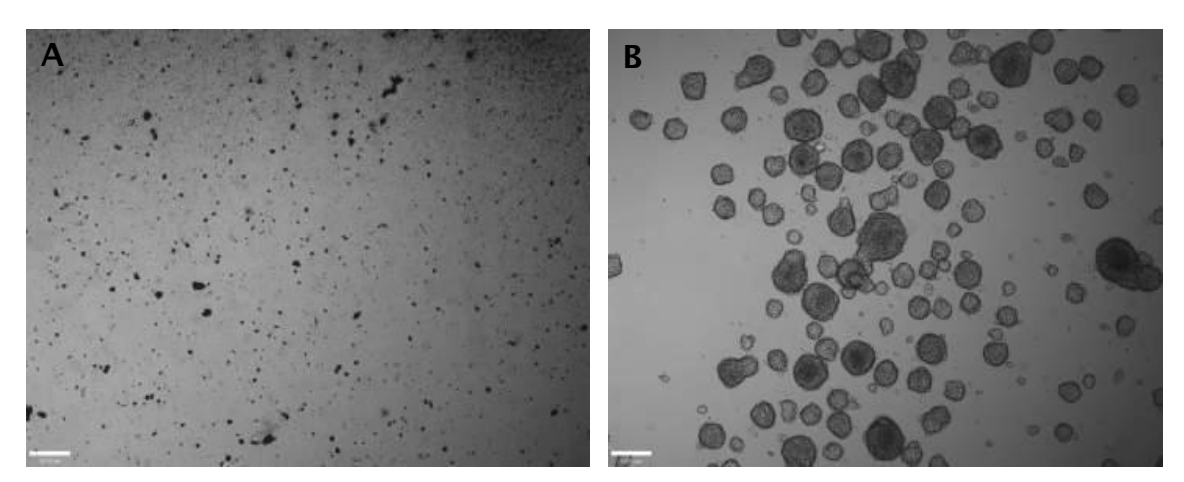


Figure 3-2 Homogenous adult mouse iris pigment epithelium and corneal limbus cells. Cells (17 DIV) from adult mouse iris and corneal limbus isolated by the same dissociation process and maintained in the same culture conditions (Medium 6).

(A) No obvious spheres were formed from adult mouse iris pigment epithelium; cells remained heavily pigmented. (B) Sphere colonies were generated with defined edges from adult mouse corneal limbus cells. Scale bar: 100 µm.

# 3.3.3 Optimal culture condition for sphere generation

To investigate the optimal culture medium for corneal limbal primary sphere formation, two basal tissue culture media, DMEM:F12 (DMEM) and Neurobasal (NB), were compared. The former is the most prevalent stem cell culture medium; while the latter was originally described for the maintenance of differentiated neurons, but was found

to be highly efficient for clonal growth and expansion of adult NS cells when combined with B27 media supplement [182]. Three media supplements N2, B27 (standard) and B27- (minus Vitamin A) were used in combination with the basal mediums to supply nutrition. All media tested were supplemented with

L- glutamine/GlutaMax, EGF, FGF2 and antibiotic/antimycotic solution.

Sphere generation efficiency in different culture mediums was investigated both at a low (10,000/ml) and medium-high (50,000/ml) initial cell density. Only spheres with a diameter of over 50µm were included for analysis. With use of N2 medium supplement, there was no apparent cell proliferation or obvious sphere formation detected from both PN and adult mouse corneal limbus. Medium composed of DMEM:F12 supplemented with B27 resulted in the formation of cell monolayers and was therefore not included for further comparison (Figure 3-5). As shown in Figure 3-3, the highest yield of primary spheres from a low initial cell density was obtained using DMEM:F12 with B27- medium supplement,  $43.50 \pm 3.78$  spheres were generated from 5000 cells (0.87 ± 0.08% efficiency). This sphere generation efficiency was significantly different when compared to all other cell culture media recipes tested (P<0.001, n=3). With a high initial seeding density (Figure 3-3), the number of primary sphere generated from DMEM/B27- (209.33  $\pm$  26.34) was higher than that with NB/B27 (138.08  $\pm$  23.24), however there was no statistical difference (P>0.05), indicating that NB/B27 and DMEM/B27- had similar capacity for primary sphere generation when high density cell plating was applied (Figure 3-4).

# Sphere Generation Effiency in different culture medium

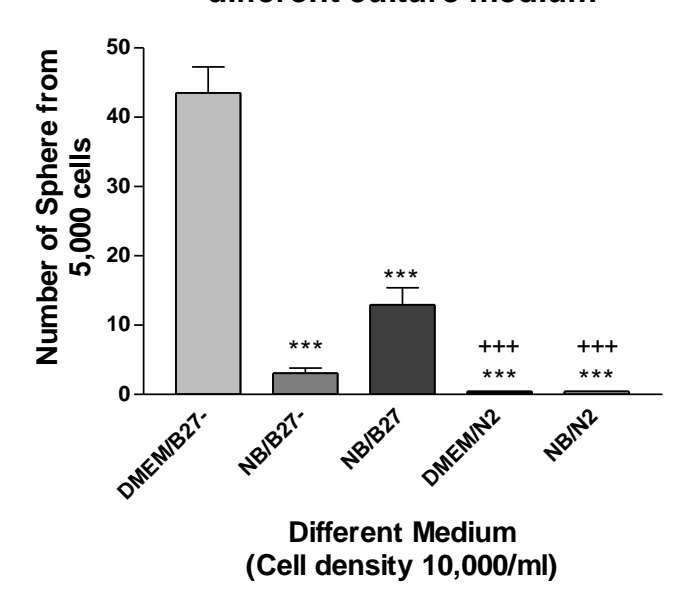


Figure 3-3 Sphere generation efficiency at low cell density in different media recipes. Quantification of total number of primary neurosphere-like clusters from adult mouse corneal limbus after 7 DIV in different culture media at low cell density (0.5ml, 10,000/ml). The results are expressed as mean ± SEM, from three separate experiments with four replicates in each experiment. Significant difference \*\*\* P<0.001 compared to DMEM/B27-. +++ P<0.001 compared to NB/B27 by ANOVA followed by the Bonferroni multiple comparison test.

The ability to form neurospheres in serum free medium was first described to select and expand neural stem cells [173]. Sphere-forming assays have also been successfully used to derive stem or progenitor cells from non-neural tissues including bone marrow, skin, inner ear, corneal limbus, ciliary body (adult retinal stem cells), retina (newborn) and IPE. In the presence of specific mitogens i.e. EGF and FGF2 serum-free media is able to support stem/progenitor cell proliferation, with gradual elimination of post mitotic non-proliferating mature cells.

We optimized the basal media and nutrition supplements for sphere generation. Consistent with other studies regarding the generation of neurospheres from CNS cells [183], we found B27 to be essential for sphere generation. Limbal sphere generation was possible using both basal media (Neurobasal A and DMEM:F12). At low cell density, it was found that DMEM: F12 supplemented with B27- lead to more efficient sphere generation. This effect was not seen when medium to high cell density was investigated.

# Sphere Generation Efficacy in different culture medium

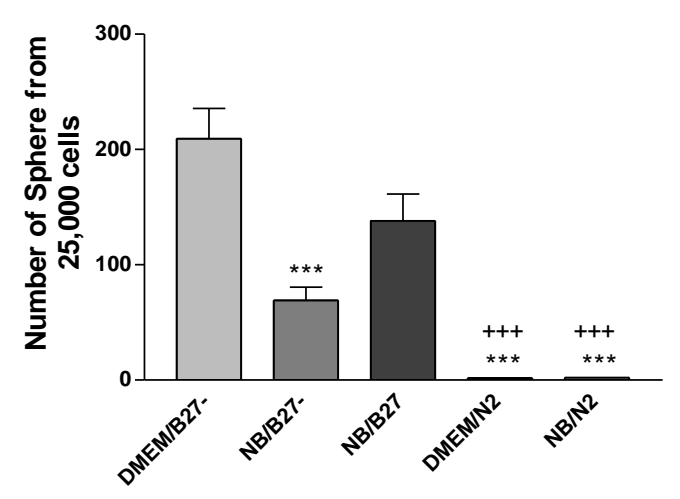


Figure 3-4 Sphere generation efficiency at high cell density in different media recipes. Quantification of total number of primary neurosphere-like clusters from adult mouse corneal limbus after 7 DIV in different culture media at high cell density (50,000 / ml). The results are expressed as mean  $\pm$  SEM, from three separate experiments with four replicates in each experiment. Significant difference \*\*\* P<0.001 compared to DMEM/B27-. +++ P<0.001 compared to NB/B27 by ANOVA followed by the Bonferroni multiple comparison test.

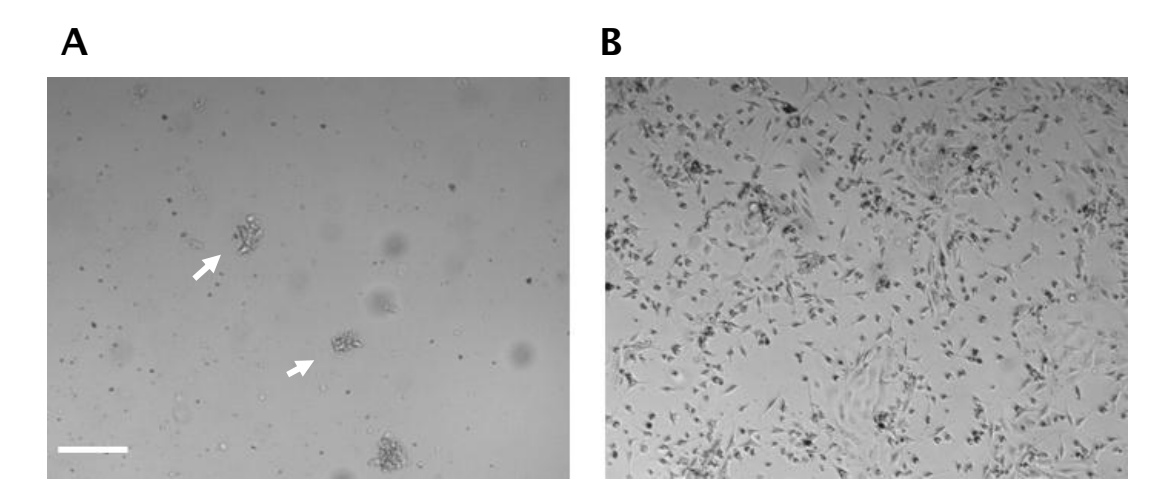


Figure 3-5 Limbal cells in non-optimal culture medium. No sphere formation was detected in N2 supplemented base culture media in the presence of mitogens, disorganized cells clumps (white arrows, size <50um) were observed after 7 DIV (A). With DMEM: F12 Glutamax/B27, cells showed monolayer growth (B). Scale bar: 50 µm.

# 3.3.4 Cell viability within sphere

Propidium iodide (PI) can penetrate the cell membranes of dying or dead cells and intercalate into double-stranded nucleic acids. After excitation under UV light, PI within the less viable cells could be detected under microscopy. The sphere cells showed good cell viability (Figure 3-6). When the size of neurospheres exceeded 100µm, an increase in cell death was observed particularly in the centre of spheres. This may due to less nutrition reaching the center of large spheres. Therefore, to maintain cell growth and viability, sphere passaging was performed every 7-12 days before the size of spheres reached 150µm.

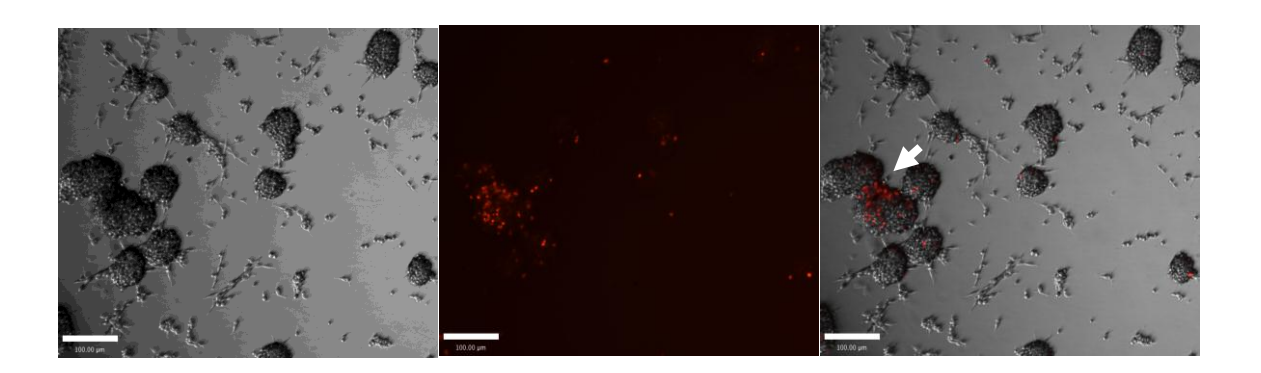


Figure 3-6 Sphere cell viability assessment

Fluorescence image merged with bright field image. Only a few PI stained (red) cells were detected in the sphere culture. Large spheres (white arrow) contained more dead cells in the centre. Most spheres showed high cell viability. Scale bar: 100µm.

# 3.3.5 Effect of growth factors on clonal growth

The number of spheres generated from adult mouse corneal limbus cultured in serum free medium in the presence and absence of EGF, FGF2 and BMP4 inhibitor (noggin) were analyzed using DMEM/B27- medium. Previously reported growth factor concentrations were used in this study [173], as shown on Table 2-1 in Chapter 2. In the presence of EGF alone, spheres with a size of over  $50\mu m$  were rarely detected (0-2 spheres per 20,000 cells). A large number of spheres were generated in the presence of FGF2 alone ( $35.92 \pm 2.21$  spheres /5000 cells) and when EGF was combined with FGF2 ( $48.75 \pm 2.97$  spheres /5000 cells). There was a significant difference in sphere generation efficiency between the groups in the presence and absence of FGF2, which is indicative that generation of spheres from adult mouse corneal limbus, is dependent upon FGF2, but not EGF.

# Number of Spheres generated from adult mouse limbus

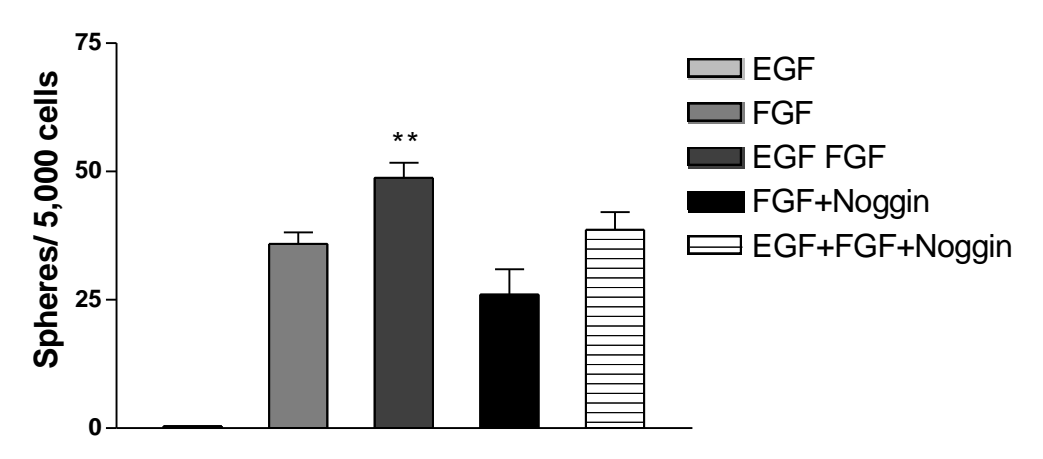


Figure 3-7 Effect of extrinsic factors on adult mouse LNS generation

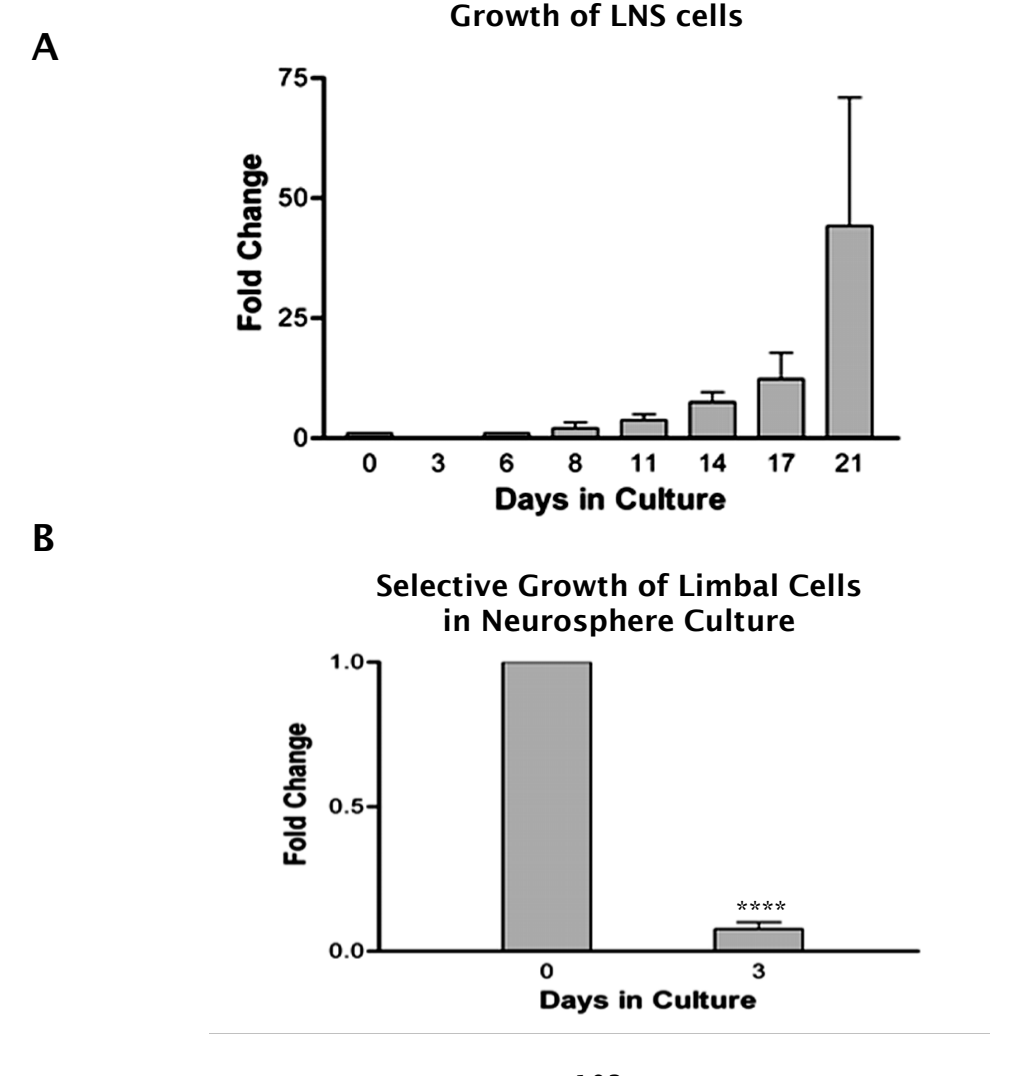
Single cell suspension from dissociated adult mouse corneal limbus were plated in 24-well plates at a density of 10,000 cells/ ml (5,000 cells/ well with 4 replicates,  $n\geq 4$ ) in DMEM/B27- and cultured with various extrinsic growth factors for 7 days. Spheres with a diameter of over 50  $\mu$ m were included for analysis. EGF: Epidermal Growth Factor; FGF: basic Fibroblast Growth Factor; N: Noggin. Results are mean  $\pm$  SEM (n=4). Significant difference \*\* P<0.01 compared to FGF by ANOVA followed by the Bonferroni multiple comparison test.

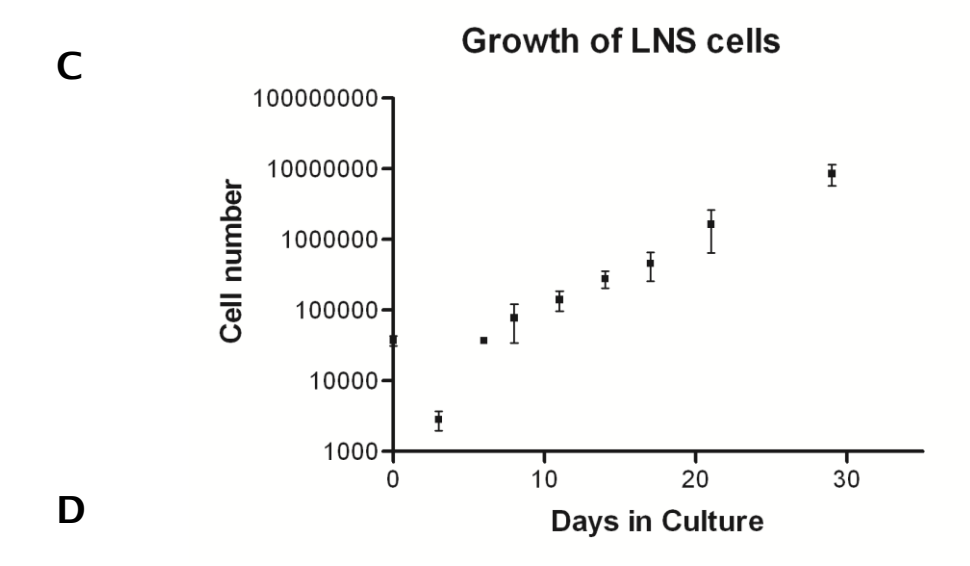
As illustrated in Figure 3-7, the combination of EGF and FGF2 produced the highest sphere generation efficiency. Compared to FGF2 supplementation alone, the combination of EGF and FGF2 reveals a significant increase in the sphere generation efficiency (p<0.01), suggestive of a synergetic effect between EGF and FGF2. This is also indicative of an optimal condition for corneal limbal sphere generation. The presence of Noggin in the culture system decreased the number of spheres formed (38.63 ± 3.47 spheres /5000 cells in FGF2+EGF+N). However, a comparison of sphere generation between the groups in the presence and absence of Noggin in the culture system (FGF2 vs. FGF+N; FGF2+EGF vs. FGF2+EGF+N) revealed no significant difference in efficiency (p>0.05), which is suggestive that inhibition of the bone morphogenetic protein pathway does not have a significant effect on sphere generation.

# 3.3.6 Cells from adult corneal limbus display self-renewal capacity

Corneal limbus derived spheres could be propagated and expanded *in vitro* by passaging for over 4-5 months. After three days in culture, over 90% of the initial cell population was gradually eliminated (Figure 3-8B). The doubling time for early passage (up to 5 weeks) spheres was approximately 4 days. The number of cells can be expanded  $9.0 \pm 2.8$  times after 16 days in sphere culture following primary sphere cell formation (Figure 3-8A). Over 30,000 cells can be harvested from  $1 \times 3$ mm of corneal limbal tissue from a single mouse eye  $(37,000 \pm 7,000, n \ge 4)$ . After 21 days in neurosphere medium, cell numbers reached approximately one million  $(1,640,000 \pm 99,400; n=4)$ , as shown in (Figure 3-8C).

The sphere generation rate of primary and sub-cultured limbal sphere was investigated in this study. As shown in Figure 3-10A, the number of limbal sphere colonies increased steadily from primary to quaternary spheres in NSA. This indicates that propagation of limbal cells from subsequent generations is also due to clonal expansion, similar to the primary spheres.





# Sphere Generation Rate of Primary and Subcultured limbal cells

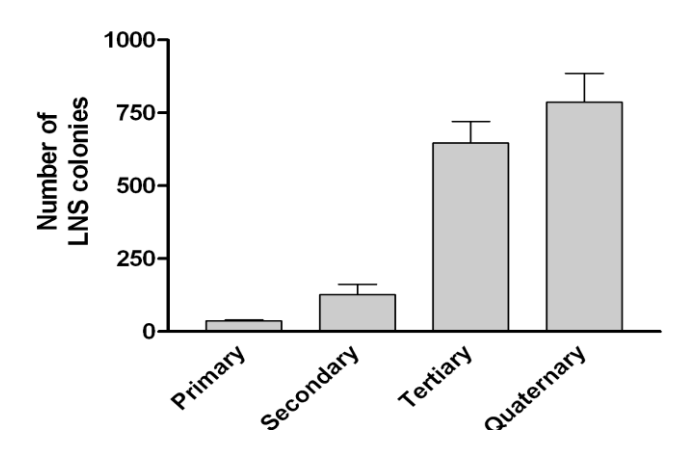


Figure 3-8 Growth features of mouse LNS cells

Single cell suspension from dissociated adult mouse corneal limbus were plated in 12-well plates at a density of 50,000 cells/ ml (5,000 cells/ well with 4 replicates,  $n \ge 4$ ) in DMEM/B27- supplemented with 20ng/ml EGF and 20ng/ml FGF2. The number of cells was counted every 3-4 DIV. Limbal spheres were passaged every 7 DIV using Accutase. Results are mean  $\pm$  SEM (n=4). (A) A growth curve of adult mouse corneal limbal neurosphere cells. Data are expressed as fold change over the number of cells initially plated ( $n \ge 4$ ). (B) Limbal cell numbers sharply decreased after three days in neurosphere culture (n=4) p<0.001 by paired t-test. (C) A growth curve of LNS cells, illustrates absolute cell numbers harvested from a single mouse eye (37,000  $\pm$  7,000, day 0) and generated via NSA cultures *in vitro* ( $n \ge 4$ ). After 21 days in neurosphere medium, cell numbers reached approximately one million (1,640,000  $\pm$  99,400; n = 4). (D) Adult mouse limbal cells were cultured and passaged at density of 10,000/ml every 7 days. Number of LNS colonies increased following subculture until the 4<sup>th</sup> genenration (maximum investigation time). Results are presented as Mean  $\pm$  SEM (n = 6).

To verify that sphere formation from corneal limbus derived cells was due to proliferation rather than cell aggregation, immunocytochemistry was carried out using antisera direct against proliferating cell nuclear antigen (PCNA), a polymerase-associated protein synthesized in early G1 and S phases of the cell cycle. We demonstrated that over 75% of cells were immunopositive for PCNA, indicating that spheres contained a significant proportion of proliferative cells (Figure 3-9).

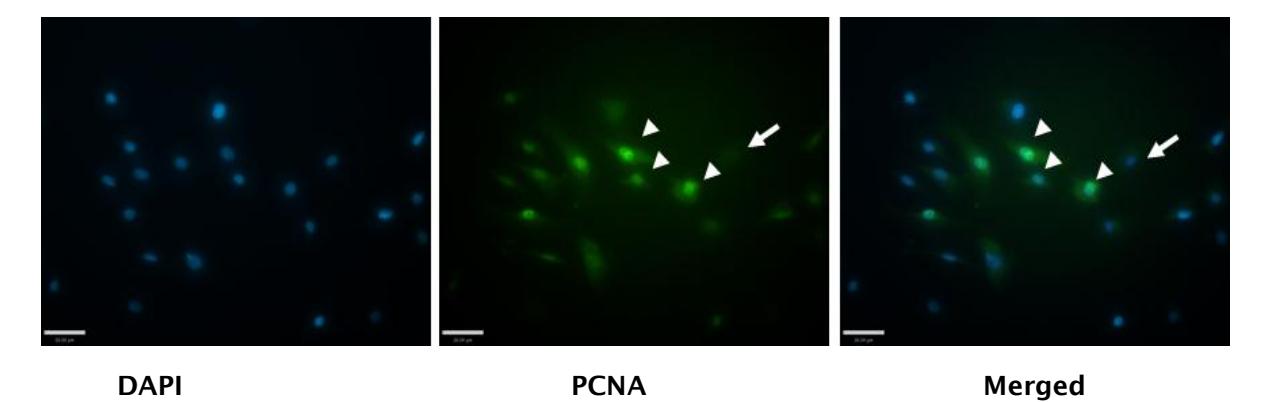


Figure 3-9 Limbal spheres expressed the proliferative marker PCNA. PCNA (proliferating cell nuclear antigen) was detected in spheres derived from adult mouse corneal limbus. Over 75% of cells were positive for PCNA (green), which colocalized with DAPI nuclear staining (blue). Arrow heads indicates positive cells, whilst arrow presents negative cell. Cells were cultured for 8 days *in vitro*. Scale bar: 26 µM.

To assess proliferation ability, secondary sphere generation was evaluated using serial dilution assays [6,90]. Serial dilution assays has been previously used to assess self-renewal of stem like cells [6,90]. Individual spheres were picked under microscopy and dissociated to single cells by enzymatic digestion and mechanical trituration. Cells were seeded at extremely low densities by serial dilution 12, 25, 50, 100, 200 and 400 cells per ml, at these extremely low densities, cell aggregation can almost be eliminated. 1, 2, 5, 9, 18, and 36 cells in 90  $\mu$ l of medium were plated into a 96 well plate (8 wells per concentration); number and size of sphere clusters generated are shown in Figure 3-10 and Figure 3-11.

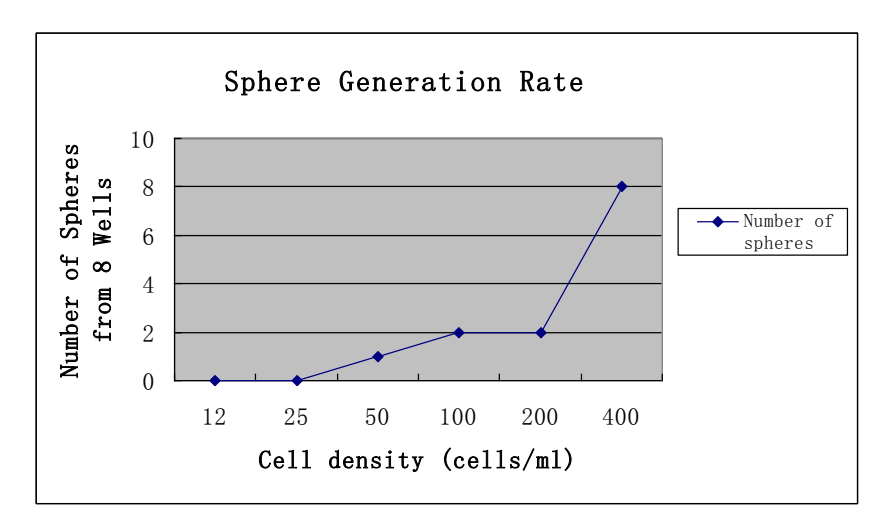


Figure 3-10 Sphere generation efficiency.

Secondary sphere generation efficiency by serial dilution assay after 14 DIV. A high cell density produced a higher sphere generation rate.

Extremely low cell densities (50-400 cells/ml) demonstrated that cells derived from murine corneal limbus support clonogenic expansion *in vitro* and are capable of producing secondary neurospheres by clonal expansion. The size and number of spheres increased with cell density (Figure 3-10, Figure 3-11). To determine the secondary clonogenic efficiency at low cell density, dissociated primary sphere cells were seeded into 96 well plates at density of 5-10 cells/well. A secondary clonogenic efficiency of approximately 1% was detected, suggesting self-renewal of sphere cells.

The sphere-forming assay was highly inefficient when single cells were seeded in single wells. We did not detect any sphere generation when the density decreased to 30 cells/ml and 10 cells/ml. In addition, no secondary spheres generation was detected from the central cornea although a few small primary spheres ( $<50\mu m$ ) were detected (Figure 3-11E-F).

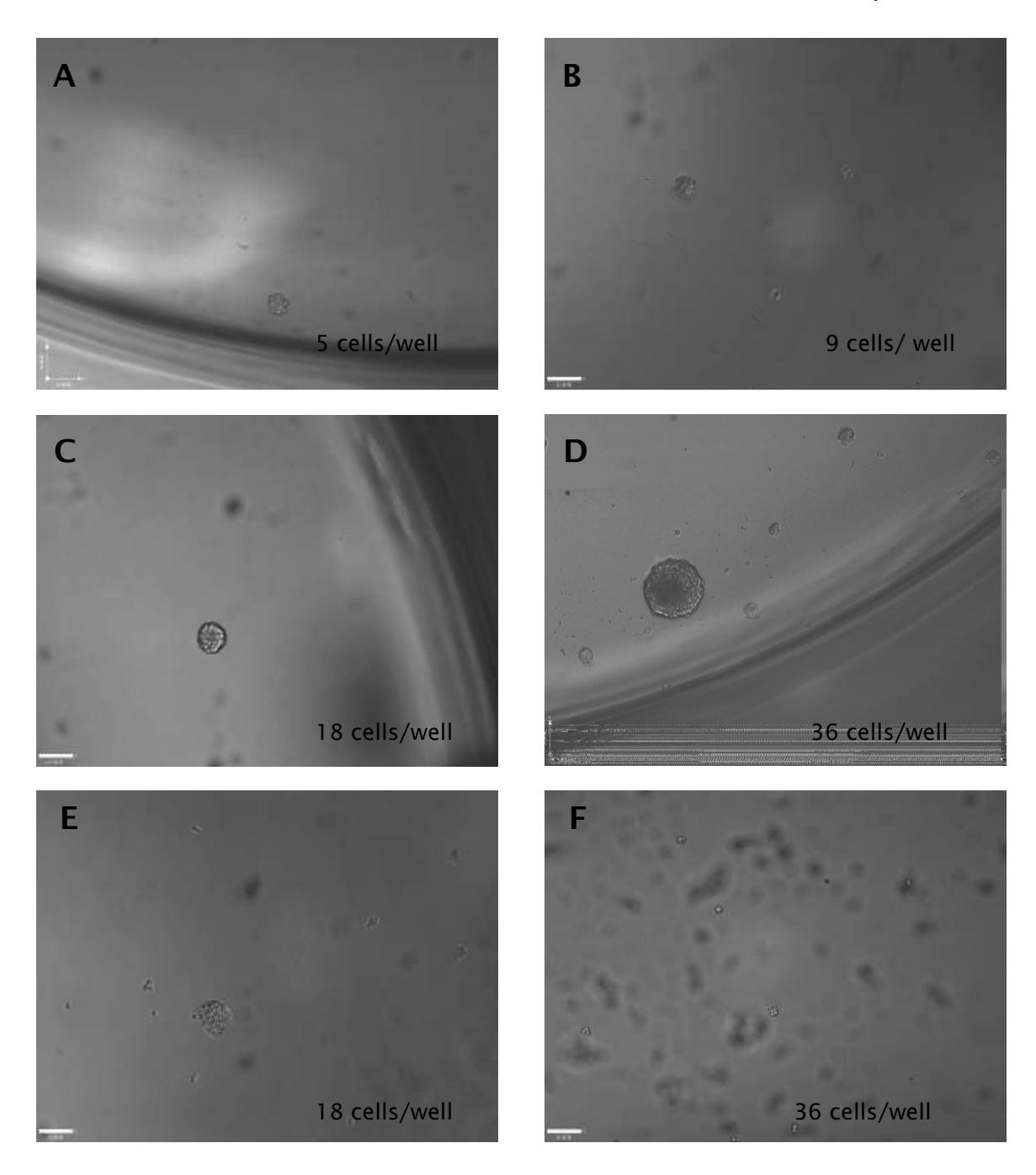
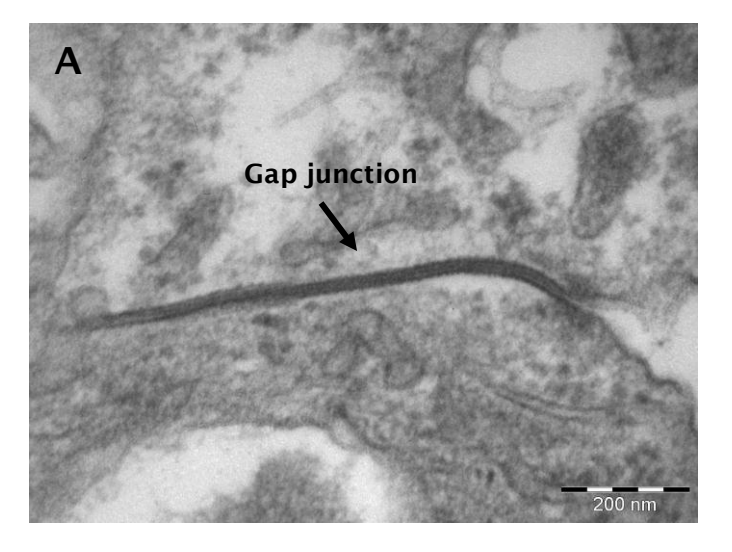


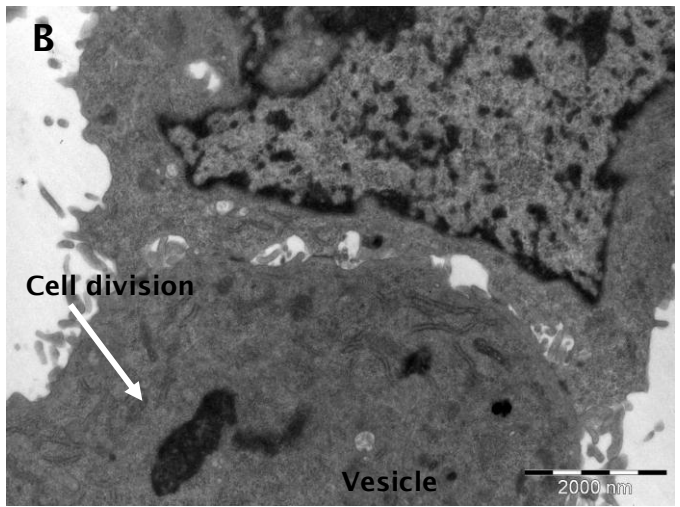
Figure 3-11 Secondary sphere generation at extreme low cell density following serial dilution assay. Secondary spheres were generated from LNS cells after14 DIV. Cell densities ranged from 10-400 cells/ml (1-36 cells/well) in 96 well plates. Higher cell density promoted sphere generation (A-D). No secondary spheres were observed from cells generated from the central cornea (E, F). Scale bar: 50µM.

## 3.3.7 Ultrastructure of sphere cells derived from adult corneal limbus

The spheres derived from the adult mouse corneal limbus were three dimensional structures. Cells within spheres were connected with each other through gap junctions (Figure 3-12A) and adherence-like junctions (Figure 3-12C). The former are communicating junctions that allow ions and small molecules to pass directly from one cell to the next. Therefore, cells connected by gap junction are electrically and chemically coordinated [181]. The latter provide strong mechanical attachments between adjacent cells. Cells within spheres also presented apparent cell division, vesicles and abundant rough endoplasmic reticulum (RER) (Figure 3-12B), indicative of active cellular mitosis, exocytosis/ endocytosis and protein synthesis. Spheres also contained some polarized cells with processes at the periphery, while melanosomes were not detected in the primary or secondary limbal spheres.

Similar to neurospheres derived from SVZ, spheres generated from the adult corneal limbus contained gap junction and immature adherence junctions. Matured tight junctions and desmosome junctions, which are found in spheres of an epithelial origin, were not detected in limbal spheres. Microvilli were previously reported to be present in the periphery of spheres derived from both epithelial (ciliary epithelium) and neural origins (SVZ) [184]. Consistent with this, cells at the periphery of our limbal spheres also contained microvilli. Melanosomes were absent in limbal spheres, whilst they have been shown to be abundant in IPE and ciliary origin sphere cells [104]. In summary, corneal limbal spheres do not have ultrastructural features in common with spheres derived from pigmented epithelial cells. Therefore they are unlikely to be generated from pigmented cells.





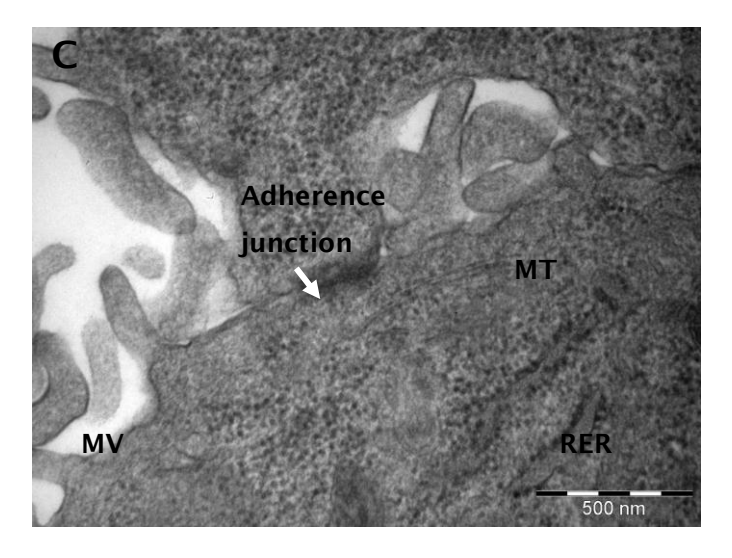


Figure 3-12 Transmission electron micrographs of adult mouse corneal limbal spheres (A, C) Gap junction and adherence-like junction were detected between cells within spheres. (B) Cell showed dissolved nuclear membrane indicative of cell division (arrow). (C) Microtubulin (MT), microvilli (mv), rough endoplasmic reticulum (RER).

# 3.4 Characteristics of corneal limbal cells

## 3.4.1 Expression of side population determinant ABCG2

We first characterized spheres derived from the limbus with an ATP-binding cassette superfamily transmembrane protein ABCG2. As a side population phenotype determinant, ABCG2 is ubiquitously expressed in stem cells from the bone marrow, skin and nervous system [104,137], it also plays an important role in the maintenance of retinal SCs [185]. It is suggested as one of the best markers for putative limbal stem cells [186]. In order to quantify the proportion of ABCG2 positive cells within neurosphere, cells were dissociated and grown as monolayers on P-L-L or P-D-L and laminin coated plates/coverslips for 24 hrs prior to immunocytochemical analysis. Approximately 90% of the cells tested were positive for ABCG2 (Figure 3-13). Flow cytometry analysis was used to confirm this.

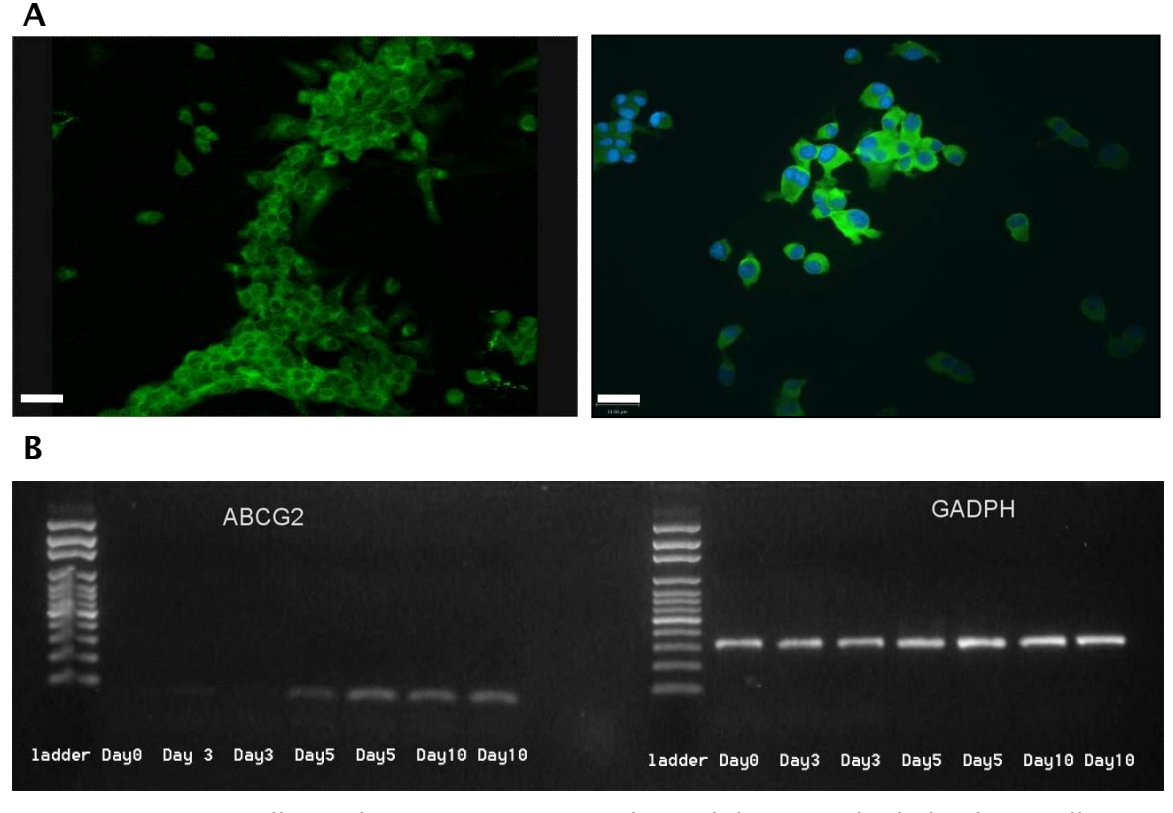


Figure 3-13 Stem cells marker ABCG2 expressed on adult mouse limbal sphere cells. Adult mouse corneal limbal sphere were dissociated into single cells and plated on P-D-L and laminin coated chamber slides for 24 hrs prior to Immunocytochemistry (ICC) (A) ABCG2 positive cells (green) were detected on over 90% of limbal sphere cells on DIV 10. Nuclei were counterstained with DAPI (blue). Scale bar: 26um (left) and 13um (right) (B) Expression of ABCG2 was confirmed with RT-PCR using specific primers.

ABCG2 expression was apparent after 5 DIV; this is the same time as spheres formation. Internal control housekeeping gene: GAPDH.

ABCG2 is a transmembrane protein; therefore, anti-ABCG2 staining is ideal for flow cytometric immunophenotyping analysis. The sphere cluster cells generated from adult mouse limbus tissue appear to be heterogeneous in cell size (FSC) and cytoplasmic granularity (SSC). The morphological heterogeneity in limbal spheres is consistent with the characteristic of neurospheres from the CNS, which also demonstrate heterogeneity of cell size, viability, cytoplasmic content and cell function [22]. As Figure 3-14 shows, in the main cell population (P1) from adult mouse corneal limbus, approximately 90% (P2) of cells were ABCG2 positive, which was in accordance with immunocytochemistry analysis.

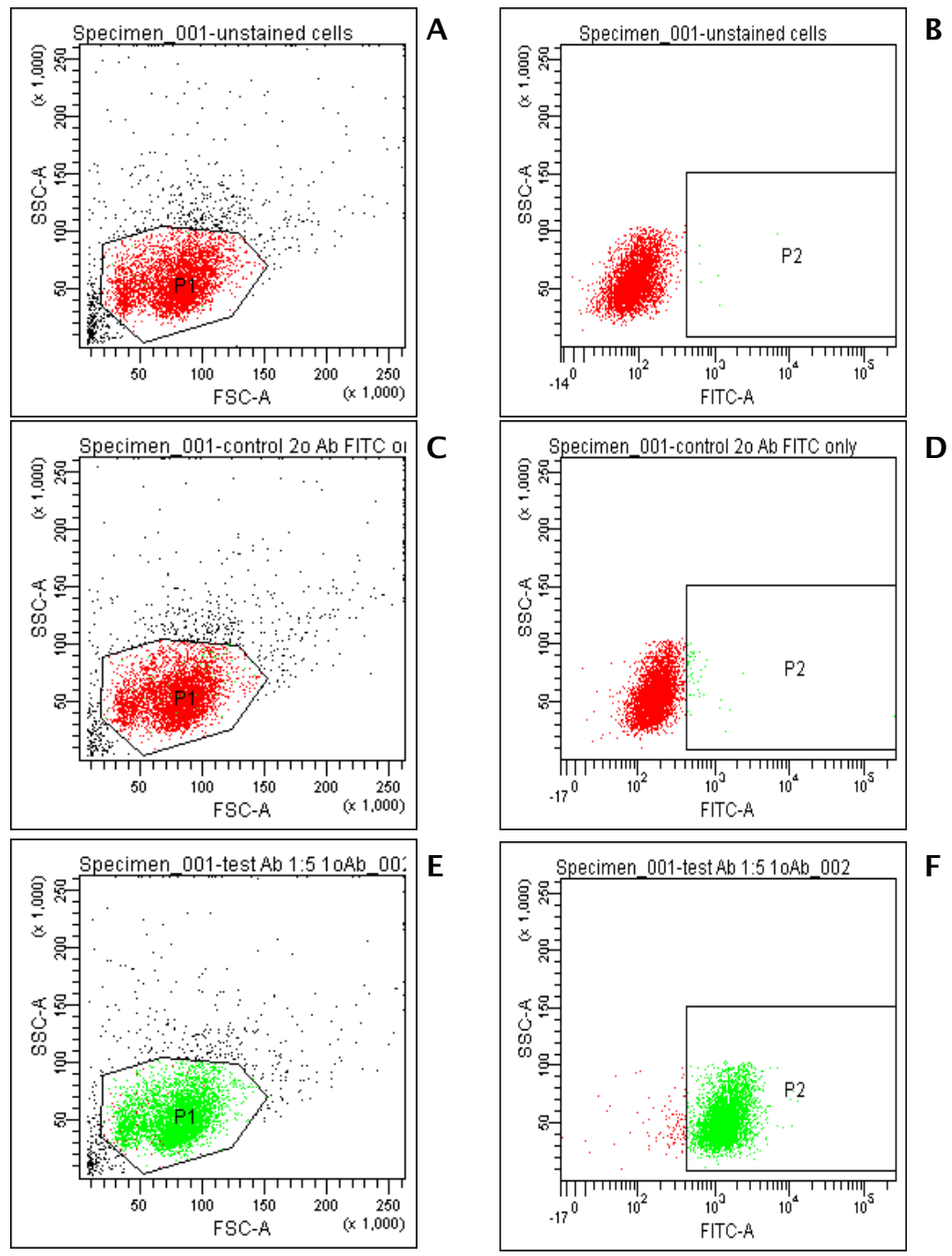


Figure 3-14 Flow cytometric analysis of cells derived from adult mouse corneal limbus. The forward scatter (FSC) versus side scatter (SSC) profile of the total limbal cell population (P2, DIV28) is shown. 5,000 cells were analysed per condition. Dots represent cells analysed by FACSAria (BD Biosciences, Oxford, UK). P1 shows the main population (90%) of total cells, and P2 represents ABCG2 positive cells within P1 population. **A, B:** Unstained single cell suspensions; **C, D:** Negative control with secondary antibody (Alexa Fluor 488-labeled donkey anti-rat IgG); **E, F:** Identification of ABCG2 positive cells. 92.9% of cells within P1 were positive for ABCG2 (dilution 1:10).

## 3.4.2 Expression of neural stem cell marker Nestin

Nestin, first identified by Hockfield and McKay, is a class VI intermediate filament protein[172]. It is predominantly expressed in early embryonic neuroepithelial stem cells in the developing CNS, and has been widely used as a marker for neural stem/progenitor cells.

Spheres derived from adult limbal tissue contain nestin-positive progenitors. To locate the nestin-positive cells within derived spheres, confocal scanning microscopy was performed at a thickness of 10 µm from top to the bottom of spheres following immunostaining. The results demonstrated that cells expressing a high level of nestin were located only at the periphery of the spheres (Figure 3-15A). For quantification of the number of nestin positive cells, spheres were then dissociated into single cells and cultured on the P-D-L and laminin coated chamber slides. We found that 32.47 ± 6.08% cells expressed nestin (Figure 3-15D-F). These results were confirmed by RT-PCR using specific primers (Figure 3-15B-C). To investigate the nestin expression level during sphere formation process, four different time points were chosen. Day 0 represent freshly isolated cells from adult corneal limbus tissue. When cultured in a serum free sphere forming system in the presence of EGF & FGF2 for three days (the second time points), the majority of mature cells were eliminated, but no sphere generation was yet detected. Day 5 and day 10 in vitro were the time points when primary spheres and subsequently secondary spheres were observed. Prior to sphere formation, there was no obvious nestin expression detected at a RNA level, but consistently high levels of nestin were detected in both primary and secondary spheres. Glyceraldehyde 3phosphate dehydrogenase (GAPDH), the house keeping gene, was used as an internal control for RT-PCR.

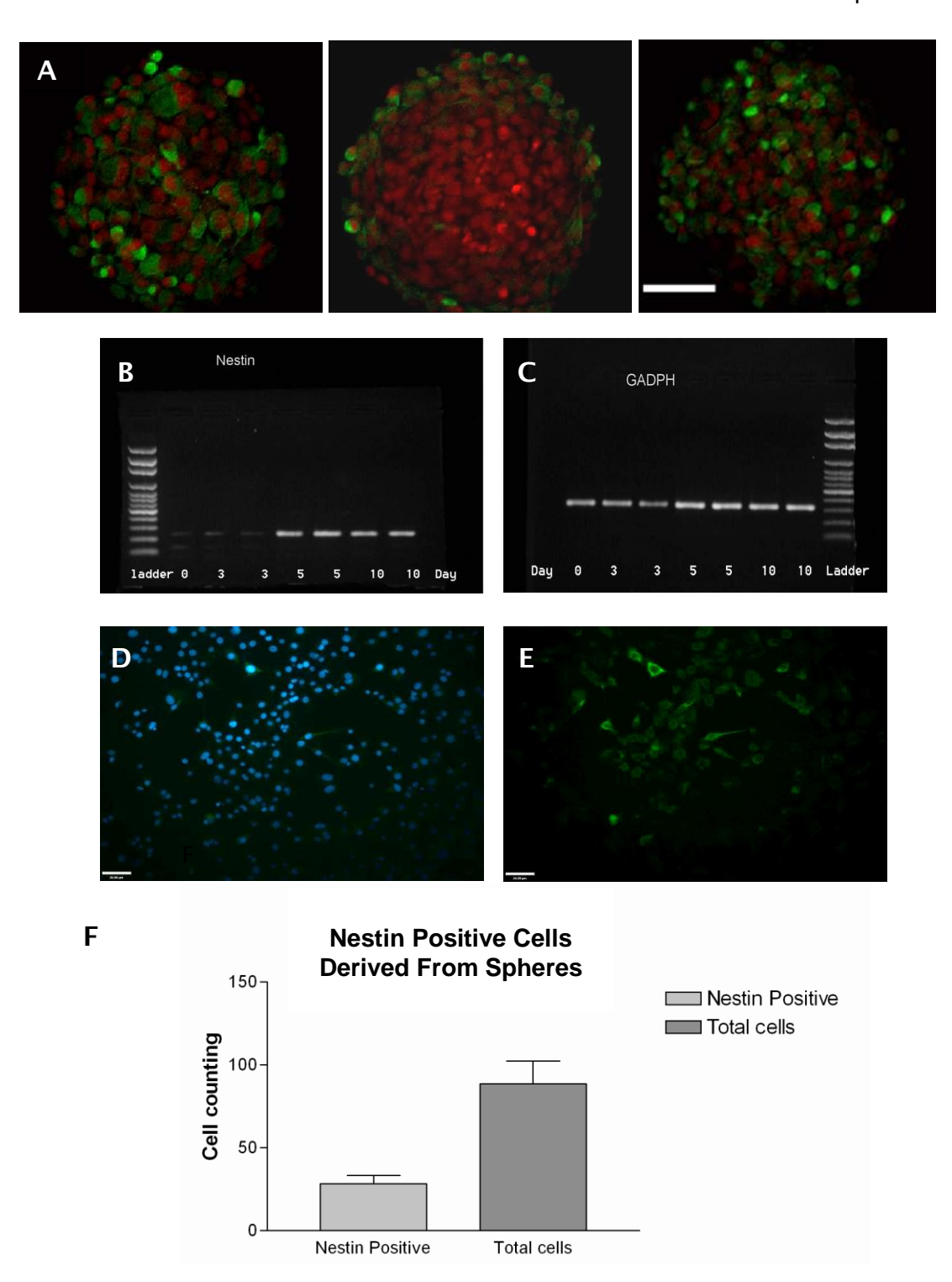


Figure 3-15 Expression of Nestin in adult corneal limbus derived spheres.

(A) Nestin positive progenitor cells (green) were located at the periphery of the spheres. The images on the left and right represent the two opposite surfaces of a sphere, while the middle image is a cross-section. Nuclei were counterstained with Sytox Orange. Scale bar: 50µm (B, C) Expression of nestin was confirmed by RT-PCR. The time of nestin appearance is concurrent with sphere formation. GAPDH was used as the house keeping gene. (B-E) Sphere cells were redissociated and seeded on P-D-L and laminin coated plates 24 hrs prior to anti-nestin immunostaining (green); nuclei were counterstained with DAPI. Scale bar: 25 µm. (F) Quantification of nestin positive cells vs. total cells.

We analyzed the three-dimensional distribution of nestin in spheres derived from adult mouse corneal limbus by immunocytochemistry. We found that nestin positive cells were mainly distributed around the periphery of spheres. This is consistent with neurospheres derived from neonatal rat and mouse forebrain [73]. However, the number of cells expressing nestin was reduced compared to neurospheres derived from the CNS. Approximately 32.57 ± 2.15% of cells expressed nestin after monolayer culture. This may be due to different cell origins or a portion of cells may have differentiated. Moe *et al.* undertook a semi-quantitative immunohistochemical analysis of adult human CB and SVZ spheres. Approximately 50% of cells within CB spheres were found to be weakly positive for nestin, while SVZ staining was much more apparently positive [181]. However, their results are not comparable to our own result as quantitation was based on weak staining, and may have been somewhat subjective. To determine the level of nestin expression, comparison with homogenous CNS derived neurosphere using quantitative RT-PCR or Western Blotting would therefore be more objective and reliable.

# 3.4.3 Expression of neural stem cells marker Sox2, Musashi1

Sox2 (Sex determining region Y-box 2), is a transcription factor that is essential for stem-cell maintenance in the CNS. It has been suggested as a universal neural stem cell marker, from embryo to adulthood [104]. Musashi1, a neural RNA-binding protein, is found selectively expressed in neural stem/ progenitor cells derived from the CNS.

Immunolabeling using anti-Sox2 showed staining localized to both the nucleus and cytoplasm in sphere derived cells (Figure 3-17). Different intracellular distribution of Sox2 in adult stem cells has previously been reported. Cytoplasmic Sox2 staining has been demonstrated in the trophectoderm of the mouse blastocyst and inner cell mass [187] as well as in hESC colonies [188]. In addition, the location of the Sox2 protein in adult ciliary margin-derived neurospheres has been reported in both the nucleus [189] and cytoplasm [137]. The reason for this redistribution of nuclear proteins to the cytoplasm remains uncertain. Observation of the Sox2 protein in the cytoplasm may reflect the start of cell differentiation when intracellular nuclear and nucleolar proteins are redistributed to the cytoplasm. Tu *et al.* reported that during the differentiation process of hematopoietic stem cells, different nuclear proteins showed noticeable redistribution to the cytoplasm [104]. Meanwhile, the use of different commercial antibodies may also lead to different intracellular distribution, especially in adult stem cells [190]. Zuk *et al.* tested commercial antibodies from different manufacturers, and found that the pluripotent nuclear markers OCT4, Sox2, and Nanog presented

distinctly different intracellular expression patterns when different commercial antibodies were used [191].

The expression of Sox2 was detected at both the RNA and protein level from limbal spheres as demonstrated in Figure 3-16. Sox2 was consistently expressed after spheres were generated and passaged for over 20 days (the maximal investigated time) as shown by RT-PCR. The expression of musashi1 was concomitant with Sox2 as shown on RT-PCR, suggesting neural potential was obtained following sphere formation.

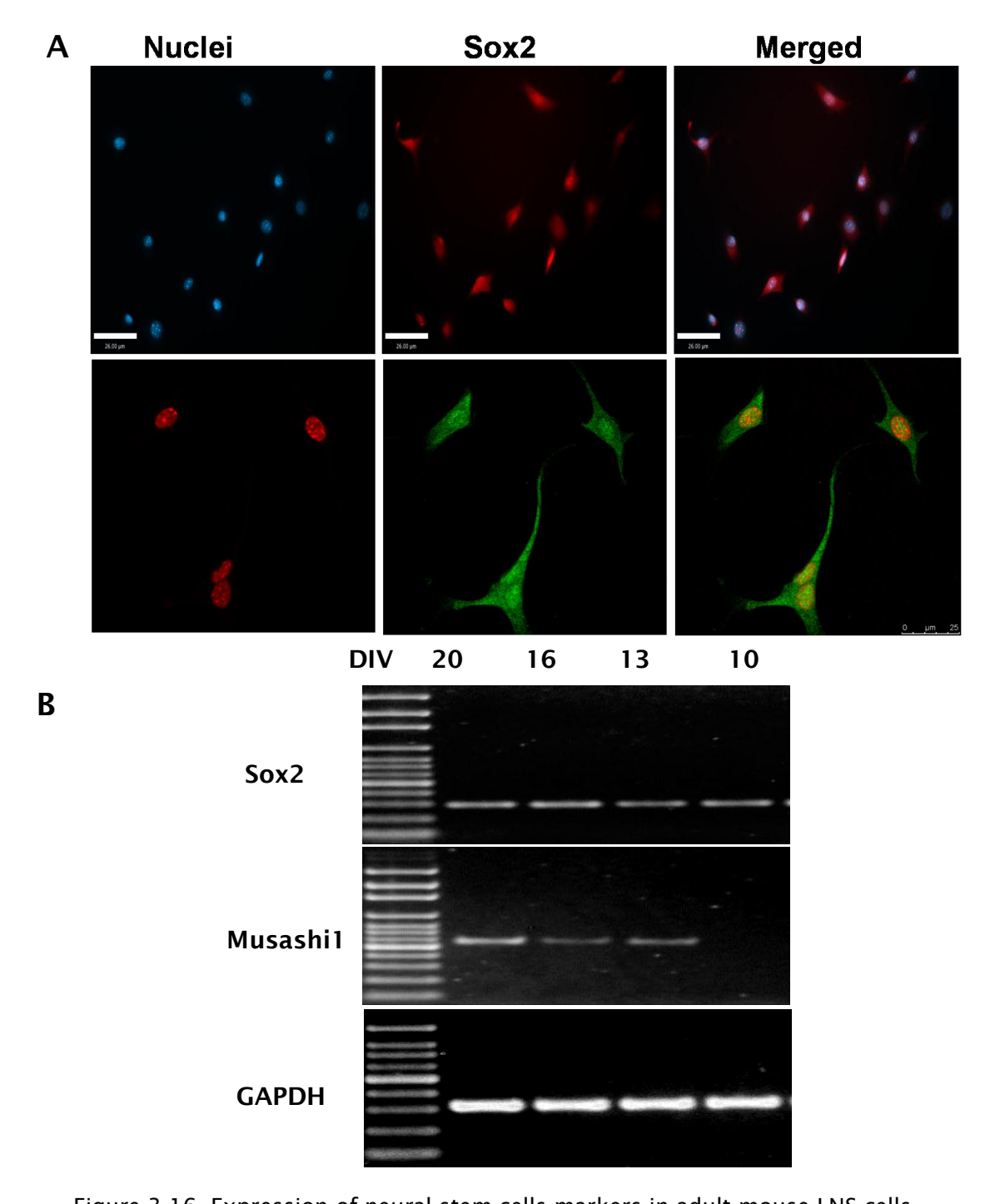


Figure 3-16 Expression of neural stem cells markers in adult mouse LNS cells. Sphere cells were re-dissociated and seeded on P-D-L and laminin coated plates 24 hrs prior to anti-Sox2 immunostaining. The fluorescent image (upper panel) and confocal images (lower panel) again demonstrate localisation of the Sox2 protein in both the nucleus and cytoplasm of the derived mouse LNS cells Scale bar- 25 µm (A). Sox2 and Musashi1 were detected from spheres by RT-PCR. Samples represent spheres cultured *in vitro* at different time point (DIV 10-20 days) Sox2 was stably expressed from DIV 10 to DIV 20 (maximal investigated time). Housekeeping gene, GAPDH was used as an internal control (B).

## 3.4.4 Expression of early differentiation neuron marker beta III tubulin

Beta-III tubulin is an early commitment marker of neuronal lineage specificiation in the primitive neuroepithelium. It is regarded as a neuron-specific marker. The antibody Tuj1 used is only reactive with neuron-specific beta-III tubulin but not with other beta tubulin isotypes in glial cells. Approximately  $31.10 \pm 3.41\%$  of corneal limbal sphere cells were positive for Tuj1 (Figure 3-17 A-C). The expression of beta-III tubulin has also been confirmed with RT-PCR using specific primers (Figure 3-17 D-E). In addition, the time at which beta-III tubulin was initially detected is in line with the time at which primary spheres form (5 DIV). The expression level remained stable in secondary and tertiary spheres up to 20 DIV (the maximal investigation time).

# 3.4.5 Lack of expression of epithelial lineage markers

To identify the origin of the sphere cells derived from the corneal limbus, two epithelium markers P63 and Cytokeratin 12 (K12) were used for immunocytochemistry and RT-PCR (Figure 3-18). The former is an epithelial stem cell marker which plays an essential role in the initiation of epithelial stratification and maturation as well as maintenance of the proliferative potential of basal keratinocytes [191]. K12 is specific for corneal keratin, composed of an intermediate filament cytoskeleton, and is seen in mature and late TAC corneal epithelial cells [22,192].

Freshly dissociated corneal limbal cells expressed high levels of K12 and P63. However, K12 expression decreased during primary sphere formation and disappeared upon secondary sphere formation. P63 was not detectable, by RT-PCR, after three days in sphere forming culture. Immunocytochemistry also confirmed this lack of corneal epithelial stem cells in the generated spheres. Together, these results suggested that the serum free culture system, in the presence of EGF and FGF2, did not promote proliferation or maintenance of mature or undifferentiated corneal epithelial lineage cells.

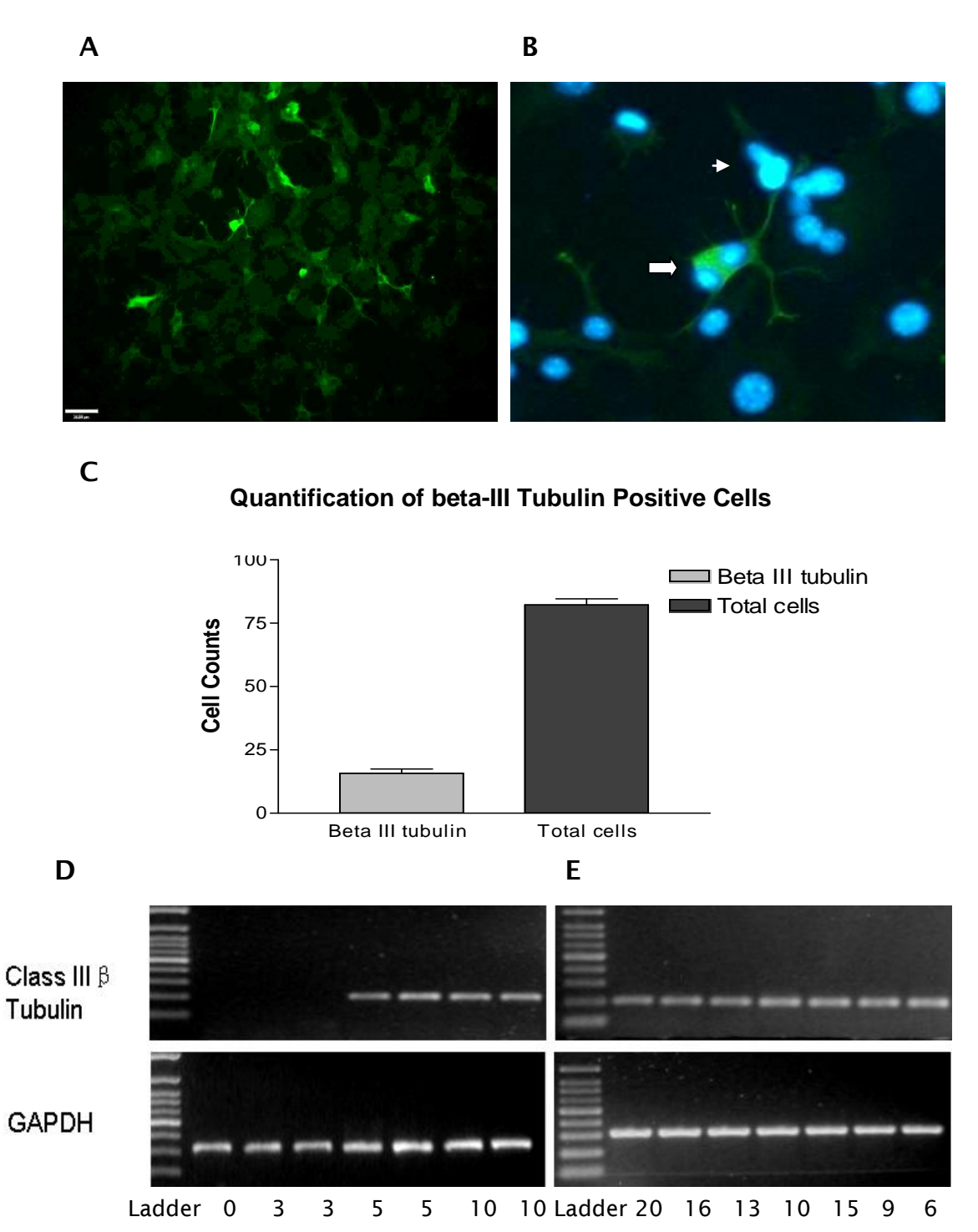


Figure 3-17 Expression of beta-III tubulin in adult corneal limbus derived spheres. **(A-B)** Sphere cells were subjected to monolayer culture for 24 hrs prior to anti beta-III tubulin immunostaining. Beta-III tubulin (green, arrow) was detected in sphere cells. Nuclei were counterstained with DAPI. Arrowhead indicates negative cells. Scale bar: 25 µm. **(C)** Quantification of beta-III tubulin positive cells vs. total cells. **(D-E)** Expression of beta-III tubulin was confirmed by RT-PCR. The numbers represent days in culture. The time of beta-III tubulin appearance is concordant with sphere formation (5 DIV), with stable expression up to 20 DIV (the maximal time investigated).



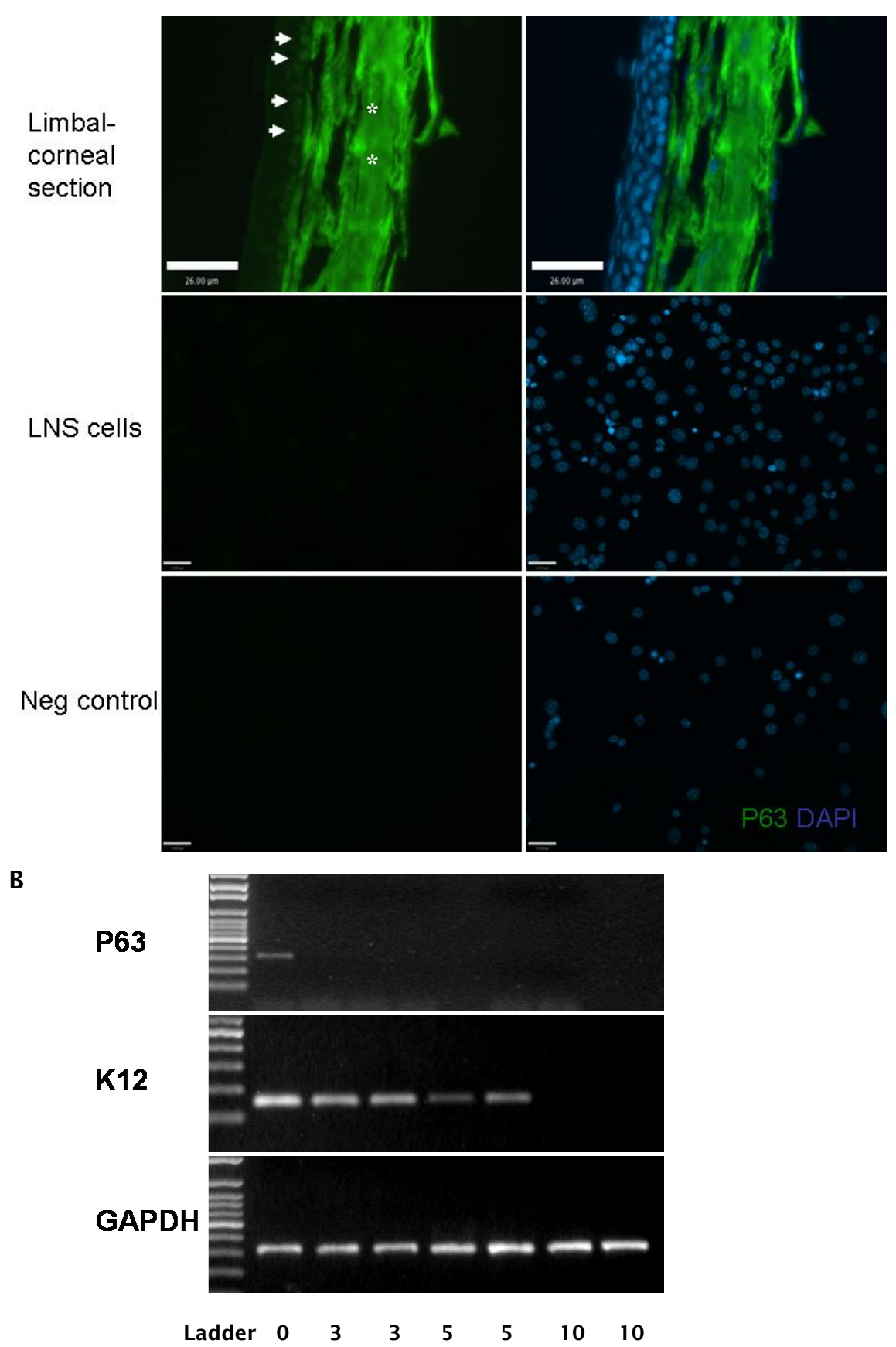


Figure 3-18 Expression of epithelial lineage markers during sphere forming culture.

(A) Immunocytochemistry analysis was negative for P63 in sphere cells (13 DIV). Representative images of P63 staining are shown on the left (green). Cell nuclei were counter stained with DAPI on the right (blue). Adult mouse limbal-corneal tissue was used as a positive control. White arrows indicate P63 positive cells in the basal layer of corneal epithelium (green). Non-specific staining was present throughout the stromal layer (\*). Negative controls were performed by omission of the primary antibody. Scale bar: 26 µm. (B) RT-PCR showed epithelial lineage markers P63 and K12 were highly expressed in freshly isolated corneal limbal cells (day 0); expression significantly decreased or was absent following sphere formation. Numbers represent number of days in culture. Primary spheres were passaged at 7 DIV.

# 3.4.6 Clonal growth corneal limbal cells are neural crest derived stem/ progenitor cells

Twist gene homolog 1 (Twist) belongs to bHLH factors, and it has been shown to play an essential role in developmental of diverse systems including neural crest cell migration and differentiation [22]. SRY-box containing gene 9 (Sox9), is expressed in the prospective neural crest and functions as a regulator for neural crest development [193]. We found that neural crest markers Twist, Sox9 and Snail were strongly expressed or detectable in adult corneal limbus derived spheres. Other stem cell markers, especially mesenchymal lineage stem cell markers such as Vimentin (Vim), CD34 antigen (CD34) and lymphocyte antigen 6 complex locus A (Sca1) and Prominin 1 (CD133) were also highly expressed in sphere cells (Figure 3-19). Only a very low level of Snail was detected in spheres derived from adult mouse corneal limbus (Figure 3-19A), although higher levels of Snail have been reported using juvenile mice [194,195]. We summarize that limbal spheres are likely to be derived from neural crest mesenchymal stem/progenitor cells, and not from cells of an epithelial lineage. Thus is possibly that the sphere are actually derived from the corneal stroma.

Sosnová *et al.* reported that CD34 positive corneal stromal cells are bone marrow-derived, by showing that in intact corneal stromal tissue, the majority of CD45 cells co-expressed CD34, while no CD34 positive/CD45 negative cells were detected [148]. CD45, a hematopoietic cell marker protein tyrosine phosphatase receptor type C, was not however detected in freshly dissociated or cultured corneal limbal cells as shown in Figure 3-19A. The lack of CD45 expression is suggestive that sphere cells are non-hematopoietic cells, but were derived from limbal neural crest mesenchymal tissue, which is consistent with the finding of Yoshida *et al.* [196].

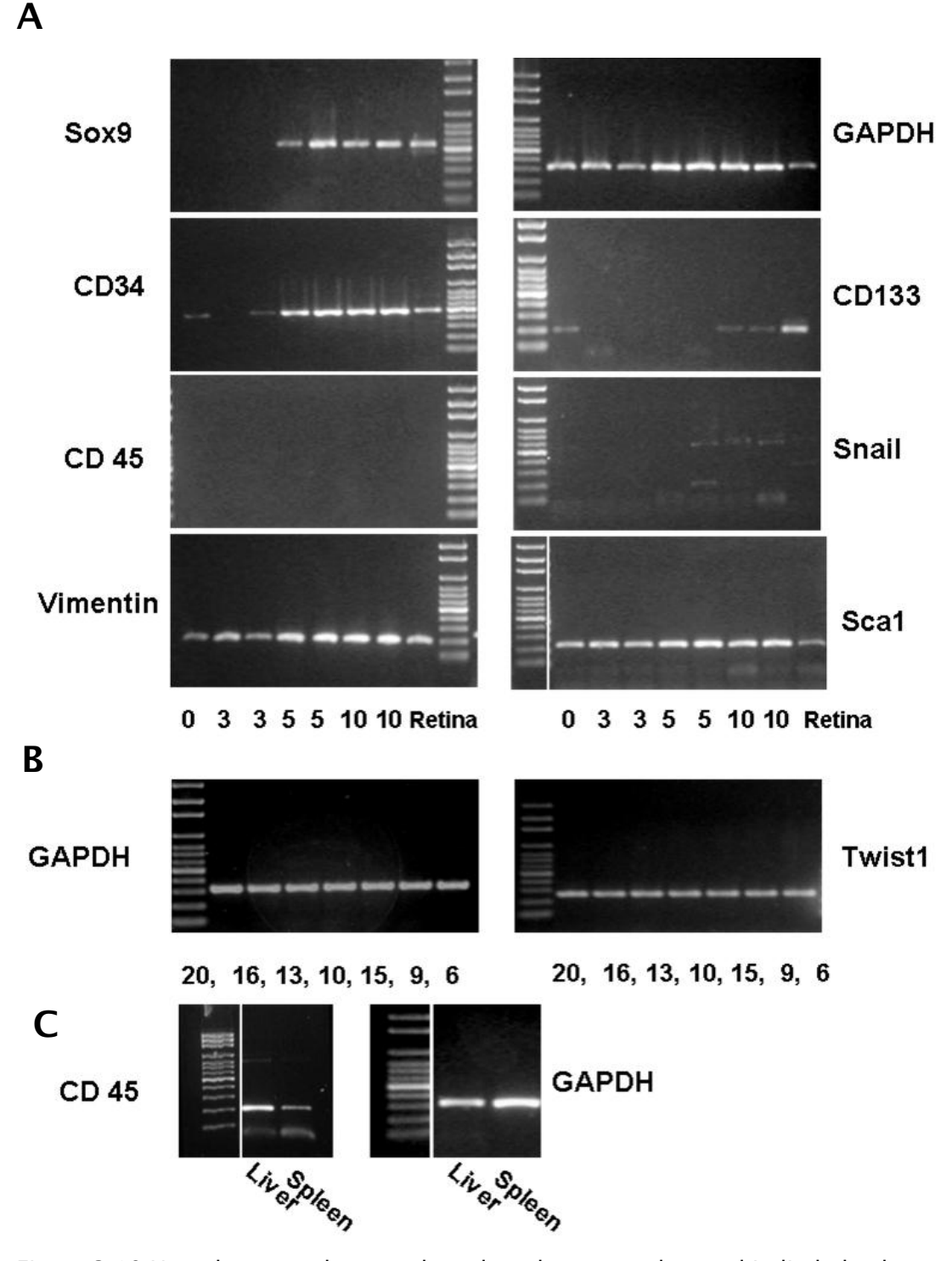


Figure 3-19 Neural-crest and mesenchymal markers were detected in limbal sphere cells. **(A)** RT-PCR shows expression of neural crest and mesenchymal markers on adult mouse limbal cells in sphere forming culture condition. Sca1 and Vimentin were consistently expressed in all samples. Numbers represent number of days in culture. Limbal spheres were passaged every 7 DIV. **(B)** Stable expression of Twist1 in secondary and tertiary LNS (DIV 9-20). **(C)** Liver and spleen tissue were used as positive controls for CD45 specific primers. Internal control: GADPH.

# 3.4.7 Effect of Noggin on gene expression of LNS cells

Noggin is a BMP4 inhibitor. It has been reported to assist acquisition of neural progenitor properties by limbal epithelial cells in neurosphere culture assays [90]. Therefore I assessed the effect of Noggin on gene expression during LNS generation. Limbal cells were cultured in optimal neurosphere culture medium (DMEM: F12 GlutaMAX™, 2% B27-, 20ng/ml EGF and 20ng/ml FGF2) in the presence or absence of 100ng/ml Noggin [6]. As demonstrated by RT-PCR in Figure 3-20, the samples cultured in the presence or absence of Noggin had similar levels of transcript expression on epithelial or neural lineage markers. They also acquired neural potential at the same timepoint. In addition, neural crest markers remained abundant following LNS generation.

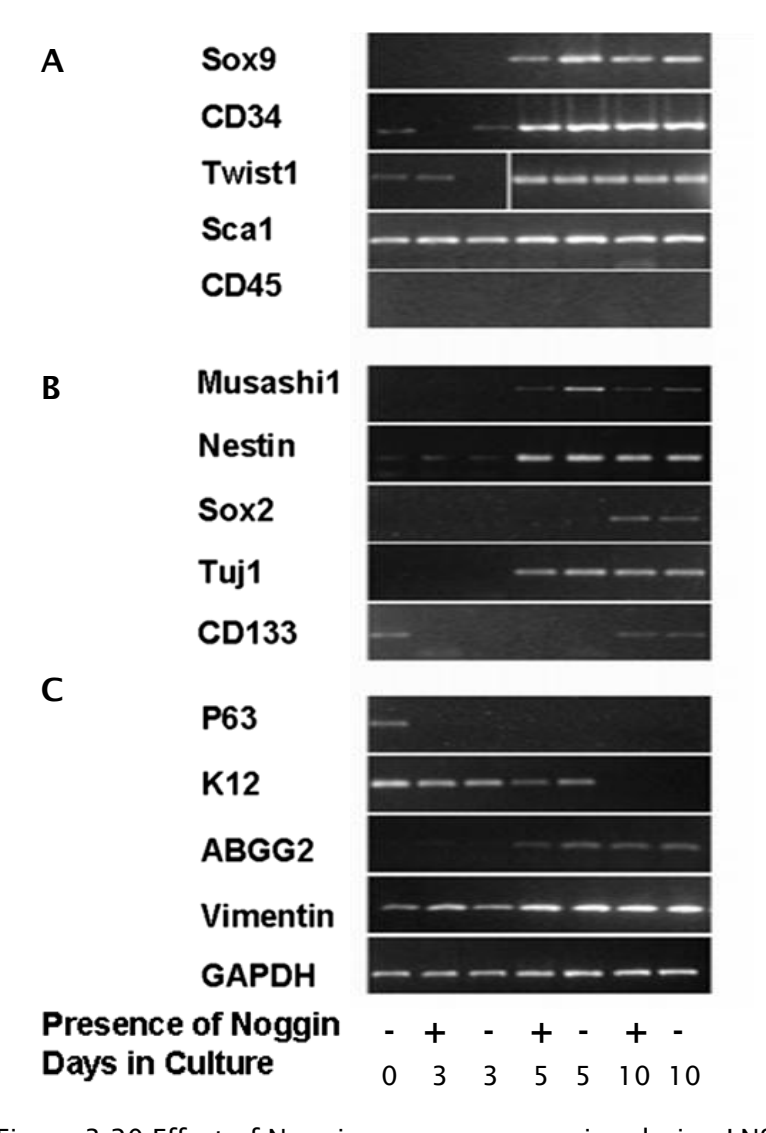


Figure 3-20 Effect of Noggin on gene expression during LNS generation.

Freshly isolated limbal cells were cultured in DMEM: F12 GlutaMAX™, 2% B27-, 20ng/ml EGF and 20ng/ml FGF2 in presence or absence of 100ng/ml Noggin. Cells were collected at day 0, 3, 5 and 10 during sphere culture. RT-PCR was conducted using gene specific primers. Day 0: Freshly isolated limbal cells. Day 1-3: No spheres detected; Day 5: Primary spheres detected; Day 10: Secondary spheres. PCRs show similar expression levels of neural crest markers (A), neural lineage markers (B), epithelial markers (P63, K12), and stem cell markers ABCG2 and Vimentin (C) on limbal cells during NS culture. GAPDH was used as internal control.

## 3.4.8 Lack of expression of retinal markers on limbal cells

To exclude the possibly of contamination from retinal or RPE cells, ranges of retinal progenitor cell markers (Pax6, Chx10, NeuroD, Crx), photoreceptor cell markers (Rhodopsin, Rhodopsin Kinase, Opsin, Recoverin) and RPE cell markers (CRALBP, bestrophin and RPE65) were investigated on fresh isolated limbal cells (div0) using RT-PCR (Figure 3-21). Freshly isolated limbal cells did not express any of these markers, except for Pax6, the eye develop master gene. The results suggest the generation of LNS is not due to contamination from either retinal cells or RPE cells during dissection. Pax6 has an essential role in the development of the retina as well as anterior of the eye [6]. It expressed on corneal epithelial stem/progenitor cells throughout the life [17,197]. Therefore, the observation of Pax6 is most likely due to cells from corneal/limbal epithelial cells.

During NS culture, LNS did not express retinal lineage markers such as Chx10 or Pax6. This also excludes the possibility of contamination from CB derived stem-like cells, where certain retinal progenitor cells markers were expressed using neurosphere culture [147,198]. Pax6 expression disappeared after 3 days in serum free neurosphere culture. This is concurrent with expression of P63, the epithelial stem markers, during the LNS culture (Figure 3-18). This is possibly due to the selective growth of neural crest limbal cells; whilst epithelial lineage cells were gradually eliminated.

Together, these results suggest generation of neurospheres from adult mouse limbus is not due to contamination of retinal, RPE or CB tissues. Retinal/RPE specific marker was absent throughout LNS generation.

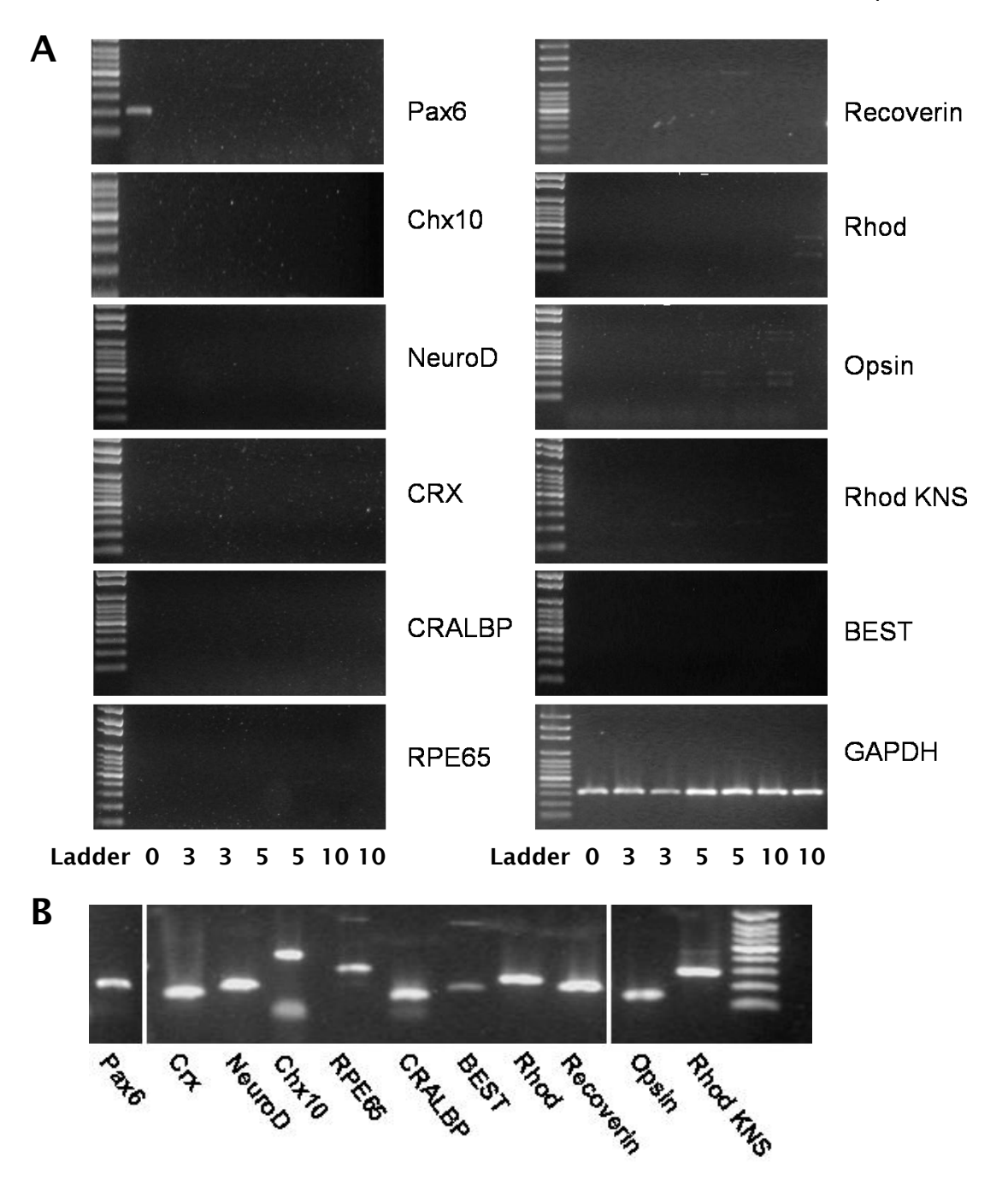


Figure 3-21 Lack of retinal markers on limbal cells

Freshly isolated limbal cells were cultured in DMEM: F12 GlutaMAX<sup>™</sup>, 2% B27-, 20ng/ml EGF and 20ng/ml FGF2. Cells were collected at day 0, 3, 5 and 10 during sphere culture. RT-PCR was conducted using gene specific primers. Day 0: Freshly isolated limbal cells. Day 1-3: No spheres detected; Day 5: Primary spheres detected; Day 10: Secondary spheres. PCR shows the absence of retinal progenitor cell, photoreceptor cell and RPE cell markers on freshly isolated limbal cells and NS cells. Pax6 was detected in freshly isolated limbal cells, was undetectable during LNS generation. GAPDH was used as internal control (A). Primers were validated using pooled cDNA from mouse retinal and RPE cells (B). Abbreviations: Rhod: Rhodopsin; Rhod KNS: Rhodopsin Kinase; BEST, Bestrophin.

# 3.5 Differentiation of LNS cells along neural lineage

We performed preliminary differentiation experiments by withdrawal of mitogens from tissue culture medium, followed by supplementation with  $1\mu$ M retinoic acid and 1-2% FBS in differentiation medium. Limbal spheres were re-dissociated and plated on to P-D-L and laminin coated plates. After 2-5 days, approximately 45% and 30% of total cells were immunopositive for Neurofilament 200 (NF) and Glial Fibrillary Acidic Protein (GFAP) respectively (Figure 3-22). However, we did notice that cells did not present typical neural morphology; this may be indicative that cells have not reached a fully mature neuronal or glial phenotype.

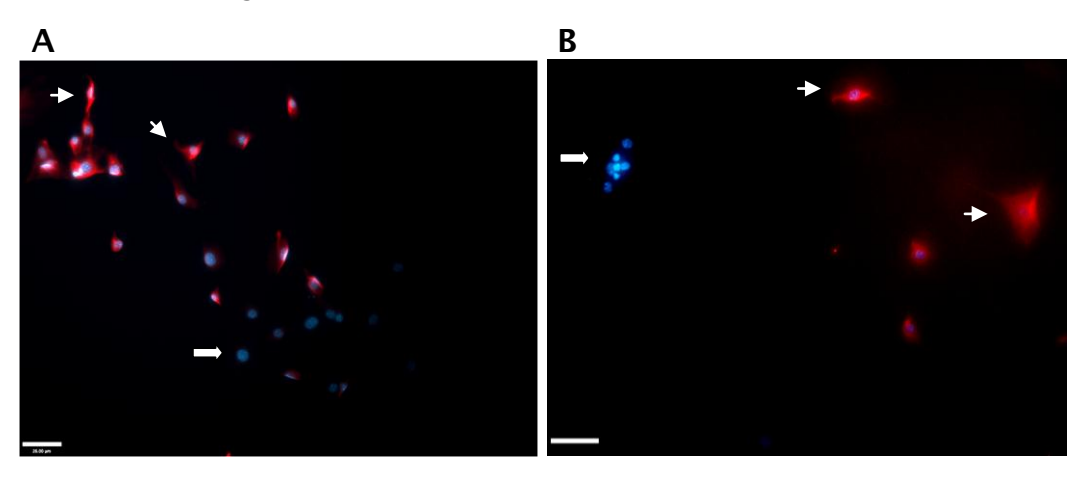


Figure 3-22 Differentiation along neuronal and glial lineages EGF and FGF2 were withdrawn, and culture medium was supplemented with  $1\,\mu\text{M}$  retinoic acid for 2-5 days, cells from limbal sphere expressed neurofilament 200 (A) and GFAP (B). Immunostained cells showed red staining in cytoplasm (arrowheads) Nuclei were counterstained with DAPI (Blue). Arrows indicate immunonegative cells. Scale bar  $25\mu\text{m}$ 

# 3.6 Discussion

#### 3.6.1 Overview

Cell therapy or transplantation is a very attractive treatment approach for degenerative diseases. However, it has proven difficult to identify practical sources of cells to generate sufficient functional tissue specific cells. Adult stem/progenitor cells isolated from surgically accessible tissues are an attractive source of autologous cells for transplantation purposes. This would not only avoid host-graft immune responses but also eliminate ethical issues and health risks associated with using certain cell sources such as ESCs [199].

The research detailed in this chapter characterises cells derived from adult mouse corneal limbus in respect of their self-renewal capacity, neural potential and origin. Limbal progenitor cells have characteristics which are reminiscent of NSC in a number of respects, indicating that limbal cells may have the potential to be a candidate resource for cell therapy.

# 3.6.2 Corneal limbal stem/progenitor cells display self-renewal and proliferative capability

Using serum free medium supplemented with mitogens, a system which is widely used for NSC derivation, we first investigated whether neurospheres could be generated from adult mouse corneal limbal cells. We found that a subpopulation of cells displayed clonogenic growth and formed neurosphere-like three dimensional structures. The culture system did not support mature cell growth, with approximately 5% of the initially isolated cells remaining after three days in culture. From a typical  $(1\times3 \text{ mm})$  limbus from one mouse eye, approximately 300 primary neurospheres were generated (diameter ≥50µm) after 7 days in vitro. Spheres could be passaged, with the ability to give rise to further generations of spheres. Sphere cells expressed proliferating cell nuclear antigen indicative of active proliferation and were highly propagated. Following one month, in this sphere forming culture assay, around  $4.5 \times 10^6$  progenitor cells could be harvested. We demonstrated that a very limited amount of limbal tissue could provide sufficient progenitor cells for further manipulation and/or transdifferentiation. This is advantageous for cell replacement purposes, where sufficient cells are required for integration, connection and restoration of function.

We then investigated whether the spheres formed in this assay system were derived from single cells by clonal growth, using a serial dilution assay. An extremely low initial seeding density (5-10 cells/well) was used to completely eliminate the possibility of cell aggregation. Secondary spheres were generated at low densities, indicating the presence of stem/progenitor cells in limbal spheres which are capable of self-renewal.

# 3.6.3 Limbal spheres have a similar ultrastructure to neurospheres, but may be generated through a different signaling pathway

Studies have characterised the ultrastructure of three dimensional neurospheres from the CNS [200] or neurosphere-like structures from the CB of the eye [104,172]. To date, no work has been published describing the ultrastructure of limbal spheres. We found that limbal spheres were not merely cell aggregates, but rather organised three dimensional structures with defined intracellular junctions. Similar to neurospheres from SVZ [104] gap junctions, which mediate chemical/ electrical communication and signalling between coupled cells, were demonstrable. Typical epithelial junctions, such as desmosome-like and tight junction-like connections which are found in CB spheres [104,172], were absent in limbal spheres. Consistent with the potent proliferative capacity of these limbal spheres mitosis was apparent in sphere cells.

Previous studies have demonstrated that neurospheres from the CNS exhibit responsiveness to both EGF and FGF2 in terms of the number of neurospheres generated and also proliferation rate [104]. The sphere forming assay used in this study showed that limbal spheres were also FGF2 dependant, while the presence of EGF alone failed to generate any spheres. This is consistent with non-neural sources of neurospheres for instance from dental pulp [172]. The difference in responsiveness to mitogens, EGF between limbal cells and NSC may imply different signalling pathways in their cell growth and proliferation.

Ciccolini et al identified neural precursors responding to both EGF and FGF-2 from mouse embryonic day 14 (E14) striatum [201]. By assessing phosphorylation of the cAMP response element-binding protein, the cells were found to initially respond to FGF-2 only, and acquire EGF responsiveness later during *in vitro* development, suggestive FGF2 promotes the acquisition of EGF responsiveness. In this study, although use of EGF alone in the culture system did not appear to generate corneal limbal neurosphere-like clusters, the combination of EGF and FGF2 demonstrated a synergetic effect and significantly increase the number of spheres in all of the

experiments carried out. The synergetic effect appears to be initiated and promoted by FGF2 too.

To summarize, limbal spheres display ultrastructural similarities with neurospheres of the CNS. They are not responsive to mitogens EGF alone, suggestinge they may be regulated through different signaling pathways.

# 3.6.4 Origin of corneal limbus derived progenitor cells

IPE cells have previously been reported to be capable of forming small spheres in NS culture assay in the presence of EGF and FGF2 [171]. However, when we cultured homogenous mouse IPE cells, following the same dissociation process used for corneal limbal cells, no NS-like structures were formed. This conflicting result may be due to the dissociation procedure used for corneal limbus tissue, which may not have been suitable for IPE cells, leading to poor IPE cell viability following digestion. Homogenous IPE cells presented as small flat and irregular clumps of heavily pigmented cells, which had a very distinct morphology compared to the three dimensional spheres formed from limbal tissue. Furthermore, reports have demonstrated that both CB and IPE derived spheres remain pigmented following sphere formation, with apparent melanosomes detected in both nestin positive and negative sphere cells [137]. In our limbal derived spheres, TEM analyses demonstrated a lack of melanosomes. Therefore, it can be concluded that limbal spheres were not derived from pigmented tissue of the CB or IPE.

The adult mouse corneal limbus and peripheral cornea contain three different cell types namely epithelium, keratocytes and endothelium. Using the same sphere culture assay, Zhao *et al.* reported isolation of progenitor cells from adult rat limbal epithelium, while others have derived progenitor cells from the stroma and endothelium of mice, rats, rabbits and humans [137,172,202]. The corneal and limbal epithelium layer develop from the epithelium of the ectoderm, while both the corneal stroma and endothelium layers are mainly derived from neural-crest mesenchymal cells, which originate from the neuroepithelium. We therefore investigated the origin of limbal derived spheres using neural crest development and migration markers.

Neural crest markers twist1, Sox9 and Snail were found to be strongly expressed or detectable in adult corneal limbus derived spheres. Concomitantly mesenchymal lineage stem cell markers including Vimentin (Vim), CD34 antigen (CD34) and lymphocyte antigen 6 complex locus A (Sca1) were also highly expressed in sphere cells. This is indicative that subpopulation of limbal derived progenitor cells originate from neural-crest mesenchymal progenitor cells.

Corneal epithelium stem cells which constantly repopulate the corneal surface reside in the basal limbal layer [29,30,33,90,134,148,203]. To determine whether there are a mixed population of corneal epithelium stem cells in the limbal derived spheres, we investigated the expression of epithelium lineage markers P63 and K12 [20]. The former is a well-known epithelial stem cell marker and the latter is expressed in mature

corneal epithelial cells and their late TACs. The expression of these two epithelial markers decreased and eventually disappeared during limbal sphere formation. Umemoto et al. demonstrate that the rodent corneal epithelial SP, represents corneal epithelial stem cells which are quiescent and do not have proliferative capability in vitro [192,198]. This is consistent with our findings that P63 expression was not detectable after three days in culture. Limbal sphere cells are more likely to be derived from stromal progenitor cells than from corneal epithelial stem cells because of the following evidence: 1) the increase of neural crest markers coinciding with a decrease in epithelial lineage markers; 2) selective growth features observed during sphere culture, with over 90% of cells eliminated during the first three days culture; and 3) a lack of typical epithelial junctions such as desmosomes or tight junctions within sphere cells. The current study cannot eliminate the possibility of a subpopulation of immature epithelial TAC which have transdifferentiated to neural crest progenitor cells. Although this study provides a number of clues that LNS cells mostly likely originate from neural crest derived limbal stroma cells, it does not provide direct evidence. A transgenic animal model that tags neural-crest originated cells would be ideal for this purpose. Yoshida et al. [34] cultured corneal neurospheres from transgenic mice encoding PO-Cre/Floxed-EGFP as well as Wnt1-Cre/Floxed-EGFP. In these transgenic mice, cells of a neural crest origin expressed GFP. The derived corneal neurospheres were GFP positive, indicating their neural crest origin. The markers detected on LNS in this study are consistent with Yoshida's cells of a neural crest origin.

Despite following the same culture system and dissociation methods, our results differ from the findings of Zhao et al., which considered that spheres with neural potential from the rat limbus were of an epithelial origin [90]. Although the author suggested that these cells were not derived from the limbal stroma, the possibility of neural crest derived stromal cells cannot be completely eliminated for a number of reasons. Firstly, there was no investigation of any neural crest markers in the sphere cells. Secondly, the author demonstrated that the decrease of P63 expression during primary neurosphere culture was concurrent with an increase of neural stem cell markers such as Nestin and Musashi 1. This may not be the primary reason that "epithelium cells acquired neural properties" since the NSA is a selective growth system. It may actually be that the culture system does not support, and actually leads to the gradual elimination of P63 positive cells; meanwhile allowing other types of progenitor cells with intrinsic neural potential to proliferate. Thirdly,  $\alpha$ -enolase, a multifunctional metabolic enzyme that has been suggested as a corneal epithelium stem cell marker [6,158], should not be considered as an epithelium-specific marker as it is widely expressed on cells of a mesenchymal origin including hematopoietic, epithelial and endothelial cells [22] and also limbal stromal mesenchymal cells [204]. Therefore, the

co-localization of nestin with  $\alpha$ -enolase in limbal derived sphere cells [31] does not necessarily lead to epithelium cells acquiring neural properties. In our limbal derived spheres, we observed a decrease of P63 which coincided with an increase of neural stem cell and neural crest markers; this may indicate the selective growth of progenitor cells originating from the neural crest. Sphere generation was not affected by the BMP4 inhibitor noggin, which suggests that cells possibly possessed intrinsic neural potential.

Bone marrow derived stem cells have been shown to possess extensive differentiation capacity and to be distributed throughout the whole cornea [158]. By transplantation of BM stem/progenitor cells from enhanced GFP (eGFP) transgenic mice into irradiated wild type mice, Nakamura *et al.* observed distribution of GFP cells throughout the cornea, with a concentration in the peripheral corneal and limbal stroma. Most of the GFP positive cells in the recipient's cornea expressed CD45, a protein tyrosine phosphatase (PTP), specifically expressed in hematopoietic cells [89,205]. Following this idea, we investigated if CD45 was expressed in our limbal derived spheres. A lack of CD45 expression in our limbal sphere cells indicated that our cells were not derived from bone marrow, but were locally sited stem/progenitor cells. This finding is consistent with previous *in vitro* studies on cultured stem/ progenitor cells from corneal stroma using the same culture system [205].

In summary, our study demonstrates that the stem/progenitor cells derived from adult mouse corneal limbus are neural crest derived mesenchymal cells, possibly from the limbal and peripheral corneal stroma. Precise dissection of corneal limbal stromal tissue will be helpful to determine cell origin, and this can only be achieved using eyes from larger animal models or human donor eyes.

# 3.6.5 Neural potential of adult mouse corneal stem/ progenitor cells

The stem/progenitor cells derived from adult mouse corneal limbus via sphere forming assay expressed neural stem cells markers including Sox2, Nestin, Musashi1 and CD133 as well as the early differentiated neural marker beta III tubulin. Following 48 hrs in differentiation conditions in the presence of a low percentage of serum and retinoic acid, low levels of neurofilament 200 and GFAP were detected in limbal cells, indicating the potential for differentiation along both neuronal and glial lineages. This is consistent with other studies of corneal stem/progenitor cells of a neural crest origin [90,148].

Neural potential has been demonstrated from corneal stroma derived progenitor cells from mice, rats, rabbits and humans [30,90], suggesting this characteristic is not restricted to species. Other studies also point to the multipotentiality of corneal stromal stem/progenitor cells [29,30,33,90,134,148,203]. Besides neural potential these cells are capable of differentiation into glial cells, adipocytes and/or chondrocytes. Although non-neural lineage potential is not the purpose of this study, further investigation would fully characterize the potential of limbal derived stem/progenitor cells.

## 3.6.6 Characteristics of progenitor cells from adult mouse corneal limbus

In conclusion, we summarize the characteristics of our limbal stem/progenitor cells derived by a NS assay in Table 3-1. The stem/progenitor cells derived from the corneal limbus have unique characteristics. Both neural stem cell and mesenchymal stem cell markers are present, but not retinal lineage markers. Neurosphere cells from adult CNS have been found to be committed to a neural fate and failed to differentiation along a retinal specific lineage [30,90,148]. We are optimistic that neural crest mesenchymal derived stem/progenitors possess more plasticity. Cells of the limbus are easily accessible from the surface of the eye, and have the ability to give rise to a significant number of progenitor cells in defined culture conditions. Limbal cells may therefore become a valuable source for autologous cell transplantation for degenerative retinal diseases.

Table 3-1 Characteristics of mouse limbal stem/progenitor cells compared with Neurospheres from CNS and neonatal retina

Marker	Limbal	Neurospheres	Neonatal retina
	spheres		(containing retinal progenitor
			cells)
Stem cell			
markers			
ABCG2	+ a	+ <sup>b</sup>	+ b
Neural stem			
cell markers			
Nestin	+ a	+ b	+ <sup>b</sup>
Musashi	+ a	+b	+b
Sox2	+ a	+ b	+ b
beta-III tubulin	+ a	+ b	+ b
CD133	+ a	+ b	+ <sup>a</sup>
Neural crest/			
Mesenchymal			
markers			
CD34	+ a	_ b	+ a
CD45	_ a	_b	_ a
Twist1	+ a		
Sca1	+ a		+ <sup>a</sup>
Snail1	+ a		_ a
Sox9	+ a		+ a
Vimentin	+ a	+ b	+ <sup>a</sup>
Eye field			
markers			
Pax6	+/- <sup>a</sup>		+ <sup>a,b</sup>
P63	_ a		
Cytokeratin 12	_ a	_b	
Rx	_ a		+ b
Crx	_ a		+ <sup>a,b</sup>
Nrl	_ a		+ b
Rhodopsin	_ a		+ a,b
Recoverin	_ a		+ a,b

<sup>+</sup> Positive, - Negative, Blank- yet to be tested;

<sup>&</sup>lt;sup>a</sup> Chapter 3, Fig. 13-21;

<sup>&</sup>lt;sup>b</sup>[86,206-208]

Xiaoli Chen Chapter Four

# 4 Chapter Four - Transdifferentiation of LNS cells towards Retinal-like Cells

# 4.1 Introduction

The limbus is readily accessible tissue. In Chapter 3, I demonstrated that LNS cells derived from the adult mouse limbus exhibit clonal growth and have neural potential. Previous studies also suggest that neural crest derived corneal stromal stem cells are multipotential and are capable of differentiation into neural cells, adipocytes and chondrocytes [179,209-211].

However, there is little known about whether neural crest derived LNS have the potential for differentiation into retinal specific neural cells. The determination of retinal cell fate, in particular towards photoreceptors, requires a comprehensive combination of intrinsic expression of transcription factors and extrinsic environmental factor-related signalling mechanisms [30,90]. Although adult stem cells have demonstrated plasticity and capacity for differentiation into cell types other than that of their origin [73,79,212-214], it is much more difficult for non-retinal lineage cells to transdifferentiate towards retinal specific phenotypes [89,91,105].

Photoreceptor-like cells can be induced from iris epithelium [89,91,105], CB stem-like cells [13,86,88,215], RPE cells [86,216], and Müller glial cells [168,217], which have the same origin as photoreceptor cells during early embryonic development. Over expression of a single or combination of several retinal development transcription factors is likely to drive these cells towards photoreceptor-like cells. However, the limbus and peripheral cornea has less common pathway with neural retinal cells than the above mentioned cell types. LNS cells originate from a transient layer called the "neural crest", while the retina develops from the neural ectoderm during early embryonic development (Figure 4-1). We noticed that retinal progenitor markers such as Chx10, and photoreceptor-specific transcription factor Crx were absent during neurosphere culture. In addition, the expression of the eye field master gene Pax6 gradually decreased during limbal cell culture in vitro, and was no longer detected following generation of primary LNSs (Figure 3-21, Chapter 3). Jomary et al. investigated the effect of exogenous Crx expression on human cornea-derived stem cells. Despite detecting several photoreceptor-specific proteins, human cornea-derived stem cells did not display light responsiveness when assessed with a cGMP enzymeXiaoli Chen Chapter Four

linked immunoassay [12]. As retinal fate determination requires activation of a comprehensive combination of intrinsic transcription factors, the over expression of single homeobox gene in LNS cells may not be sufficient to activate the relevant transcription network to drive them towards retinal lineages.

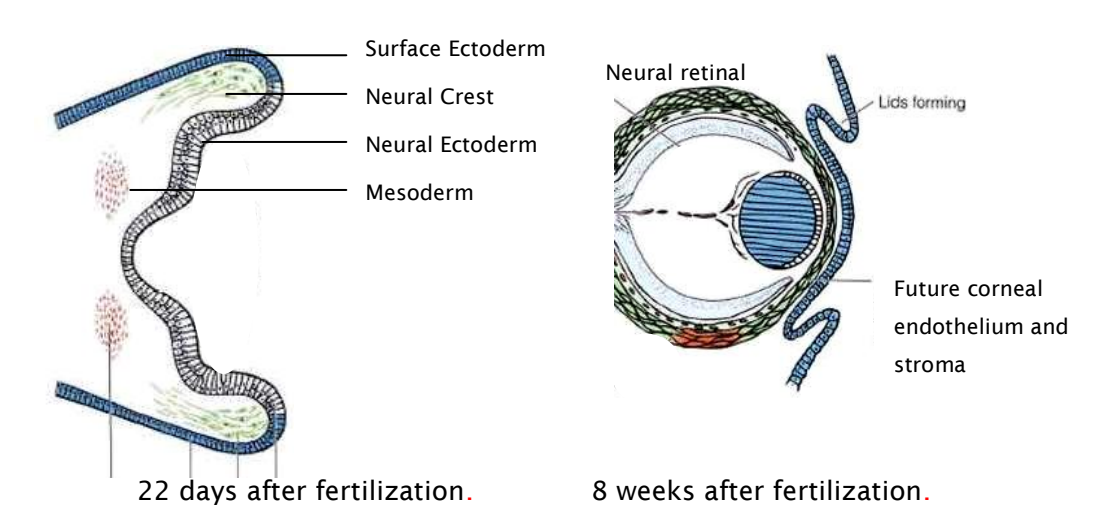


Figure 4-1 Human eye development.

These images illustrate the origin of the human eye. Corneal stroma and endothelium develop from the neural crest (Green), while the neural retina originates from the neural ectoderm (black). Adapted from Forrester *et al.* 2008.

Extrinsic environmental factors have also been shown to have an influence in promoting stem/progenitor cells differentiation into retinal cell phenotypes [8]. Watanabe and Raff (1990) demonstrated that uncommitted retinal progenitor cells (E15 retinal cells) can differentiate into rod photoreceptors when co-cultured with P1 retinal cells in vitro [6,159,161]. On the contrary, the generation of rod photoreceptors by P1 retinal cells was partially inhibited by co-culture with other type of cells or uncommitted retinal cells. This phenomenon indicates that P1 retinal cells produce signals that promote rod cell determination, differentiation and/or survival. By use of a co-culture assay, highly undifferentiated ESCs [160] or stem/ progenitor cells from non-retinal sources [110,161] expressed retinal and/ or photoreceptor specific markers in vitro. Although these short distance diffusible signals and their related signalling pathway(s) are unclear [159,161,218], co-culture with developing retinal cells has been used to investigate the potential of other cell types to commit to a retinal lineage [159]. In a study of rodent limbal neurosphere cells, photoreceptor markers including opsin and rhodopsin kinase were observed following co-culture with P1 retinal cells [6,159,161,215,218]. The activation of retinal transcription factors

Xiaoli Chen Chapter Four

including Nrl, Crx and other mature photoreceptor markers were detected. Therefore, to investigate the potential of neural-crest originated LNS cells for transdifferentiation into retinal lineage, co-culture with developing retinal cells is possibly more efficient.

The aim of this study was to assess the transdifferentiation potential of LNS cells, when exposed to a photoreceptor differentiation promoting environment. An *in vitro* coculture system was applied to allow neurotrophic factors released by neonatal retinal cells to direct the differentiation of LNS cells, omitting the possibility of cell contamination. The LNS cell morphology and ultrastructural features were monitored upon differentiation; the expression of retinal lineage specific markers was investigated at both a protein and transcript level.

#### 4.2 Methods

#### 4.2.1 Neonatal retinal cell dissociation and culture

Whole retinas were dissected from PN day 1-3 mice. Eyes were enucleated immediately following sacrifice by cervical dislocation. Following puncture of the sclera at the ora serrata with a 30G needle (BD Plastipak), the eyes were cut in half along the equator with microsurgical scissors. The retina detached from the posterior eye cup spontaneously. Following blunt separation from the optic nerve, retinas were collected into DMEM: F12 medium.

Enzymatic digestion, using a commercially available papain dissociation kit (Worthington-Biochemical, Berkshire, UK), was used for retinal cell dissociation as per manufactures' instructions. In brief, minced retinal tissue was incubated with a mixture of papain (20 units/ml) and DNase (0.005%) for approximately 40 min at 37°C. After gentle trituration, an equal volume of papain inhibitor containing 10% ovomucoid and 0.005% DNase in Earle's balanced saline solution was added. Cell suspensions were then filtered using 100µm cell strainers (BD Falcon) to eliminate large cell clumps. Following centrifugation at 150G for 5 min, cell pellets were resuspended and gently triturated in inhibitor solution. After a second centrifugation at 150G for 5 min, cell pellets were resuspended in neural differentiation medium.

#### 4.2.2 Indirect co-culture assay

To promote neurosphere cell differentiation towards photoreceptors, sphere cells derived from adult corneal limbus were plated onto Poly-D-Lysine (P-D-L) (Sigma-Aldrich) and laminin (Sigma-Aldrich) coated wells and co-cultured with dissociated P1-3 mouse retinal cells using Millicel CM inserts (pore size 0.4 µm; Millipore) for 1-2 weeks, as illustrated in Figure 4-2A. Differentiation medium contained Neurobasal A media (Invitrogen), 2% B27, 0.5mM L-Glutamine (Sigma-Aldrich), 0.5-1% FBS (Sigma-Aldrich), 1µM retinoic acid (RA, Sigma-Aldrich) and 1 ng/ml brain-derived neurotrophic factor (BDNF, R&D system). Half of the medium was changed every other day.

LNS grew as a monolayer when exposed to differentiation conditions. Cell morphology was investigated using phase contrast microscopy. The expression of retinal specific genes was conducted using RT-PCR and/or immunocytochemistry. In order to study ultrastructural changes following induction, LNSs were grown on Millicel CM insert membranes, with P1-3 mouse retinal cells (Figure 4-2B).

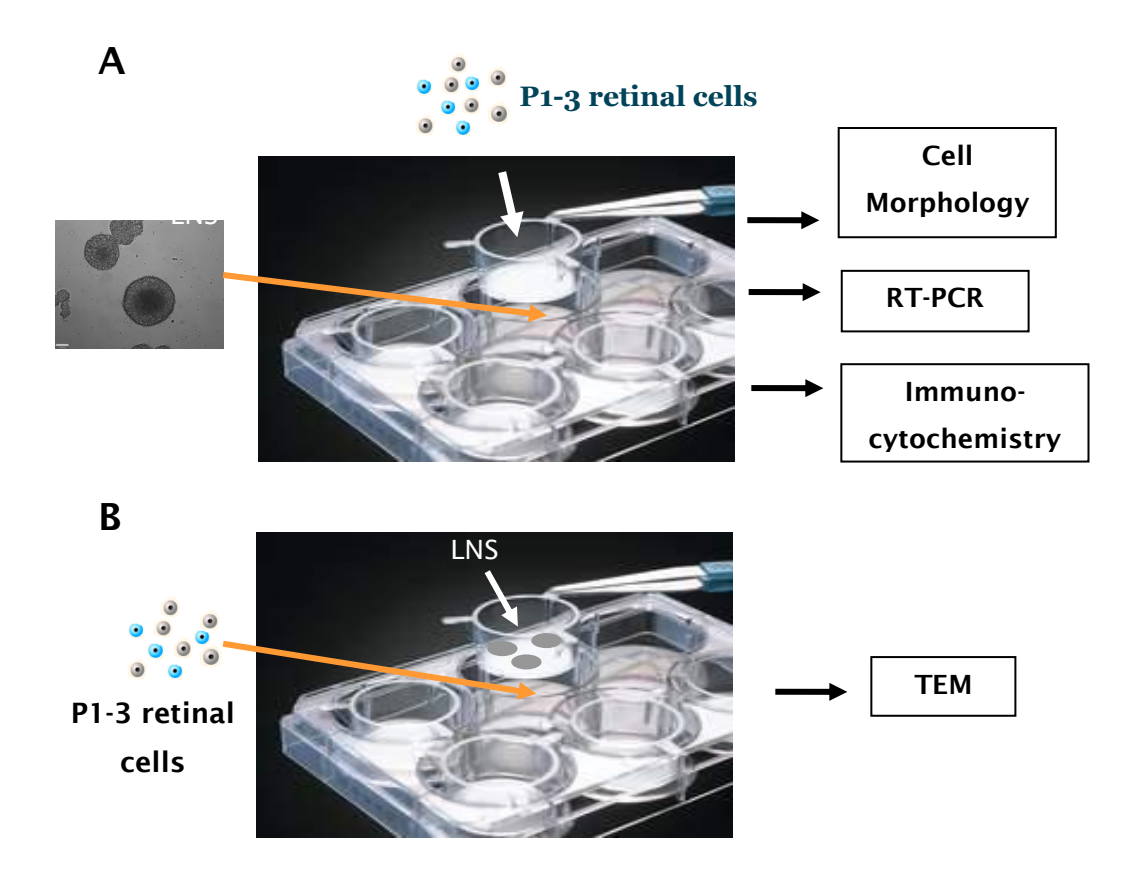


Figure 4-2 Co-culture System for Retinal Lineage Differentiation Millicel CM inserts (pore size  $0.4~\mu m$ ) were used in this co-culture system. The permeable membrane allows neurotrophic factors to diffuse through, while avoiding cell contamination. (A) Shows the co-culture system and the following cell characterisation experiments. (B) Shows modified co-culture system for investigating ultrastructure of induced LNS cells.

#### 4.2.3 Reverse transcription polymerase chain reaction

RNA extraction, cDNA synthesis and polymerase chain reaction were conducted as described in Chapter 2, Section 2.4. Total RNA was isolated and cDNA synthesis was performed following manufactures' protocols using RNeasy Plus (Qiagen, West Sussex, UK) and High Capacity cDNA Reverse Transcription Kit (Applied Biosystems). cDNA was amplified using gene specific primers (Table 4-1). Cycles used were (denaturing for 30 sec at 94°C; annealing for 30 sec at 60°C, extension for 30 sec at 72°C for 35 cycles, unless stated otherwise). Electrophoresis was performed on a 1.5% agarose gel. The gels were stained with Ethidium Bromide (Sigma-Aldrich) and viewed under a UV illuminator (UVP High Performance, Cambridge, UK). Photos were captured on a CCD camera, using Doc-It®LS Image software (UVP High Performance, Cambridge, UK).

Melting curve analyse were conducted on Rotogene 6000 real time thermo-analyser (Qiagen, West Sussex, UK) following real time PCR using SYBR green and commercially designed rhodopsin primers. PCR reactions consisted of 5ul of cDNA (at approximately 50ng/µl), 1ul of reconstituted primer mix (PrimerDesign, Southampton, UK), 10ul of 2 × precision mastermix with SYBRgreen (PrimerDesign, Southampton, UK) and 4ul of PCR-grade water. The Rotorgene run setting were according to the standard protocol suggested for custom qPCR assay by PrimerDesign: enzyme activation for 10 min at 95 °C, followed by 45 cycles of 15 seconds denaturation at 95°C, 60 seconds annealing and extension at 60 °C. A Melt was performed with ramping from 60-95 °C with fluorescence data collection at 0.5 increments. All samples were run in duplicate. Negative control omitted transcriptase in reverse transcription reaction. cDNA from retinal tissue was used as a positive control.

Table 4-1 Primer sequences used for phenotypic analysis and expected product sizes in co-culture study.

Primers Name	Sequence	Amplicon Size (bp) <sup>a</sup>
Bestrophin_F	CTACAAGCGCTTTCCCACTC	165
Bestrophin_R	CGGATTCGACCTCCAAGATA	
Crx_F*	ATCCAGGAGAGTCCCCATTT	506
Crx_R*	GGCAGAGATGGGCTGTAAGA	
CRX_F	CCCATACTCAAGTGCCCCTA	122
CRX_R	CCTCACGTGCATACACATCC	
Lhx2_F*	GCCATGCTGTTCCACAGTC	509
Lhx2_R*	AAGTGCAAGCGGCAATAGAC	
Pax6_F*	CAGTTCTCAGAGCCCCGTAT	489, 456
Pax6_R*	CTAGCCAGGTTGCGAAGAAC	
RPE65_F	CGGACTTGGGTTGAATCACT	282
RPE65_R	AGTCCATGGAAGGTCACAGG	
Rhodopsin_F	TCACCACCACCTCTACACA	216
Rhodopsin_R	TGATCCAGGTGAAGACCACA	
Rhodopsin kinase_F	AGCCCGAGGAGAAGGTAG	285
Rhodopsin kinase_R	CCCACGTCCTGAATGTTCTT	
Six6_F*	AAACCGCAGACAAAGAGACC	510
Six6_R*	AATACCCGCAGGAGACTCAA	
GAPDH_F	GGGTGTGAACCACGAGAAAT	323
GAPDH_R	ACACATTGGGGGTAGGAACA	
β-Actin_F	TGTTACCAACTGGGACGACA	392
β-Actin_R	TCTCAGCTGTGGTGGTGAAG	
Rhodopsin_F <sup>b</sup>	TCAGAAGGCAGAGAAGGAAGT	109
Rhodopsin_R <sup>b</sup>	CTGGTGGGTGAAGATGTAGAAG	

<sup>&</sup>lt;sup>a</sup> Base Pairs; F: forward; R: reverse

<sup>&</sup>lt;sup>b</sup> Primers were designed and manufactured by PrimerDesign LTD (Southampton, UK)

<sup>\*</sup> Cycles for PCR: denaturing for 30 sec at 94°C; annealing for 30 sec at 60°C, extension for 30 sec at 72°C for 1 cycle; then denaturing for 30 sec at 94°C, annealing for 30 sec at 55°C, extension for 30 sec at 72°C for the following 34 cycles.

#### 4.2.4 Immunocytochemistry

Immunocytochemistry was conducted as described in Chapter 2, Section 2.2. In brief, cells were fixed with 4% PFA for 15-20 min at 4°C. Following permeabilization and blocking with 0.1 mM PBS supplemented with 0.1% Triton X-100 and 5% donkey block serum for 0.5-1 hr at rt, cells were incubated with primary antibodies (See Table 4-2) overnight at 4°C. Following gentle washing, specific IgG secondary antibodies, conjugated to an Alexa Fluor 488 or Alexa Fluor 555 (Invitrogen) at a concentration of 1:500 in PBS, were incubated at rt for 1-2 hrs. Negative controls omitted the primary antibody. Nuclei were counterstained with 10ng/ml DAPI. To quantify the percentage of cells expressing a particular phenotypic marker, the number of positive cells was determined relative to the total number of cells (DAPI labeled nuclei) [6]. A total of 500-1000 cells were counted per marker.

Table 4-2 Primary antibodies for immunocytochemical analysis in co-culture study.

Antibody	Specificity	Company	Conc.
Bestrophin	RPE cells	Abcam	1:100
beta-III tubulin	Early differentiated neurons	Covance	1:500
Neurofilament 200	Neurons	Sigma Aldrich	1:500
Rhodopsin	Photoreceptors	Sigma Aldrich	1:250
RPE65	RPE cells	Abcam	1:200
Syntaxin3	Synapse composition	Abcam	1:500

#### 4.2.5 Transmission Electron Microscopy (TEM)

To investigate the ultrastructure of induced LNS cells, LNSs were cultured on cell insert membranes as shown in Figure 4-2B. P1-P3 mouse retinal cells were cultured underneath the membranes to provide extrinsic factors. Cell inserts together with LNS were fixed in  $100~\mu l$  of primary fixative containing 0.1 M sodium cacodylate buffer, 3% glutaraldehyde, 4% PFA and 0.1 M PIPES buffer, pH 7.4 for 15 min at rt. Further processing was performed in the Biomedical Image Unit, University of Southampton. In brief, following initial fixation the specimens were rinsed in 0.1M PIPES buffer, postfixed in 1% buffered osmium tetroxide (1 hr), rinsed in PIPES buffer, block stained in 2% aqueous uranyl acetate (20 min) followed by dehydration in a graded series of ethanols up to 100% and embedded in TAAB resin (TAAB Laboratories, Aldermaston,

UK). Gold sections were cut on a Leica OMU 3 ultramicrotome (Leica (UK) Ltd, Milton Keynes, Bucks, UK), stained with Reynolds lead stain and imaged on a Hitachi H7000 transmission electron microscope with a SIS megaview III digital camera (Hitachi High-Technologies Corporation, Maidenhead, Berkshire, UK).

#### 4.3 Results

#### 4.3.1 Cell morphology change following differentiation

Cell morphology was monitored using light microscopy following withdrawal of mitogens and culture on P-D-L and laminin coated tissue culture plates with neural differentiation media. After 24 hrs, spherical cell clusters started to attach to the surface of tissue culture plates and began to grow as a monolayer. Peripheral cells started to grow out from the cell cluster and displayed a neuron like phenotype with dendritic processes. The cells at the centre of the differentiated LNS, were much darker compared to the peripheral region. To fully assess the morphology of individual cells *in vitro*, I dissociated the LNS into single cells and cultured them at a density of 100,000 cell/ml in 6-well tissue culture plates with neural differentiation media. The cells displayed a variety of morphological features. Typical neuron-like cells with dendritic and axonal processes were observed as shown in Figure 4-3A. In addition, small pigment cell islands were also observed (Figure 4-3B).

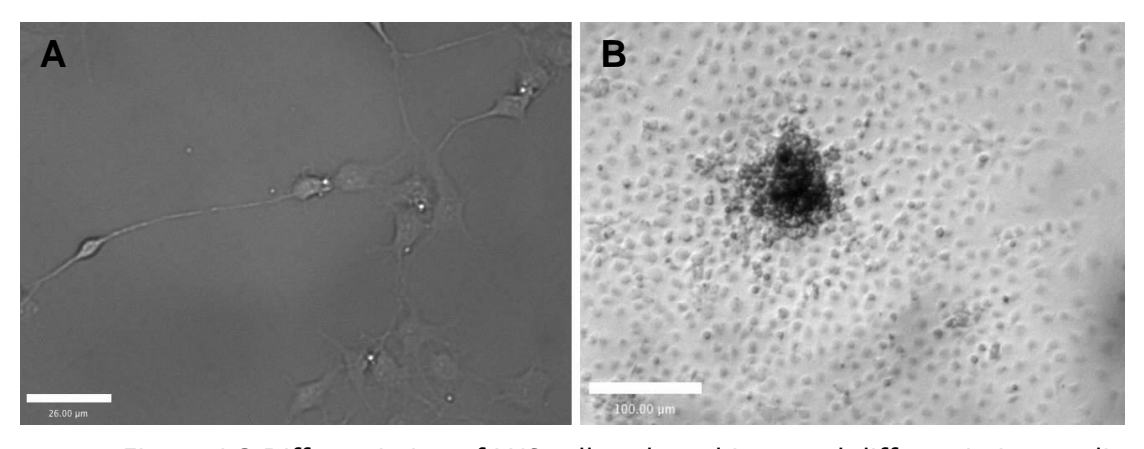


Figure 4-3 Differentiation of LNS cells cultured in neural differentiation media (A) LNS cells displayed neuronal morphology with neurite like processes following culture in neural differentiation media for 7-10 days *in vitro*. (B) LNS derived cells displayed pigment islands. Scale bar: 26 μm (A) 100 μm (B)

#### 4.3.2 Ultrastructural changes following differentiation

Cell ultrastructure was investigated following co-culture for 7-10 days. A comparison between the LNS cells before and after co-culture conditions was carried out using TEM. Following co-culture, cellular junctions such as gap junction and immature adherence junctions found in LNS, were not apparent (Figure 4-4C). These junctions provide mechanical or electrical connection for the cells within neurospheres. On the contrary, putative presynaptic dense bodies (Figure 4-4A, arrow), non-motile primary cilia (Figure

4-4B) and immature melanosome-like structures (Figure 4-4D), were observed following differentiation. These features indicate cell maturation or the beginnings of lineage specification. We did not observe mature synaptic structures. The cilia noted in cocultured LNS were identified as sensory cilia, consisting of an axoneme of nine doublet microtubules, with a lack of key central pair of microtubules that were involved in ciliary motility [176]. Although these non-motile 9+0 primary cilia are not specific to retinal lineage cells, the same subtype of cilia are present in photoreceptor and RPE cells.

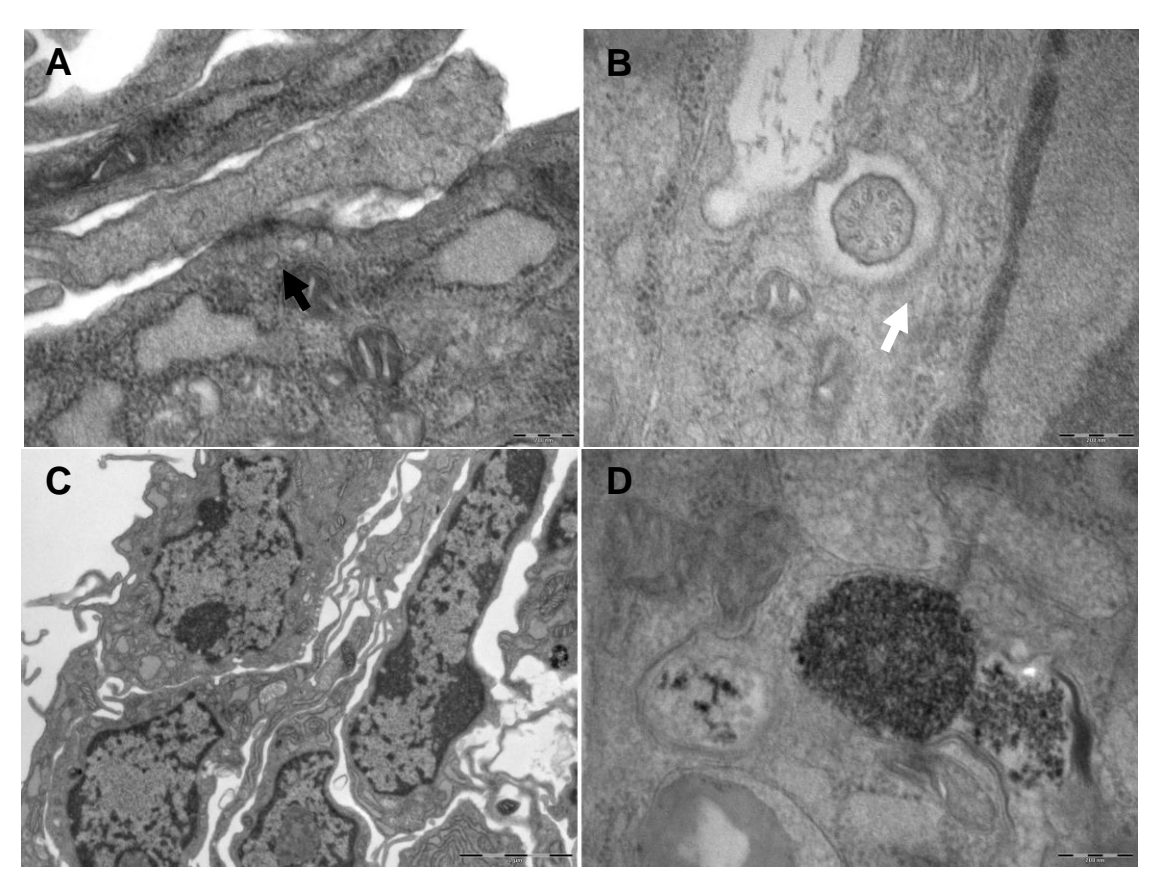


Figure 4-4 TEM images of differentiated limbal spheres

Putative presynaptic dense bodies were present (**A**, black arrow); Cell junctions were not apparent (**C**); immature melanosome like structure (**D**) and 9+0 non motile cilia were detected on induced limbal cells (**B**, white arrow). Scale bar: 200nm (A-D).

#### 4.3.3 Expression of retinal progenitor cell markers

As previously described [219] cultured PN1-3 murine retinal cells can release diffusible rod promoting factors, which can promote stem cell differentiation or transdifferentiation towards rod photoreceptors. Cell inserts with a semi-permeable membrane were utilised to avoid cell contamination, while still allowing the passage of diffusible factors.

We investigated the expression of retinal progenitor cell markers including Pax6 (Paired box gene 6), Lhx2 (LIM homeobox 2), Crx (cone and rod homeobox) and Six6 (SIX homeobox 6) on the induced LNS at the early stages of differentiation using RT-PCR. Results represent two independent co-culture experiments. Pooled cDNA extracted from neonatal and adult mice were used as positive control for mouse progenitor markers. Co-cultured limbal cells omitting transcriptase during cDNA synthesis was used as negative to exclude the possibility of non-specific amplification or possibility of contamination.

As shown in Figure 4-5, low levels of Lhx2 was detected on approximately 60% of samples after 2-4 days of co-culture, while expression of Pax6 and Six6 at transcript level was observed on most of samples(n=4-5). No bands were detected with the negative control. As shown in Chapter 3 (Figure 3-22), Pax6 was detected in freshly isolated limbal cells or intact limbal tissue. During neurosphere culture, the expression of Pax6 gradually decreased to an undetectable level. However during co-culture, expression of Pax6 was strongly upregulated. This indicates that some endogenous signals were upregulated in response to a retinal differentiation promoting environment.

The expression of Crx at transcript level was assessed using Crx gene specific primers. The size of predicted Crx amplicom was 506bp. As shown on Figure 3-22, bands were detected on 2 out of 4 co-cultured LNS samples. However, their sizes were slightly larger than 506bp. PCR was conducted on the same samples using a second pair of intron spanning Crx primers (Crx 122). Transcript Crx was not detected on any of co-cultured LNS samples using Crx122 primers. Therefore, Crx was still under detectable following co-culture with developing retinal cells.

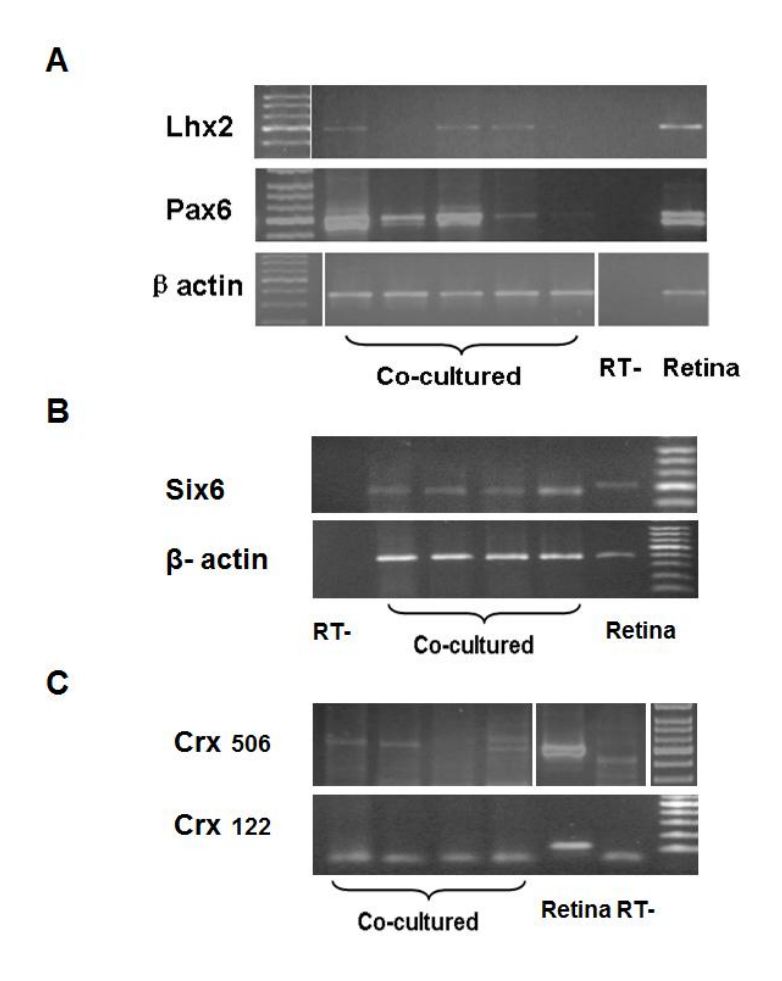


Figure 4-5 Expression of retinal progenitor cell markers in LNS derived cells Transcripts Pax6, Lhx2 and Six6 were detected by RT-PCR in LNS cells after short term (2-4 days) co-culture with neonatal retinal cells (A & B). Two pairs of intron-spanning Crx gene specific primers, were used to assess the expression of the photoreceptor progenitor cell marker Crx. Numbers represent the predicted amplicon size. Bands larger than 506bp were detected on LNS cells using Crx506 primers, while transcript Crx was not detected using Crx122 primers. Unspecific amplification/primer dimers were observed on both LNS cells and RT- on Crx122. Pooled neonatal and adult retinal cDNA was used as a positive control for retina-specific gene expression. RT-omitted reverse transcriptase. Results represent 4-5 independent experiments. β-actin was used as cDNA quality control.

#### 4.3.4 Detection of photoreceptor specific markers by RT-PCR

Following 7-10 days co-culture, Rhodopsin and Rhodopsin Kinase were both detected in co-cultured LNS cells as shown by RT-PCR (Figure 4-6). Results represent six independent co-culture experiments. Similar sized PCR products were detected in co-

cultured LNS cells and retinal tissue using gene specific rhodopsin primers. Following real-time PCR using SYBRgreen and a second pair of commercially designed rhodopsin primers, a melting curve analysis was used to confirm the expression of rhodopsin at transcript level. As shown in Figure 4-6B, amplicons from retinal cDNA and co-cultured LNS cells showed the same DNA melting temperature. Hence, the expression of rhodopsin was confirmed by two assays measuring both size and melting pattern. Rhodopsin was detected consistently, while the level of rhodopsin kinase varied between experiments. In approximately half of the experiments conducted, expression of rhodopsin kinase was weak or under detectable.

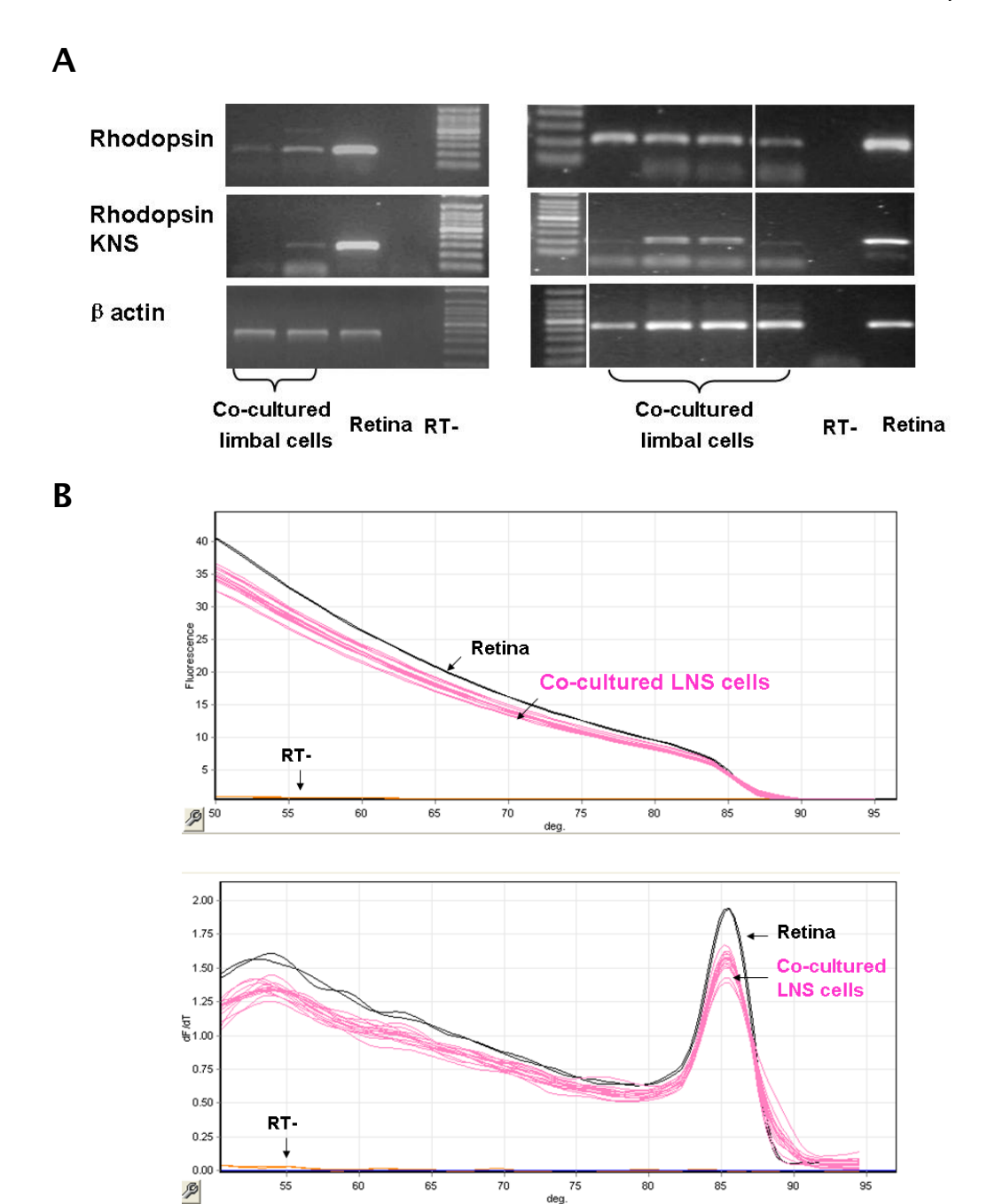


Figure 4-6 Expression of photoreceptor specific genes in derived LNS cells RT-PCR was performed with gene specific primers. Retinal cDNA was used as a positive control for photoreceptor specific genes. Negative controls (RT-) omitted reverse transcriptase. (A) Electrophoresis was used to check the presence of DNA fragments on 1.5% agarose gels. Expression of rhodopsin was detected in co-cultured LNS cells and retinal tissue. (B) A melting curve analysis (dissociation curve) was conducted following real-time PCR using SYBR green and commercially designed rhodopsin primers. Amplicons from retinal cDNA (black) and co-cultured LNS cells (pink) exhibited the same melting temperature of 85.3 °C. –dF/dT: the rate of change of fluorescence vs. temperature; deg: degree.

In order to examine whether there is endogenous expression of Rhodopsin and Rhodopsin Kinase in limbal cells at a transcript level, freshly isolated limbal cells and primary RPE cells were investigated. The photoreceptor specific markers were absent in freshly isolated limbal cells, but expressed after induction (Figure 4-7). Taken together, these results suggest that expression of rhodopsin and rhodopsin kinase in induced LNS cells was not due to contamination from retinal or RPE cell during dissecting.

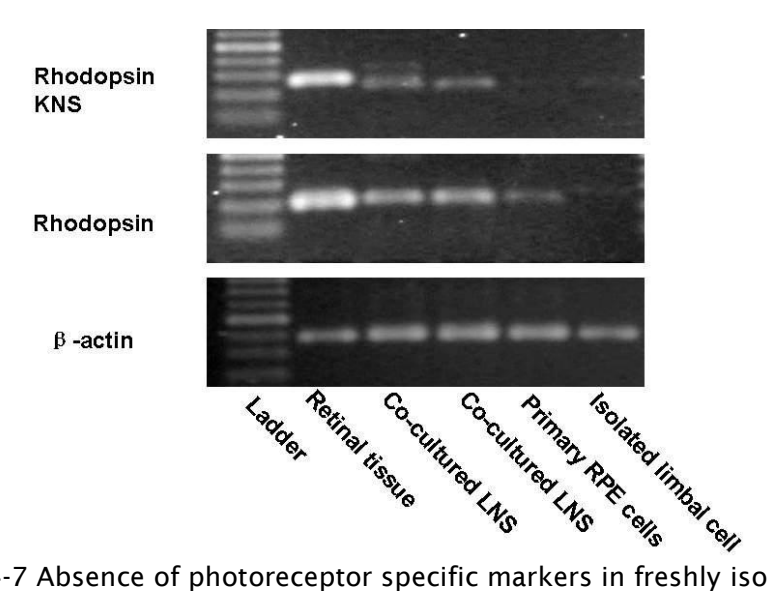


Figure 4-7 Absence of photoreceptor specific markers in freshly isolated limbal cells. Rhodopsin and Rhodopsin kinase were absent in freshly isolated limbal cells. Low levels of Rhodopsin were detected in primary RPE cells. RT-PCR was performed with gene specific primers. Retinal cDNA was used as a positive control for the photoreceptor specific genes.  $\beta$ -actin was used as cDNA quality control.

## 4.3.5 Detection of photoreceptor, neural and synaptic markers by immunocytochemistry.

Immunocytochemistry was conducted after 7-10 days, using co-cultured LNS cells and LNS cells without co-culture. The rod photoreceptor specific marker Rhodopsin, matured neuronal marker Neurofilament 200 and the major synaptic component marker, Syntaxin3 were examined.

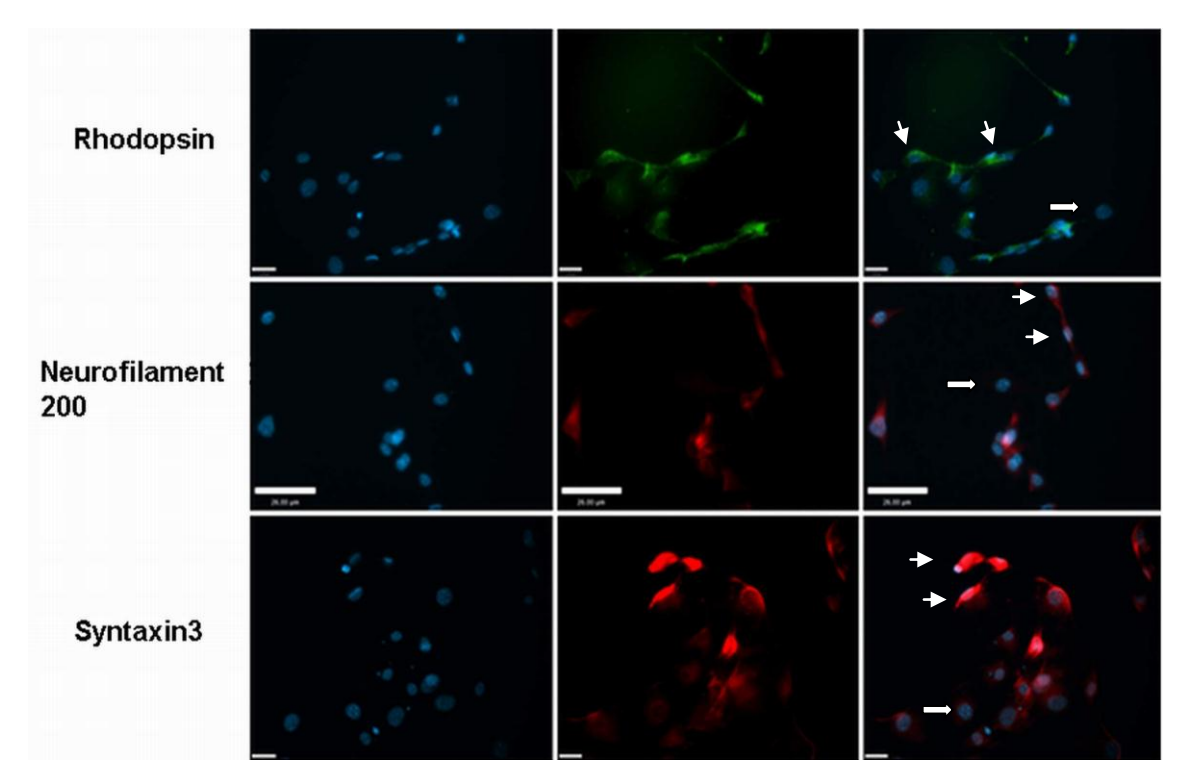
As shown in Figure 4-8 and Figure 4-9,  $13.64 \pm 2.76 \%$  of LNS cells were immunopositive for rhodopsin following co-culture with P1-3 mouse retinal cells. Rhodopsin positive cells had a dendritic morphology, with staining in both the cells

body and cytoplasmic processes. Approximately  $12.47 \pm 5.27 \%$  of cells exhibited strong immunoreactivity to Syntaxin3 (Figure 4-12).

In the control condition (without co-culture), few Rhodopsin positive cells were detected (1.19  $\pm$  0.39 %). Statistical analysis showed significant difference between the two groups in the presence and absence of co-culture (P <0.0001, unpaired t-test).

We also investigated the expression of the mature neuronal marker, neurofilament 200, in both co-culture and non co-culture conditions. A larger number of LNS were immunopositive for NF200 (31.40  $\pm$  2.71%), compared to the control condition (10.44  $\pm$  1.65%) (Figure 4-8 and Figure 4-9). The results suggest that there is a statistically significant difference between the two groups (P <0.001, unpaired t-test).

Α



В

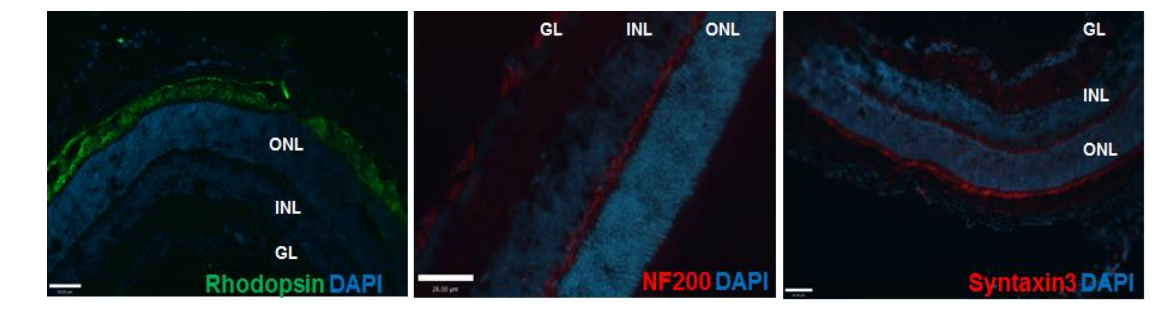
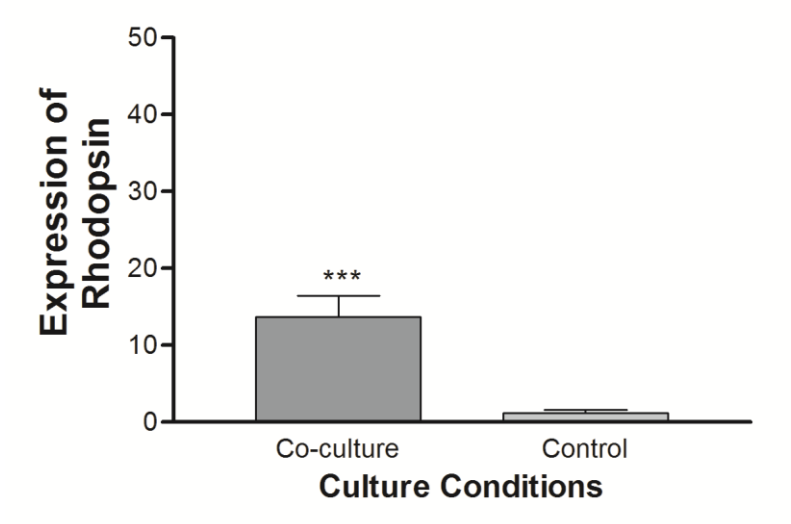


Figure 4-8 Immunocytochemistry of LNS cells in co-culture condition. (A) Immunocytochemistry was conducted on LNS cells following 1 week of co-culture with neonatal retinal cells. Cells were stained with antibodies directed against Rhodopsin, Neurofilament 200 and Syntaxin3. Cell nuclei were counter stained in blue with DAPI, Scale bar neurofilament:  $26~\mu m$ ; Rhodopsin & Syntaxin3:  $13\mu m$ . Arrow heads indicate immunopositive cells, and arrows show immunonegative cells. (B) Mouse retinal sections were used as positive controls for immunostaining with anti-rhodopsin, NF200 and syntaxin3. As expected, rhodopsin labeled rod photoreceptors (green), NF200 staining identified horizontal and ganglion cells (red), and Syntaxin showed immunoreactivity with photoreceptor cells and bipolar cells (red) in the retina. Cell nuclei were counter stained in blue with DAPI. ONL: outer nuclear layer, INL: inner nuclear layer, GL: ganglion layer, scale bar:  $26\mu m$ .

# A Percentage of Rhodopsin Positive Cells in Co-culture and Control Conditions



## B Percentage NF200 positive cells in co-culture and control conditions

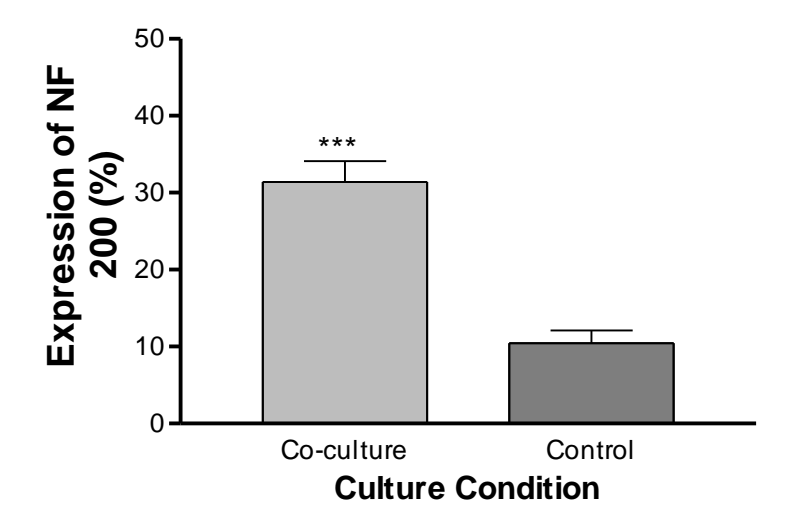


Figure 4-9 The percentage of Rhodopsin and NF 200 positive cells from adult LNS cells following 7-10 days differentiation in co-culture and control conditions. Cells were cultured in differentiation media containing RA and BDNF, in the presence or absence (control) of co-culture with P1-3 mouse retinal cells. The results are expressed as mean  $\pm$  SEM (n $\geq$ 6), from at least three separate experiments. Significant

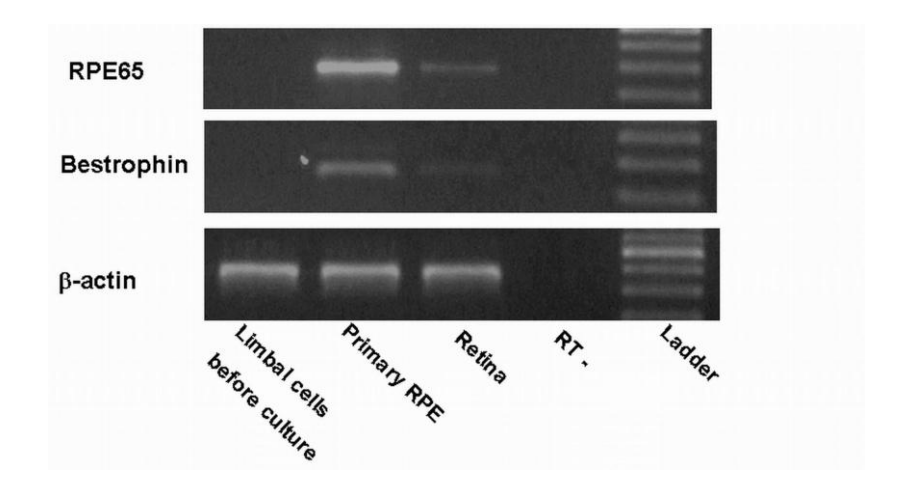
difference, \*\*\* P<0.001 by unpaired t-test.

#### 4.3.6 Expression RPE specific markers

In order to investigate whether the pigmented cells observed under differentiation conditions were RPE-like cells, the expression of RPE specific markers including RPE protein 65 (RPE65) and bestrophin were examined at both a transcript and protein level. Firstly, the expression of both genes were undetectable in freshly isolated limbal cells (Figure 4-10A, Lane one). This excludes the possibility of contamination from RPE cells during dissection of mouse corneal limbus. Similar to the preceding findings (Figure 4-3), RPE65 and Bestrophin were present in co-cultured limbal cells at transcript levels (Figure 4-10B). Weak bands of both genes also were observed on freshly dissected retinal tissues. This is possibly due to contamination of RPE cells during dissection of retinal tissues.

Immunocytochemistry was used to investigate expression of RPE specific markers at a protein level. As shown in Figure 4-11, a subpopulation of LNS cells were immunopositive for both RPE65 and Bestrophin under co-culture conditions. As expected, RPE65 was observed in the cytoplasm, while Bestrophin staining was localised in the cell membranes of LNS cells. Approximately 20% of cells expressed PRE65 under co-culture condition and 7% in control condition (Figure 4-10). This was statistically significant (P <0.05, unpaired t-test).





В

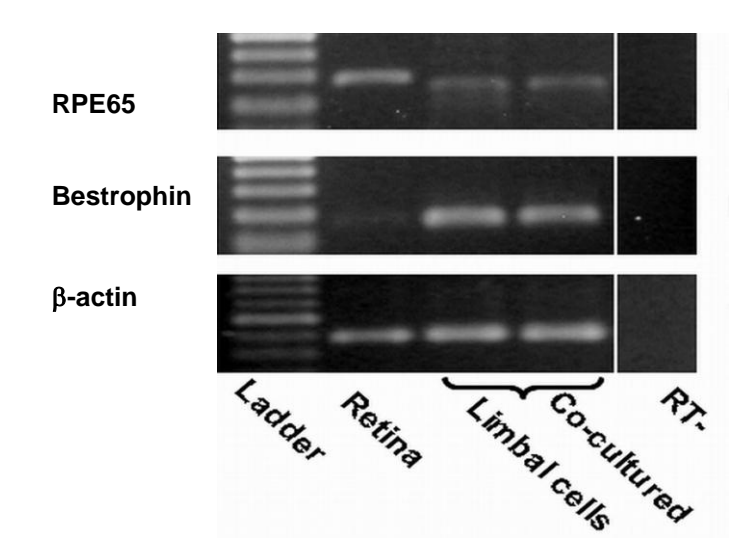
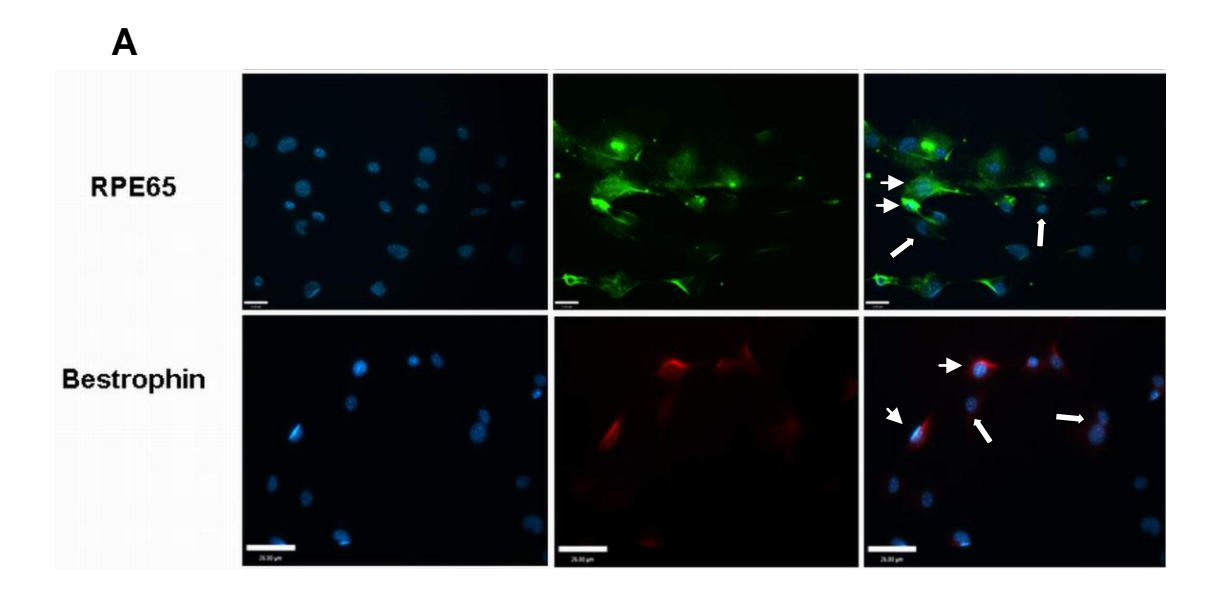


Figure 4-10 Expression of RPE specific markers at a transcript level RT-PCR was performed with gene specific primers. Retinal cDNA and primary RPE cells were used as positive controls. Negative controls (RT-) omitted reverse transcriptase. RPE specific markers RPE65 and Bestrophin, were absent in freshly isolated limbal cells. Low levels of Bestrophin were expressed in the retinal tissue. This is due to contamination of retina with RPE cells during dissection; the strong expression of RPE65 in the retina is in accordance with previous reports (15).



В

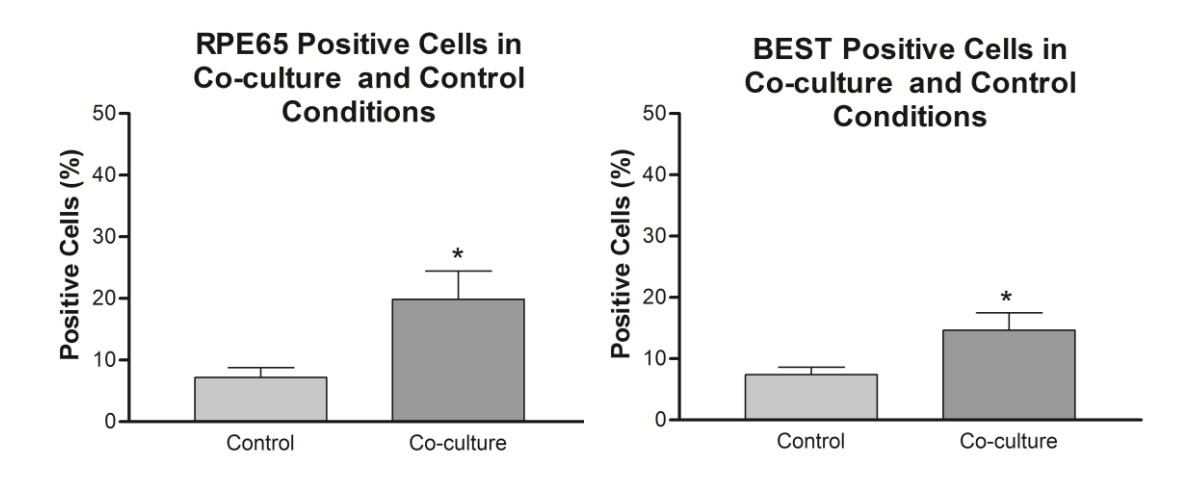
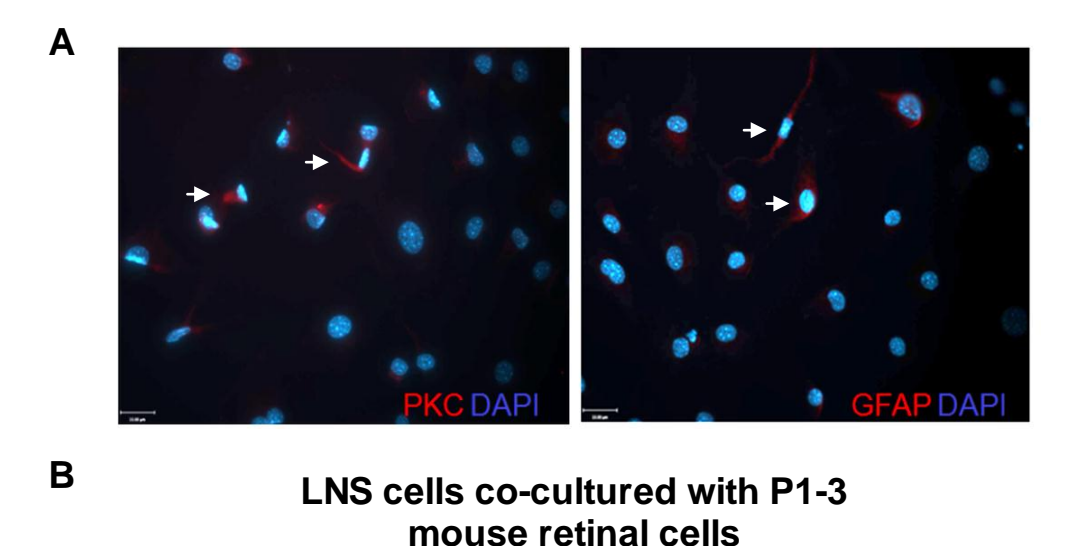


Figure 4-11 Expression of RPE specific markers at a protein level Immunocytochemistry was conducted on LNS cells following 1 week in co-culture with neonatal retinal cells. (A) Cells were stained with antibodies directed against Bestrophin and RPE65 (arrowheads). Cell nuclei were counter stained in blue with DAPI. Arrows indicate the immunonegative cells in the same field. Scale bar RPE65:  $13\mu m$ , Bestrophin:  $26 \mu m$ . (B) percentage of RPE65 positive cells and Bestrophin positive cells in co-culture and control condition. Results are expressed as mean  $\pm$  SEM, from at least three separate experiments. Significant difference \* P <0.05, by unpaired t-test.

#### 4.3.7 Cell populations of LNS in co-culture with neonatal retinal cells

In vitro cultured P1-3 mouse retina provides a retinal/photoreceptor promoting environment. Following culture in this environment, LNS expressed the neural marker NF200 and GFAP (Figure 4-12), neural retinal markers Rhodopsin, PKC (Figure 4-12) and Syntaxin3 and RPE specific markers RPE65 and Bestrophin. Induced LNS cells were a mixed cell population, displaying a diverse range of morphological features and expressing different cell markers. The percentage of LNS expressing each marker was shown in Figure 4-12.



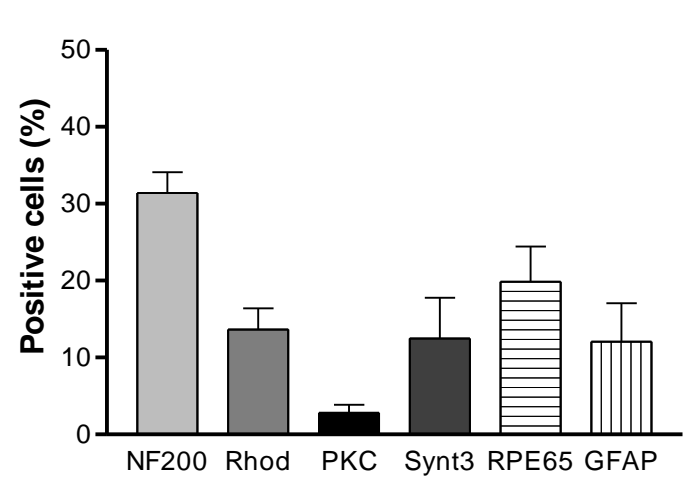


Figure 4-12 Cell populations observed from LNS co-cultured with neonatal retinal cells (A) Immunocytochemistry was conducted on LNS cells following 1 week in co-culture with neonatal retinal cells. Induced LNS cells were stained with antibodies directed against PKC (Bipolar cell marker, arrowheads) and GFAP (glial cell marker, arrowheads). Cell nuclei were counter stained in blue with DAPI. Scale bar: 13μm. (B) The percentage of cells expressing each marker is expressed as mean ± SEM, from at least three separate experiments. NF200, neurofilament 200; Rhod, Rhodopsin; PKC, protein kinase C; Synt3, Syntaxin3; RPE65, RPE protein 65; GFAP, glial fibrillary acidic protein.

#### 4.4 Discussion

The results demonstrated above show the derived LNS cells have potential for differentiation towards neural cells, including towards retinal-like cells.

A number of early retinal progenitor cell markers were detected during early differentiation, indicating LNS cell transdifferentiation involves upstream regulators of retinal formation genes. The LIM homeobox transcription factor Lhx2 and master regulator of eye development Pax6 were present in LNS cells after short term co-cultured with neonatal retinal cells. Both transcription factors have previously showed to be synergistically cooperate to trans-activate downstream target genes to establish and maintain a definitive retinal identity [159,160]. In mice, Six6 has been reported to play an important role in the formation of the ventral optic stalk, as well as in the specification and differentiation of the neural retina [220]. As expected, we also detected Six6 at the same early differentiation stage. Crx plays a crucial role in specifying the photoreceptor lineage. It acts as a trans-activator directly regulating the expression of many photoreceptor genes [73]. However, the expression of Crx gene was not confirmed in the early differentiation stage of LNS cells. Further experimental investigations are needed to estimate whether LNS cells were regulated by an alternative pathway, or an unknown Crx isoform.

LNS cells expressed mature retinal specific markers including Rhodopsin and Rhodopsin Kinase following co-culture with neonatal retinal cells, with approximately 10% of cells immunopositive for rhodopsin. The expression of rhodopsin at the transcript level has been validated by two assays measuring both size and melting temperature of amplified cDNA from co-cultured LNS cells. Neurofilament and synaptic components were also expressed, as would be expected in differentiated retinal cells. Interestingly, these cells also formed small pigmented cell islands. RPE specific markers including RPE65 and Bestrophin were detected at both a protein and transcript level. This implies that both photoreceptor cells and RPE cells can be derived from the same cell resource. Expression of photoreceptor and RPE specific markers at a transcript level indicates endogenous expression of these photoreceptor and RPE specific genes.

By comparing co-cultured LNS with the control population (non co-culture), we observed an increase in the expression of rhodopsin, NF200 and RPE65 in response to exposure to developing retina. This is in accordance with previous reports that neonatal retinal cells can promote stem / progenitor cell differentiation towards retinal lineage [221,222]. Co-cultured LNS represent a heterogeneous population in terms of

morphological features and expression of markers including neural and RPE markers. These observed differences are possibly due to heterogeneity of the NSA or a mixed cell population of co-cultured retinal cell. Although a heterogeneous cell population exist in adult limbus derived cells, the results suggest that a small population of co-cultured cells were directed toward a matured neural or photoreceptor like state.

Other accessible autologous cell resources, such as bone marrow stromal cells, have been considered as a treatment for degenerative retinal diseases. Tomita *et al.* investigated the potential of BM stromal cells for retinal integration and differentiation by co-culture with retinal explants from rhodopsin knockout mice [110,158-160]. Bone marrow stromal cells failed to express rhodopsin in this environment. This may be because bone marrow cells originate from the endoderm.

The data we demonstrate here highlights a promising new candidate progenitor cell source for photoreceptor and RPE cell generation. The corneal limbus is one of the most readily accessible regions in the human eye. The stromal layer from the peripheral cornea and limbus is clear of the visual axis. It represents 90% of the thickness of the front wall of the eye. Hence cells can be readily harvested from this area without compromising ocular function. As intra-ocular surgery is not required to obtain these cells, surgical complications such as endophthalmitis and intraocular haemorrhage are avoided. In addition, LNS are adult cells and so the risk of tumour formation following transplantation is significantly reduced. To date, adult corneal/ limbal stromal stem cells with neural potential have been successfully derived from the following species: human [146], bovine [30] rabbit [33] and mouse [32]. This suggests that the existence of limbal stromal stem/ progenitor cells is not species specific. The data presented here expands the concept of the plasticity of neural crest derived stromal progenitor cells. These results suggest further research is warranted to enhance the transdifferentiation efficiency of these cells.

# 5 Chapter Five - Investigation of LNS cell functionality and integration *in vitro*

#### 5.1 Introduction

Neurons are electrically excitable cells. They process and transmit information by electrical and chemical signaling. As demonstrated in Chapter Four, a subpopulation of LNS cells exhibited mature neural cell markers or retinal specific markers when cultured in a retinal developing environment. The next important question is whether these neural like cells possess functional properties.

In excitable cells, especially neurons, voltage-gated ions channels are critical for cell functionality. They are transmembrane ion channels activated by changes in electrical potential across the cell membrane. Activation causes a change in conformation of the channel protein, allowing influx or efflux of specific ion. Hence, a rapid and coordinated depolarization is triggered in response to a voltage change. The existence of voltage-gated ions channels has been used previously to prove the functionality of derived neuron or photoreceptor-like cells [90,148]. Methods used include single cell electrophysiological recording [6,223,224] and an intracellular specific ion indicator assay [223]. Functional cells displayed a non-linear relationship between voltage and membrane current in electrophysiology recording [6,224], or a flux of intracellular ions in response to the potential stimuli [223].

Photoreceptors are specialized types of neurons that respond to light and convert light energy to an electrical pulse. When a photon of light arrives at the photoreceptors, retinol undergoes a conformational change from the 11-cis form to an all-trans form, subsequently forming activated transducin. The latter activates cGMP phosphodiesterase which breaks down cGMP into 5'-GMP. This reduction of cGMP allows cGMP-gated cation channels to be closed, preventing the influx of positive ions (sodium), which hyperpolarize the cell membrane. This hyperpolarization causes voltage-gated calcium channels to close, and calcium level in the photoreceptor cell decrease [6,224]. As a result, the neurotransmitter glutamate which is released by photoreceptors also drops, causing electrical potential change in bipolar cells. Therefore, the change of intracellular calcium concentration upon light stimulation reflects the response of the cell to light.

To detect the change of intracellular calcium concentration, highly ion specific fluorescent calcium indicator dyes have been developed since last century. They greatly enhanced the efficiency and sensitivity to measure intracellular calcium in various systems. However, when using fluorescent dyes to assess the light responsiveness of photoreceptors, the light necessary to excite the fluorescent dye also provides a strong stimulus to the cells themselves. Despite this potential drawback in the measurement of light responsiveness, a light-induced reduction of cytoplasmic free calcium was previously detected in a number of studies on developing photoreceptors and photoreceptor-like cells [42]. These photoreceptor-like cells include encephalic photoreceptors from chick brain and photoreceptor-like cells derived from genetically modified RPE cells [168,175,224].

To achieve restoration of vision, derived photoreceptor-like cells need to be functional, as well as capable of integrating into the retina to form appropriate connections with inner retinal cells [168,175]. MacLaren et al. showed that post mitotic rod photoreceptor precursor cells successfully integrated into the adult retina after transplantation into the SRS [62]. The grafted cells were seen to be present in the outer nuclear layer of host retinas, exhibiting photoreceptor like morphology, appropriate orientation, and synaptic connections with inner retinal neurons. Sensitivity to low light stimuli, was enhanced in the host mice when compared with sham-injected controls [62]. Other studies, using photoreceptor-like cells, also investigated their capacity to integrate within host retina. Zhao et al. transplanted limbal epithelium derived cells into the vitreous cavity of PN day 7 wildtype rat eyes [62]. A very small population of grafted cells expressed the photoreceptor-specific marker opsin. However, incorporation into the outer nuclear layer was not convincing, as the host retina lost its highly laminated structure. Intravitreally transplanted cells need to migrate through the inner limiting membrane, inner nuclear layer, inner plexiform layer and outer plexiform layer in order to reach the outer nuclear layer, where photoreceptors reside. Therefore, the incorporation process is much more difficult through the inner retinal path. Akagi et al. co-cultured iris-derived photoreceptor like cells, with rat embryonic retinal explants (E18.5) for up to 2 weeks in vitro. The cells of the retinal explants completed differentiation in vitro and formed three layers, however outer segments were not observed in this co-culture system. A very small number of transdifferentiated photoreceptor-like cells migrated into the ONL and expressed rod-opsin [6]. Derived from readily accessible adult tissue, LNS cells are an ideal autologous cells resource. The immune response and subsequent damage could be completely avoided using autologous cells; hence LNS cells have fewer barriers to successful transplantation. However, little is known about whether limbal cells can integrate into the retina to form connections with inner retinal cells.

The aim of this study was to assess the functionality of LNS derived neural or photoreceptor like cells and their potential for integration into retinal tissue *in vitro*. Via the calcium flux assay, the existence of voltage-gated ions channels and possible light responsiveness was investigated in this study. By culturing the fluorescently labeled LNS cells with neonatal retinal explants, the capability of LNS integration into retinal tissues was assessed *in vitro*.

#### 5.2 Methods

#### 5.2.1 Cell dissociation and culture

Limbal cells were dissected from 8 week old mice and enzymatically dissociated using Trypsin, collagenase and hyaluronidase. Cells were maintained DMEM:F12GlutaMAX<sup>™</sup> with 2% B27, 20ng/ml FGF2 and EGF at 37°C. For neural differentiation, mitogens were withdrawn and cells were cultured in Neurobasal<sup>™</sup>A medium containing 2% B27, 0.5mM L-Glutamine, 0.5-1% FBS, 1µM RA and 1ng/ml BDNF. For transdifferentiation, LNS cells were co-cultured with developing retinal cells (P1-3) for 5-7 days.

Developing retinal cells were dissected from PN day 1-3 mice and dissociated using enzymatic digestion (See Chapter 2, Section 2.6.2). Freshly isolated developing retinal cells were plated onto cell inserts and co-cultured with LNSs to provide conditioned media. To validate the calcium assay in this study, P1 retinal cells were cultured on P-D-L and Laminin coated plates in neural differentiation media for 2-5 days.

Cell functionality was investigated utilizing a calcium influx/efflux assay on three groups of cells as follows:

- 1) LNS cells co-cultured with developing retinal cells in neural differentiation media.
- 2) LNS cells cultured in neural differentiation media only (negative control).
- 3) In vitro cultured P1-3 retinal cells (positive control).

#### 5.2.2 Calcium influx imaging

Calcium imaging was conducted as described in Chapter 2, Section 2.7. Briefly, cells were incubated for 30 min in Fluo-4 acetoxymethyl (AM) ( $4\mu$ M, Invitrogen) in HBSS (Invitrogen) plus non-ionic detergent ( $10\mu$ M; Pruronic F-127, Invitrogen) at  $37^{\circ}$ C. Prior to imaging, excess dye was washed out and cells were equilibrated in HBSS to allow the AM to be cleaved by cytoplasmic esterase. Cells were imaged at  $20\times$  magnification, and fluorescence was simulated with light wavelengths near 488nm and acquired near 520nm. Images were captured every 10-30 sec, at an acquisition time of 500ms by a cooled camera on an inverted microscope (Leica) and analyzed using Improvision Volocity software. Intracellular calcium concentration was presented as fluorescence intensity (raw pixel intensities). Mean background intensity was subtracted from each cellular region to minimize the noise and vibration due to staining or fluorescence fading (F = cellular average-background average). All cells were then normalized by their initial intensity F/F0 [88]. A Trypan blue exclusion assay was used to assess cell

viability following calcium influx imaging. Images were captured in 6 areas per condition. The percentage of viable cells was calculated as follows:

Viable cells (%) =  $\frac{\text{Total number of viable cells per field}}{\text{Total number of cells per ml per field}} \times 100$ 

#### 5.2.3 Live Cell tracking

Qdots (Qtracker 655, Invitrogen) were used for cell tracking in cell integration experiments. The detailed methodology is described in Chapter 2, Section 2.8.2. Briefly, adult LNS cells were dissociated into single cells using Accutase. Cells were then incubated in Qdot labelling solution (10nM) in full culture media for 60 min at 37°C. Followed by two washes with full medium, Qdot labelled cells were viewed under a Leica fluorescence microscope to estimate the labelling efficiency with an excitation filter at 535 +/- 20 nm and an emission filter at 565nm long pass. Approximately 40-60% of cells were labelled.

#### 5.2.4 Cell integration assessment in vitro

In vitro cell integration was assessed using direct co-culture of Qdot labelled cells with neonatal mouse retinal explants. The detailed methodology is described in Chapter 2, Section 2.8.3. Briefly, dissociated Qdot labelled cells were collected and plated on Transwell® membranes (pore size 0.4  $\mu$ m, Corning®, New York, USA). Retinal tissue was dissected under microscopy from PN day 1-3 mice and transferred to the Transwell membrane. The photoreceptor layers of explants were adjacent to Qdot labelled cells, as demonstrated in Figure 2-9, Chapter 2.

Following co-culture for a week in DMEM/F12Glutamax media supplemented with 2% B27 and 1% FBS, the retinal tissues and cells were subjected for immunohistochemistry and integration analysis. Samples were fixed using 4% PFA for 30-60 min at 4°C. Following incubation in 30% sucrose in 0.1M PBS overnight at 4°C, samples were embedded in OCT and sectioned at15 µm using a cryostat. Slides were dried at 37°C for 2 hrs or rt for 24 hrs. For immunostaining, slides were permeabilized and blocked with 0.1mM PBS supplemented with 0.1% Triton X-100 and 5% donkey block serum for 1 hr at rt. Rhodopsin antibody (Sigma Aldrich, 1:250) was incubated with slides overnight at 4°C. The following day specific IgG secondary antibodies, conjugated to an Alexa Fluor 488 (Invitrogen) at a concentration of 1:500 in PBS, were incubated at rt for 2 hrs. Negative controls omitted the primary antibody. Nuclei were counterstained with 10ng/ml DAPI.

#### 5.3 Results (1) electrical excitability of induced LNS cells

5.3.1 Intracellular free calcium was labeled by a calcium indicator in retinal cells and LNS cells in neural differentiation conditions.

LNS cells cultured in neural differentiation conditions displayed a dendritic morphology with long neural processes prior to the calcium assay (Figure 5-1A). To validate this calcium assay, neonatal retinal cells were cultured *in vitro* and used as positive control (Figure 5-1C).

Following incubation with the calcium indicator Fluo-4, the entire cell body including the nucleus of developing retinal cells and co-cultured LNS cells displayed green fluorescence (Figure 5-1C, D). The cellular fluorescence intensity, minus the background signal, was calculated and compared using *in vitro* cultured retinal cells and co-cultured LNS cells. There was no significant difference in fluorescence intensity between co-cultured LNS cells and neonatal retinal cells (P>0.05, unpaired t-test, Figure 5-1E), suggesting they have similar intracellular calcium concentration. This also provided a baseline for the following calcium influx and efflux assay.

Following calcium efflux/influx assay, cell viability was assessed using Trypan blue staining. Most of cells  $(91.07\pm6.51\%)$  displayed intact cell membrane (Figure 5-1B). This indicates that the cells were viable during the calcium assay. Thus, the activity of calcium channel reflects live cell functionality.

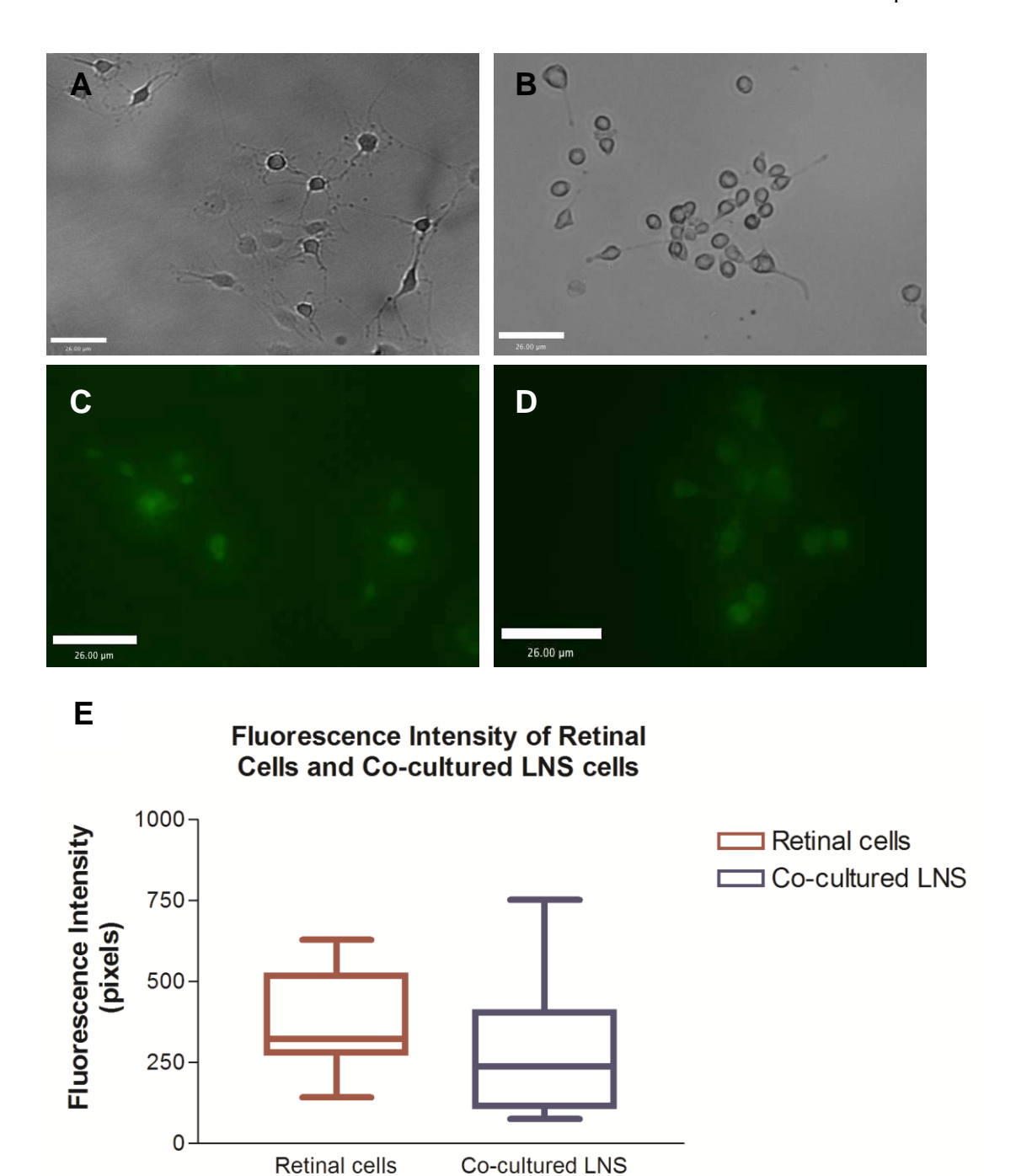


Figure 5-1 Intracellular  $Ca^{2+}$  concentration in developing retinal cells and cocultured LNS cells. **(A)** Phase contrast image of LNS derived cells loaded with calcium indicator Fluo-4; **(B)** Trypan blue staining after calcium assay, showing intact cell membranes; **(C)** *In vitro* cultured developing retinal cells and **(D)** LNS derived cells exhibited green fluorescence following incubation with the calcium indicator Fluo-4. Scale bar:  $26\mu m$ . **(E)** To calculate the cellular fluorescence intensity, background fluorescence was subtracted from individual cells: F= F0 (cellular) - F0 (average background). There was no significant difference between fluorescence intensity in the two cell types ( $n \ge 22$ , unpaired t-test).

Fluo-4 stains both free intracellular and extracellular calcium. When culture condition changed, however, the fluorescence intensity of the LNS cells exhibited difference. With the same incubation procedure, cells cultured in high concentration serum (10%) media exhibited same level as the background fluorescence (Figure 5-2).



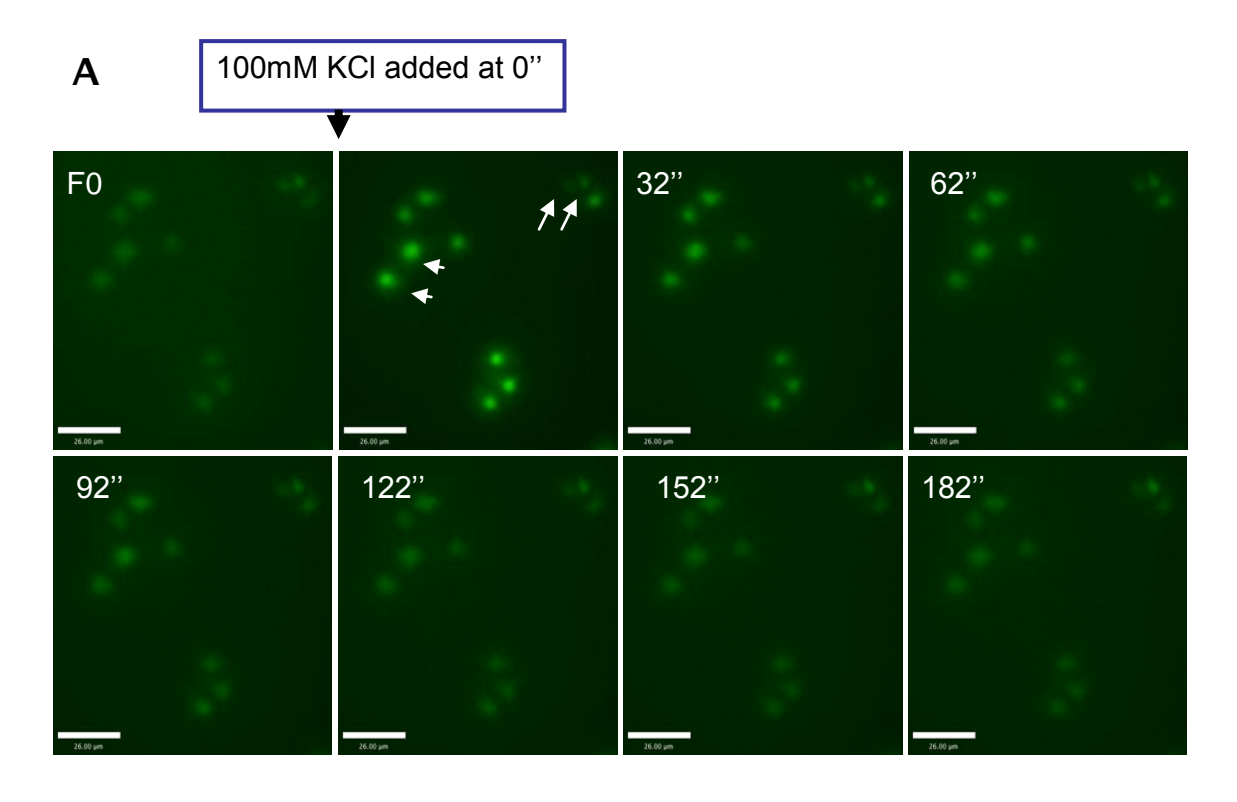
Figure 5-2 Differences in intracellular fluo-4 intensity due to culture condition LNS cells exhibited different intracellular fluorescence intensities when cultured under different conditions. (A) LNS cells in non co-culture differentiation media (1% FBS). (B) LNS cells cultured in differentiation media containing 10% FBS; (C) Developing retinal cells. Scale bar:  $26\mu m$ .

## 5.3.2 Voltage stimulus evoked a Ca<sup>2+</sup> influx in induced LNS cells and developing retinal cells.

Electrical excitability is one of the characteristics of neural lineage cells. To assess the electrical excitability of LNS derived cells, the change of intracellular free calcium was monitored using the calcium indicator Fluo-4 [168,175]. A significant influx of free calcium was evoked by stimulation with high concentrations of K<sup>+</sup>, indicating the existence of voltage-gated calcium channels in the induced limbal cells. The intensity of florescence (F) represents the concentration of free calcium within the cells, and the calcium influx or efflux was displayed individual cellular fluorescence intensity normalized to their initial values (F/F0). Neonatal mouse retinal cells were cultured in the same conditions and used as a positive control.

As demonstrated in Figure 5-3, a significant influx of free calcium was evoked by stimulation with high concentrations of K<sup>+</sup>, indicating the existence of voltage-gated calcium channels in the induced limbal cells. Approximately 60% of induced cells demonstrated excitability. A change in intracellular calcium concentration was not noted in induced limbal cells in the absence of depolarizing stimulus (HBSS control). Neonatal mouse retinal cells cultured *in vitro* also displayed the same reactivity (Figure 5-4). Voltage stimulation was monitored over time. Both cell types showed a similar response, with a quick and significant influx of calcium upon stimulation. The

intracellular free calcium level gradually effluxed after the peak, reaching the prestimulation level at approximately 300s following stimulation (Figure 5-3).



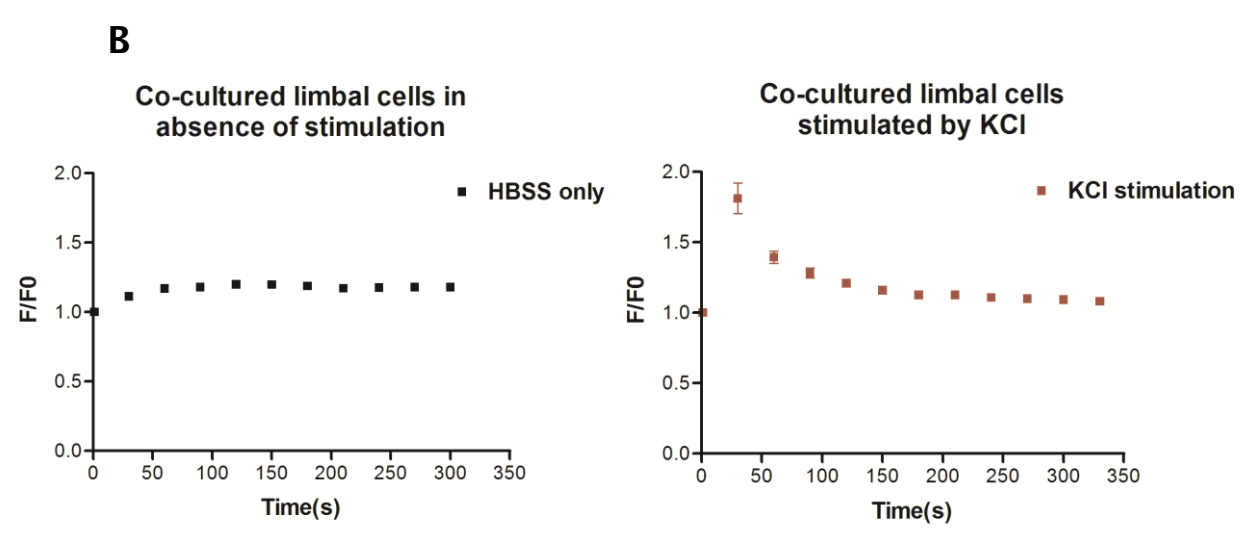
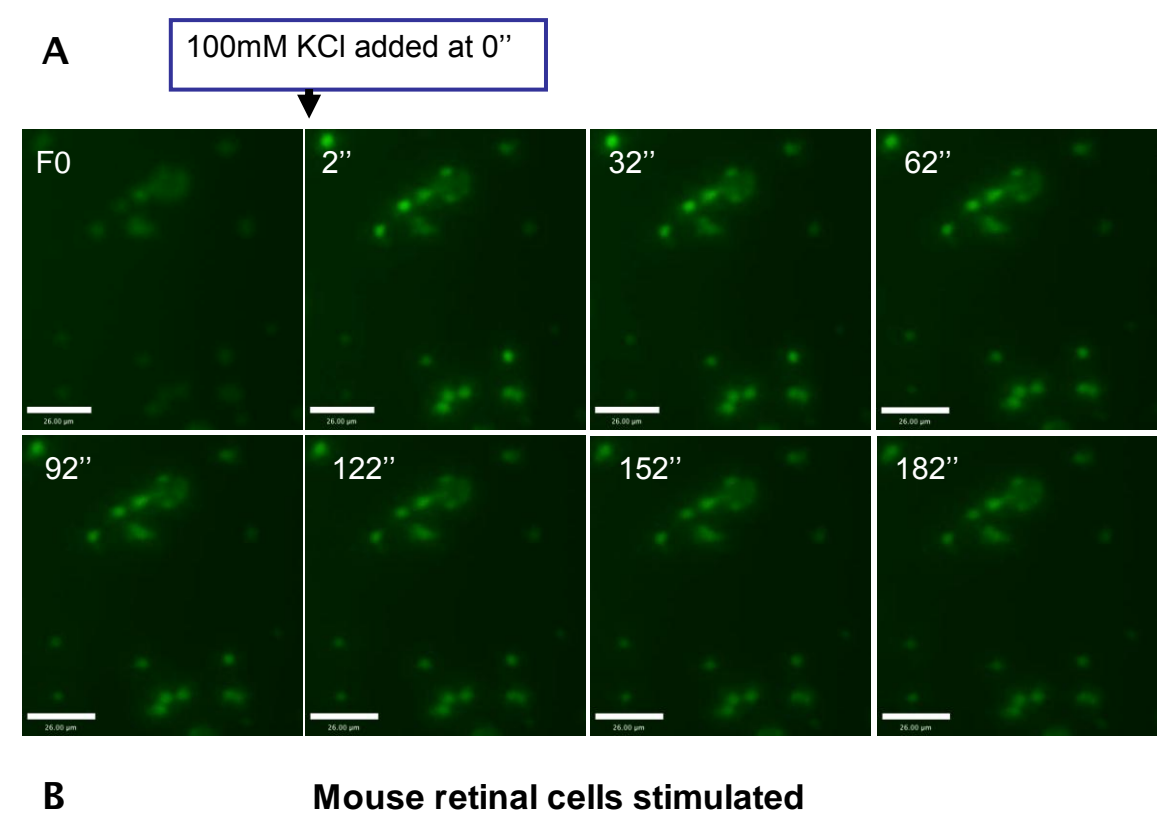


Figure 5-3 Co-cultured LNS cells exhibit calcium influx following a depolarizing stimulus. LNS co-cultured with developing retinal cells were loaded with free calcium indicator Fluo-4. 100mM KCl was added at time 0". Images show free calcium (green fluorescence) of individual cells before and after K+ stimulation against time in seconds. A rapid influx of calcium was observed at 2" upon stimulation, and a slow calcium efflux was observed. Arrowheads indicate two responsive cells with calcium influx; whist arrows show two non-respondsive cells in the same field. Graph depicts the fluorescence intensity (F/F0) changes of individual cells upon non stimulation (HBSS) and depolarizing stimulus by KCl (n≥12). The results suggest that co-cultured cells possess voltage gated calcium channels which are excitable.



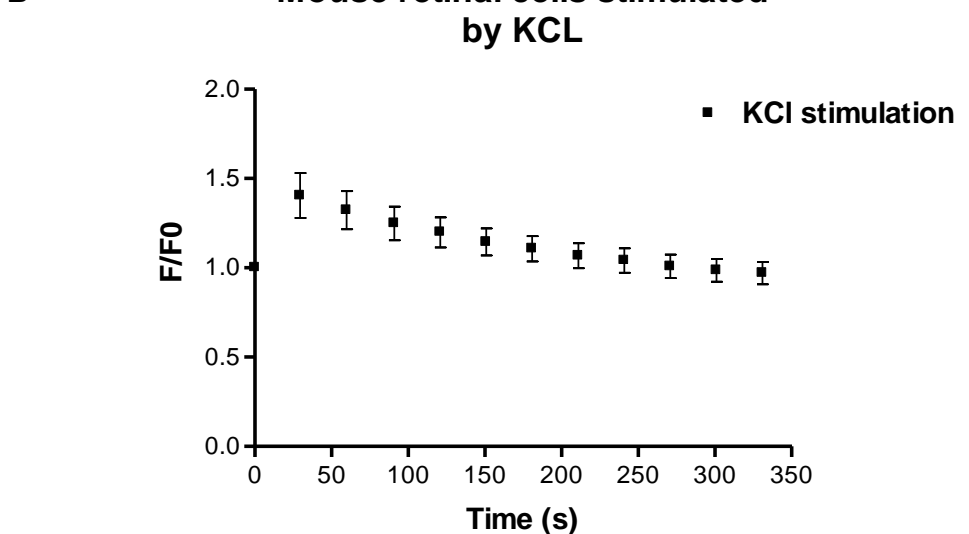


Figure 5-4 P1 retinal cells exhibit calcium influx following a depolarizing stimulus. P1 retinal cells cultured *in vitro* were loaded with free calcium indicator Fluo-4. Cells were stimulated by 100nM KCl at time 0". Images show free calcium (green fluorescence) of individual cells before and after  $K^+$  stimulation, against time. A rapid influx of calcium was observed after 2" upon stimulation, and a slow calcium efflux was observed. The graph depicts the fluorescence intensity (F/F0) changes in individual cells upon a depolarizing stimulus ( $n \ge 12$ ), suggesting they are excitable and possess voltage gated calcium channel.

LNS cells cultured in neural differentiation conditions in the absence of developing retinal co-culture also displayed dendritic cell morphology. It remains unclear whether these cells are functional. Therefore, a further experiment was conducted using non co-cultured limbal cells.

As demonstrated in Figure 5-5, high voltage stimulating 100 mM K<sup>+</sup> did not cause an increase in intracellular free calcium. Similar to the non-stimulated condition, where only loading buffer (HBSS) was added, the intracellular fluorescence intensity was the same as pre-stimulation level. These results suggest that LNS cells acquired functional properties via co-culture with developing retinal cells.

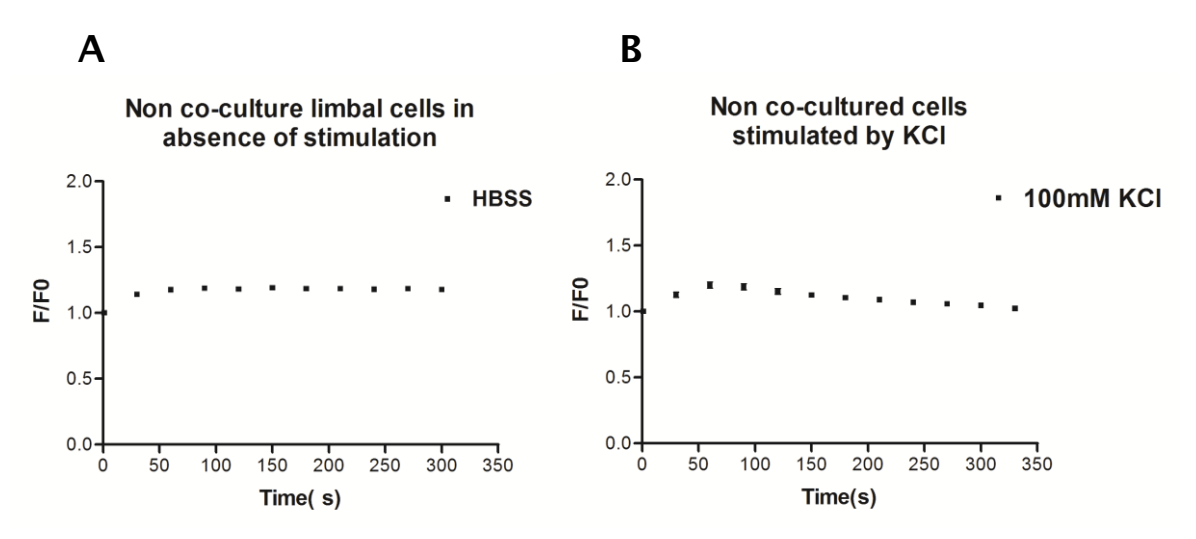


Figure 5-5 Effect of depolarizing stimulus on non co-cultured LNS cells. LNS cells were cultured in defined neural differentiation media in the absence of co-culture for 7 days. Fluo-4 was loaded as free calcium indicator. (A) The cells were stimulated by control buffer solution (HBSS) at time 0". The fluorescence intensity following stimulation is close to the baseline ( $F/F0\approx1$ ). (B) Cells were stimulated by 100mM KCl, a depolarizing stimulus, at time 0". The fluorescence intensity following stimulation is close to the baseline ( $F/F0\approx1$ ), similar to the negative control condition. ( $n\geq12$ ). This result suggests that non co-cultured cells do not possess functional voltage gated calcium channels.

### 5.3.3 Light response was not detected on developing retinal cells using calcium influx/efflux assay.

Light responsiveness is the specific function of photoreceptor cells. Several studies have used calcium influx/efflux assays to demonstrate the light sensitivity of photoreceptor like cells from different resources [6,168]. Before using this assay to test induced limbal cells, a validation experiment was carried out in developing retinal cells. Light hyperpolarizes photoreceptors and causes the closure of cGMP-gated channel, which eventually leads to a decrease in the concentration of intracellular calcium.

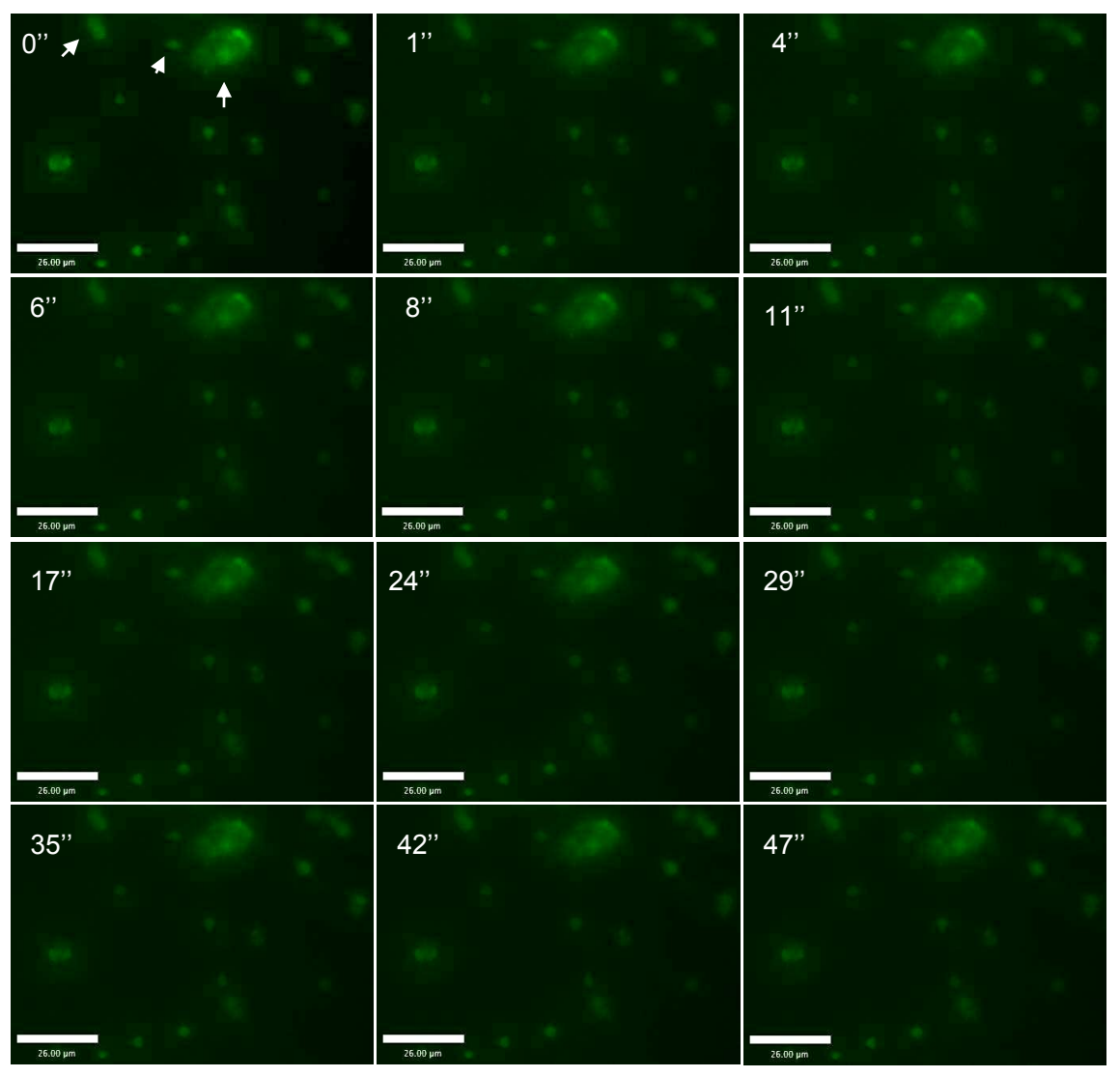
P1 mouse retinal cells were dissociated and cultured in neural differentiation media for 2-3 days prior to loading with fluo-4. Previous studies suggest that the same light source that excites the fluorescent calcium indicator was also used for light stimulation of cells [168,175,224]. To detect possible rapid changes in fluorescence intensity, images were taken approximate every 2 seconds (maximal speed). The shutter remained open, and retinal cells were continually photostimulated. The change in fluorescence intensity was monitored as a function of light responsiveness.

Figure 5-6A shows a series of images taken from 0 to 47 secs from a random field of *in vitro* cultured retinal cells. There was no obvious change in intracellular calcium concentration observed in the developing retinal cells upon light stimulation. *In vitro* cultured retina cells are a mixed cell population, including seven different types of neurons. Among these, only photoreceptor cells and ganglion cells are light responsive. In order to detect a small population of light responsive cells, the analyses were conducted in two different ways:

- (1) monitoring the ratio of F/F0 for individual cell against all time points (Figure 5-6B)
- (2) calculating overall intracellular fluorescence intensity (mean  $\pm$  SEM), as demonstrated in Figure 5-6C.

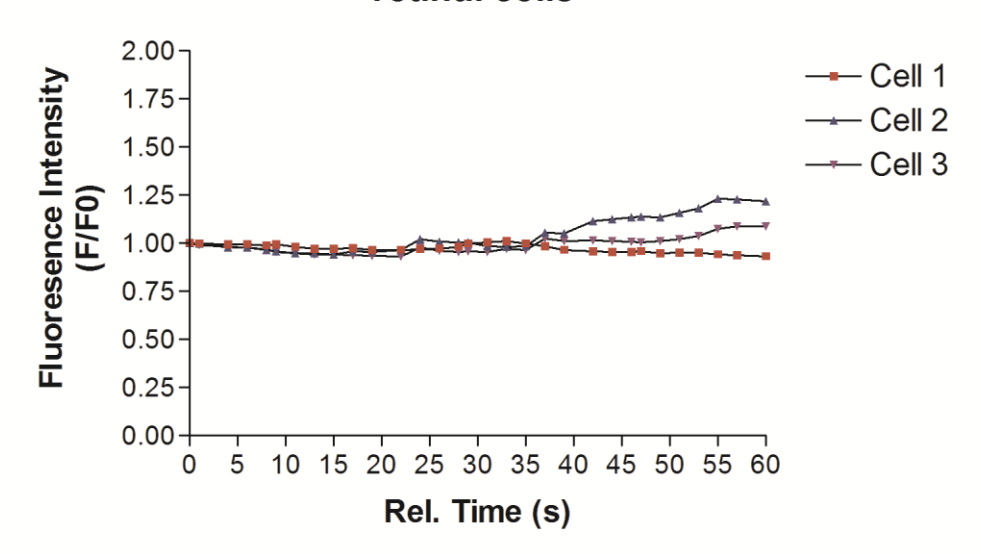
Both graphs show the ratios of F/F0 against time are close to 1, suggesting intracellular calcium concentration in the retinal cells remain unchanged following continual light stimulation. The expected reduction in intracellular calcium concentration was not detectable using this method. Results indicate that this method has limitations as a photostimulation assay. It is not an ideal method to investigate whether induced limbal cells have developed the physiological features of photoreceptor cells.

Α



В

Light response of individual retinal cells



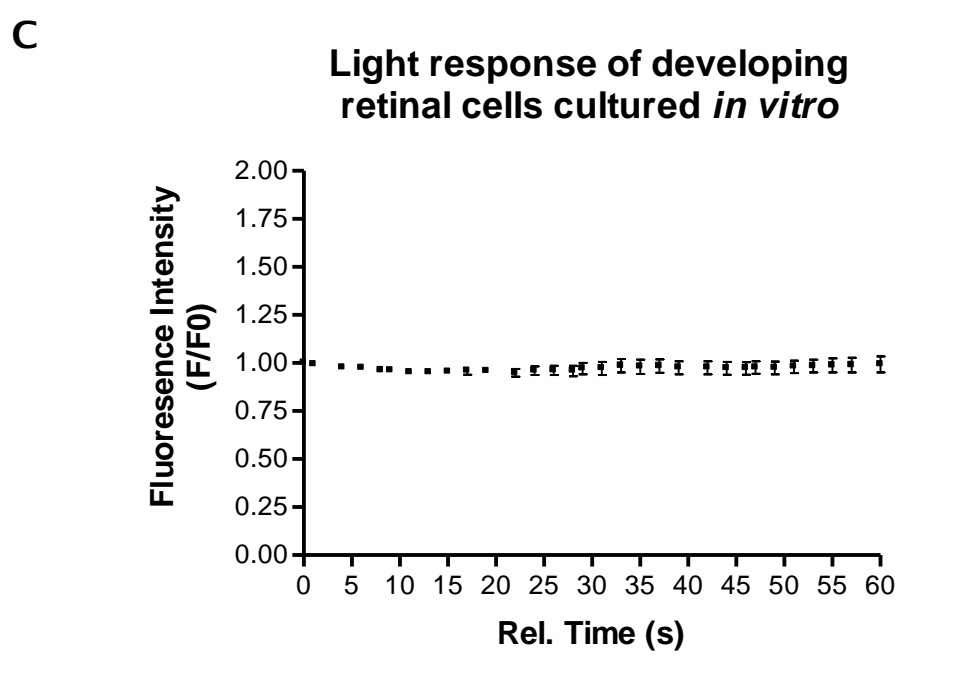


Figure 5-6 light response of *in vitro* cultured developing retinal cells using Fluo-4 calcium assay. **(A)** Cells were excited and stimulated using a 488 nm light source. Images were captured using the maximum shutter speed (< 2 seconds), with an exposure time of 500ms each. The fluorescence images show retinal cells loaded with Fluo-4 upon light stimulation against time. **(B)** Graph represents change in calcium concentration from three chosen cells (white arrows in **A**). Mean background intensity was subtracted from each cellular region to minimise the noise and vibration due to staining or fluorescence fading (F = cellular average-background average). All cells were then normalized by their initial intensity F/FO, and then plotted against time [175]. **(C)** Graph illustrates the change of intracellular fluorescence intensity upon light stimulation from all cells in randomly chosen imaging fields (mean ± SEM, n>50). Result represents three independent experiments.

#### 5.4 Results (2) integration into retinal tissues in vitro

#### 5.4.1 Optimization of Qdot labeling for integration studies

The Qdot loading procedure was tested and optimized based on the manufactures' protocol. LNS cells were incubated with Qdot loading solution for 30 min at varying concentrations (5, 10, 15 and 20mM). The higher concentrations improved the labeling efficiency. However, free Qdots remained in the media after standard washing procedures when the concentration exceeded 10 mM (Figure 6-5). This could possibly lead to false cell integration results if the remaining dye were taken up by the host retinal tissue/cells. Therefore, the time of incubation was increased to 45 min, 1 hr, 3 hrs and overnight respectively at a concentration of 10mM. Overnight incubation led to a much higher proportion of cell death, with an incubation time of between 1- 3 hrs, there was no obvious difference in labeling efficiency and cell viability. Thus, a concentration of 10nM and incubation time 60 mins was selected for cell labeling and integration experiments.

The labelling efficiency was approximately 50% in both human and mouse LNS cells. There was no free floating dye detected in the media (Figure 5-7A). The Qdot florescence was distributed throughout the cytoplasm (Figure 5-7).

#### 5.4.2 Qdot labeled cells rapidly decreased in co-culture system

The majority of Qdot (655nm) labelled cells showed very bright red fluorescence, as demonstrated in Figure 5-7. The fluorescence intensity decreased with time due to cell division and subsequent dilution of the intracellular Qdot particles. In LNS cells, the fluorescence was detectable up to one month after labelling (maximum observation time).

Before integration assessment, Qdot labelled LNS cells were continuously cultured as neurosphere for 5-7 days (Figure 5-8A). They were then dissociated into single cells and cultured on cell inserts. Neonatal retinal explants were then placed on the same cell insert, with their photoreceptor layer adjacent to Qdot labelled LNS cells (Figure 5-8B). In this co-culture system, the number of Qdot labelled LNS cells decreased rapidly. Figure 5-7C & D shows that less than 10% of cells retained Qdots within their cell bodies.

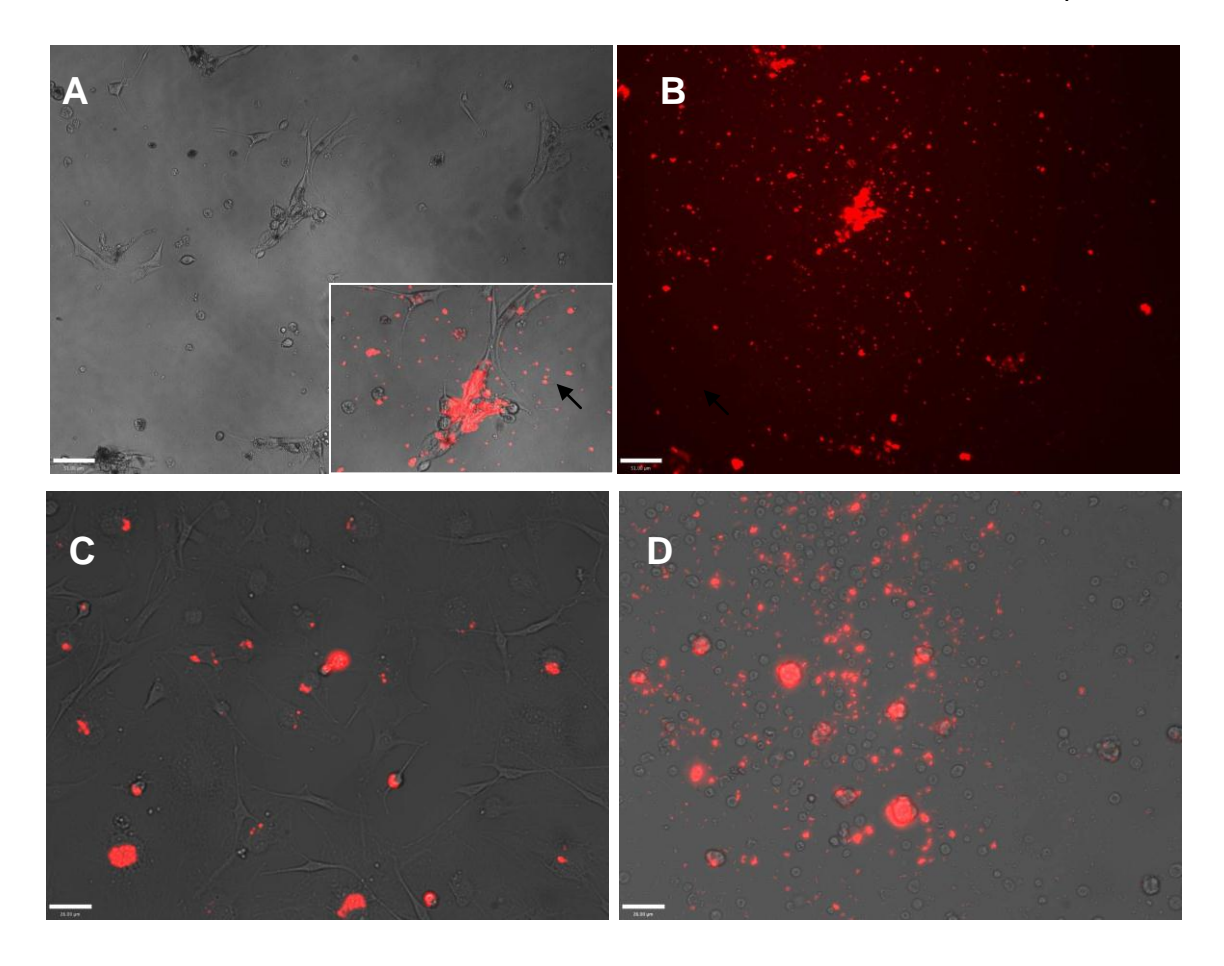


Figure 5-7 Labelling of mouse and human LNS derived cells using Qdot nanoparticles. Free floating Qdots (black arrow) remained in the media when high concentrations of Qdots were used to label mouse LNS cells (A, B & D). Qdot labeling was observed in approximately 50% human limbal cells (C). Cells from both species were labeled with similar efficiency and cellular distribution. Scale bar: 26 µm.

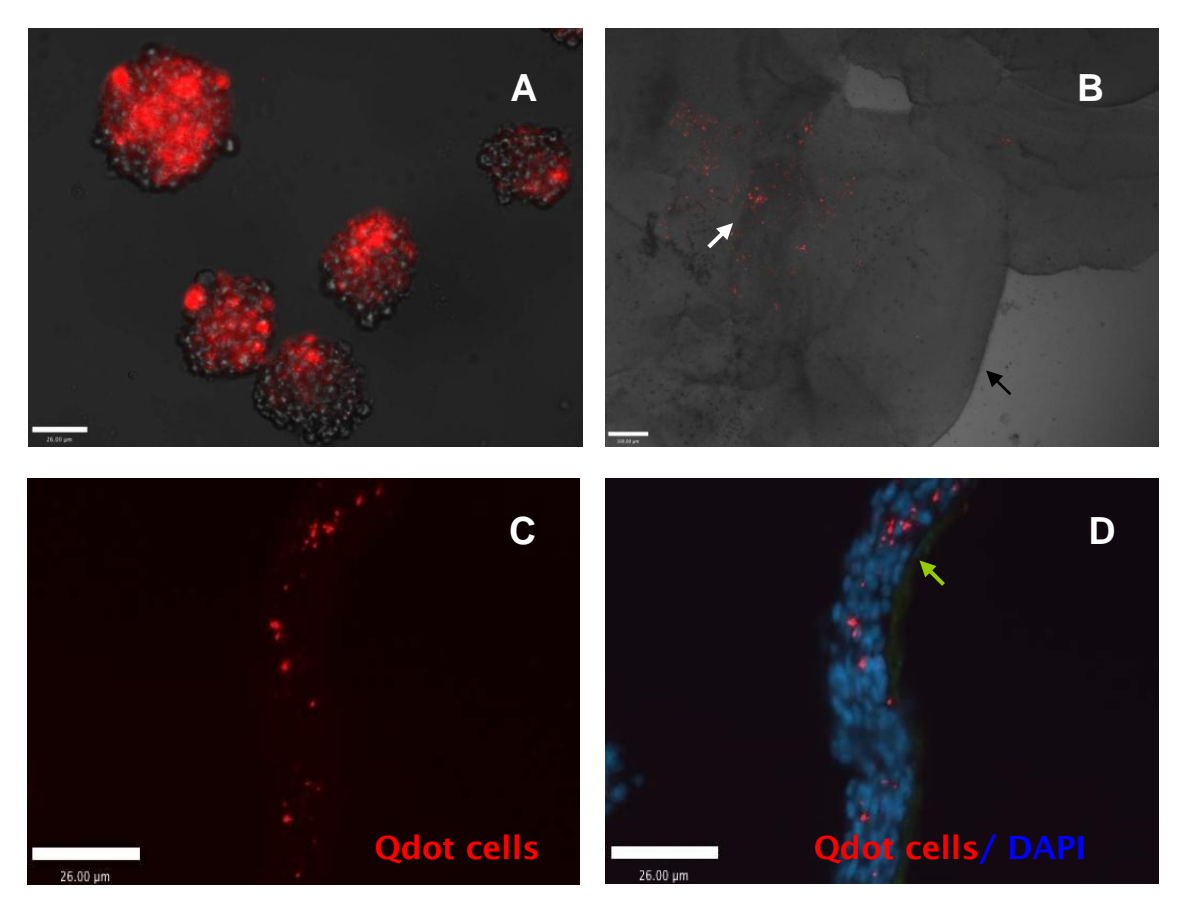


Figure 5-8 Qdot labeled LNS cells in neurosphere culture and co-culture system.

(A) Cells were labeled with bright red fluorescence in the neurosphere culture. The merged fluorescence and bright field image shows that cells and Qdot labeling overlapped, with no free floating Qdots in the media. (B) Shows the Qdot labeled cells in the co-culture system. The retinal tissues were directly cultured on LNS derived cells, with ganglion layer facing up. Through semitransparent retinal tissue (black arrow), the Qdot labeled cells were visible (white arrow). (C, D) show Qdot labeled LNS cell layers (red) on Transwell membrane (green arrow). DAPI was used to stain cell nuclei (blue). Less than 10% of cells retained fluorescent Qdots within their cell bodies. Scale bar: 26um

#### 5.4.3 LNS cells rarely integrated into developing retinal tissue in vitro

Following direct co-culture with developing retinal tissue for 5-7 days, the whole culture system including cells, retinal tissue and Transwell membrane were sectioned and stained for rhodopsin immunoreactivity.

As demonstrated into Figure 5-9, LNS cells were evenly distributed on the membrane surface, although only approximately 10% of cells were still labeled with Qdots following 5-7 days culture. The morphology of the outer nuclear layer of the retina still remained after 2-3 days in culture. The photoreceptor layer of the retinal tissue was confirmed with immunostaining against photoreceptor specific protein, rhodopsin (bright green fluorescence, Figure 5-9). Approximately 1% of Qdot cells migrated into the photoreceptor layer from the subretinal space. They exhibited double labeling with red Qdots and green rhodopsin (orange fluorescence, Figure 5-9C & D). However, the majority of the LNS cells remained unincorporated (Figure 5-9A & B).

This assay showed limitations for cell integration assessment. There was a gap present between dot labeled cells and some of the retinal tissues (Figure 5-9A & B). The labeled cells appeared to attach to the membrane. Therefore, there was a lack of direct contact between LNS cells and retinal tissues in some of the samples. This may limit the ability of cells to integrate. The use of unsorted Qdot labeled cells also decreases the sensitivity of this assay, 50-60% of cells were Qdot labeled after initial loading, however less than 10% of cells retained Qdot fluorescence on the Transwell membranes.

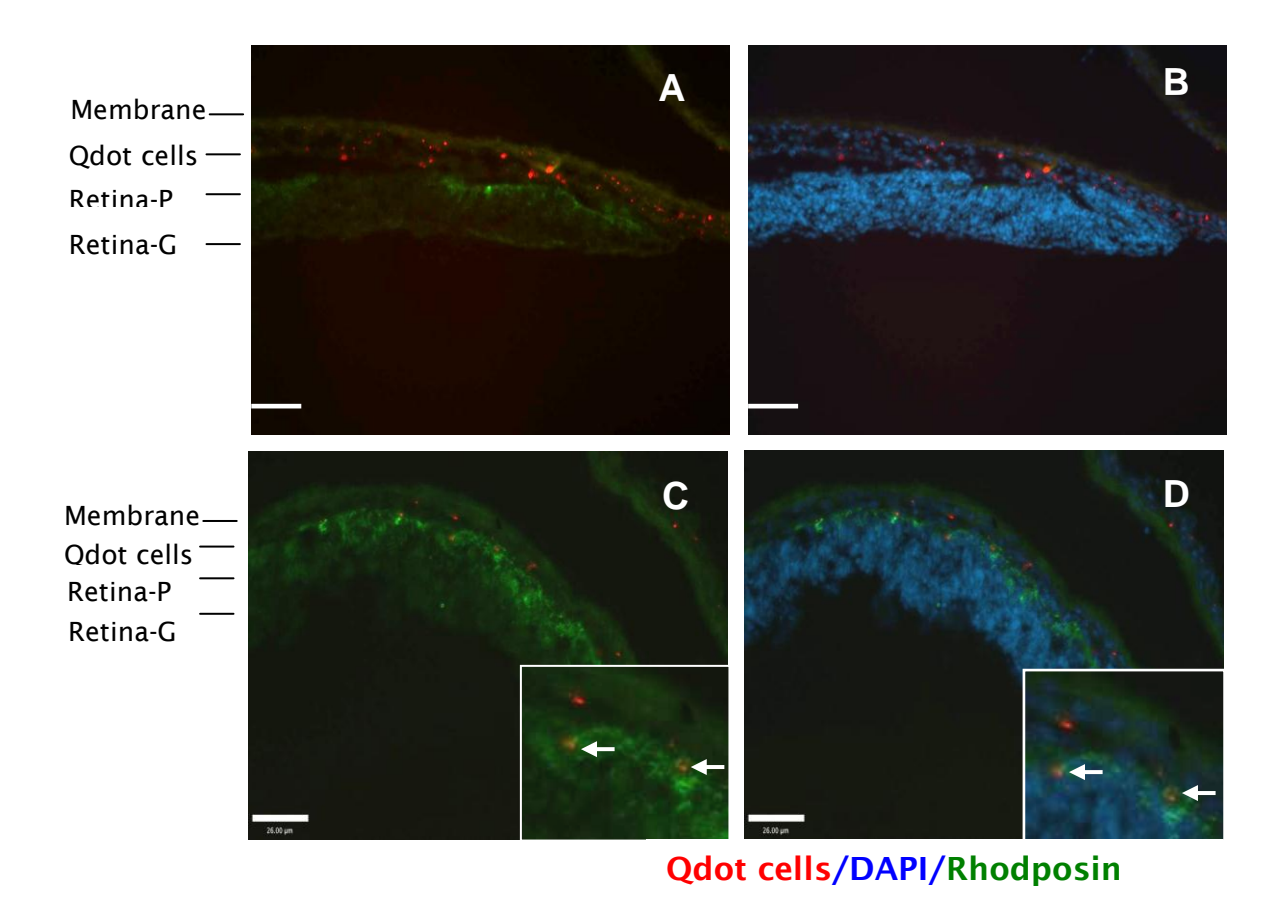


Figure 5-9 Integration of Qtracker labeled LNS cells in vitro.

LNS cells (Qdot labeled cells) were cultured on Transwell membranes. Approximately 10% of LNS exhibited red fluorescence. Developing retinal tissues were placed on top of Qdot labeled LNS cells. To confirm the orientation of retinal tissues, sections were immunostained with Rhodopsin (bright green fluorescence). The photoreceptor layer (bright green) was adjacent to Qdot labeled cells. ( $\bf B, D$ ) show merged images nuclei stained using DAPI. A small proportion of Qdot labeled cells integrated into the photoreceptor layer (in orange,  $\bf C, D$  white arrow); while the majority of LNS cells remained unincorporated ( $\bf A, B$ ). Scale bar:  $26\mu m$ . Abbreviation: Retina-P: retinal photoreceptor layer; Retina-G: retinal ganglion cell layer.

#### 5.5 Discussion

For transplantation and visual rescue, grafted cells must be functional as well as capable of incorporation into the inner retina. Therefore, functionality and integration of LNS derived cells were assessed in this chapter.

#### 5.5.1 Functionality of induced LNS cells

LNS cells cultured in neural differentiation conditions were similarly labelled with calcium indicator as retinal neurons. On the contrary, LNS differentiated in high concentration of serum were unlabelled and not visible under fluorescence microscopy. They did not show typical neuronal like morphology, but were observed as large, flat fibroblast like cells with elongated processes protruding from the cell bodies. This is accordance with previous reports that neural crest derived stem/progenitor cells differentiate into fibroblast cell types when exposed to high percentages of serum [168,175]. This difference in cell labelling using calcium indicator was also observed by Liang *et al.* 2008, they reprogrammed RPE cells into photoreceptor like cells [30]. Only the cells displaying a neuron like morphology were labelled with calcium indicator while the remaining non-reprogrammed RPE cells were not visible under fluorescence microscopy. Therefore, the difference in calcium indicator labelling between cells may due to variation in cell membrane components or due to differences in the concentration of intracellular free calcium.

The presence of functional voltage gated calcium channel was detected in co-cultured LNS cells. Upon exposure to a depolarizing stimulus, approximately 60% of the cocultured LNS cells exhibited an obvious calcium influx, similar to the response seen in the positive control (retinal cells). A 2-3 times increase in fluorescence intensity was detected. Calcium influx was an acute response, which occurred within 2 seconds of stimulation. While it took more than 5 minutes to efflux the intracellular calcium to the pre-stimulation level. The negative control omitting KCI, did not cause a significant increase in intracellular fluorescence. In addition, over 90% of cells showed good viability following this calcium assay, suggesting calcium influx was not due to the damage to the cell membrane. These controls ensured that the observed calcium influx was the result of activation of voltage-gated calcium channels. By contrast, LNS cells maintained in non co-culture condition did not exhibit a similar response, despite some cells displaying a neural-like morphology. These cells also expressed neuronal marker neurofilament 200 as demonstrated in Section 3.5, in Chapter 3. However, the fully-functional voltage gated calcium channels had not developed yet. Thus, these non co-cultured LNS cells probably are not functional.

The use of the calcium assay for the functionality assessment allowed a number of cells to be assessed at the same time. As demonstrated in Chapter 4, only approximately 10% of induced LNS cells expressed photoreceptor specific markers. Therefore, the use of the calcium assay has advantages in the assessment of single cell functionality as well as quantifying a population of cells. Chick retinal cells at embryonic day 16 (E16) have previously been used as positive control, showing light responsiveness by the calcium flux assay [168]. These cells were at the early stage of photoreceptor cell development, as the rhodopsin transcripts first appears in the inferior chick retina at E15 [225]. In the current study, in vitro cultured retinal cells derived from P1-3 mice were used in order to validate the method. These cells were at the peak of rod photoreceptor genesis, expressing rhodopsin at the protein level and consisting of postmitotic rod photoreceptor cells. Therefore, they are at a later development stage than previously reported E16 chick retinal cells. P1-3 mouse retinal cells were able to be maintained in the same low-serum medium as LNS cells in vitro for over 24 days. Similar to LNS cells, most of the retinal cells were viable after the calcium efflux assay and also following light stimulation. However, over 60 seconds of consistent photostimulation did not induce a detectable light response from P1-3 mouse retinal cells by calcium assay.

Photo-transduction is a rapid response process in vivo. Liang et al. also showed that most of the calcium efflux from photoreceptor cells occurred during the first 0.5 minutes following stimulation [168]. The failure to detect a response to light stimulation using calcium indicator may due to the limitations of this assay. Firstly, the light used to excite the fluorescence calcium indicator is also acts as a light stimulus to the cells. Therefore, initial fluorescence intensity (F0) does not represent the baseline of calcium concentration in the dark, but after short photostimulation. Secondly, to detect and quantify a fluorescent signal, other light sources need be avoided. The fluorescence indicator also has the possibility of fading when exposed to strong light sources. The failure to detect light sensitivity may also be due to lack of an appropriate control in this study. Photoreceptor outer segments are undergoing development in mice at age p1-3. Previous reports demonstrates that neonatal mice (p12) have a lower light sensitivity than adult (P45) mice, although the results varied between studies from 1.5 fold to 50-fold [226]. This age-dependent change in light sensitivity may have affected the results in this chapter. Liang et al detected a reduction in fluorescence intensity in E16 chick retinal cells. The basis for the difference between our results and these may be due to the different retinal development patterns in mice and chicks [227].

In this study, the calcium influx/efflux assay did not successfully detect the light responsiveness of retinal cells in vitro. Therefore, it cannot be used to determine whether induced LNS cells were light responsive. Two alternative methods to assess light sensitivity have been previously reported: enzyme linked cGMP assay and electrophysiological recording [168]. The former is an immunoassay to quantify the amount cGMP from tissues/cells. As the hydrolysis of cGMP by cGMP phosphodiesterase is one of the key steps in the phototransduction cascade, light responsiveness can be quantified as a reduction of total cGMP following exposure to light. Jomary et al. conducted the cGMP assay on genetic modified mouse CB epithelial cells in vitro [87,88]. The cGMP level in the dark was 3.2 times higher than in the light. However, this assay cannot be used for in situ analysis of single live cells. The sensitivity of the immunoassay as well as the efficiency of generation photoreceptorlike cells will influence the result. Electrophysiological analysis is a powerful tool for characterizing visual transduction in single cells as well as in tissues. Akagi et al. demonstrated a light induced hyperpolarization of genetically modified iris cells from rats and monkeys [87]. The cells also displayed partially depolarized resting potential in the dark, the electrophysiological feature of the photoreceptors. Electrophysiological recording could be an idea method to further assess the in vitro photoreceptor specific functionality in our future work.

#### 5.5.2 Integration of LNS cells in direct co-culture system

Rod genesis occurs after birth in mice. Neonatal mouse retina can provide an optimal condition for mature photoreceptor cell integrate into the outer nuclear layer [88]. Retinal explants cultures are a good model for *in vitro* assessment of retinal cell transplantation [62]. In this study, for the first time we have investigated the capacity for LNS cells to integrate and migrate within retinal tissue. The co-culture LNS cells integrated into developing neural retinal explants, and expressed the photoreceptor specific marker rhodopsin, although the number of incorporated grafted cell was very small.

Compared to other non-eye field retinal stem cell resources, LNS cells appear more promising. Studies using rat hippocampus derived neural stem cells [88,228] and bone marrow stromal cells [228] have also been shown to migrate into host retinas. Although these studies demonstrated successful integration into animal models or retinal explants, the majority of grafted cells migrated into the INL or GNL instead of ONL. Bone marrow stromal stem cells can express a range of retinal/neuronal markers e.g. neurofilament 200, GFAP, PKC $\alpha$ , and recoverin following migration into retinal

explants. However, no Rhodopsin positive cells were detected [146]. Similar results were observed from hippocampus derived neural stem cells [146].

Cell integration into the retina remains challenging. Despite being derived from the same origin as the neural retina, iris or CB derived cells have also shown limited ability for integration into retina [228]. The proportions of cells which integrated into embryonic retinal explants or retina from degeneration animal models were very small. Studies using retinal progenitor cells from embryonic retina have also shown little integration into host retina, although mature retinal phenotypes were observed following subretinal transplantation [88,229]. MacLaren *et al.* investigated the optimal cell resource for functional integration into adult retina [115,230]. The cells which migrated and integrated were shown to be post mitotic rod precursor cells. Besides morphological integration, expression of mature retinal markers as well as ribbon synapse proteins in the integrated spherule was observed. The eye receiving subretinal transplantation also showed an increase in light-induced pupil constriction. Therefore, the ontogenetic stage of transplanted cells is important for successful cell integration.

The reasons that such a small number of LNS cells (<1%) integrated into retinas was possibly not only due to the donor cells, but also the conditions of the host tissue and limitations of the direct co-culture system in use. Host microenvironment is essential for inducing cell differentiation and migration. In a study involving transplantation of IPE derived cells, the grafted cells expressed the photoreceptor specific marker rhodopsin when they were transplanted into subretinal space of embryonic chicken (E5) eyes. On the contrary, they did not express rhodopsin or other neural markers such as β-III Tubulin and GFAP when they were transplanted into the vitreous cavity. Their morphological features also suggest that they did not differentiation into neuronal cells [62]. In this study, the ONL layers of the co-culture retinal explants retained normal morphology. However, other layers were disrupted rapidly when cultured in vitro. This possibly affected the host microenvironment. On the other hand, the use of unsorted Qdot labeled cells decreased the sensitivity of this assay. Less than 10% of labeled LNS cells exhibited fluorescence in the direct co-culture system. In addition, intracellular distributed of Qdot particles was uneven. Therefore, Qdot cell labeling appears not suitable for the investigation into whether new synaptic connection is formed.

Even though only a small number of LNS cells integrated into the ONL of retinal explants, this study demonstrated a promising autologous cell resource. Future investigation will aim to enhance the integration efficiency through optimization of both donor cells and host environment. FACS sorting will give the ability to deliver a

concentrated population of labeled cells, thereby allowing donor cells to be fully tracked following transplantation into SRS. The may give a more true representation of cell integration. A previous study showed that cells from more defined differentiation stages, particularly post-mitotic cells which are committed to a photoreceptor fate (Nrl positive cells), are more capable of integration into the photoreceptor layer of mice [215]. The host retina at the peak of rod genesis provides an optimal microenvironment for photoreceptor differentiation and cell integration. Therefore, further *in vivo* experiments are required to fully assess the retinal lineage transdifferentiation potential and integration ability of LNS cells.

In summary, the data described provide the functional evidence that LNS derived photoreceptor-like cells possess voltage-gated calcium channel and exhibited electrical excitability. In addition, a small number of cells showed the ability to integrate into retinal tissue *in vitro*. These results highlight a potential candidate progenitor cell source for retinal repair. Further research is warranted to enhance the transdifferentiation efficiency and integration ability of these LNS derived cells.

# 6 Chapter Six - Human LNS cell culture and transdifferentiation

#### 6.1 Introduction

From front to back, the human limbus consists of three major layers namely the epithelial, stromal and endothelial layers. The epithelial layer accounts for 10 percent of the thickness of the limbus, while the remaining 90 percent is composed of the stromal layer. Both layers are readily accessible without intraocular surgery; hence they are an ideal autologous source for cell therapy.

Putative corneal epithelial stem cells were located in the basal layer of the limbal epithelial layer. Clinically, they have been successfully used in the treatment of partial and unilateral limbal stem cell insufficiency (LSCI) caused by chemical or heat burns. From a 1mm² biopsy sample, limbal stem cells can be cultured/expanded *in vitro*, and utilized for corneal surface restoration [62]. Long-term follow-up demonstrated the stability of regeneration of the corneal epithelium and significant improvement in patients' comfort and visual acuity [24,231].

The stroma consists of tightly packed collagen fibrils, with quiescent neural crest derived keratocytes between its lamellae layers. Studies in mice, rabbits and other animal species demonstrate the existence of stem/progenitor cells in the corneal/limbal stroma [24,231]. They exhibit neural potential [32,33,90,145,148,203]. In 2005, Uchida *et al.* derived sphere-clusters from human corneal stromal cells (keratocytes), which expressed neural proteins including beta-III tubulin, neurofilament M (NFM), and GFAP *in vitro*. The human stromal neurosphere cells could be cultured *in vitro* from donors up to 78 years of age [32,33,90,145,148,203]. Du *et al.* investigated the characteristics of human limbal stromal cells. They display clonal growth and side population characteristics, which are key features of adult stem cells. The cells were also multipotent, expressing neural, chondrocyte and keratocyte lineage specific markers when cultured in different induction conditions [29].

In previous chapters, I have demonstrated that stem/progenitor cells with neural potential can be derived from adult mice. They express diverse neural lineages markers, including Sox2, nestin, Musashi 1, beta-III tubulin and neurofilament 200. When co-cultured with developing retinas, they expressed retinal lineage specific markers including Lhx2, Rhodopsin and Rhodopsin kinase, and possessed voltage

gated calcium channel. It is unknown whether human limbus derived cells have the same potential for transdifferentiation. Therefore, the purpose of this study is to

- (1) determine whether LNS cells can be derived from adult, especially aged human limbal tissue.
- (2) investigate whether derived human LNS can differentiate into retinal specific neuron-like cells *in vitro*.

Human limbal tissues from donor eyes and live patients were utilized for cell culture. To fully assess the effect of age on LNS culture, tissue was obtained from aged donors from 66 to 97 years of age. After optimisation of the cell dissociation and culture methods, investigations were conducted on the neural potential of derived limbal cells and their potential for transdifferentiation towards a retinal lineage.

#### 6.2 Methods

#### 6.2.1 Sample collection

The use of human limbal tissue was conducted in accordance with the World Medical Association Declaration of Helsinki, the Ethical Principles for Medical Research Involving Human Subjects. This study (REC: 10/H0502/19) was approved by Southampton & South West Hampshire Research Ethics Committee A to utilize corneal limbal tissue from donor eyes and residue limbal tissue from live patients following pterygium surgery.

Human limbal tissues from donor eyes used in this study were from two resources:

1) residue corneal–scleral rims after routine corneal grafting and 2) corneal and limbal tissues from Bristol Eye Bank which were not appropriate for clinical use. In accordance with the Human Tissue Act 1961, only tissues from donors where appropriate consent for research purposes has been obtained were made available for use in this study. Tissues containing corneal limbal rims were collected from 18 individual donors, with an age range from 66-97 years old. Three female, 10 male and five donors of unknown gender were included.

Surplus limbal tissue from live patients undergoing routine pterygium surgery was also collected. A Pterygium is a benign growth of the conjunctiva. Routine surgery includes excision of pterygium combined with conjunctival autografting, which is an effective treatment to prevent recurrence [30]. A graft is taken from the superior bulb conjunctiva and limbus to cover the excision region. Normally the graft contains surplus tissue (about 1×1mm) to ensure that the excised area can be sufficiently covered. We obtained residual tissue from the graft which would otherwise be discarded after the surgery. Patients were invited to take part in this study if they were due to undergo routine corneal surgery, and given a patient information leaflet. If happy to take part, patients were then consented. Six patients undergoing pterygium surgery (2 female and 4 male) were recruited. Their ages ranged from 34 to 85 years of age.

#### 6.2.2 Human limbal cells dissociation form donor eyes

The tissue obtained from donor eye contained cornea and a narrow rim of anterior sclera only (Figure 6-1). A 2-3mm wide corneal-limbal rim was dissected from the remaining sclera and central corneal. After washing with HBSS, the tissue was cut into 2-3mm pieces. Limbal tissue was then dissociated using three different protocols:

Protocol 1) Incubation in collagenase (78 U/ml), hyaluronidase (38 U/ml) and M2 (Sigma-Aldrich) solution at 37°C for 3-4 hours.

Protocol 2) Incubation in 2.5U/ml Dispase II (Gibco- Invitrogen) and HBSS solution at 4°C overnight [232]. The cells and tissues were then digested in collagenase (78 U/ml), hyaluronidase (38 U/ml) and M2 solution at 37°C for 3-4 hours.

Protocol 3) Incubation in collagenase (78 U/ml), hyaluronidase (38 U/ml) and M2 solution at 37°C overnight.

Cell strainers (70 nm, BD Falcon™) were used to remove undigested tissue; any remaining cell clumps were then triturated to a single cell suspension using a 1 ml pipette. Following centrifugation at 500G for 5 min, cell pellets were re-suspended in a known volume of full neurosphere media DMEM: F12GlutaMAXTM supplemented with 2% B27, 20ng/ml EGF and 20ng/ml FGF2 for cell enumeration and subsequent culture. Cells were plated at a density of 50,000/ml for neurosphere culture. Fresh growth factor mix EGF/FGF2 (20ng/ml) was added every other day. Half of the medium was changed every 3-4 days.

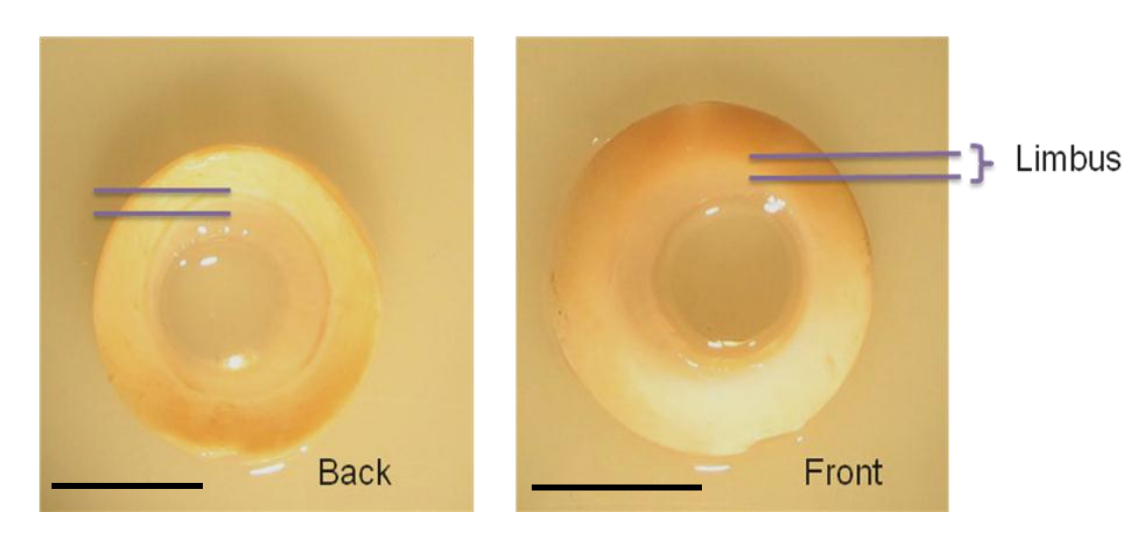


Figure 6-1 Human corneal–scleral rims (residual tissue) from grafting surgery. Images show human donor corneal–scleral rims used in this study. After routine corneal grafting, surplus limbal tissues were collected for neurosphere culture. A 2-3mm wide corneal-limbal rim (between the two lines) was dissected from the remaining sclera and cornea. There was no contamination from other cell such as iris, CB or retina. Scale bar: 10 cm

#### 6.2.3 Human limbal cells dissociation from pterygium samples

The maximum amount of surplus limbal tissue available from pterygium surgery was  $1 \times 1$ mm. Cell dissociation and/or culture protocols were adapted from mouse limbal cell dissociation methods (Chapter 2, Section 2.1), or as previously reported for explants cultures [30].

For serum free sphere forming culture, limbal tissue was incubated in 0.025% (w/v) trypsin/EDTA (Sigma-Aldrich) at 37°C for 10-12 min. One volume of DMEM: F12 with 10% FBS was added to stop digestion. After washing with HBSS, the cells and tissues were incubated in collagenase (78 U/ml) and hyaluronidase (38 U/ml) mix in M2 medium at 37°C for 30 min. Cells were plated into 0.5ml DMEM: F12GlutaMAX<sup>TM</sup> supplemented with 2% B27 and 20ng/ml of EFG and 20ng/ml FGF2.

For explants cultures, tissue was cultured in DMEM: F12GlutaMAX<sup>™</sup> supplemented with 5% FBS, 2% B27, 20ng/ml EGF and 20ng/ml FGF2 for 7-10 days, until monolayer cells grew out of the explants. Monolayer cells were then dissociated with Accutase and subject to serum free sphere forming culture assay in the presence of mitogens.

#### 6.2.4 Co-culture with human and mouse developing retinal

Detailed method of the co-culture protocol with mouse neonatal retinal cells are described in Chapter 2, Section 2.6.3. Briefly, human LNS were plated onto P-D-L and laminin coated plates and co-cultured with dissociated P1-3 mouse retinal cells using Millicel CM inserts (pore size 0.4  $\mu$ m; Millipore) for 1-2 weeks. Differentiation medium contained Neurobasal A media, 2% B27, 0.5 mM L-Glutamine, 0.5-1% FBS, 1 $\mu$ M retinoic acid and 1 ng/ml brain-derived neurotrophic factor (BDNF, R&D system). Half of the medium was changed every other day.

Human developing retinas (45-56 days post-conception) were collected from collaborators in the Division of Human Genetics, at the University of Southampton. Human retinal cells were dissociated using a Papain kit (Washington) as per manufactures' instructions and cultured on cell Inserts for 5-7 days in medium containing DMEM: F12 Glutamax™, 2% B27 and 10% FBS prior to co-culture with human LNS cells.

LNS grew as monolayer when exposed to differentiation conditions. Cell morphology was investigated using phase contrast microscopy. The expression of retinal specific markers was assessed by RT-PCR and/or immunocytochemistry (Figure 6-2).

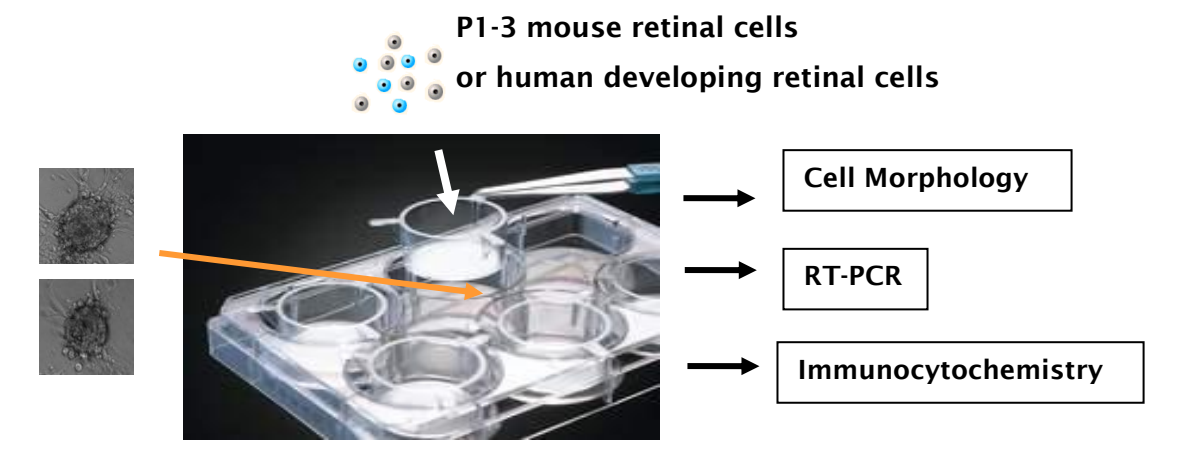


Figure 6-2 Co-culture system for human LNS cells differentiation towards retinal lineage. Millicel CM inserts (pore size  $0.4~\mu m$ ) were used in this co-culture system. The permeable membrane allowed neurotrophic factors to go through, while avoiding cell contamination. Cell characterisation was conducted on human LNS cells following co-culture with P1-3 mouse retinal cells or human developing retinal cells.

#### 6.2.5 Immunocytochemistry

For immunostaining, slides were permeabilized and blocked with 0.1 mM PBS supplemented with 0.1% Triton X-100 and 5% donkey block serum for 1 hr at rt. Primary antibodies were incubated overnight at 4°C. After gentle washing, specific IgG secondary antibodies, conjugated to an Alexa Fluor 488 at a concentration of 1:500 in PBS, were incubated at rt for 2 hrs. Negative controls omitted the primary antibody. Nuclei were counterstained with 10ng/ml DAPI. The antibodies used in this study are listed in Table 6-1.

Table 6-1 Primary antibodies used for human LNS cell immunocytochemical analysis.

Antibody	Specificity	Company	Conc.
Nestin	Neural stem cells	Millipore	1:100
Sox2	Neural stem cells	Santa Cruz	1:250
Bestrophin	RPE cells	Abcam	1:100
beta-III tubulin	Early differentiated neurons	Covance	1:500
Rhodopsin	Photoreceptors	Sigma-Aldrich	1:250
RPE65	RPE cells	Abcam	1:200

#### 6.2.6 Reverse transcription polymerase chain reaction

RNA extraction, cDNA synthesis and polymerase chain reaction were conducted as described in Chapter 2, Section 2.4. Total RNA was isolated and cDNA synthesis was performed as per manufacturers' instructions using a RNeasy Plus kit (Qiagen, West Sussex, UK) and a High Capacity cDNA Reverse Transcription Kit (Applied Biosystems). cDNA was amplified using gene specific primers (Table 6-2) using step cycles (denaturing for 30 sec at 94°C; annealing for 30 sec at 60°C and extension for 30 sec at 72°C for 35 cycles, unless mentioned otherwise). Electrophoresis was performed on a 1.5% agarose gel. The gels were stained with Ethidium Bromide and viewed under a UV illuminator (UVP High Performance). Photos were captured using a CCD camera, using Doc-It®LS Image software (UVP High Performance).

Table 6-2 Gene specific primers used for human LNS cell RT-PCR analysis.

Gene	Primer sequence	Size
Human_Bestrophin_F	ATTTATAGGCTGGCCCTCACGGAA	359
Human_Bestrophin_R	TGTTCTGCCGGAGTCATAAAGCCT	
Human_Chx10_F	ATTCAACGAAGCCCACTACCCAGA	229
Human_Chx10_R	ATCCTTGGCTGACTTGAGGATGGA	
Human_Crx_F	TATTCTGTCAACGCCTTGGCCCTA	253
Human_Crx_R	TGCATTTAGCCCTCCGGTTCTTGA	
Human_GAPDH_F	ACCACAGTCCATGCCATCAC	450
Human_GAPDH_R	TCCACCACCCTGTTGCTGTA	
Human_Lhx2_F	CAAGATCTCGGACCGCTACT	284
Human_Lhx2_R	CCGTGGTCAGCATCTTGTTA	
Human_Opsin(sw)_F	TACCTGGACCATTGGTATTGGCGT	379
Human_Opsin(sw)_R	TAAGTCCAGCCCATGGTTACGGTT	
Human_Pax6_F	CGGAGTGAATCAGCTCGGTG	300(5a),258(5a)
Human_Pax6_R	CCGCTTATACTGGGCTATTTTGC	
Human_RPE65_F	GCCCTCCTGCACAAGTTTGACTTT	259
Human_RPE65_R	AGTTGGTCTCTGTGCAAGCGTAGT	
ªHuman_Rx_F	GAATCTCGAAATCTCAGCCC	279
ªHuman_Rx_R	CTTCACTAATTTGCTCAGGAC	
*Human_Six3_F	CGAGCAGAAGACGCATTGCTTCAA	394
*Human_Six3_R	CGGCCTTGGCTATCATACATCACA	
<sup>a</sup> Human_Sox2_F	CCCCGGCGCAATAGCA	448
<sup>a</sup> Human_Sox2_R	TCGGCGCCGGGAGATACAT	
Human_Rhodopsin_F	CACCACAGAAGGCAGAGA	378
Human_Rhodopsin_R	AGGTGTAGGGGATGGGAGAC	

<sup>\*</sup>Six3: Annealing Temp: 55°C, MgCl2: 2mM; all other primers: Annealing Temp: 60°C,

<sup>&</sup>lt;sup>a</sup>: Non-intron-spanning primers

#### Results

#### 6.2.7 Effective generation human LNS from donor limbal tissues

Human limbal tissue is much harder and thicker than mouse corneal. In order to obtain sufficient cells for culture, the cell dissociation was re-optimised as described in the Methods in this chapter. Following Protocol 1, the majority of the limbal sample remained as intact tissue following digestion, showing a poor cell dissociation effect. All cells were cultured in 0.5ml of full media in 24 well plates. After 2 weeks culture, there were no typical neurospheres detected following Protocol 1 cell dissociation.

Following protocol 2, approximately half of the tissues were digested. There were 20-30 LNSs generated following 10 days in serum free sphere forming culture. The spheres generated were up to  $25\mu m$  in diameter (Figure 6-3A). Beside the clonal growth feature, a subpopulation of human limbal cells exhibited a dendritic morphology and grew as a monolayer in the serum free culture media (Figure 6-3B). To investigate the neural potential of human LNS cells, the cells were dissociated into single cells and plated on P-D-L and Laminin coated plates for 24 hrs prior to immunostaining. Approximately  $8.83 \pm 1.31\%$  (Mean  $\pm$  SEM) cells expressed the neural stem cell marker nestin, as demonstrated in Figure 6-3.

Protocol 3 was the most efficient for human limbal cell dissociation. The majority of the intact limbal tissue was digested following overnight incubation with the collagenase / hyaluronidase enzyme mix. Cell viability was accessed using a Trypan blue assay, showing 90% cell viable. Following culturing for 7-10 days in the serum free neurosphere culture system, over 100 LNSs were generated from all donor eyes (Figure 6-4). Human LNS displayed a smooth surface, with sizes ranging from 50-150 $\mu$ m in diameter. Human LNSs were generated from donor tissue with an age range from 72-97 years. Although a subpopulation of human limbal cells generated a cell monolayer in the serum free culture media, neurospheres were efficiently generated from donor limbal rim tissues. Approximately 34.80  $\pm$  2.19% (Mean  $\pm$  SEM) limbal cells were immunoreactive with the neural stem cell marker nestin when Protocol 3 was used. This is significantly higher compared with protocol 2 (two-tailed unpaired t-test, P<0.001, Figure 6-5). The cells also expressed the transcription factor, Sox2, as shown Figure 6-4. The Sox2 protein was localized to both the nucleus and cytoplasm.

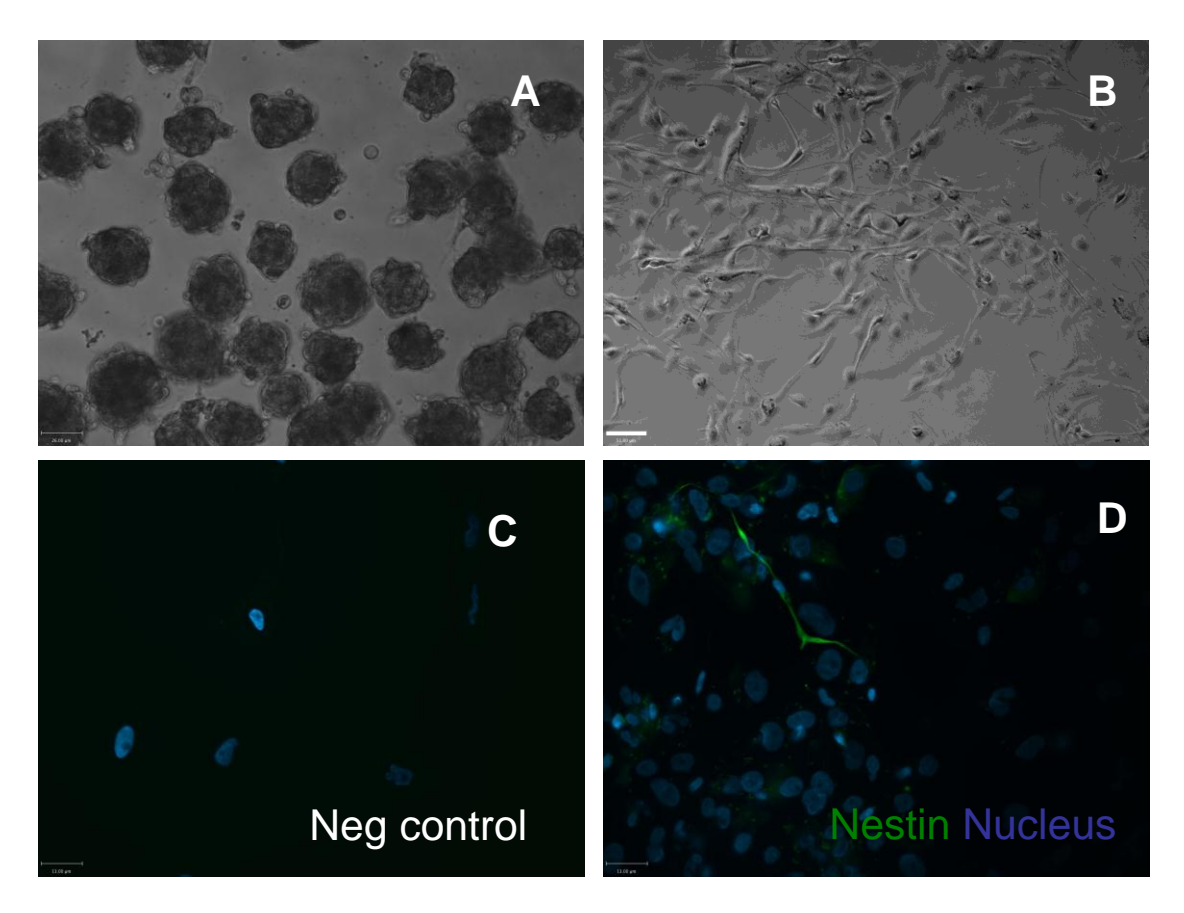


Figure 6-3 Human LNS cells from a 79 years old male using Protocol 2. Small spheres (diameter  $\leq 25~\mu m$ ) were generated after 10 days in culture **(A)**. A subpopulation of cells grew as monolayer **(B)**; Negative control for immunofluorescence primary antibody was omitted **(C)**; Green fluorescence shows the Nestin positive cells in the culture. Approximately  $8.83 \pm 1.31\%$  (Mean  $\pm$  SEM) cells expressed nestin **(D)**. Scale bar: A:  $26\mu m$ , B:  $52\mu m$ , C & D:  $13\mu m$ 

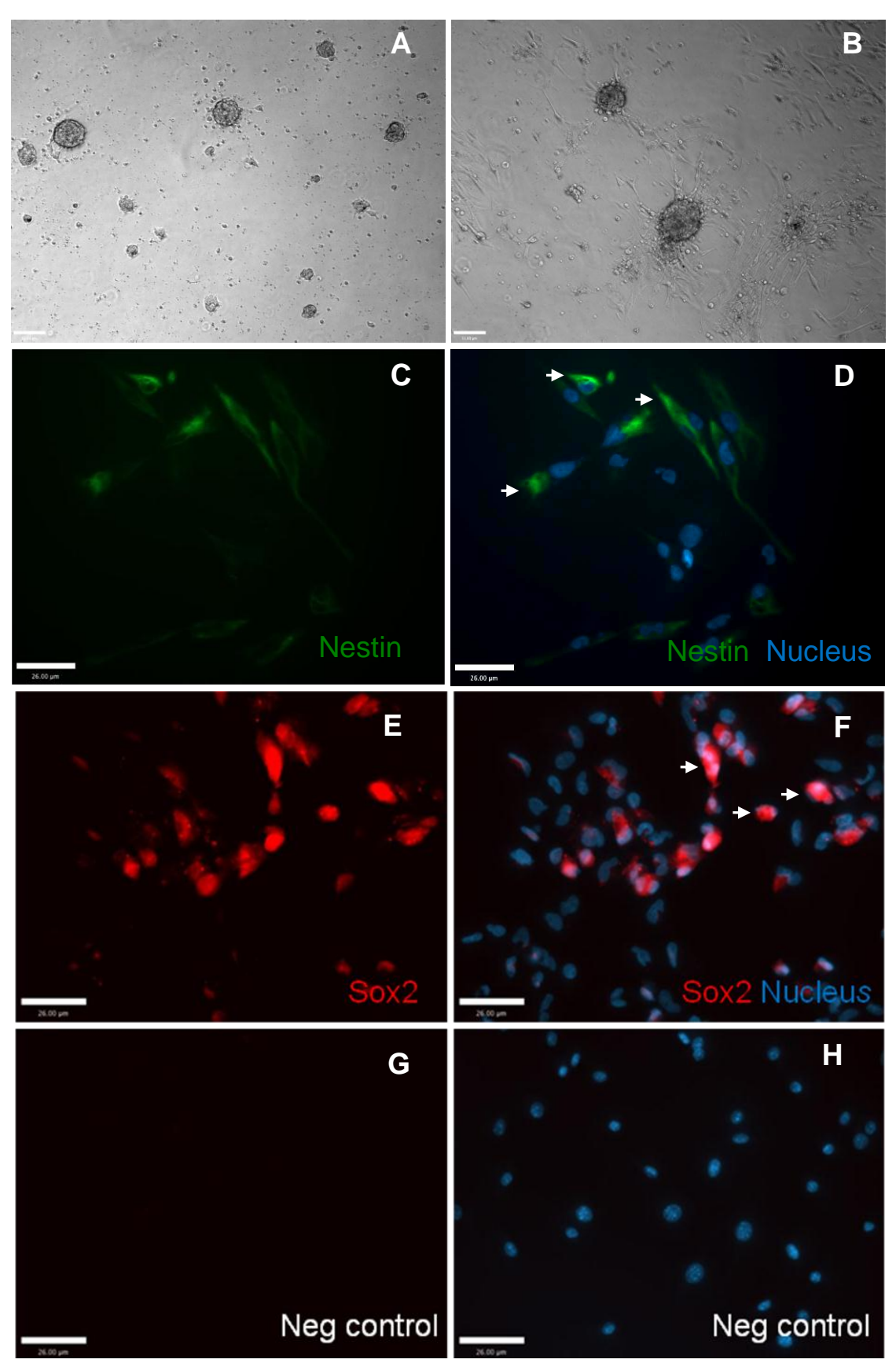
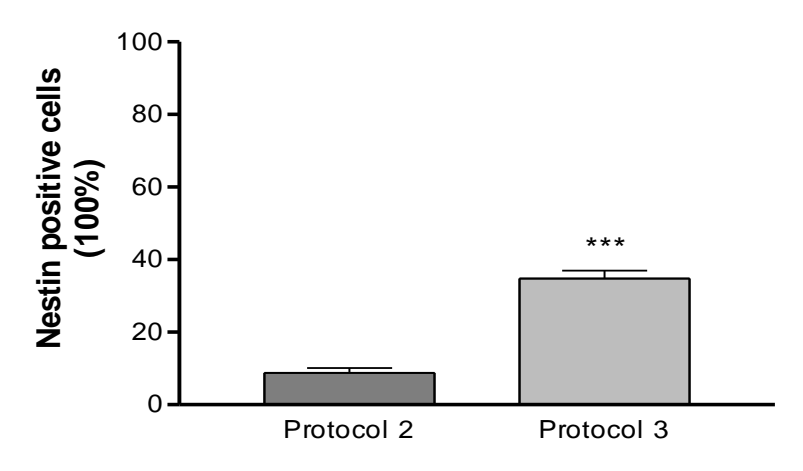


Figure 6-4 Human LNS cells from 74 - 80 years old donor eyes using Protocol 3 Human LNS generated after 7 days in culture were 50-100  $\mu m$  in diameter (A & B). Negative control for immunofluorescence omitted primary antibody (G & H). Human LNS cells expressed the neural stem cells marker nestin (C & D, arrowheads, green) and Sox2 (E & F, arrowheads, Red). Sox2 was located in both the nucleus and cytoplasm. Scale bar: A & B 50  $\mu m$ , C-H 26  $\mu m$ 

## Percentage of Nestin Positive cells from Human LNS cultured in vitro



### Cell dissociation from human donor limbal rim

Figure 6-5 Optimal cell dissociation protocol for LNS cell culture. Donor limbal rims were subjected to different cell dissociation protocols, followed by a neurosphere forming culture system in the presence of EGF and FGF2. Human derived primary LNS were re-dissociated into single cells and plated on P-D-L and Laminin coated plates 24 hrs prior to immunostaining. There was no LNS generated using protocol 1. Percentage of nestin positive cells is expressed as mean  $\pm$  SEM (n=3). Significant difference \*\*\* P<0.001 compared between protocol 2 and 3 by a two-tailed unpaired t-test.

## 6.2.8 Secondary LNS were generation from Primary human LNS, although a small number of samples lost clonal growth features.

Human donor LNS cells can be subcultured to generate secondary neurospheres and cryopreserved for future use. Following subculture, 2 of the 8 samples (77 & 74 years old male donors) lost their ability to proliferate by clonal expansion. Characterisation was carried out on the subcultured cells. Figure 6-6 demonstrated the expression of the neural stem cell markers Sox2 and Nestin and the early differentiated neuronal marker beta-III tubulin (Tuj1) by immunocytochemistry. Nestin, Sox2 and beta-III tubulin were strongly expressed when the cells were proliferating by clonal expansion (Figure 6-6, Left). However in the samples which lost clonal growth in the NSA, the neural stem /progenitor cell markers, Nestin and Sox2, were weak or undetectable (Figure 6-6, right). Beta-III tubulin expression remained similar in both neurosphere and monolayer limbal cells.

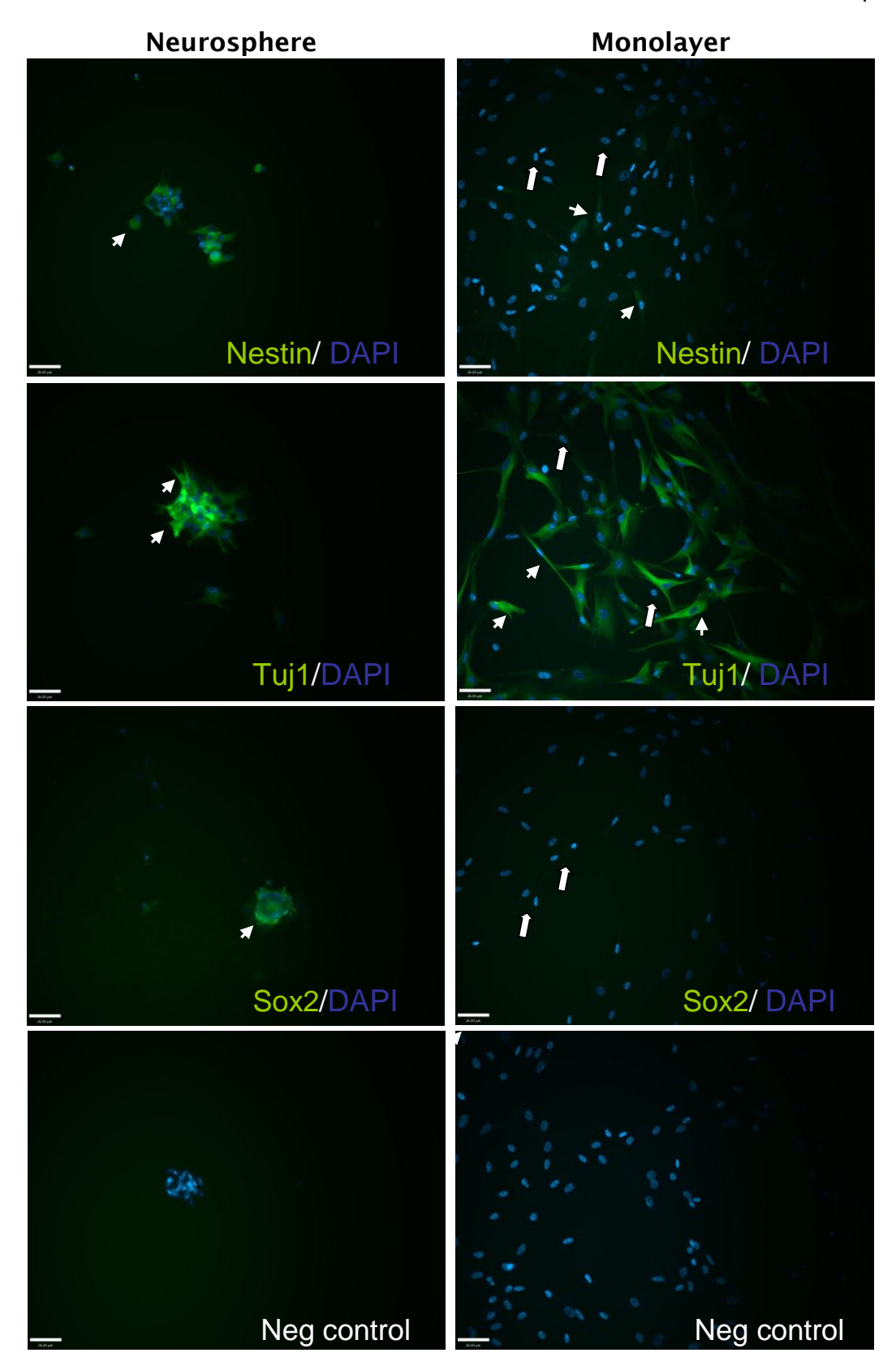


Figure 6-6 Neural potential of subcultured human LNS cells.

Human LNSs derived from donor eyes were subcultured in sphere forming medium (DMEM: F12GlutaMAX™ with 2% B27, 20ng/ml EFG, 20ng/ml FGF2). Approximately half of the samples spontaneously gave rise to monolayers after subculture (right panel). Expression of the neural stem cell markers Sox2 and Nestin was weak or undetectable

in monolayer cells, while expression of beta-III tubulin (Tuj1) was consistent. Arrowheads indicate immunopositive cells, while arrows show negative cells. Strong expression of all three markers were observed in cells continuously grown as neurospheres (right panel). Scale bar: 25µm

#### 6.2.9 Human LNS culture from Pterygium surgery

Five samples were collected from patients who underwent routine pterygium surgery. Initially two samples from patients (72 year old female and 55 year old male) were dissociated into single cells and cultured in the serum free sphere forming assay in the presence of mitogens (EFG and FGF2). However, the majority of the cells gradually died under these culture conditions. Neither the formation of sphere-like structures nor cell proliferation was observed after 14 days in culture.

The remaining 3 samples were subjected to explants culture in the presence of both serum and mitogens [88,176]. Cells grew out from the explants and formed a monolayer from two samples (35 and 40 year old males). Following sphere forming subculture, the cells formed cells clumps attached to the culture plate, conventional neurospheres with a smooth surface or typical size (≥50µm) were not detected (Figure 6-7). No cell proliferation or growth was observed from the third sample which was from an 85 year old male.

From Pterygium surgery, samples were typically less than  $1 \times 1$  mm in size, and were obtained from the superficial layer of the limbus. The serum free sphere forming assay in the presence of mitogens, supported the growth of LNS from human donor eyes, however it did not support the growth of limbal cells derived from pterygium patients. This may be due to the very small number of cells which were obtained. Of which, the majority were possibly epithelial cells from the conjunctiva. Explants culture in the presence of low concentrations of serum was a more supportive environment. The two successful cultures were from patients aged 35 and 40 years old, while the one from patient aged 85 failed. It appears that age, the size of the sample and culture method affect human limbal cell growth.

Immunocytochemistry was carried out to investigate whether limbal cells had neural potential in these two successful explants cultures. Approximately 3-5% of cells expressed Nestin. Interestingly, the nestin positive cells were detected on the monolayer of cells growing out from the sphere like cell clumps, but not in the in the sphere-forming cells (Figure 6-7). Conversely, the early differentiated neuronal marker

beta-III tubulin was detected in the sphere-like cell clumps (Figure 6-7), with approximately 90% of cells being immunopositive for TUJ1.

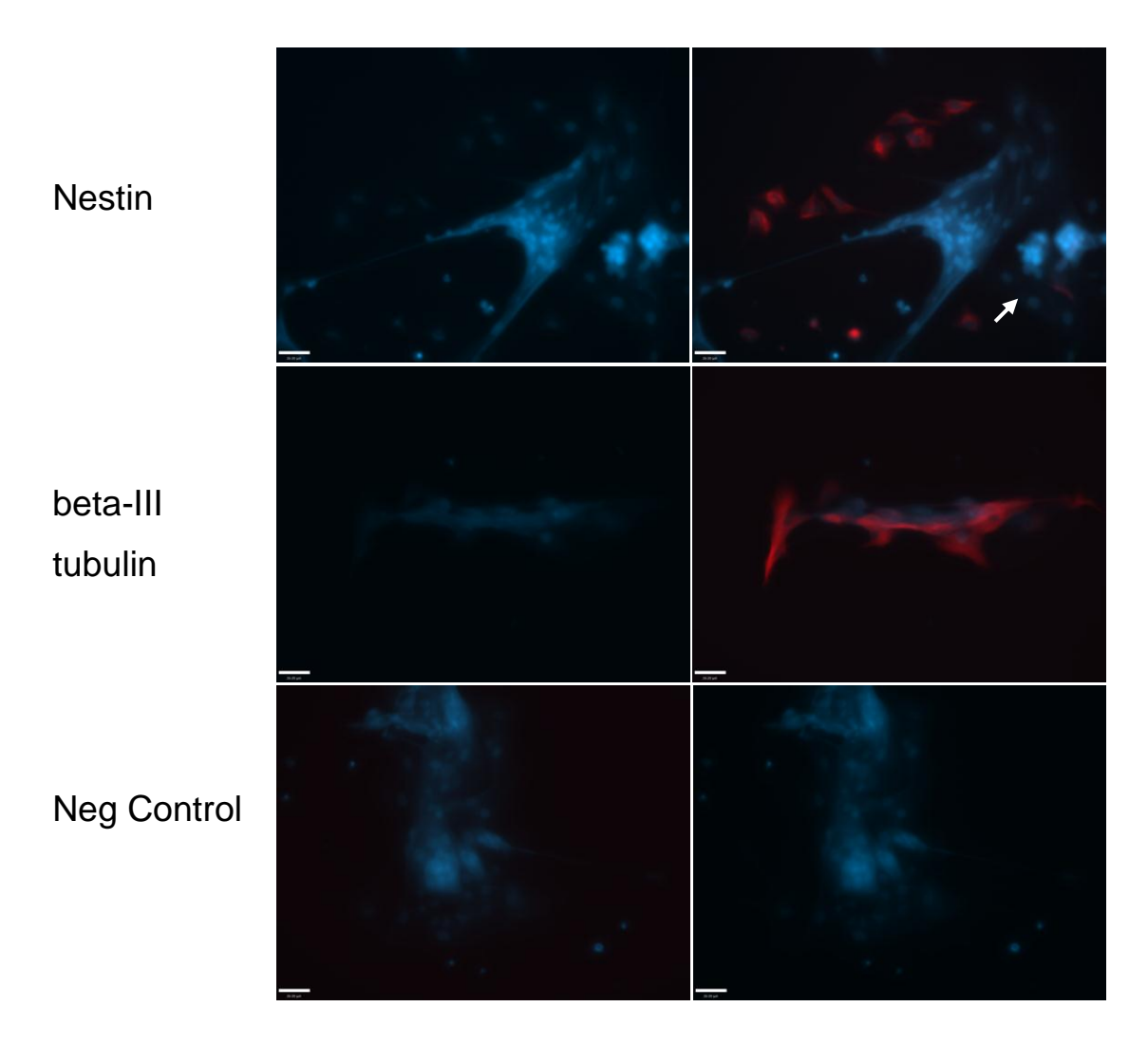


Figure 6-7 Culture of limbal cells from live patients

Limbal cells were cultured from  $1\,\text{mm}^2$  of limbal tissue from a 35 years old patient who underwent pterygium surgery. Following explants culture and subsequent serum free neurosphere forming culture, sphere-like cell clumps formed (white arrow). Expression of Nestin was absent in the sphere-like cell clumps, but was detected in monolayer cells (red). Nuclei were counterstained with DAPI (blue). Beta-III tubulin was detected in the majority of cell clumps (red). Cells were in different plains of focus, due to clonal growth. Therefore, the images were not evenly focused. Scale bar:  $26\mu\text{m}$ .

Here we demonstrated that cells with neural potential can be derived from less than 1 mm2 of superficial limbal tissues from adult patients. They expressed the neural stem/ progenitor marker nestin and beta-III tubulin. Our preliminary data is based on 5 five patients. The tissues were not from the pathological region of pterygium site, but from the healthy limbal region, hence it represents the characteristics of ex vivo limbal cells derived from healthy individuals. Increasing the sample size is necessary to determine the effect of age on the derivation and expansion of human limbal cells and their neural potential.

## 6.2.10 Expression of retinal progenitor markers were detected on human LNS derived cells by RT-PCR

Several methods were used to promote human LNS cell differentiation towards retinal like phenotypes, including the use of extrinsic factors such as Shh, Taurine and RA [88,176] and a co-culture assays. To investigate the potential of human LNS cell transdifferentiation towards retinal-like cells, both neonatal mouse retinal cells and early human developing retinal cell were used for the co-culture assay.

The expression of retinal progenitor cell markers including Pax6 (Paired box gene 6), Lhx2 (LIM homeobox 2), Rx (retinal homeobox), Crx (cone and rod homeobox), Six3 (SIX homeobox 3) and Chx10 (also known as Vsx2, visual system homeobox 2) were investigated on the human LNS cells following differentiation for approximately 5 days. The results represent 2 independent experiments by RT-PCR. cDNA extracted from foetal and adult human retina was used as a positive control for human progenitor markers. Co-cultured limbal cells omitting transcriptase during cDNA synthesis were used as negative control to exclude the non-specific amplification or possible contamination (Figure 6-8).

As shown (Figure 6-8, Lane 1-4), low levels of Lhx2 and Pax6 were detected in all samples co-cultured with mouse developing retina or Shh/Taurine/RA conditions. No band was detected in the negative control (Figure 6-8, lane 5). Rx was present in 50% of above samples. On the contrary, human LNS cells co-cultured with human early developing retinal cells or non-inducing control condition, did not express the above retinal developing transcription factors (Figure 6-8, lane 6-8). Expression of Chx10 and the downstream transcription factors, such as Crx and Six3, were either undetectable or appeared at an incorrect size in all conditions.

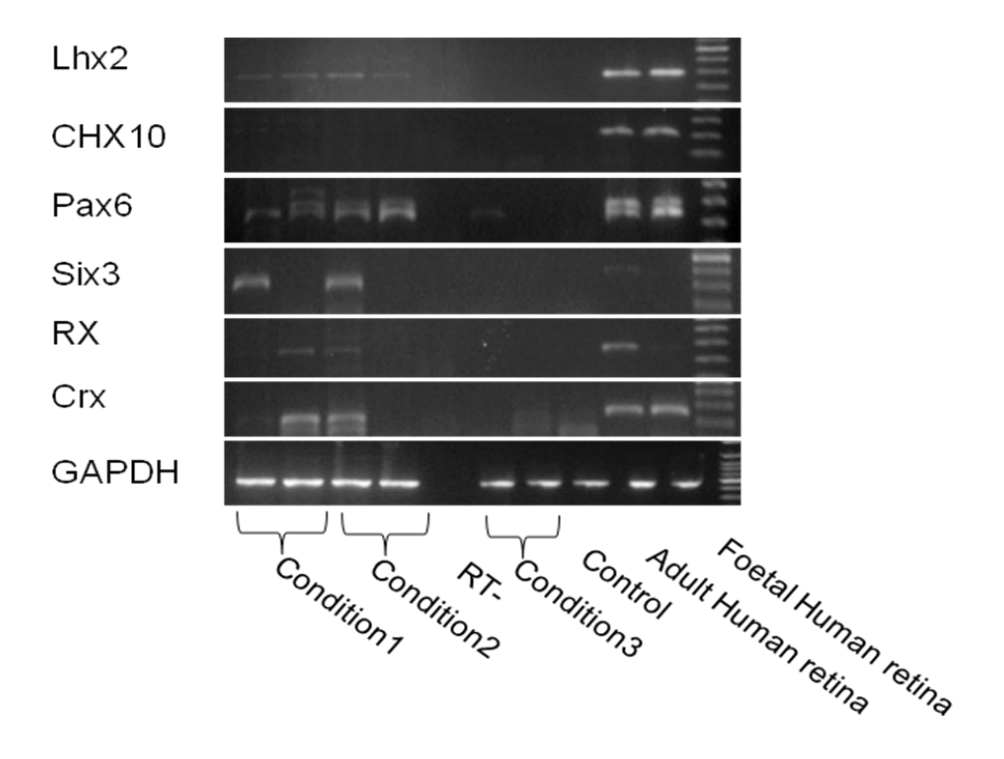


Figure 6-8 Expression of retinal development transcription factors in induced human LNS. Human LNS cells derived from donor eyes were cultured in retinal lineage promoting conditions. Total RNA was extracted from human LNS and RT-PCR was performed using gene specific primers. RT- omitting reverse transcriptase.

Condition 1: human LNS cells co-cultured with mouse developing retinal cells;

Condition 2: human LNS cells cultured in differentiation media in the presence of Shh/RA/Taurine. Condition 3: human LNS cells co-cultured with human foetal retinal cells (post conception 56 days). Positive controls: adult human retinal cDNA (from donor retina, proved by Southampton and South West Hampshire Research Ethics Committee B, REC: 08 /H0504/191) and foetal retinal cells (post conception 56 days). GAPDH was used as cDNA the housekeeping gene.

#### 6.2.11 Absence of mature retinal lineage markers in human LNS derived cells

Unlike mouse LNS cells, human derived LNS cells did not express mature retinal cell markers such as blue Opsin (cone photoreceptor marker), Rhodopsin (rod photoreceptor marker) and RPE65 (RPE cell marker), regardless of the retinal-lineage-promoting conditions used (Figure 6-9). There were traces RPE65 detected from cells cultured in non-inducing condition (control). An inappropriately sized non-specific band was observed on most of the derived LNS samples using the rhodopsin specific primers. The size was smaller than predicted (378bp), as shown on the positive control using adult human retinal cDNA (human retina- A). This suggests that human LNS cells did not express rhodopsin following three different induction conditions.

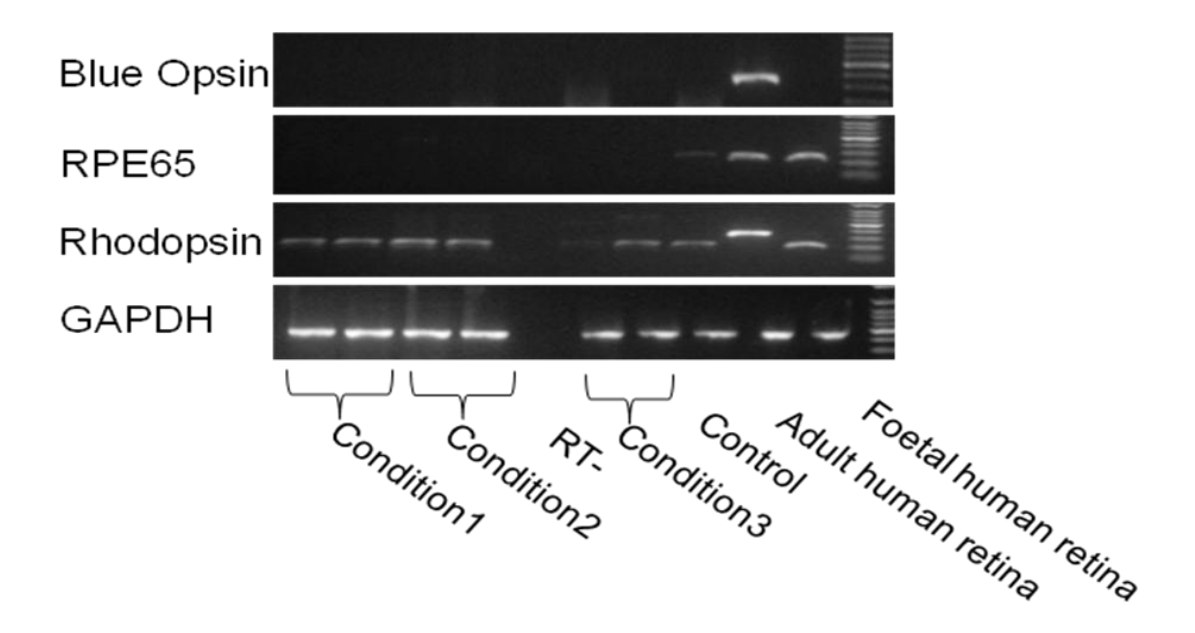


Figure 6-9 Absence of mature retinal lineage markers in human LNS derived cells. RT-PCR was performed using gene specific primers. Human adult retinal cDNA was used as a positive control for photoreceptor specific genes. Negative control (RT-) omitted reverse transcriptase. Results represent two independent experiments. Condition 1: human LNS cells co-cultured with mouse developing retinal cells; Condition 2: human LNS cells cultured in differentiation media in the presence of Shh/RA/Taurine. Condition 3: human LNS cells co-cultured with human foetal retina (post conception 56 days). GAPDH was used as cDNA quality control. Human foetal retinal cells (post conception 56 days) were also used as a control.

#### 6.2.12 Human Foetal retinal cells

In vitro cultured human foetal developing retinal cells (post conception 56 days), were utilized to provide a retinal lineage differentiation environment in this study. The gene expression of early human foetal retinal cells was investigated at both transcript level and protein level. Transcription factors import for retinal development including Lhx2, Pax6, Chx10 and Crx were detected in foetal retina (Figure 6-9, Lane 10). However, as expected mature photoreceptor or RPE markers were undetectable (Figure 6-9, Lane 10), indicating the absence of photoreceptor cell development at this stages.

Foetal retinal tissues/ cells (post conception 49-56 days) were examined with matured photoreceptor cell specific marker Rhodopsin by immunocytochemistry. As shown (Figure 6-10), rhodopsin was not detected at this stage.

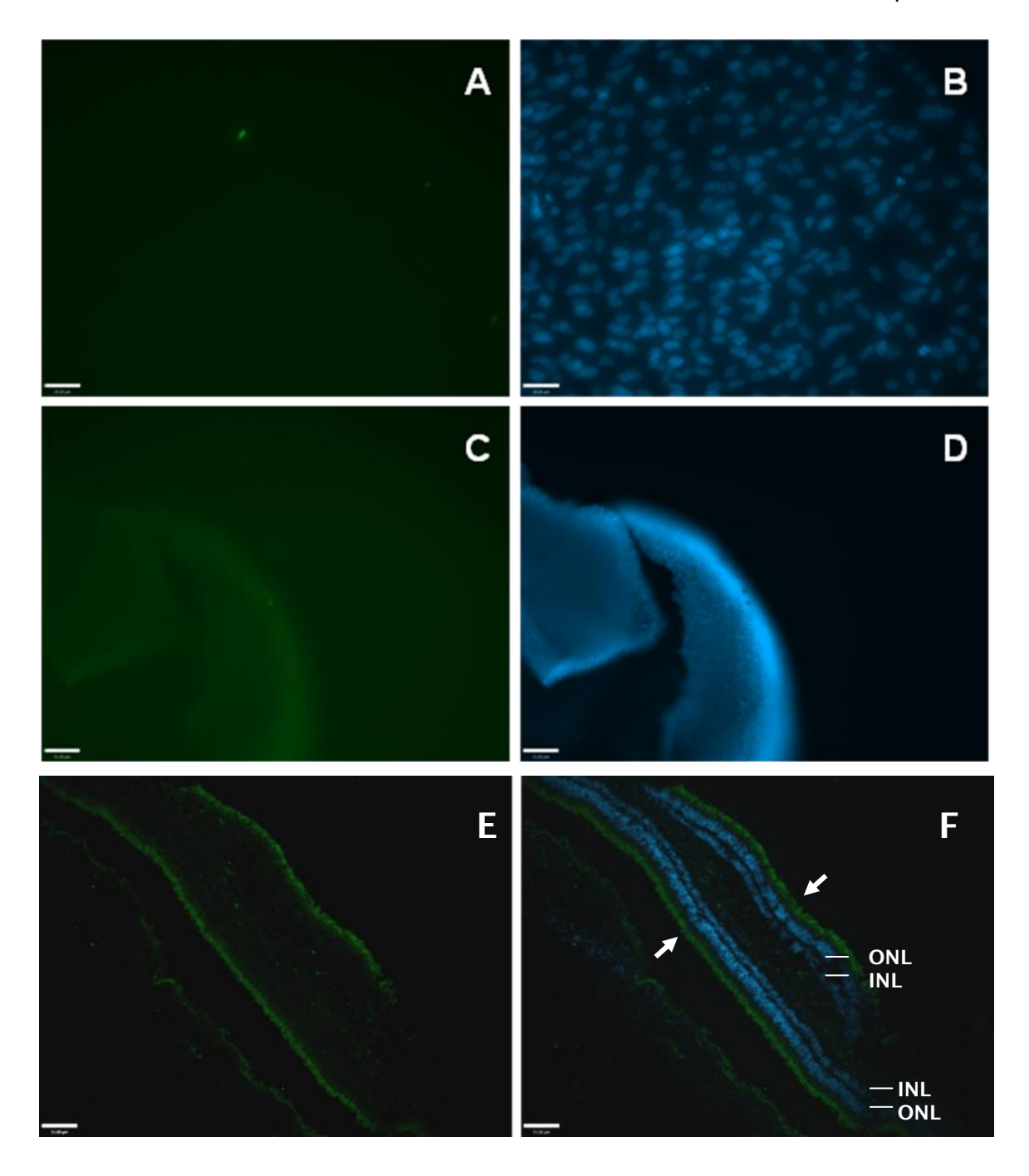


Figure 6-10 Rhodopsin was not expressed in human foetal retinal cells (post conception 49-56 days). Immunostaining using the rod photoreceptor specific marker Rhodopsin (green Immunofluorescence) was conducted on cultured retinal cells (A & B) and on whole-mount retinal tissue (C-D). B & D present the merged images of anti-rhodopsin and DAPI nuclear staining (blue). Adult human retinal tissues from donor eyes were used as a positive control. Rhodopsin was detected in the photoreceptor layer of retina (in green, arrows, E & F). ONL: outer nuclear layer; INL: inner nuclear layer. Scale bar: A-B: 26  $\mu$ m; C-F: 100  $\mu$ m.

## 6.2.13 Absence of photoreceptor markers on human LNS cells by immunocytochemistry

Human LNS cells from aged donors were co-cultured with human foetal retinal cells for 5-7 days then subjected to immunocytochemistry (Figure 6-11). Cells were stained for the rod photoreceptor specific marker Rhodopsin, and RPE specific markers bestrophin and RPE65 as shown in Figure 6-11, A-C). No rhodopsin or RPE65 expression was observed however approximately 10% of cells were weakly positive for Bestrophin. Rhodopsin was not detected in human LNS cells when co-cultured with mouse neonatal retinal cells or when culture conditions were supplemented with extrinsic factors HH/Taurine/RA (Figure 6-11, D-F).

The immunocytochemical results were in accordance with the results at a transcript level by RT-PCR (Figure 6-9). As shown in this chapter, although essential retinal progenitor markers including Lhx2, Pax6 and Rx were expressed in human LNS derived cells *in vitro* following induction, mature photoreceptor specific markers such as Rhodopsin and Blue opsin were undetectable.

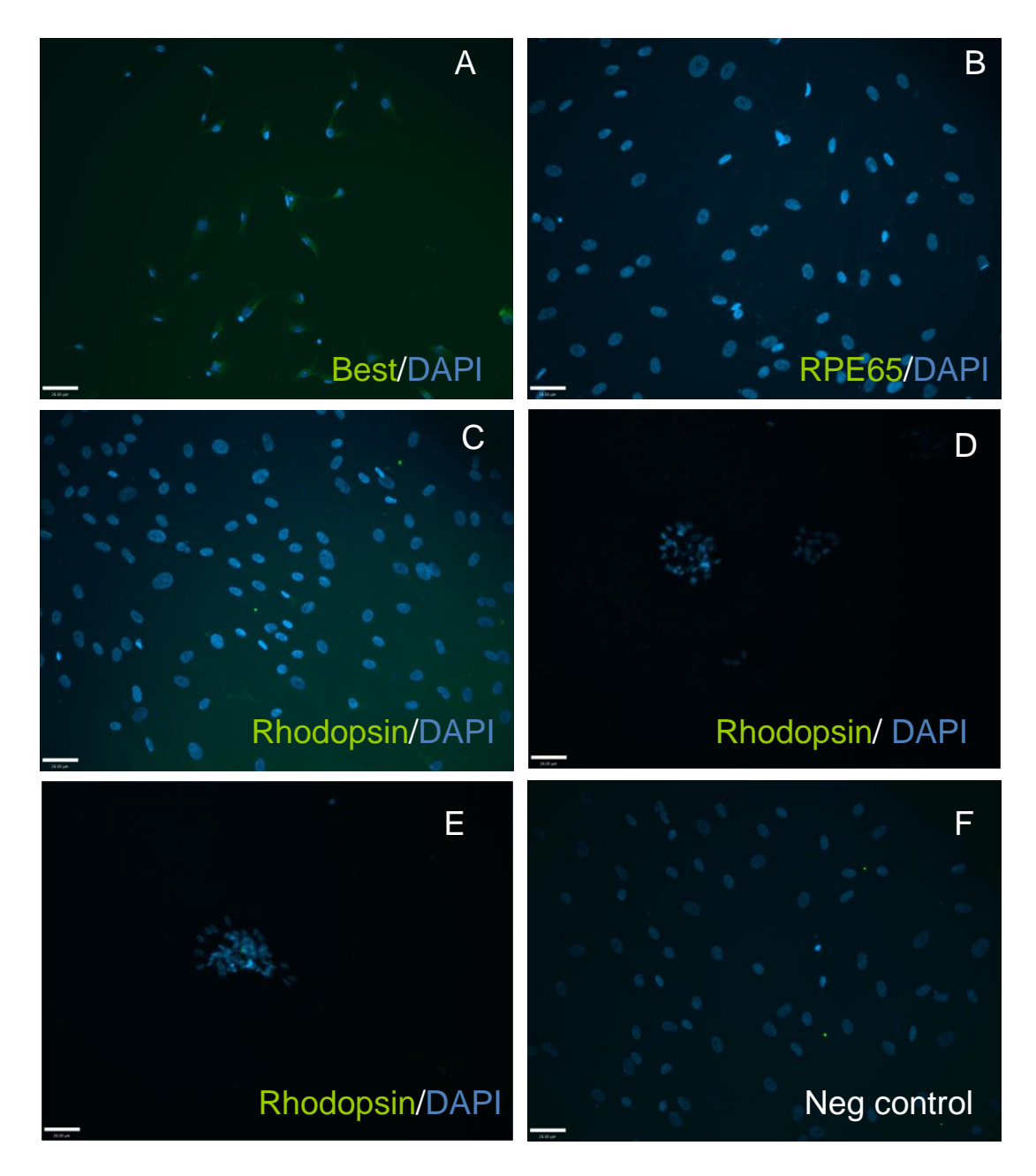


Figure 6-11 Absence of photoreceptor markers in human LNS cells by immunocytochemistry. LNS cells derived from aged donors were co-cultured with human developing retina (post conception 64 days, A-C). LNS cells did not express rhodopsin or RPE65. Bestrophin was detected in approximately 10% of cells; **(D)** LNS cells were co-cultured with neonatal mouse retinal cells; **(E)** LNS cells cultured in differentiation media in the presence of SHH/Taurine/RA. Best: Bestrophin; Scale bar:  $26\mu m$ .

#### 6.3 Discussion

For the first time, human limbal cells from both aged donor eyes and live patients were used for generation of neurosphere. This study optimized and verified cell dissociation and culture methods. Neurospheres were successfully generated from aged donor limbal tissues up to 94 years of age, indicative of the potential of the limbus as an autologous cell resource. The size of the human eyeball allows precisely dissecting corneal limbal tissue to avoid cell contamination from iris, CB or retina. Therefore, this study also confirmed that the derived LNSs were from the corneal limbus. Like cells derived from mouse and other animals [6,144], human LNS cells expressed neural stem cell markers including Sox2, nestin and beta-III tubulin, suggesting the derivation of neural progenitor cells from adult/aged human limbus. The distribution of Sox2 was found to be in both the cytoplasm and nucleus in primary human derived LNS. Following subculture, a small number of samples lost expression of neural stem/ progenitor marker Sox2 and/or nestin in the neurosphere culture media. This was possibly due to cell differentiation and loss of stemness.

Following exposure to a retinal developing environment provided by mouse neonatal retinal cells or extrinsic factors (Shh/taurine/RA), human LNS cells derived from donor eyes expressed a number of early retinal progenitor cell markers. Include LIM homeobox transcription factor Lhx2 and master regulator of eye development Pax6. The former is required to specify the retinal lineage [32,90,148], while the latter is required for eye morphogenesis for most species including humans. It is also required for the multipotential state of retinal progenitor cells [220]. The presence of both Lhx2 and Pax6 is in accordance with the findings in Chapter 5, which show the same upstream regulators have been activated in retinal like cells derived from mouse LNS. In addition, Rx, a transcription factor involved in the development, specification and maintenance of retinal progenitor cells was also detected in some of the induced samples. Crx plays a crucial role in specifying the photoreceptor lineage [197], but the expression of Crx was not confirmed in induced human LNS cells. This is consistent with the finding from Chapter 5, and further experiments are needed to confirm whether LNS cells are regulated by an alternative pathway, or by an unknown Crx isoform.

Although certain transcription factors which are essential for retinal development were detected, none of the induced human LNS expressed mature photoreceptor markers such as Rhodopsin or Blue-Opsin following culture in the three different inducing conditions. In Chapter 5, we demonstrated that photoreceptor markers were present in retinal-like cells derived from mouse LNS. This difference may be due to development

and specification of human retinal-like cells requiring more complicated endogenous and exogenous regulation compared to mouse cells. For example, rat derived iris cells required less genetic modification to adopt a photoreceptor phenotype when compared to primate cells. A single transcription factor Crx was sufficient for rat cells, while a combination of transcription factors was required in primates [73,213]. ESCs from human, monkey and mouse can differentiate into photoreceptor cells through a stepwise pathway in *vitro* [88]. The signaling pathways and transcription factors activated in this process differ between human and mouse derived ESCs. Due to the species differences, the diffusible photoreceptor promoting factors released by mouse neonatal retinal cells were possibly insufficient to promote human cell transdifferentiation towards retinal-like cells.

Foetal human retinal cells at 7-8 weeks post-conception were collected in this study. Immunostaining showed that the mature photoreceptor specific marker rhodopsin was absent from intact whole retinal tissues or cultured retinal cells, indicative of a lack of rod genesis at this stage. This is accordance with previous reports that rod genesis starts at 10.5 foetal weeks (post conception), when rod-specific proteins NRL and NR2e3 are detected. The second phase of human rod genesis occurs later, with expression of rod opsin (rhodopsin) at approximately week 15 [109]. In this study, the foetal retinal cells (7-8 weeks) appeared unable to promote human LNS cell transdifferentiation towards retinal-like cells. Neither retinal development transcription factors nor mature photoreceptor markers were detected at a transcript level or protein level. An observation from Watanabe et al. may explain this: the rod promoting activity of diffusible signals was only observed in rodent neonatal neural at the peak of rod genesis. The retinal cells from embryonic day 15 (E15), the peak of cone genesis, did not have the same effect [233]. In addition, other tissues including adult neural retina, neonatal thymus, cerebrum or cerebellum do not have a retinal specific promoting effect either. Therefore, in vitro cultured human retinal cells from foetal week 7-8 may be an inappropriate stage for promoting photoreceptor differentiation.

It is very encouraging that human LNS expressed retinal progenitor markers when exposed to several defined factors including Sonic Hedgehog (Shh), Taurine and retinoic acid (RA). Shh has been shown to be the key inductive signal in patterning of vertebrate embryonic tissues, including the ventral neural tube. It is involved in formation of the ventral optic cup, specification of the dorso-ventral polarity within the optic vesicle, and governing of ocular morphogenesis [160,234]. Besides specification of the eye field during embryonic development, Shh also has been implicated in control of retinal development in vertebrates [235,236], and is required for maintenance of RPC proliferation [237]. Studies show that inhibiting Shh and twhh (tiggy-winkle

Xiaoli Chen Chapter Six

hedgehog) by antisense oligonucleotides reduces and delays photoreceptor differentiation in zebrafish. Conversely, addition of Shh increases the percentage of photoreceptors in rat retinal explants. Another factor, RA, plays an important role in early eye development as well as in the differentiation, maturation and survival of photoreceptors [238].

This is the first time that the effects of the Shh signal pathway, RA and taurine have been investigated on the transdifferentiation potential of neurosphere cells derived from human limbus. This positive retinal lineage promoting effect was consistent with the reports on other cell/tissue resources including embryos or retinal progenitor cells. [239,240]. An activation of Shh signaling has also been detected on co-cultured rat limbal cells using microarray gene chip expression profile analysis [235,236,238-240]. In this study, the combination of the three factors had a similar retinal lineage promoting effect as *in vitro* cultured neonatal mouse retinal cells, suggesting that mechanisms involving the Shh signaling pathway may lead to the activation of retinal development transcription factors in human LNS cells.

In summary, this preliminary data demonstrates the characteristics of LNS cells derived from aged human donors and live patients. The cells derived display clonal growth, and exhibit neural lineage markers when cultured in a retinal lineage inducing environment. Derived human LNS cells expressed eye/retinal development transcription factors including Lhx2, Pax6 and RX, although some retinal transcription factors and mature photoreceptor specific markers were not detected. This is the first study on the transdifferentiation potential of human limbus derived progenitor cells towards a retinal lineage. As a readily accessible progenitor cell resource that can be derived from individuals up to 94 years of age, limbal neurosphere cells may open up promising avenues towards the development of novel approaches for the treatment of degenerative retinal diseases.

# 7 Chapter Seven – Introduction of Crx gene into LNS cells by Lentiviral Vector

#### 7.1 Introduction

Genetic modification may be used to promote cells to differentiation/
transdifferentiation along specific lineages [6]. In Chapter 3, I demonstrated that LNS
have neural stem/progenitor cell properties. By co-culture with developing retinal cells
in vitro, approximately 10% of LNS cells expressed retinal lineage specific markers,
including photoreceptor markers at both a transcript and protein level. However, the
efficiency of generation photoreceptor-like cells is low. In addition, co-culture with
animal derived cells is not clinically applicable. I therefore wanted to investigate
whether exogenous expression of Crx, a key regulator of early photoreceptor fate in
the developing retina, can drive LNS acquisition of retinal-like cells properties.

Crx is the earliest photoreceptor-specific gene expressed in developing rods and cones [8,86-88]. In humans, mutations in Crx cause autosomal dominate cone-rod dystrophy, RP or Leber's congenital amaurosis [73]. In a study of homozygous Crx knockout mice (Crx - ), photoreceptor cells failed to develop outer segments [73]. A serial analysis of gene expression (SAGE) was conducted using libraries generated from mature and developing mouse retina. It was shown that 46% of photoreceptor-enriched genes are Crx-dependent [241]. Studies using mouse, primate and human cells have shown that exogenous expression of Crx alone or together with Otx2 *in vitro* expanded adult iris or ciliary epithelial cells, drove them to express photoreceptor specific markers, such as rhodopsin, blue-cone opsin and PDE [242]. Furthermore, the resulting cells were found to have functional activity associated with photoreceptors, using a cyclic GMP assay [8,87,88] or with electrophysiological recording [8,87]. By transient Crx expression, Jomary *et al.* detected photoreceptor specific markers including rhodopsin, cyclic nucleotide-gated cation channel-3, blue-cone opsin, and beta-6-PDE on human limbal cell [88]. However, functional activity was not detected by the cyclic GMP assay.

Lentiviral vectors (LVV) are a type of retrovirus, which includes the human immunodeficiency virus (HIV). HIV based LVV have the advantages of efficient transfection, integration and long-term expression of target genes in various types of cells [8]. A series of modifications have been made to HIV-derived LVVs in order to produce safer gene transfer vectors [243]. These modifications prevent structural sequences from being incorporated into the viral genome. Thus the virus is unable to

reproduce after it has infected the target host cell. The new LVVs, known as third generation LVVs, have been modified to remove packaging signals and unnecessary accessory genes, which has further improved safety and enhanced viral titres. The LVV-Crx-GFP used in the study was a gift from Dr. J Cooke and Prof A Dick (Bristol Eye Research Center, UK). Figure 7.1 illustrates the final LVV with mouse Crx cloned into following viral assembly within the packaging cell line. This virus is able to transfect a host cell once and cannot excise itself. Therefore, the virus cannot replicate and spread itself automatically. The vector contained the WPRE (Woodchuck Hepatitis Virus (WHP) Post-transcriptional Regulatory Element) to stabilize mRNA and increase the gene expression.

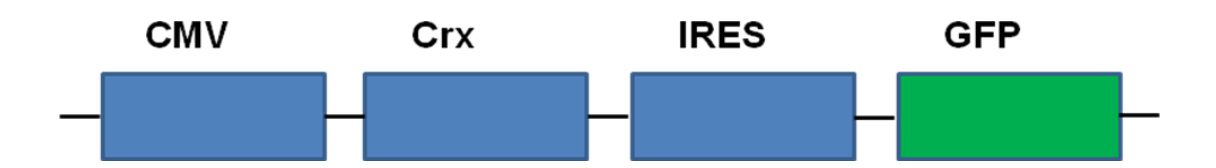


Figure 7-1 Schematic representation of a Crx and GFP lentiviral vector.

A heterologous promoter (cytomegalovirus, CMV) drives the expression of a transgene (Crx), followed by the IRES (internal ribosome entry site) which allows for the continued translation of the expression marker (eGFP). The transgene is composed of full-length mouse Crx coding region. Image was from Dr. J Cooke and Prof. A Dick, Bristol Eye Research Center.

The aim of this study was to investigate whether a LVV carrying Crx, can induce LNS to more efficiently adopt a photoreceptor-like phenotype. Green fluorescent protein was introduced along with Crx, so that the successfully transfected cells can be identified. The resulting cells will be characterized by immunocytochemistry and RT-PCR using photoreceptor specific markers.

#### 7.2 Methods

#### 7.2.1 Cell culture

Limbal cells were dissected from 8 week old mice and enzymatically dissociated using Trypsin, collagenase and hyaluronidase as described in section 2.1.2 in Chapter2. Cells were maintained in the full neurosphere culture media containing DMEM F12/Glutamax™/B27- in the presence of 20ng/ml EGF, 20ng/ml FGF2 and 5ng/ml heparin for 7 days before transfection.

#### 7.2.2 Cell transfection

Multiplicity of infection (MOI) is the ratio of infectious agents to infection targets. In this chapter, concentrations of 1, 2.5 and 5 MOI were used for LNS cell transductions.

MOI = The number of LVV (infectious agents)

Number of LNS cells (target cells)

LVV solution required ( $\mu$ I) =  $\frac{\text{Total cells required x MOI } (1/2.5/5)}{\text{The viral titre x } 1000}$ 

The LVV-Crx-GFP and control LVV-GFP vectors were a generous gift from Dr J Cooke and Prof A Dick. Before transfection, primary LNS cells were dissociated into single cells using Accutase. Cells were plated into 96-well plates at a density of 1×10<sup>6</sup>cells/ml in DMEM: F12/Glutamax<sup>™</sup>/B27 in the presence of 20ng/ml FGF2 and transfected with LVV-Crx-GFP at 1, 2.5 and 5 MOI. LVV-GFP (5 MOI) and non-transfected cells were used as negative controls. Cells were transferred into 6 well plates after 5 days and subsequently cultured in DMEM: F12 Glutamax<sup>™</sup>/2% B27/ 1% FBS. Medium was exchanged every 2-3 days. Cell characterisation was conducted 10 and 26 days post-transfection by immunocytochemistry and/or RT-PCR (Figure 7-1).

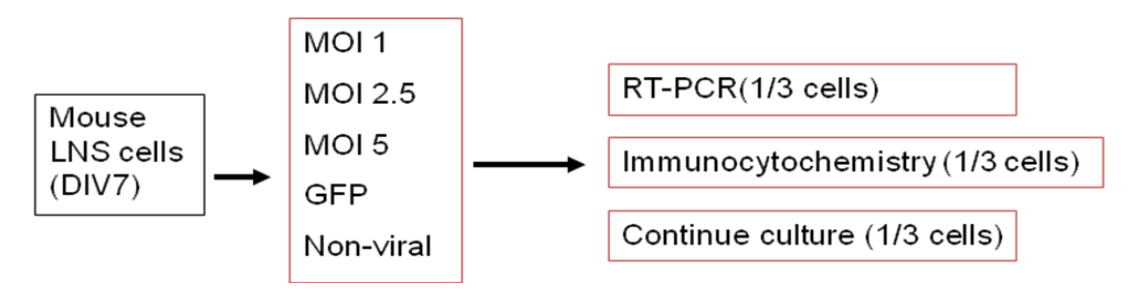


Figure 7-2 Crx transduction plan.

The diagram illustrates the Crx transduction plan using LVV-Crx-GFP. Cell characterisation was conducted at a protein level (immunocytochemistry) or transcript level (RT-PCR) on day 10 and day 26.

#### 7.2.3 RT-PCR

RNA extraction, cDNA synthesis and polymerase chain reaction were conducted as described in Chapter 2, Section 2.4. Total RNA was isolated and cDNA synthesis was performed using RNeasy Plus (Qiagen) and High Capacity cDNA Reverse Transcription Kit (Applied Biosystems). cDNA was amplified using gene specific primers (Table 4-1). Cycles used were denaturing for 30 sec at 94°C; annealing for 30 sec at 60°C, extension for 30 sec at 72°C for 35 cycles. Electrophoresis was performed on a 1.5% agarose gel. Two different sets of Crx primers were used in RT-PCR in order to validate Crx transduction (Crx\_1) and investigate endogenous expression of Crx (Crx\_2) respectively.

Table 7-1 Primer sequences used for phenotypic analysis on transduced LNS

Primers Name	Sequence	Amplicon Size (bp)
Crx_1_F	CCCATACTCAAGTGCCCCTA	122
Crx_1_R	CCTCACGTGCATACACATCC	
Crx_2_F	ATCCAGGAGAGTCCCCATTT	506
Crx_2_R	GGCAGAGATGGGCTGTAAGA	
Rhodopsin_F	TCACCACCACCTCTACACA	216
Rhodopsin_R	TGATCCAGGTGAAGACCACA	
Rhodopsin kinase_F	AGCCCGAGGAGAAGGTAG	285
Rhodopsin kinase_R	CCCACGTCCTGAATGTTCTT	
β-Actin_F	TGTTACCAACTGGGACGACA	392
β-Actin_R	TCTCAGCTGTGGTGGAAG	

Crx\_1 primer pair for validation of Crx transduction

Crx\_2 primer pair, for investigation of endogenous Crx expression

#### 7.2.4 Immunocytochemistry

Immunocytochemistry was conducted as described in Chapter 2 (Section 2.2.) Transduced LNS cells on post transfection on day 10 and 26 were fixed with 4% PFA for 15-20 min. Following permeabilization and blocking with 0.1% Triton X-100 PBS with 5% DBS for 0.5-1 hrs at rt, cells were incubated with primary antibodies overnight at 4°C. Antibodies used in this study include mouse anti-rhodopsin (1: 250 Sigma Aldrich), rabbit anti- blue-opsin (1: 200 Abcam) and mouse anti-GFP (1:500 Abcam), as detailed in Table 2-2 in Chapter 2. After rinsing 3 x 10 mins with PBS, cells were incubated with secondary antibody (Alexa Fluor 488 /555, 1:500) for 2 hrs at rt. nuclei counterstained with DAPI. Negative controls were incubated with secondary antibody only.

#### 7.3 Results

# 7.3.1 Expression of GFP on LNS cells following transfection with LVV-CRX-GFP and LVV-GFP vectors

Following transfection with LVV-Crx-GFP or LVV-GFP, LNS cells grew as NS in DMEM:F12/Glutamax<sup>™</sup>/B27 in the presence of 20ng/ml FGF2 during first 5 days. Non-transfected cells did not exhibit any fluorescence, while LVV-GFP cells display bright green fluorescence as shown in Figure 7-3. The GFP signal reached a plateau by 72-96 hours post-transfection and gradually decrease over time. After approximately 20 days, fluorescence was not observed in GFP control cells.

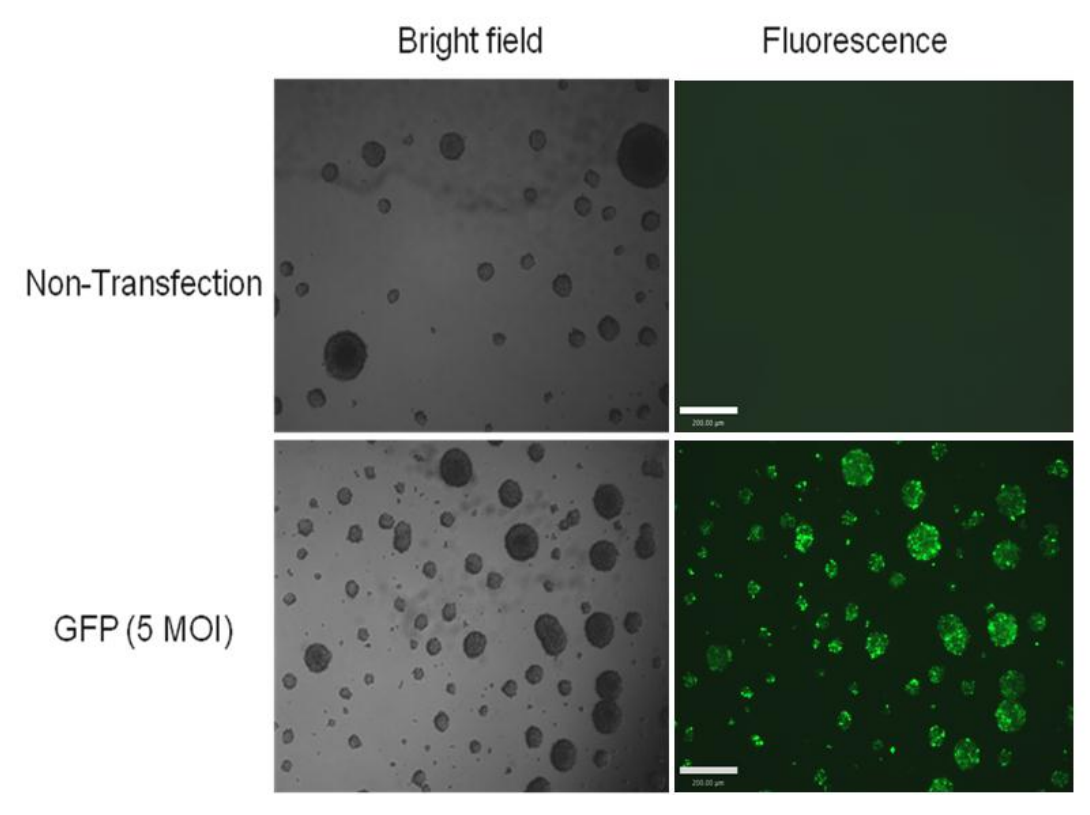


Figure 7-3 Bright field and GFP images of LNS cells transduced with LVV-GFP or non-transfected cells. Images illustrate t LVV-GFP transduced cells three days after transfection (bottom). Bright green fluorescence was observed, which typically reached a plateau by 72-96 hours. Representative bright field and fluorescent microscopy images are shown on the left and right, respectively. Control cells (top) did not exhibit any green fluorescence. Cells in both conditions showed typical NS growth features. Scale bar:  $200\mu m$ 

The concentration of LVV-Crx-GFP was optimised using 1, 2.5 and 5 MOI. Crx transfected cells from three vector concentrations are shown in Figure 7-4. The cells exhibited much fainter GFP fluorescence compared to the control vector (LVV-GFP) transduced LNS cells. The fluorescence also reached a plateau by 72-96 hours post-transfection, and decreased gradually until it was undetectable after 7-10 days. All cells showed typical NS growth features. However, the presence of more single floating cells was observed in the cells transduced with an MOI of 5. This was possibly due to cytotoxicity at this higher concentration.

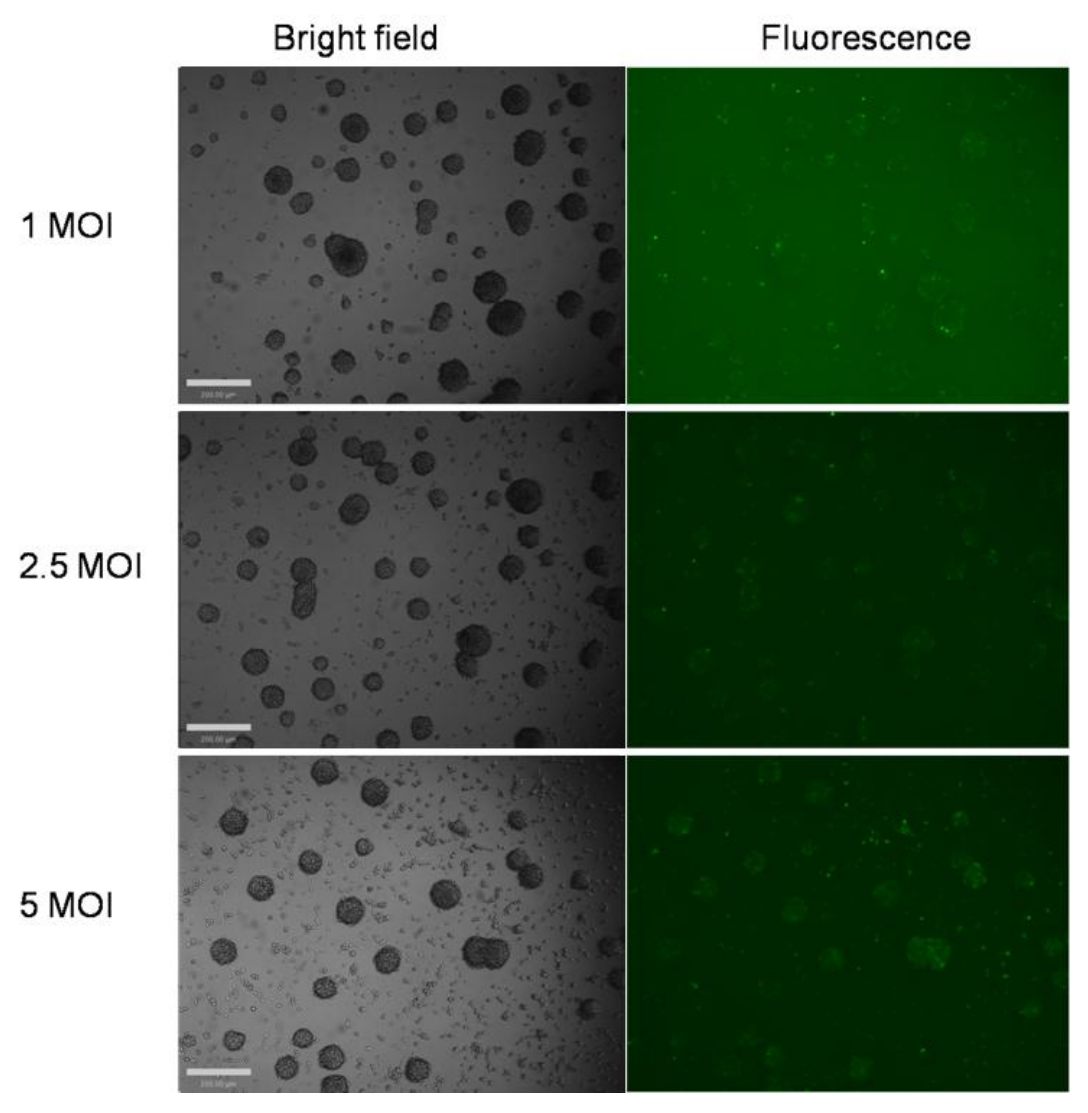


Figure 7-4 Bright field and fluorescent microscopy images of LNS cells transduced with LVV-CRX-GFP. Images illustrate cells transduced with LVV-Crx-GFP at MOIs of 1, 2.5 and 5 three days post- transfection. Weak green fluorescence was observed using all three concentrations, which reached a plateau by 72-96 hours. Representative bright field and GFP images are shown on the left and right, respectively. Cell in both conditions showed typical NS growth features. Scale bar: 200µm

#### 7.3.2 Validation the Crx expression by RT-PCR

LNS cells were transduced by LVV in serum free medium containing 20ng/ml FGF2. No further FGF2 was used to supplement growth medium. LNS started growing as monolayers 5 days after transfection. Cells were then maintained in growth medium with a low concentration of serum (1% FBS).

The primer pair (Crx\_1, Table 7-1) amplifying encoding region of Crx gene, was use to validate transduction of Crx into LNS cells. LVV have the advantages of prolonged gene expression *in vitro* and *in vivo* [244], therefore, we tested whether Crx was expressed in cells 10 days post-transfection. As shown in Figure 7-5, single strong bands were observed on Crx transduced cells and neonatal retinal cDNA by RT-PCR. The size of the amplification was close to the predicted 122bp. Whist transcript Crx was absent on the GFP control and non-transduction control.

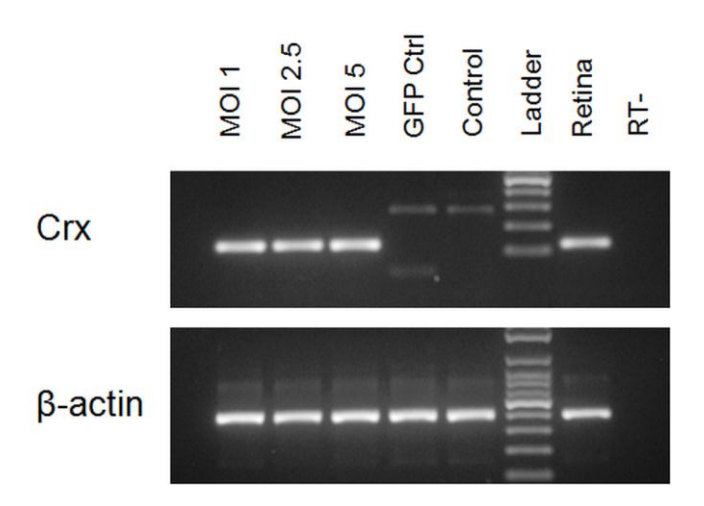


Figure 7-5 Validation of Crx transfection by RT-PCR

RT-PCR was performed to confirm the introduction of Crx on LVV-Crx transduced LNS cells. Total RNA was extracted from LNS cells 10 days post-transfection. The Crx gene specific primers were utilized to amplify the encoding region of mouse Crx. RT-PCR shows abundant expression of exogenous Crx on LNS cells following transduction with 1, 2.5 and 5 MOI LVV-Crx-GFP. Transcript Crx was absent on control conditions. The extra bands observed on control conditions were unspecific amplification. GFP ctrl: LNS transfected with LVV-GFP, Ctrl: non-transfected control. Positive control was neonatal retinal. RT- omitting transcriptase. Internal control:  $\beta$ -actin.

To investigate whether endogenous Crx was activated following transduction, a second pair of Crx primers (Crx\_2, Table 7-1) were designed to amplify a 500bp cDNA covering both the untranslated and encoded region within the Crx gene as demonstrated in Figure 7-6 A. The LVV-Crx-GFP vector used in this study did not contain the Un-Translated Region (UTR). Therefore, only endogenous Crx can be amplified using this primer pair. A single band was observed on LNS cells transfected with 2.5 MOI LVV-Crx-GFP (Figure 7-6 B).

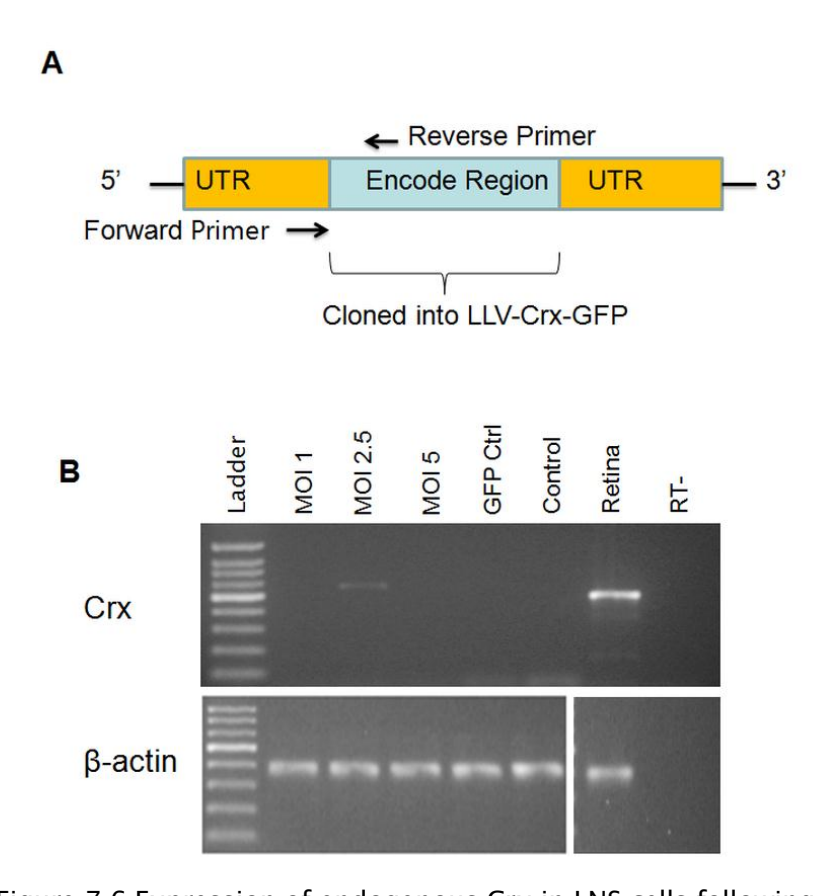


Figure 7-6 Expression of endogenous Crx in LNS cells following transduction. (A) A diagram illustrating the location of the primer pair (black arrows) used to detect endogenous Crx expression at a transcript level only the encoded region of Crx was cloned into the LVV. In order to detect endogenous Crx, the primer pair was designed to cover the 5' UTR. (B) Samples used were 10 days post-transfection. Total RNA was extracted from LVV-Crx-GFP transduced LNS cells. RT-PCR showing expression of endogenous Crx detected on LNS cells transduced by 2.5 MOI LVV-Crx-GFP. GFP ctrl: LNS transfected with LVV-GFP, Ctrl: non-transfected control. Positive control was mouse retinal cDNA, RT- omitting transcriptase. Internal control: β-actin.

# 7.3.3 Expression of rod photoreceptor markers at a transcript level, but not at a protein level following LVV-Crx-GFP transfection

The LVV encoding Crx was used in an attempt to reprogram limbal derived cells along a photoreceptor differentiation pathway. The first question is whether LNS could differentiate towards rod photoreceptor-like cells, upon exogenous expression of Crx. After 10 days differentiation, RT-PCR and immunofluorescence staining were conducted using rod specific markers including rhodopsin and rhodopsin kinase. RT-PCR analysis for rhodopsin and rhodopsin kinase showed single strong bands present in the LNS cells transduced with 1 and 2.5 MOI LVV-Crx-GFP, suggestive of the expression of both rod specific markers at a transcription level. In the control conditions or with the higher concentration of LVV-Crx-GFP (5 MOI), bands were much weaker or absent at these markers (Figure 7-7). The expression of rod photoreceptor markers decreased gradually, and was barely detected by 26 days post-transduction using all viral vector concentrations.

No LNS cells were found to be immunoreactive with rhodopsin 10 or 26 days LVV-Crx-GFP post-transfection. Rhodopsin staining was also not observed in control conditions (cells transfected with GFP control vector or non-transfected cells). The GFP signal decreased in the culture in all the transfection conditions. 26 days post-transfection, GFP was detected in approximately 15% of LVV-GFP transduced cells, however GFP fluorescence was barely detectable in LVV-Crx-GFP transduced cells using an anti-GFP antibody.

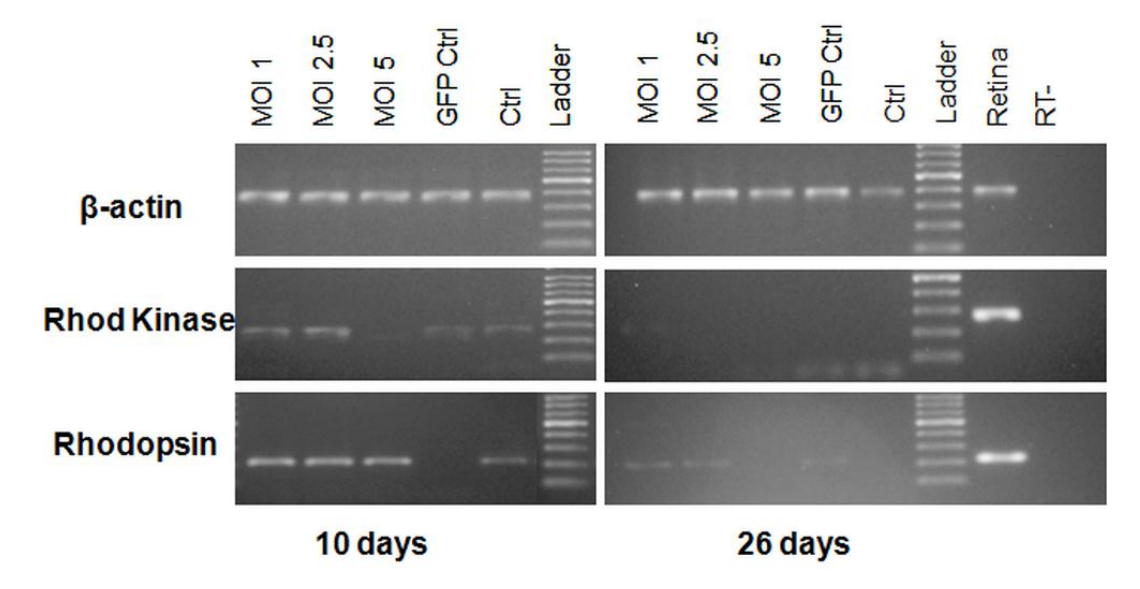


Figure 7-7 Rod specific markers detected on LVV-Crx-GFP transduced LNS cells by RT-PCR. Total RNA was extracted from LVV-Crx-GFP transduced LNS cells, and RT-PCR was conducted using gene specific primers. GFP ctrl: LNS transfected with LVV-GFP; Ctrl: non-transfection control. Samples on the left are from 10 days post-transfection, and samples on the right are 26 days post-transfection. Positive control was mouse retinal cDNA, RT- omitting transcriptase. Expression of both rhodopsin kinase and rhodopsin was detected on LVV-Crx-GFP transduced cells at MOI of 1 and 2.5 on the 10th day post transduction. Bands were weaker or absent on the control conditions and 5 MOI transduced cells. The expression of rod specific markers was barely detected 26 days following transduction. Internal control: β-actin.

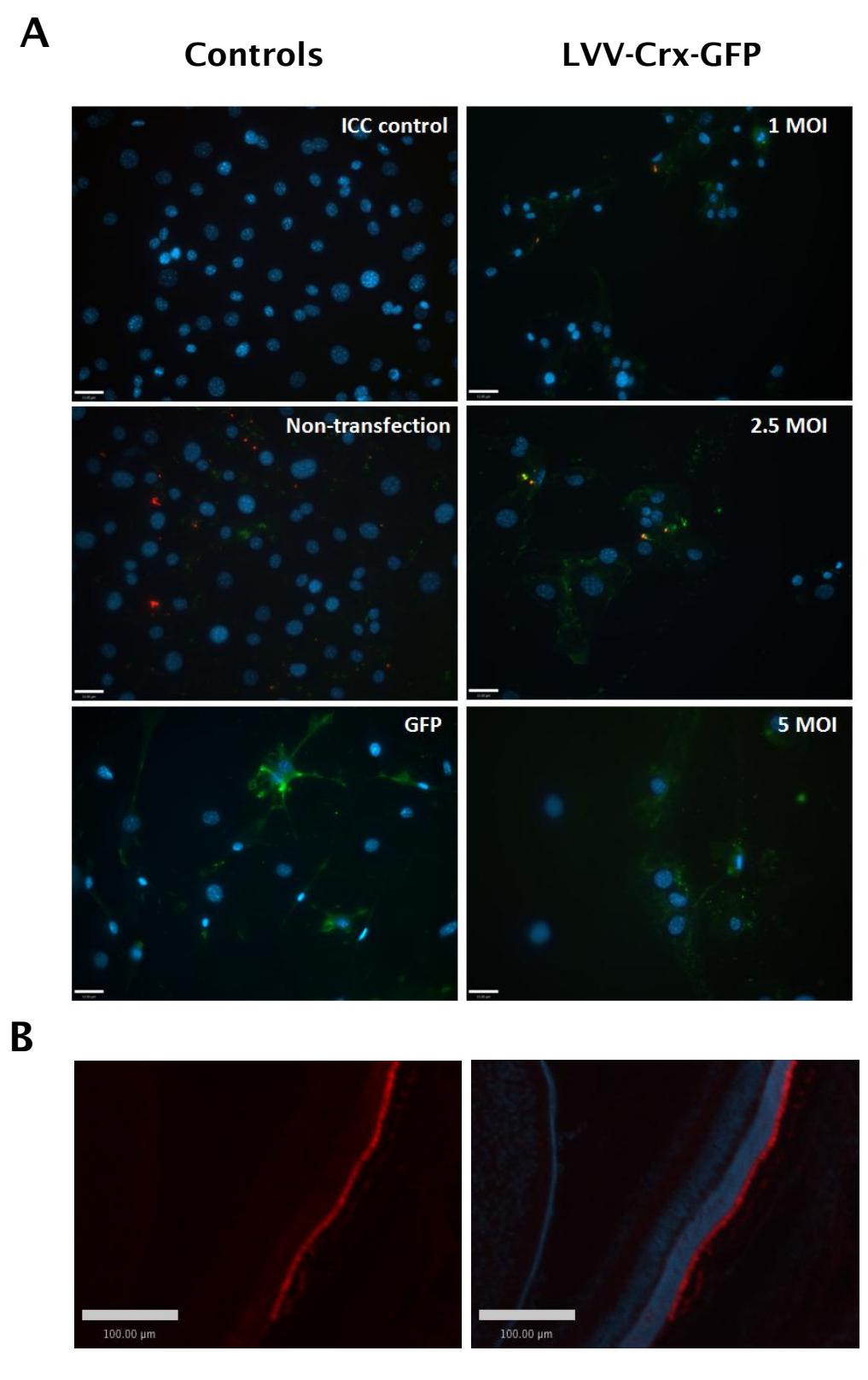


Figure 7-8 Absence of rhodopsin expression on transduced LNS cells by immunocytochemistry. **(A)** Rhodopsin immunostaining was conducted on LVV-Crx-GFP transfected LNS cells (right) and controls (left) 26 days post-transduction. GFP fluorescence was amplified using anti-GFP immunostaining (green). Immunostaining analysis for rhodopsin did not show any positive cells on all conditions tested (red).

GFP was barely detected on LVV-Crx-GFP transduced cells. Approximately 15% of LVV-GFP transfected cells were GFP positive. Representative images of control and LVV-Crx-GFP transduced are shown on the left and right, respectively, as indicated. Ctrl: non-transfected cells. GFP: LNS transfected with LVV-GFP. Scale bar:  $13\mu m$  (B) P8-10 mouse retinal tissue was used as a positive control. Rhodopsin was detected in the photoreceptor layer (red). Scale bar:  $100 \mu m$ .

### 7.3.4 Upregulation of cone photoreceptor markers at a protein level following LVV-CRX-GFP transfection

We also investigated whether LNS could differentiate towards cone photoreceptor-like cells upon forced expression of Crx. Immunocytochemical staining was conducted using the cone specific marker blue opsin 26 days post-transduction. Approximately 23% of blue opsin positive cells were detected on LNS cells transduced with 2.5 MOI LVV-Crx-GFP, and less than 10% on the cells transfected with 1 or 5 MOI LVV-Crx-GFP. Blue opsin expression was also noted in 2-6% of cells transduced with the GFP control virus and in cells which had not been transduced (Figure 7-9). In this study, 2.5 MOI LVV-Crx-GFP shows the trend to increase the expression of cone marker expression. It also changed the morphology of LNS cells, and neurite-like long cytoplasmic processes were observed on the cells in this condition (Figure 7-9A, 2.5 MOI).

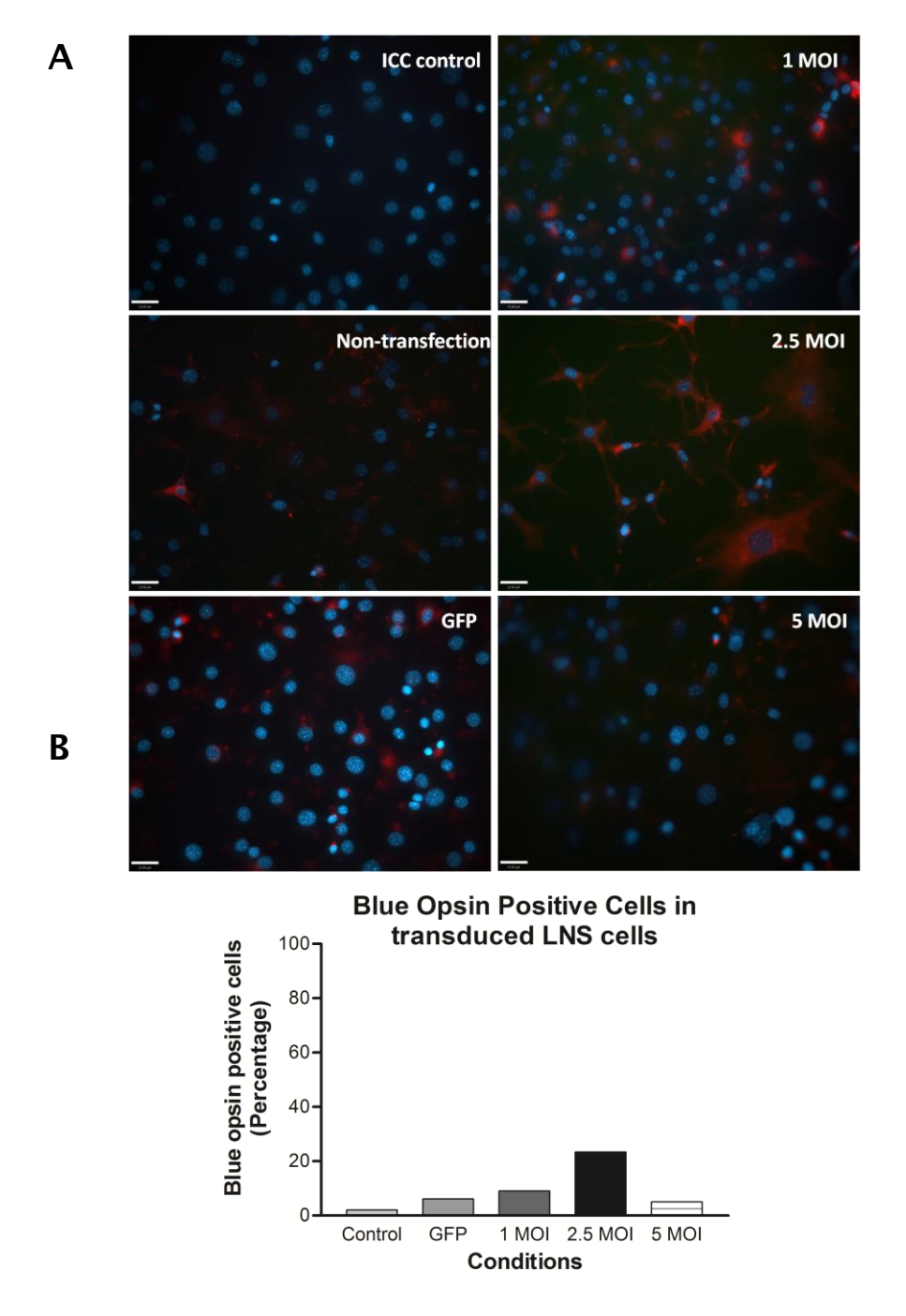


Figure 7-9 Expression of blue opsin on transduced LNS cells detected by immunocytochemistry. **(A)** Blue opsin immunostaining was conducted on LVV-Crx-GFP transfected LNS cells and the control cells 26 days post-transduction. Immunostained cells showed red staining in cytoplasm. GFP was barely detected on Crx transduced cells. **(B)** Immunostaining analysis showed 23.3% of cells transduced with an MOI of 2.5 were positive for blue opsin. In the non-transfected control (Control), GFP control (GFP) and 1 and 5 MOI LVV-Crx-GPF transduced cells, 2.2%, 6.1%, 9.0% and 5.0% of cells were immunopositive for blue opsin, respectively. Results were from one experiment. For analysis, 200-400 cells for each condition were analyzed from 3-4 randomly chosen fields. Scale bar: 13µm.

#### 7.4 Discussion

The results here present a single experiment of genetic modification on LNS. The forced expression of Crx via a LVV in LNS cells activated endogenous Crx. In addition, downstream regulation genes such as rhodopsin and blue opsin showed the trends of upregulation at a transcript and protein level, respectively. The study performed the initial optimisation on the concentration of LVV-Crx-GFP for transfection into LNS cells. A concentration of 2.5 MOI LVV-Crx-GFP appeared to be an optimal transducing condition. It activated endogenous Crx and induced highest percentage of LNS expressing blue opsin.

Crx can bind to and trans-activate regulatory elements in various photoreceptor-specific genes, which indicate that Crx may be able to directly control expression of these genes [245]. The Crx gene alone has been transfected into a number of cells sources in an attempt to promote cell differentiation along a photoreceptor-like pathway. The successful generation of photoreceptor-like cells has been reported from iris and CB epithelium cell, which have the same origin as the retina during embryonic development [73]. The transduced cells were immunoreactive to photoreceptor specific markers including rhodopsin, recoverin or blue opsin. A similar effect of driving non-retinal cells towards a photoreceptor lineage was not observed using other transcription factors such as NeuroD or Nrl, despite their important roles in photoreceptor fate regulation [8,13,87,88].

In this preliminary genetic modification study, neural-crest derived LNS cells were shown to have a high degree of plasticity. Through internal regulation with the transcription factor Crx, rod and cone specific markers were detected by RT-PCR or immunocytochemistry. This is consistent with the results from Chapter 4, which demonstrated that photoreceptor-like cells can be generated from LNS cells via exposure to a retinal development environment. The forced expression of Crx using LVVs has been carried out on adult rat hippocampus derived NSC, which are capable of self-renewal and differentiation into neuron and glial cells [88]. However no photoreceptor markers were detected on NSCs upon transduction with the Crx gene [228]. Akita *et al.* transplanted NSCs into E18 rat retinal explants [13]. The grafted NSC expressed neuronal and glial markers, but failed to express retinal cell specific markers. Therefore, neither transduction with Crx nor a microenvironment of developing retina promoted NSCs differentiation along a retinal lineage. Plasticity towards retinal-like cells does not widely exist in other source of adult stem cells.

In this study, rhodopsin positive cells were not observed following LVV-Crx-GFP transfection. However, to my knowledge, this is the first time that expression of rhodopsin at a transcript level has been reported. Using gene specific primers which covered both the UTR and coding region of the Crx gene, a single band was detected by RT-PCR. This may indicate activation of endogenous Crx in limbus derived progenitor cells following Crx transfection. However, the size of the amplicom generated from Crx-LVV transfected cells is slightly larger than the positive control retinal tissue, as shown on Fig 6-9. Therefore, whether endogenous Crx was upregulated following the introduction of Crx remains to be proven. Further studies using alternative methods, such as DNA sequencing or restriction digests, are necessary to exclude the possibility of amplification from the insertion sequence of the LVV vector.

A combination of other transcription factors such as Otx2, NeuroD or Nrl, may enhance the generation of rod-like cells. The Nrl gene is essential for rod photoreceptor cell specification. It is expressed in developing and mature rods. Nrl-eGFP transgenic reporter mice provide a useful tool in the identification of a definite rod photoreceptor cells fate [228]. Areas for future research include: 1) use of a combination of transcription factors such as Crx with NeuroD, Chx10 or Otx2, which may improve the strength and efficiency of transduction of LNS cells; 2) assessment of whether transduced cells possess functional properties; and 3) assessment of whether transduced cells are capable of integration into the ONL of the retina following subretinal transplantation.

The results presented in this chapter were from a single experiment. This was due to the limited time available towards the end of the project. Also the amount of LVV-Crx-GFP vector available was inadequate for a replication study. Construction and production of more LVV-Crx-GFP are planned in order to replicate this experiment and verify the expression of endogenous Crx in the future. To summarise, the preliminary data presented in this chapter shows the potential of LNS cells to differentiate into photoreceptor-like cells through genetic modification. Further efforts using a combination of other transcription factors may enhance the strength and efficiency of driving LNS cells along retinal lineages.

### 8 Chapter Eight - Final Discussion

### 8.1 Thesis summary

The studies detailed in this thesis characterize neural colonies (neurospheres) derived from adult mouse and human limbus, and for the first time explore their potential for transdifferentiation towards retinal like cells *in vitro*.

The investigations on self-renewal, neural potential, origin and ultrastructure, provide comprehensive knowledge of the neurosphere cells derived from adult corneal limbus. The cells displayed clonal expansion and expressed a wide range of stem cell and neural lineage markers. Adult LNS cells appear to be stem/progenitor cells from neural crest derived limbal stroma, instead of transformed limbal epithelial or bone marrow derived cells. The studies also present the first ultrastructural characterisation of LNS. They exhibited similar morphology and microstructure to neurospheres derived from the CNS.

Following culture in a retinal development microenvironment, LNS derived cells displayed mature neural markers and exhibited electrical excitability. For the first time this demonstrates that neural crest derived limbal stromal stem/progenitor cells are capable of transdifferentiation towards a retinal lineage, displaying photoreceptor / RPE specific markers and electrical excitability *in vitro*. A subpopulation of LNS cells integrated into the photoreceptor layer of retinal explants *in vitro*.

A further study was performed using human limbal tissue from donor eyes and from patients undergoing pterygium surgery. Human LNS cells have been successfully derived from donors aged up to 94-year old. A final preliminary study introducing exogenous Crx, the key photoreceptor fate regulation transcription factor, has shown an activation of endogenous Crx and a trend towards up-regulation of downstream photoreceptor genes. This indicates that internal regulation may also be utilized to encourage LNS cells to acquire photoreceptor-like properties.

Ultimately the results presented here highlight a valuable autologous cell resource to generate retinal-like cells for tissue repair. Much of the work provides the first evidence on the transdifferentiation potential of neural-crest derived limbal stromal stem/progenitor cells as a candidate cell resource for retinal repair. This will allow us and other research groups to pursue further work with the common goal of generating functional autologous photoreceptor/RPE cells.

#### 8.2 Implications for stem cell therapy for retinal disease

Cell therapy is an attractive approach for the treatment of degenerative retinal diseases. In many such diseases, the inner retinal neurons remain largely intact. The spatially organised inner neural network is still functional for receiving and transmitting signals to the CNS. Therefore, if photoreceptors can be transplanted at the optimal site and form synaptic connections with the next neurons (bipolar cells) within retinas, visual function may be restored. In addition, the retina possesses unique advantages due to its anatomical features and the development of ophthalmic surgical techniques. The SRS, the potential space between photoreceptors and RPE cells, provides an ideal site for cell delivery. Synaptic integration and improvements in retinal function have been demonstrated following photoreceptor precursor cell transplantation into animal models of retinal degeneration [135]. Several studies have also demonstrated grafting cells integration in to adult retina, displaying typical photoreceptor morphology [62].

Whilst the studies presented in this thesis used adult/aged corneal limbus derived neurosphere cells, various sources of stem/progenitor cells are currently being investigated in order to identify the ideal cell type for the treatment of degenerative retinal diseases. However, there is still a lack of practical cell resources for clinical application. Utilizing embryonic or foetal tissues is difficult due to limited resources, ethical issues and risks associated with tumour formation [5,64,135]. In addition, transplant rejection may occur due to chronic immune responses. As reported recently, in the absence of immune modulation there is a 90% loss of integrated allogeneic photoreceptors by 4 months, and this increases to almost 100% at 6 months [114]. iPSCs, generated from somatic cells via introduction of transcription factors, can provide immune matched cells for transplantation. However, the possibility of mutagenesis due to viral vector integration or tumour formation remains [120]. Although a small population of CB epithelial cells exhibit clonal growth and express neural/retinal progenitor markers, the existence of true stem cells in the CB remains controversial [124,125]. In addition, it is technically challenging to harvest autologous CB cells.

#### 8.2.1 A new candidate autologous cell resource for degenerative retinal diseases

The results presented here highlight an attractive autologous cell resource derived from corneal limbus, for the treatment of degenerative retinal diseases. This is a readily accessible area between the conjunctiva/sclera and the transparent cornea, where the superficial layers are amenable to tissue harvesting. In Chapter 3, it was shown that neural colonies (neurospheres) were successfully derived from adult mouse cells using a NSA, which is a *bona fide* serum-free culture system. The cells expressed a wide range of neural stem/progenitor markers, and gave rise to mature neuron-like cells following differentiation. LNS derived cells were also capable of self-renewal. Robust expansion *in vitro* can therefore provide sufficient progenitor cells for further manipulation and/or transdifferentiation.

LNSs in this study are likely to have originated from neural-crest limbal stromal cells rather than epithelial cells or bone marrow derived cells. The result presented here differs from observations by Zhao et al., which demonstrated that a NSA accompanied with inhibition of BMP4 signaling encouraged limbal epithelial progenitor cells to acquire neural properties [3]. These cells could also be subsequently differentiated into either functional neurons or cells which expressed photoreceptor specific markers. The author excluded the stromal origin simply by the observation that no neurospheres were generated from rat limbal stroma in the NSA culture system. However, other research groups have demonstrated that neurospheres can be generated from corneal/limbal stroma from rodents, cows, rabbits and humans [6]. In addition it is not possible to surgically separate epithelial from stromal layers in rodent eyes without cell contamination. Therefore, the use of specific markers is necessary to identify cell origin. In Chapter 3, following neurosphere generation, continuous expression of a diverse range of neural-crest markers was shown. The neural crest markers were upregulated in synchrony with expression of neural lineage markers. While a downregulation of epithelial lineage markers was concurrent with elimination of over 90% of cells within the first three days of culture. These observations suggest that LNS generation is likely to be from neural crest derived corneal stromal progenitor cells. Inhibition of BMP4 did not change the gene expression profile or affect LNS forming capacity, which is suggestive that BMP4 inhibition is not critical in the generation or maintenance of LNSs. In addition, on comparison of the ultrastructure of limbal neurospheres with well characterised neurospheres derived from the CNS [30,32,33,90] and the CB [104]. Tight- and desmosome junctions, typical in spheres of an epithelial origin, were absent. This suggests that sphere formation was unlikely to be due to reprogramming of epithelial cells to a neural lineage [202].

Several studies have demonstrated that bone marrow derived cells can migrate to the corneal/limbal stroma [30,90,148], with expression of the hematopoietic stem cell marker (CD34) and leukocyte marker (CD45) in the stromal layer of the cornea and limbus, but not in the epithelial or endothelial layers. In our study, we found that limbal derived neurosphere cells expressed CD34, but were negative for CD45, indicating that LNS are stromal keratocyte progenitor cells. This supports previous studies suggesting that corneal/limbal stromal keratocytes are multipotent neural crest stem cells capable of differentiating into a neural lineage [90,196].

Cell contamination from retinal cells and RPE cells is possible due to the small size of the mouse eye. However we are confident that LNS cells were not derived from retinal cells or RPE cells. In Chapter 3, a range of neural retinal markers and RPE markers were found to be absent in freshly isolation limbal cells as well as LNSs cultured *in vitro*. Therefore the acquisition of retinal-like cell properties observed in Chapter 4 was not due to contamination from retinal/ RPE cells during dissection. In Chapter 6, the generation of human LNS cells from live patients and donor limbal rims also confirmed that LNS cells were from limbal tissues, rather than from tissues of a retinal origin.

#### 8.2.2 Derivation of excitable retinal-like cells from adult LNS cells

Consistent with previous reports, our neural crest derived corneal LNS cells were immunopositive for a range of neural lineage markers [90,148,172]. In this study, we confirmed that following neural differentiation, a sub-population of cells displayed a typical neural morphology and expressed mature neural markers, as detailed in Chapter 3 and 4.

This is the first time that neurosphere cells generated from neural-crest derived limbal stroma have shown the potential for transdifferentiation into photoreceptor and RPE like cells. In Chapter 4, expression of retinal development transcription factors including Lhx2 and Pax6 were observed in LNS cells following 3-4 days culture in a retinal developing microenvironment provided by a co-culture system. The subsequent expression of photoreceptor specific markers as well as other retinal/RPE markers was observed at a transcript and/or protein level. Morphologically, differentiated LNS also displayed putative presynaptic dense bodies and sensory cilia after differentiation. The latter is the same subtype of cilia which is present in photoreceptor and RPE cells [30,90,146,148]. These typical retinal cell features have not been observed in transduced hippocampus-derived adult NSC or induced bone marrow stromal stem cells [219].

Furthermore, I demonstrate in Chapter 5, for the first time, that induced LNS cells possess voltage-gated calcium channels capable of electrical excitability. The acute calcium influx response was similar to the response seen in retinal cells, which were used as a positive control. Voltage gated calcium channels and their mediated release of neurotransmitters play an important role in the functionality of the retina [88,146,160]. These channels also regulate calcium homeostasis, cell metabolism, cytoskeletal dynamics, gene expression and cell death in photoreceptor [246-248]. Functional voltage-dependent channel has also been observed in iPSCs derived photoreceptor-like cells [247,249]. Due to the limitations of fluorescent calcium indicators for use in the assessment of light responsiveness, it remains to be seen whether LNS cell acquired this unique function of photoreceptor cells. Electrophysiological recording may be an ideal alternative method to utilise for further investigation *in vitro*.

#### 8.2.3 Transdifferentiation potential of human LNS cells towards a retinal lineage

I extended this study to human limbal cells, using tissue from aged individuals. In Chapter 5, LNSs were generated from tissue from donors up to 94 years of age. These cells expressed neural stem cell/progenitor markers including nestin, Sox2 and beta-III tubulin. This study also provided information on the derivation of limbal cells with neural potential from 1 mm<sup>2</sup> of superficial limbal tissues from live patients.

This is the first study on the transdifferentiation potential of human limbus derived progenitor cells towards a retinal lineage. Although mature photoreceptor/RPE markers were undetectable, human LNS expressed retinal progenitor markers including Pax6, Lhx2 and Rx when co-cultured with developing mouse retinal cells or exposed to extrinsic factors such as Shh, RA and Taurine. The use of extrinsic factor modulation is valuable as it indicates the use of animal tissue/cells can be avoided in the future. It is encouraging that endogenous retinal development transcription factors were shown to be up-regulated in human LNS cells. These results suggest that in vitro expanded human LNS cells may be a potential autologous cell resource for the treatment of retinal degenerative diseases. Further research using extrinsic pathway regulators or genetic modification to introduce intrinsic transcription factors, may promote LNS cells to acquire retinal-like cell properties in vitro. To ultimately prove that LNS cells can give rise to RPE cells and photoreceptors, comprehensive evidence is required. These include expression of mature photoreceptor/RPE specific markers, and demonstration of their functionality such as light responsiveness for photoreceptor cells, and ability to phagocytose ROS for RPE cells both in vitro and in vivo.

#### 8.2.4 Genetic modification of LNS cells

Co-culture of LNS cells with animal tissue/cells in Chapter 3 and 4 explored the potential for differentiation along retinal lineages. However, the use of animal tissue/cells is not clinically applicable. A preliminary experiment was therefore performed in order to investigate the effect of ectopic expression of Crx on LNS cells, as detailed in Chapter 7. Possible endogenous Crx activation and a trend towards upregulation of photoreceptor markers were observed. Ectopic expression of Crx was however not sufficient to drive LNS cell differentiation to mature rod photoreceptor-like cells. It should be noted that this potential has not been detected from other source of non-eye field stem cells, such as neural stem cells derived from the hippocampus [223]. Therefore, LNS can be used more readily for retinal cell derivation than non eye-field stem cell resources. Genetic modification by ectopic expression of retinal development transcription factors has been shown to promote CB epithelial cells or IPE cells to express photoreceptor-specific markers [13,88]. The efficiencies of 50-90% rhodopsin positive cells from rat or primate CB and IPE cells have been reported previously by introducing transcription factors including Crx, Otx2 and NeuroD [8,86,87,169]. The derived photoreceptor-like cells hyperpolarised after light stimulation [86,88]. A more recent study demonstrated introduction of factors Otx2 and Crx, with the modulation of Chx10, led to a strong enrichment of functional photoreceptor-like cell from human CB derived cells [88]. Therefore, combination with other retinal/photoreceptor developing transcription factors may enhance the effect of driving the LNS towards photoreceptor-like cells [169].

Despite the encouraging results from genetic modified CB and IPE, it remains challenging to generation "true" photoreceptor cells from adult stem cells. Adult CB epithelial cells were previously identified as retinal stem cells [86,168,169,213]. Their stem cell properties and capacity for generation of photoreceptor cells have been questioned [128]. Gualdoni *et al.* investigated the effect of previously reported methods on driving CB derived cells into photoreceptor cells. None of the culture conditions or introduced transcription factors including NeuroD, Chx10, Crx, and Nrl can effectively activate Nrl-regulated photoreceptor differentiation program [3,135]. Therefore, the potential of CB cells to generate "true photoreceptor" cells are yet to be determined. The author suggests reprogramming and/or trans-differentiation would be required to use CB cells as a source for the generation of photoreceptors [135]. LNS cells would also be an optimal cell resource for reprogramming and/or trans-differentiation. They are readily accessible, highly proliferative and multipotent. iPSCs can be generated from mouse and human somatic cell by introduction of four transcription factors including OCT4, SOX2, c-Myc and KLF4. Due to the risks such as

insertional mutagenesis or tumor formation, it has been suggested to use a minimal number of transcription factors and to eliminate oncogenic factors [135]. This goal can be achieved through selection of optimal candidate cell resources. Kim *et al.* generated iPSCs from adult mouse and human neural stem cells by ectopic expression of single transcription factor Oct4 [250-252]. As demonstrated in Chapter 3, a diverse range of neural stem markers including Sox2, were detected on LNS cells. The multipotential capability of limbal stroma derived stem/progenitor cells have been reported by different research groups [250]. Dravida *et al.* showed that stem cells derived from human corneal-limbal stroma, expressed the ESC marker SSEA-4 (stage specific embryonic antigen-4) and other stem cell markers important for maintaining an undifferentiated state [29,30,90,148,149]. Therefore, LNS cells may become an ideal cell resource for single-factor reprogramming or transdifferentiation due to their existing stem/progenitor cell properties, multipotency and plasticity.

#### 8.3 Future Plans

The studies present in this thesis, provide the first information on LNS cells transdifferentiation towards retinal-like cells. As a new candidate cell resource for retinal repair, many new avenues have been opened up for further studies. The following section describes some of the work which will be continued in our group.

#### 8.3.1 Functional assessment - light responsiveness in vitro

The expression of photoreceptor specific markers is not sufficient to definitively prove cell identity. Light responsiveness, a unique function of photoreceptor cells, needs to be further investigated. Functional photoreceptors are partially depolarised in the dark. This is due to positively charged ions entering cyclic-nucleotide gated channels when cGMP is bound to those channels. Upon light stimulation, cGMP is hydrolyzed into GMP, which causes closure of cyclic-nucleotide gated channels and stops positive ions entering. Thus, photoreceptors become hyperpolarized. Electrophysiological recording can be utilised to measure the change of membrane potential and detect light responsiveness in single cells [149].

As a continuation of the work described in Chapter 5, electrophysiological recording by patch clamp will be used to measure the electrical potential across cell membranes in the light and dark. Neonatal mouse retinal cells cultured *in vitro* will be used as positive control to validate the assay. Adult mouse LNS cells maintained in non coculture conditions will be used as negative control.

#### 8.3.2 Investigation of Nrl-activation using gene reporter mice

Nrl is a basic motif-leucine zipper transcription factor that is expressed in developing and mature rods. It has an essential role in rod fate specification [88]. A deletion of Nrl (Nrl<sup>-/-</sup>) leads to loss of rod function and a change of photoreceptor layer morphology *in vivo* [212-214]. The Nrl-eGFP transgenic reporter mouse model has been previously used to select optimal cell for retinal repair [214]. In this mouse model, developing rod photoreceptors are tagged with GFP.

Further work will assess definite rod generation from LNS cells using this mouse model [62]. Nrl-eGFP mouse derived LNS cells will be subjected to co-cultured assay, extrinsic factors stimulation or genetic modification with retinal development transcription factors. We will monitor and quantify the percentage of GFP labelled cells in these

conditions to assessed LNS cells' capability in generation new photoreceptor cells [62,135].

#### 8.3.3 To enhance the efficiency of photoreceptor-like cell generation

#### 8.3.3.1 Combined introduction of photoreceptor development transcription factors

Genetic modification is a high throughput method utilised to promote stem cell differentiation toward a specific fate(s). Hence it has great potential in regenerative medicine. Retinal specific neuronal differentiation is regulated by a complex transcriptional network. The transcription factors Crx and Otx2 play an essential role in retinal lineage commitment [135]. Combined transduction with Otx2 and Crx, together with the modulation of Chx10, greatly enhanced the efficiency of generation functional photoreceptor-like cell from human CB derived cells [73,82,83,213,253]. Electrophysiological and behavioural tests showed improvements in visual function, following transplantation of transduced cells into animal models of retinal disease. Whilst Nrl, NeuroD, Rx, Ngn2, or Mash1 did not affect rod nor cone photoreceptor differentiation [169]. LNS cells are derived from the anterior eye; therefore they have certain intrinsic factors leading them to become eye field cells. Ectopic expression of combined transcription factors including Crx/Otx2 may enhance the strength and efficiency of photoreceptor-like cell generation from LNS cells.

#### 8.3.3.2 Regulation of signalling pathways

Several extrinsic factors have been reported for use in directing ESC differentiation toward retinal progenitor cells and subsequently to photoreceptors through a stepwise comprehensive differentiation procedure [169]. Factors used include Noggin (BMP4 inhibitor) DKK1, Shh, Activin A and Taurine.

The work presented in Chapter 6, suggests extrinsic factors including Shh, Taurine and RA induce human LNS cell to express retinal progenitor markers such as Pax6, Lhx2 and Rx at a transcript level. This is similar to the effect of the co-culture assay. In the case of heterogeneous progenitor cells differentiating into retinal neurons, extrinsic factors have also been demonstrated to direct regulation or act synergistically with co-culture assays. It has been reported that Activin A and Taurine can induce expression of photoreceptor specific markers such as rhodopsin, opsin and recoverin from bone marrow stromal cells [109]. Zhao *et al.* found that DKK1 and Shh significantly increased the number of rhodopsin kinase positive cells when corneal limbal progenitor cells were co-cultured with PN1 retinal cells [144]. Further detailed studies

are however required to determine the functionality of these derived photoreceptor-like cells.

The defined extrinsic factors and their effect on heterogeneous stem/progenitor cell differentiation along retinal lineages may help us to understand the mechanisms involved in retinal specific neuronal development. In addition, they also have a number of advantages compared to other assays such as co-culture with animal tissue and genetic modification in terms of safety for prospective clinical application.

#### 8.3.4 Functionality and integration assessment following transplantation

#### 8.3.4.1 *In vivo* transplantation studies

Wild type mice (C57BL/6, P1) and a mouse model of retinal degeneration (Ccl2\*/Cx3Cr1\*/) will be utilized for transplantation studies. Rod genesis peaks at PN day 1 in mice. Therefore PN1 mice will be used to provide an optimal microenvironment to promote photoreceptor specific differentiation and to facilitate integration into the ONL [6]. A degenerative retinal phenotype is present in Ccl2\*/Cx3Cr1\*/is apparent by 5 weeks of age. We will therefore transplant cells into knockout mice at 6-8 weeks. If photoreceptor-like cells can be derived from human and mouse LNS cells through genetic modification as detailed in section 8.5.3.1, they will be transplanted into retinal degeneration animal model. The GFP tagged donor cells will be dissociated into single cells and transplanted into the SRS of recipient mice transsclerally. We will use previously suggested immunosuppression to minimise the effect of inflammation or rejection caused by allogeneic or xenogeneic donor cells [62].

We will set up three groups for transplantation experiments: a) control group on which no surgical procedures will be conducted; b) a sham injection group in which the same surgical procedure will be conducted, but without cell transplantation to eliminate possible effect due to the surgical intervention; and c) cell transplantation group. We anticipate that 6-8 animals per treatment group should be sufficient to obtain the required results [120].

#### 8.3.4.2 LNS cell differentiation and integration in vivo

The ability of transplanted cells to integrate within host tissue is crucial for cell therapy. In Chapter 5, I performed a preliminary *in vitro* cell integration study using neonatal retinal explants and Qdot labelled LNS cells. Due to the limitations of the Qdot tracking assay, the majority of grafted cells were not fluorescently labelled. In addition, the

retinal explants lost the typical laminated morphology in the organotypic culture system.

In the future, *in vivo* transplantation will be used to assess cell integration and synaptic connection. LVV-GFP, a generous gift from Dr. J Cooke and Prof A Dick will be used to genetically label LNS cells. As shown in Chapter 7, bright GFP cells were observed following transfection. Successfully GFP tagged LNS cells will be sorted for subretinal transplantation into neonatal wildtype mice. LNS cells genetically modified with combined retinal development transcription factors will also be tagged with GFP, and transplanted into the SRS of Ccl2\*/Cx3Cr1\*.

Recipient mice will be sacrificed at a number of time points following transplantation. Host retina will be examined at 1, 2 and 4 weeks post transplantation by immunohistochemistry. Photoreceptor specific markers including rhodopsin and recoverin will be used. The location and phenotype of transplanted cells (GFP tagged) will be assessed too. We will also investigate photoreceptor specific synaptic connections using anti-bassoon antibodies [62].

#### 8.3.4.3 Assessment of visual function following transplantation

If optimal photoreceptor cell phenotypes and integration can be achieved, functional studies will be performed to assess if transplanted cells are light-responsive and functionally connected. Result from all three groups (control, sham injection and transplantation) will be analyse to avoid bias.

The following experiments will be carried out 3-4 weeks post transplantation: optokinetic drum test and electroretinography. The optokinetic drum has been used as an appropriate tool to examine the visual perception and visual acuity of mouse. We will investigate head-tracking responses. The measurement of extracellular field potential may also be carried out as previously reported [62]. We will stimulate the retinal tissue *in vitro* with light, and measure the electrical potential produced by excitable cells using extracellular microelectrodes.

#### 8.3.5 Studies on human LNS cells

The work presented in Chapter 6, provides information on isolation and culture of LNS cells from aged human donor tissue. The presence of retinal progenitor markers at transcript level on human LNS cells following culture in conducive environment suggests their potential for transdifferentiation towards a retinal lineage. Future work will continue the investigation on clonal growth, neural potential and ultrastructural

characteristics of human LNS cells. More samples will be collected from live patients. By using genetic modification, extrinsic factors and transplantation in to SRS of animal models, it is hope that the feasibility of transdifferentiation human LNS cell along retinal lineages will be revealed.

#### **Reference List**

- [1] A. Schermer, S. Galvin, and T. T. Sun, Differentiation-related expression of a major 64K corneal keratin in vivo and in culture suggests limbal location of corneal epithelial stem cells, J. Cell Biol., 103 (1986) 49-62.
- [2] H. P. Scholl, M. Fleckenstein, I. P. Charbel, C. Keilhauer, F. G. Holz, and B. H. Weber, An update on the genetics of age-related macular degeneration, Mol. Vis., 13 (2007) 196-205.
- [3] S. A. Cicero, D. Johnson, S. Reyntjens, S. Frase, S. Connell, L. M. Chow, S. J. Baker, B. P. Sorrentino, and M. A. Dyer, Cells previously identified as retinal stem cells are pigmented ciliary epithelial cells, Proc. Natl. Acad. Sci. U. S A, 106 (2009) 6685-6690.
- [4] H. J. Kaplan, T. H. Tezel, A. S. Berger, and L. V. Del Priore, Retinal transplantation, Chem. Immunol., 73 (1999) 207-219.
- [5] T. Leveillard, S. Mohand-Said, and J. A. Sahel, Retinal repair by transplantation of photoreceptor precursors, Med. Sci. (Paris), 23 (2007) 240-242.
- [6] X. Zhao, A. V. Das, S. Bhattacharya, W. B. Thoreson, J. R. Sierra, K. B. Mallya, and I. Ahmad, Derivation of neurons with functional properties from adult limbal epithelium: implications in autologous cell therapy for photoreceptor degeneration, Stem Cells, 26 (2008) 939-949.
- [7] D. A. Lamba, M. O. Karl, C. B. Ware, and T. A. Reh, Efficient generation of retinal progenitor cells from human embryonic stem cells, Proc. Natl. Acad. Sci. U. S. A, 103 (2006) 12769-12774.
- [8] C. Jomary, S. E. Jones, and A. J. Lotery, Generation of light-sensitive photoreceptor phenotypes by genetic modification of human adult ocular stem cells with Crx, Invest Ophthalmol. Vis. Sci., 51 (2010) 1181-1189.
- [9] Y. Hirami, F. Osakada, K. Takahashi, K. Okita, S. Yamanaka, H. Ikeda, N. Yoshimura, and M. Takahashi, Generation of retinal cells from mouse and human induced pluripotent stem cells, Neurosci. Lett., 458 (2009) 126-131.
- [10] H. Ikeda, F. Osakada, K. Watanabe, K. Mizuseki, T. Haraguchi, H. Miyoshi, D. Kamiya, Y. Honda, N. Sasai, N. Yoshimura, M. Takahashi, and Y. Sasai, Generation of Rx+/Pax6+ neural retinal precursors from embryonic stem cells, Proc. Natl. Acad. Sci. U. S. A, 102 (2005) 11331-11336.
- [11] F. Osakada, Z. B. Jin, Y. Hirami, H. Ikeda, T. Danjyo, K. Watanabe, Y. Sasai, and M. Takahashi, In vitro differentiation of retinal cells from human pluripotent stem cells by small-molecule induction, J. Cell Sci., 122 (2009) 3169-3179.
- [12] S. G. Giannelli, G. C. Demontis, G. Pertile, P. Rama, and V. Broccoli, Adult human Muller glia cells are a highly efficient source of rod photoreceptors, Stem Cells, 29 (2011) 344-356.
- [13] M. Haruta, M. Kosaka, Y. Kanegae, I. Saito, T. Inoue, R. Kageyama, A. Nishida, Y. Honda, and M. Takahashi, Induction of photoreceptor-specific phenotypes in adult mammalian iris tissue, Nat. Neurosci., 4 (2001) 1163-1164.
- [14] V. A. Wallace, Stem cells: a source for neuron repair in retinal disease, Can. J. Ophthalmol., 42 (2007) 442-446.

[15] J. V. Forrester, The eye: basic sciences in practice, Saunders Elsevier, Edinburgh 2002.

- [16] C. F. Bahn, R. M. Glassman, D. K. MacCallum, J. H. Lillie, R. F. Meyer, B. J. Robinson, and N. M. Rich, Postnatal development of corneal endothelium, Invest Ophthalmol. Vis. Sci., 27 (1986) 44-51.
- [17] J. M. Wolosin, M. T. Budak, and M. A. Akinci, Ocular surface epithelial and stem cell development, Int. J. Dev. Biol., 48 (2004) 981-991.
- [18] R. I. Freshney, G. Stacey, and J. M. Auerbach, Culture of human stem cells, Hoboken, N.J.: Wiley-Interscience, 2007.
- [19] C. Murphy, J. Alvarado, R. Juster, and M. Maglio, Prenatal and postnatal cellularity of the human corneal endothelium. A quantitative histologic study, Invest Ophthalmol. Vis. Sci., 25 (1984) 312-322.
- [20] G. Cotsarelis, S. Z. Cheng, G. Dong, T. T. Sun, and R. M. Lavker, Existence of slow-cycling limbal epithelial basal cells that can be preferentially stimulated to proliferate: implications on epithelial stem cells, Cell, 57 (1989) 201-209.
- [21] G. M. Seigel, W. Sun, R. Salvi, L. M. Campbell, S. Sullivan, and J. J. Reidy, Human corneal stem cells display functional neuronal properties, Mol. Vis., 9 (2003) 159-163.
- [22] U. Schlotzer-Schrehardt and F. E. Kruse, Identification and characterization of limbal stem cells, Exp. Eye Res., 81 (2005) 247-264.
- [23] E. C. Alfonso, Treatment of severe ocular-surface disorders with corneal epithelial stem cell transplantation, Arch. Ophthalmol., 118 (2000) 123-124.
- [24] G. Pellegrini, C. E. Traverso, A. T. Franzi, M. Zingirian, R. Cancedda, and L. M. De, Long-term restoration of damaged corneal surfaces with autologous cultivated corneal epithelium, Lancet, 349 (1997) 990-993.
- [25] K. Tsubota, Y. Satake, M. Kaido, N. Shinozaki, S. Shimmura, H. Bissen-Miyajima, and J. Shimazaki, Treatment of severe ocular-surface disorders with corneal epithelial stem-cell transplantation, N. Engl. J. Med., 340 (1999) 1697-1703.
- [26] K. Higa and J. Shimazaki, Recent advances in cultivated epithelial transplantation, Cornea, 27 Suppl 1 (2008) S41-S47.
- [27] P. A. Cauchi, G. S. Ang, A. zuara-Blanco, and J. M. Burr, A systematic literature review of surgical interventions for limbal stem cell deficiency in humans, Am. J. Ophthalmol., 146 (2008) 251-259.
- [28] G. A. Secker and J. T. Daniels, Corneal epithelial stem cells: deficiency and regulation, Stem Cell Rev., 4 (2008) 159-168.
- [29] S. Uchida, S. Yokoo, Y. Yanagi, T. Usui, C. Yokota, T. Mimura, M. Araie, S. Yamagami, and S. Amano, Sphere formation and expression of neural proteins by human corneal stromal cells in vitro, Invest Ophthalmol. Vis. Sci., 46 (2005) 1620-1625.
- [30] Y. Du, M. L. Funderburgh, M. M. Mann, N. SundarRaj, and J. L. Funderburgh, Multipotent stem cells in human corneal stroma, Stem Cells, 23 (2005) 1266-1275.

[31] N. Polisetty, A. Fatima, S. L. Madhira, V. S. Sangwan, and G. K. Vemuganti, Mesenchymal cells from limbal stroma of human eye, Mol. Vis., 14 (2008) 431-442.

- [32] T. Mimura, S. Amano, S. Yokoo, S. Uchida, T. Usui, and S. Yamagami, Isolation and distribution of rabbit keratocyte precursors, Mol. Vis., 14 (2008) 197-203.
- [33] M. L. Funderburgh, Y. Du, M. M. Mann, N. SundarRaj, and J. L. Funderburgh, PAX6 expression identifies progenitor cells for corneal keratocytes, FASEB J., 19 (2005) 1371-1373.
- [34] T. Umemoto, M. Yamato, K. Nishida, J. Yang, Y. Tano, and T. Okano, Limbal epithelial side-population cells have stem cell-like properties, including quiescent state, Stem Cells, 24 (2006) 86-94.
- [35] M. A. Goodell, Multipotential stem cells and 'side population' cells., Cytotherapy. 4(6):507-8, (2002).
- [36] T. Mimura, S. Yokoo, M. Araie, S. Amano, and S. Yamagami, Treatment of rabbit bullous keratopathy with precursors derived from cultured human corneal endothelium, Invest Ophthalmol. Vis. Sci., 46 (2005) 3637-3644.
- [37] S. Yokoo, S. Yamagami, Y. Yanagi, S. Uchida, T. Mimura, T. Usui, and S. Amano, Human corneal endothelial cell precursors isolated by sphere-forming assay, Invest Ophthalmol. Vis. Sci., 46 (2005) 1626-1631.
- [38] R. S. Fishman, The Nobel Prize of 1906, Arch. Ophthalmol., 125 (2007) 690-694.
- [39] H. Kolb, E. Fernandez, and R. Nelson, Webvision: the organization of the retina and visual system, Bethesda, Md.: National Library of Medicine: National Center for Biotechnology Information [electronic resource], 2007.
- [40] R. H. Masland, The fundamental plan of the retina, Nat. Neurosci., 4 (2001) 877-886.
- [41] A. Lukats, A. Szabo, P. Rohlich, B. Vigh, and A. Szel, Photopigment coexpression in mammals: comparative and developmental aspects, Histol. Histopathol., 20 (2005) 551-574.
- [42] P. A. Hargrave and J. H. McDowell, Rhodopsin and phototransduction: a model system for G protein-linked receptors, FASEB J., 6 (1992) 2323-2331.
- [43] Dale Purves, George J Augustine, David Fitzpatrick, Lawrence C Katz, Anthony-Samuel LaMantia, James O McNamara, and and S Mark Williams, Neuroscience, Sinauer Asociates Inc., 2001.
- [44] O. Strauss, The retinal pigment epithelium in visual function, Physiol Rev., 85 (2005) 845-881.
- [45] S. Binder, B. V. Stanzel, I. Krebs, and C. Glittenberg, Transplantation of the RPE in AMD, Prog. Retin. Eye Res., 26 (2007) 516-554.
- [46] R. W. Young, Visual cells, Sci. Am., 223 (1970) 80-91.
- [47] G. Soubrane, W. M. Haddad, and G. Coscas, Age-related macular degeneration, Presse Med., 31 (2002) 1282-1287.

[48] A. Lotery, X. Xu, G. Zlatava, and J. Loftus, Burden of illness, visual impairment and health resource utilisation of patients with neovascular age-related macular degeneration: results from the UK cohort of a five-country cross-sectional study, Br. J. Ophthalmol., 91 (2007) 1303-1307.

- [49] N. M. Bressler, L. A. Frost, S. B. Bressler, R. P. Murphy, and S. L. Fine, Natural course of poorly defined choroidal neovascularization associated with macular degeneration, Arch. Ophthalmol., 106 (1988) 1537-1542.
- [50] J. R. Vingerling, C. C. Klaver, A. Hofman, and P. T. de Jong, Epidemiology of age-related maculopathy, Epidemiol. Rev., 17 (1995) 347-360.
- [51] R. D. Jager, W. F. Mieler, and J. W. Miller, Age-related macular degeneration, N. Engl. J. Med., 358 (2008) 2606-2617.
- [52] S. Ennis, C. Jomary, R. Mullins, A. Cree, X. Chen, A. Macleod, S. Jones, A. Collins, E. Stone, and A. Lotery, Association between the SERPING1 gene and age-related macular degeneration: a two-stage case-control study, Lancet, 372 (2008) 1828-1834.
- [53] R. J. Klein, C. Zeiss, E. Y. Chew, J. Y. Tsai, R. S. Sackler, C. Haynes, A. K. Henning, J. P. SanGiovanni, S. M. Mane, S. T. Mayne, M. B. Bracken, F. L. Ferris, J. Ott, C. Barnstable, and J. Hoh, Complement factor H polymorphism in agerelated macular degeneration, Science, 308 (2005) 385-389.
- [54] J. R. Yates, T. Sepp, B. K. Matharu, J. C. Khan, D. A. Thurlby, H. Shahid, D. G. Clayton, C. Hayward, J. Morgan, A. F. Wright, A. M. Armbrecht, B. Dhillon, I. J. Deary, E. Redmond, A. C. Bird, and A. T. Moore, Complement C3 variant and the risk of age-related macular degeneration, N. Engl. J. Med., 357 (2007) 553-561.
- [55] A. Swaroop, K. E. Branham, W. Chen, and G. Abecasis, Genetic susceptibility to age-related macular degeneration: a paradigm for dissecting complex disease traits, Hum. Mol. Genet., 16 Spec No. 2 (2007) R174-R182.
- [56] R. A. Pagon and S. P. Daiger, Retinitis Pigmentosa Overview, (1993).
- [57] S. B. Bressler, Introduction: Understanding the role of angiogenesis and antiangiogenic agents in age-related macular degeneration, Ophthalmology, 116 (2009) S1-S7.
- [58] D. V. Alfaro, Age-related macular degeneration: a comprehensive textbook, Philadelphia; London: Lippincott Williams & Wilkins, 2006.
- [59] A. Klettner and J. Roider, Comparison of bevacizumab, ranibizumab, and pegaptanib in vitro: efficiency and possible additional pathways, Invest Ophthalmol. Vis. Sci., 49 (2008) 4523-4527.
- [60] I. Semkova, F. Kreppel, G. Welsandt, T. Luther, J. Kozlowski, H. Janicki, S. Kochanek, and U. Schraermeyer, Autologous transplantation of genetically modified iris pigment epithelial cells: a promising concept for the treatment of age-related macular degeneration and other disorders of the eye, Proc. Natl. Acad. Sci. U. S A, 99 (2002) 13090-13095.
- [61] Submacular surgery trials randomized pilot trial of laser photocoagulation versus surgery for recurrent choroidal neovascularization secondary to agerelated macular degeneration: II. Quality of life outcomes submacular surgery trials pilot study report number 2, Am. J. Ophthalmol., 130 (2000) 408-418.

[62] R. E. MacLaren, R. A. Pearson, A. MacNeil, R. H. Douglas, T. E. Salt, M. Akimoto, A. Swaroop, J. C. Sowden, and R. R. Ali, Retinal repair by transplantation of photoreceptor precursors, Nature, 444 (2006) 203-207.

- [63] E. L. Berson and F. A. Jakobiec, Neural retinal cell transplantation: ideal versus reality, Ophthalmology, 106 (1999) 445-446.
- [64] U. Bartsch, W. Oriyakhel, P. F. Kenna, S. Linke, G. Richard, B. Petrowitz, P. Humphries, G. J. Farrar, and M. Ader, Retinal cells integrate into the outer nuclear layer and differentiate into mature photoreceptors after subretinal transplantation into adult mice, Exp. Eye Res., 86 (2008) 691-700.
- [65] J. S. Meyer, M. L. Katz, J. A. Maruniak, and M. D. Kirk, Embryonic stem cell-derived neural progenitors incorporate into degenerating retina and enhance survival of host photoreceptors, Stem Cells, 24 (2006) 274-283.
- [66] U. Schraermeyer, G. Thumann, T. Luther, N. Kociok, S. Armhold, K. Kruttwig, C. Andressen, K. Addicks, and K. U. Bartz-Schmidt, Subretinally transplanted embryonic stem cells rescue photoreceptor cells from degeneration in the RCS rats, Cell Transplant., 10 (2001) 673-680.
- [67] N. D. Radtke, R. B. Aramant, M. J. Seiler, H. M. Petry, and D. Pidwell, Vision change after sheet transplant of fetal retina with retinal pigment epithelium to a patient with retinitis pigmentosa, Arch. Ophthalmol., 122 (2004) 1159-1165.
- [68] G. Halder, P. Callaerts, and W. J. Gehring, Induction of ectopic eyes by targeted expression of the eyeless gene in Drosophila, Science, 267 (1995) 1788-1792.
- [69] P. A. Georgala, C. B. Carr, and D. J. Price, The role of Pax6 in forebrain development, Dev. Neurobiol., 71 (2011) 690-709.
- [70] T. Glaser, L. Jepeal, J. G. Edwards, S. R. Young, J. Favor, and R. L. Maas, PAX6 gene dosage effect in a family with congenital cataracts, aniridia, anophthalmia and central nervous system defects, Nat. Genet., 7 (1994) 463-471.
- [71] D. Arendt, Evolution of eyes and photoreceptor cell types, Int. J. Dev. Biol., 47 (2003) 563-571.
- [72] P. H. Mathers, A. Grinberg, K. A. Mahon, and M. Jamrich, The Rx homeobox gene is essential for vertebrate eye development, Nature, 387 (1997) 603-607.
- [73] A. K. Hennig, G. H. Peng, and S. Chen, Regulation of photoreceptor gene expression by Crx-associated transcription factor network, Brain Res., 1192 (2008) 114-133.
- [74] A. Nishida, A. Furukawa, C. Koike, Y. Tano, S. Aizawa, I. Matsuo, and T. Furukawa, Otx2 homeobox gene controls retinal photoreceptor cell fate and pineal gland development, Nat. Neurosci., 6 (2003) 1255-1263.
- [75] B. F. Del, K. Tessmar-Raible, and J. Wittbrodt, Direct interaction of geminin and Six3 in eye development, Nature, 427 (2004) 745-749.
- [76] X. Huang and J. P. Saint-Jeannet, Induction of the neural crest and the opportunities of life on the edge, Dev. Biol., 275 (2004) 1-11.

[77] D. Sela-Donenfeld and C. Kalcheim, Regulation of the onset of neural crest migration by coordinated activity of BMP4 and Noggin in the dorsal neural tube, Development, 126 (1999) 4749-4762.

- [78] R. W. Young, Cell differentiation in the retina of the mouse, Anat. Rec., 212 (1985) 199-205.
- [79] X. J. Yang, Roles of cell-extrinsic growth factors in vertebrate eye pattern formation and retinogenesis, Semin. Cell Dev. Biol., 15 (2004) 91-103.
- [80] R. Ohsawa and R. Kageyama, Regulation of retinal cell fate specification by multiple transcription factors, Brain Res., 1192 (2008) 90-98.
- [81] J. R. Martinez-Morales, I. Rodrigo, and P. Bovolenta, Eye development: a view from the retina pigmented epithelium, Bioessays, 26 (2004) 766-777.
- [82] F. Beby, M. Housset, N. Fossat, G. C. Le, F. Flamant, P. Godement, and T. Lamonerie, Otx2 gene deletion in adult mouse retina induces rapid RPE dystrophy and slow photoreceptor degeneration, PLoS. One., 5 (2010) e11673.
- [83] J. R. Martinez-Morales, V. Dolez, I. Rodrigo, R. Zaccarini, L. Leconte, P. Bovolenta, and S. Saule, OTX2 activates the molecular network underlying retina pigment epithelium differentiation, J. Biol. Chem., 278 (2003) 21721-21731.
- [84] M. Nguyen and H. Arnheiter, Signaling and transcriptional regulation in early mammalian eye development: a link between FGF and MITF, Development, 127 (2000) 3581-3591.
- [85] K. Yasumoto, K. Yokoyama, K. Takahashi, Y. Tomita, and S. Shibahara, Functional analysis of microphthalmia-associated transcription factor in pigment cell-specific transcription of the human tyrosinase family genes, J. Biol. Chem., 272 (1997) 503-509.
- [86] T. Akagi, M. Mandai, S. Ooto, Y. Hirami, F. Osakada, R. Kageyama, N. Yoshimura, and M. Takahashi, Otx2 homeobox gene induces photoreceptor-specific phenotypes in cells derived from adult iris and ciliary tissue, Invest Ophthalmol. Vis. Sci., 45 (2004) 4570-4575.
- [87] C. Jomary and S. E. Jones, Induction of functional photoreceptor phenotype by exogenous Crx expression in mouse retinal stem cells, Invest Ophthalmol. Vis. Sci., 49 (2008) 429-437.
- [88] T. Akagi, J. Akita, M. Haruta, T. Suzuki, Y. Honda, T. Inoue, S. Yoshiura, R. Kageyama, T. Yatsu, M. Yamada, and M. Takahashi, Iris-derived cells from adult rodents and primates adopt photoreceptor-specific phenotypes, Invest Ophthalmol. Vis. Sci., 46 (2005) 3411-3419.
- [89] J. Kohyama, H. Abe, T. Shimazaki, A. Koizumi, K. Nakashima, S. Gojo, T. Taga, H. Okano, J. Hata, and A. Umezawa, Brain from bone: efficient "meta-differentiation" of marrow stroma-derived mature osteoblasts to neurons with Noggin or a demethylating agent, Differentiation, 68 (2001) 235-244.
- [90] S. Yoshida, S. Shimmura, N. Nagoshi, K. Fukuda, Y. Matsuzaki, H. Okano, and K. Tsubota, Isolation of multipotent neural crest-derived stem cells from the adult mouse cornea, Stem Cells, 24 (2006) 2714-2722.

[91] C. R. Bjornson, R. L. Rietze, B. A. Reynolds, M. C. Magli, and A. L. Vescovi, Turning brain into blood: a hematopoietic fate adopted by adult neural stem cells in vivo, Science, 283 (1999) 534-537.

- [92] S. Hombach-Klonisch, S. Panigrahi, I. Rashedi, A. Seifert, E. Alberti, P. Pocar, M. Kurpisz, K. Schulze-Osthoff, A. Mackiewicz, and M. Los, Adult stem cells and their trans-differentiation potential--perspectives and therapeutic applications, J. Mol. Med., 86 (2008) 1301-1314.
- [93] S. Yoshida, S. Shimmura, N. Nagoshi, K. Fukuda, Y. Matsuzaki, H. Okano, and K. Tsubota, Isolation of multipotent neural crest-derived stem cells from the adult mouse cornea, Stem Cells, 24 (2006) 2714-2722.
- [94] P. V. Algvere, L. Berglin, P. Gouras, and Y. Sheng, Transplantation of fetal retinal pigment epithelium in age-related macular degeneration with subfoveal neovascularization, Graefes Arch. Clin. Exp. Ophthalmol., 232 (1994) 707-716.
- [95] N. D. Radtke, R. B. Aramant, H. M. Petry, P. T. Green, D. J. Pidwell, and M. J. Seiler, Vision improvement in retinal degeneration patients by implantation of retina together with retinal pigment epithelium, Am. J. Ophthalmol., 146 (2008) 172-182.
- [96] J. W. Streilein, N. Ma, H. Wenkel, T. F. Ng, and P. Zamiri, Immunobiology and privilege of neuronal retina and pigment epithelium transplants, Vision Res., 42 (2002) 487-495.
- [97] J. W. Streilein, Ocular immune privilege: therapeutic opportunities from an experiment of nature, Nat. Rev. Immunol., 3 (2003) 879-889.
- [98] K. Warfvinge, J. F. Kiilgaard, H. Klassen, P. Zamiri, E. Scherfig, W. Streilein, J. U. Prause, and M. J. Young, Retinal progenitor cell xenografts to the pig retina: immunological reactions, Cell Transplant., 15 (2006) 603-612.
- [99] H. Wenkel and J. W. Streilein, Analysis of immune deviation elicited by antigens injected into the subretinal space, Invest Ophthalmol. Vis. Sci., 39 (1998) 1823-1834.
- [100] X. Zhang and D. Bok, Transplantation of retinal pigment epithelial cells and immune response in the subretinal space, Invest Ophthalmol. Vis. Sci., 39 (1998) 1021-1027.
- [101] S. Crafoord, P. V. Algvere, E. D. Kopp, and S. Seregard, Cyclosporine treatment of RPE allografts in the rabbit subretinal space, Acta Ophthalmol. Scand., 78 (2000) 122-129.
- [102] J. K. Olson and S. D. Miller, Microglia initiate central nervous system innate and adaptive immune responses through multiple TLRs, J. Immunol., 173 (2004) 3916-3924.
- [103] D. S. Gregerson and J. Yang, CD45-positive cells of the retina and their responsiveness to in vivo and in vitro treatment with IFN-gamma or anti-CD40, Invest Ophthalmol. Vis. Sci., 44 (2003) 3083-3093.
- [104] M. C. Moe, R. S. Kolberg, C. Sandberg, E. Vik-Mo, H. Olstorn, M. Varghese, I. A. Langmoen, and B. Nicolaissen, A comparison of epithelial and neural properties in progenitor cells derived from the adult human ciliary body and brain, Exp. Eye Res., 88 (2009) 30-38.

[105] T. R. Brazelton, F. M. Rossi, G. I. Keshet, and H. M. Blau, From marrow to brain: expression of neuronal phenotypes in adult mice, Science, 290 (2000) 1775-1779.

- [106] A. Hermann, S. Liebau, R. Gastl, S. Fickert, H. J. Habisch, J. Fiedler, J. Schwarz, R. Brenner, and A. Storch, Comparative analysis of neuroectodermal differentiation capacity of human bone marrow stromal cells using various conversion protocols, J. Neurosci. Res., 83 (2006) 1502-1514.
- [107] I. A. Grivennikov, Embryonic stem cells and the problem of directed differentiation, Biochemistry (Mosc.), 73 (2008) 1438-1452.
- [108] A. J. Joannides, C. Fiore-Heriche, A. A. Battersby, P. Athauda-Arachchi, I. A. Bouhon, L. Williams, K. Westmore, P. J. Kemp, A. Compston, N. D. Allen, and S. Chandran, A scaleable and defined system for generating neural stem cells from human embryonic stem cells, Stem Cells, 25 (2007) 731-737.
- [109] F. Osakada, H. Ikeda, M. Mandai, T. Wataya, K. Watanabe, N. Yoshimura, A. Akaike, Y. Sasai, and M. Takahashi, Toward the generation of rod and cone photoreceptors from mouse, monkey and human embryonic stem cells, Nat. Biotechnol., 26 (2008) 215-224.
- [110] X. Zhao, J. Liu, and I. Ahmad, Differentiation of embryonic stem cells into retinal neurons, Biochem. Biophys. Res. Commun., 297 (2002) 177-184.
- [111] H. Kawasaki, H. Suemori, K. Mizuseki, K. Watanabe, F. Urano, H. Ichinose, M. Haruta, M. Takahashi, K. Yoshikawa, S. Nishikawa, N. Nakatsuji, and Y. Sasai, Generation of dopaminergic neurons and pigmented epithelia from primate ES cells by stromal cell-derived inducing activity, Proc. Natl. Acad. Sci. U. S. A, 99 (2002) 1580-1585.
- [112] M. Haruta, Y. Sasai, H. Kawasaki, K. Amemiya, S. Ooto, M. Kitada, H. Suemori, N. Nakatsuji, C. Ide, Y. Honda, and M. Takahashi, In vitro and in vivo characterization of pigment epithelial cells differentiated from primate embryonic stem cells, Invest Ophthalmol. Vis. Sci., 45 (2004) 1020-1025.
- [113] M. J. Martin, A. Muotri, F. Gage, and A. Varki, Human embryonic stem cells express an immunogenic nonhuman sialic acid, Nat. Med., 11 (2005) 228-232.
- [114] S. Arnhold, H. Klein, I. Semkova, K. Addicks, and U. Schraermeyer, Neurally selected embryonic stem cells induce tumor formation after long-term survival following engraftment into the subretinal space, Invest Ophthalmol. Vis. Sci., 45 (2004) 4251-4255.
- [115] D. M. Chacko, J. A. Rogers, J. E. Turner, and I. Ahmad, Survival and differentiation of cultured retinal progenitors transplanted in the subretinal space of the rat, Biochem. Biophys. Res. Commun., 268 (2000) 842-846.
- [116] J. H. Stern and S. Temple, Stem cells for retinal replacement therapy, Neurotherapeutics., 8 (2011) 736-743.
- [117] G. Qiu, M. J. Seiler, C. Mui, S. Arai, R. B. Aramant, de Juan E Jr, and S. Sadda, Photoreceptor differentiation and integration of retinal progenitor cells transplanted into transgenic rats, Exp. Eye Res., 80 (2005) 515-525.
- [118] C. A. Haas, L. J. DeGennaro, M. Muller, and H. Hollander, Synapsin I expression in the rat retina during postnatal development, Exp. Brain Res., 82 (1990) 25-32.

[119] J. Lakowski, Y. T. Han, R. A. Pearson, A. Gonzalez-Cordero, E. L. West, S. Gualdoni, A. C. Barber, M. Hubank, R. R. Ali, and J. C. Sowden, Effective transplantation of photoreceptor precursor cells selected via cell surface antigen expression, Stem Cells, 29 (2011) 1391-1404.

- [120] E. L. West, R. A. Pearson, S. E. Barker, U. F. Luhmann, R. E. MacLaren, A. C. Barber, Y. Duran, A. J. Smith, J. C. Sowden, and R. R. Ali, Long-term survival of photoreceptors transplanted into the adult murine neural retina requires immune modulation, Stem Cells, 28 (2010) 1997-2007.
- [121] J. Yu, M. A. Vodyanik, K. Smuga-Otto, J. ntosiewicz-Bourget, J. L. Frane, S. Tian, J. Nie, G. A. Jonsdottir, V. Ruotti, R. Stewart, I. I. Slukvin, and J. A. Thomson, Induced pluripotent stem cell lines derived from human somatic cells, Science, 318 (2007) 1917-1920.
- [122] K. Takahashi, K. Tanabe, M. Ohnuki, M. Narita, T. Ichisaka, K. Tomoda, and S. Yamanaka, Induction of pluripotent stem cells from adult human fibroblasts by defined factors, Cell, 131 (2007) 861-872.
- [123] O. Comyn, E. Lee, and R. E. MacLaren, Induced pluripotent stem cell therapies for retinal disease, Curr. Opin. Neurol., 23 (2010) 4-9.
- [124] A. J. Carr, A. A. Vugler, S. T. Hikita, J. M. Lawrence, C. Gias, L. L. Chen, D. E. Buchholz, A. Ahmado, M. Semo, M. J. Smart, S. Hasan, C. L. da, L. V. Johnson, D. O. Clegg, and P. J. Coffey, Protective effects of human iPS-derived retinal pigment epithelium cell transplantation in the retinal dystrophic rat, PLoS. One., 4 (2009) e8152.
- [125] C. Cattoglio, G. Facchini, D. Sartori, A. Antonelli, A. Miccio, B. Cassani, M. Schmidt, K. C. von, S. Howe, A. J. Thrasher, A. Aiuti, G. Ferrari, A. Recchia, and F. Mavilio, Hot spots of retroviral integration in human CD34+ hematopoietic cells, Blood, 110 (2007) 1770-1778.
- [126] F. Jia, K. D. Wilson, N. Sun, D. M. Gupta, M. Huang, Z. Li, N. J. Panetta, Z. Y. Chen, R. C. Robbins, M. A. Kay, M. T. Longaker, and J. C. Wu, A nonviral minicircle vector for deriving human iPS cells, Nat. Methods, 7 (2010) 197-199.
- [127] D. E. Buchholz, S. T. Hikita, T. J. Rowland, A. M. Friedrich, C. R. Hinman, L. V. Johnson, and D. O. Clegg, Derivation of functional retinal pigmented epithelium from induced pluripotent stem cells, Stem Cells. 27(10):2427-34, (2009).
- [128] V. Tropepe, B. L. Coles, B. J. Chiasson, D. J. Horsford, A. J. Elia, R. R. McInnes, and D. van der Kooy, Retinal stem cells in the adult mammalian eye, Science, 287 (2000) 2032-2036.
- [129] I. Ahmad, A. V. Das, J. James, S. Bhattacharya, and X. Zhao, Neural stem cells in the mammalian eye: types and regulation, Semin. Cell Dev. Biol., 15 (2004) 53-62.
- [130] A. M. Das, X. Zhao, and I. Ahmad, Stem cell therapy for retinal degeneration: retinal neurons from heterologous sources, Semin. Ophthalmol., 20 (2005) 3-10.
- [131] T. Akagi, M. Mandai, S. Ooto, Y. Hirami, F. Osakada, R. Kageyama, N. Yoshimura, and M. Takahashi, Otx2 homeobox gene induces photoreceptor-specific phenotypes in cells derived from adult iris and ciliary tissue, Invest Ophthalmol. Vis. Sci., 45 (2004) 4570-4575.

[132] A. V. Das, J. James, J. Rahnenfuhrer, W. B. Thoreson, S. Bhattacharya, X. Zhao, and I. Ahmad, Retinal properties and potential of the adult mammalian ciliary epithelium stem cells, Vision Res., 45 (2005) 1653-1666.

- [133] T. Inoue, B. L. Coles, K. Dorval, R. Bremner, Y. Bessho, R. Kageyama, S. Hino, M. Matsuoka, C. M. Craft, R. R. McInnes, F. Tremblay, G. T. Prusky, and K. D. van der, Maximizing functional photoreceptor differentiation from adult human retinal stem cells, Stem Cells, 28 (2010) 489-500.
- [134] Y. Inoue, Y. Yanagi, Y. Tamaki, S. Uchida, Y. Kawase, M. Araie, and H. Okochi, Clonogenic analysis of ciliary epithelial derived retinal progenitor cells in rabbits, Exp. Eye Res., 81 (2005) 437-445.
- [135] S. Gualdoni, M. Baron, J. Lakowski, S. Decembrini, A. J. Smith, R. A. Pearson, R. R. Ali, and J. C. Sowden, Adult ciliary epithelial cells, previously identified as retinal stem cells with potential for retinal repair, fail to differentiate into new rod photoreceptors, Stem Cells, 28 (2010) 1048-1059.
- [136] N. D. Bull and K. R. Martin, Concise review: toward stem cell-based therapies for retinal neurodegenerative diseases, Stem Cells, 29 (2011) 1170-1175.
- [137] A. MacNeil, R. A. Pearson, R. E. MacLaren, A. J. Smith, J. C. Sowden, and R. R. Ali, Comparative analysis of progenitor cells isolated from the iris, pars plana, and ciliary body of the adult porcine eye, Stem Cells, 25 (2007) 2430-2438.
- [138] G. Thumann, Development and cellular functions of the iris pigment epithelium, Surv. Ophthalmol., 45 (2001) 345-354.
- [139] T. Abe, M. Yoshida, Y. Yoshioka, R. Wakusawa, Y. Tokita-Ishikawa, H. Seto, M. Tamai, and K. Nishida, Iris pigment epithelial cell transplantation for degenerative retinal diseases, Prog. Retin. Eye Res., 26 (2007) 302-321.
- [140] G. A. Limb and J. T. Daniels, Ocular regeneration by stem cells: present status and future prospects, Br. Med. Bull., 85 (2008) 47-61.
- [141] S. Joly, V. Pernet, M. Samardzija, and C. Grimm, Pax6-positive Muller glia cells express cell cycle markers but do not proliferate after photoreceptor injury in the mouse retina, Glia, 59 (2011) 1033-1046.
- [142] C. B. Del Debbio, S. Balasubramanian, S. Parameswaran, A. Chaudhuri, F. Qiu, and I. Ahmad, Notch and Wnt signaling mediated rod photoreceptor regeneration by Muller cells in adult mammalian retina, PLoS. One., 5 (2010) e12425.
- [143] I. Ahmad, C. B. Del Debbio, A. V. Das, and S. Parameswaran, Muller glia: a promising target for therapeutic regeneration, Invest Ophthalmol. Vis. Sci., 52 (2011) 5758-5764.
- [144] A. Kicic, W. Y. Shen, A. S. Wilson, I. J. Constable, T. Robertson, and P. E. Rakoczy, Differentiation of marrow stromal cells into photoreceptors in the rat eye, J. Neurosci., 23 (2003) 7742-7749.
- [145] S. Arnhold, P. Heiduschka, H. Klein, Y. Absenger, S. Basnaoglu, F. Kreppel, S. Henke-Fahle, S. Kochanek, K. U. Bartz-Schmidt, K. Addicks, and U. Schraermeyer, Adenovirally transduced bone marrow stromal cells differentiate into pigment epithelial cells and induce rescue effects in RCS rats, Invest Ophthalmol. Vis. Sci., 47 (2006) 4121-4129.

[146] M. Tomita, T. Mori, K. Maruyama, T. Zahir, M. Ward, A. Umezawa, and M. J. Young, A comparison of neural differentiation and retinal transplantation with bone marrow-derived cells and retinal progenitor cells, Stem Cells, 24 (2006) 2270-2278.

- [147] G. A. Secker and J. T. Daniels, Limbal epithelial stem cells of the cornea, Stembook, Cambridge (MA): Harvard Stem Cell Institute, 2009.
- [148] C. Brandl, C. Florian, O. Driemel, B. H. Weber, and C. Morsczeck, Identification of neural crest-derived stem cell-like cells from the corneal limbus of juvenile mice, Exp. Eye Res., 89 (2009) 209-217.
- [149] S. Dravida, R. Pal, A. Khanna, S. P. Tipnis, G. Ravindran, and F. Khan, The transdifferentiation potential of limbal fibroblast-like cells, Brain Res. Dev. Brain Res., 160 (2005) 239-251.
- [150] Y. Jiang, B. N. Jahagirdar, R. L. Reinhardt, R. E. Schwartz, C. D. Keene, X. R. Ortiz-Gonzalez, M. Reyes, T. Lenvik, T. Lund, M. Blackstad, J. Du, S. Aldrich, A. Lisberg, W. C. Low, D. A. Largaespada, and C. M. Verfaillie, Pluripotency of mesenchymal stem cells derived from adult marrow, Nature, 418 (2002) 41-49.
- [151] A. Hemmati-Brivanlou and D. Melton, Vertebrate embryonic cells will become nerve cells unless told otherwise, Cell, 88 (1997) 13-17.
- [152] D. C. Weinstein and A. Hemmati-Brivanlou, Neural induction in Xenopus laevis: evidence for the default model, Curr. Opin. Neurobiol., 7 (1997) 7-12.
- [153] H. Grunz and L. Tacke, Neural differentiation of Xenopus laevis ectoderm takes place after disaggregation and delayed reaggregation without inducer, Cell Differ. Dev., 28 (1989) 211-217.
- [154] P. A. Wilson and A. Hemmati-Brivanlou, Induction of epidermis and inhibition of neural fate by Bmp-4, Nature, 376 (1995) 331-333.
- [155] P. A. Wilson, G. Lagna, A. Suzuki, and A. Hemmati-Brivanlou, Concentration-dependent patterning of the Xenopus ectoderm by BMP4 and its signal transducer Smad1, Development, 124 (1997) 3177-3184.
- [156] G. Pellegrini, P. Rama, F. Mavilio, and L. M. De, Epithelial stem cells in corneal regeneration and epidermal gene therapy, J. Pathol., 217 (2009) 217-228.
- [157] R. J. Tsai, L. M. Li, and J. K. Chen, Reconstruction of damaged corneas by transplantation of autologous limbal epithelial cells, N. Engl. J. Med., 343 (2000) 86-93.
- [158] X. Zhao, A. V. Das, W. B. Thoreson, J. James, T. E. Wattnem, J. Rodriguez-Sierra, and I. Ahmad, Adult corneal limbal epithelium: a model for studying neural potential of non-neural stem cells/progenitors, Dev. Biol., 250 (2002) 317-331.
- [159] D. Altshuler and C. Cepko, A temporally regulated, diffusible activity is required for rod photoreceptor development in vitro, Development, 114 (1992) 947-957.
- [160] T. Watanabe and M. C. Raff, Diffusible rod-promoting signals in the developing rat retina, Development, 114 (1992) 899-906.

[161] Y. Sugie, M. Yoshikawa, Y. Ouji, K. Saito, K. Moriya, S. Ishizaka, T. Matsuura, S. Maruoka, Y. Nawa, and Y. Hara, Photoreceptor cells from mouse ES cells by co-culture with chick embryonic retina, Biochem. Biophys. Res. Commun., 332 (2005) 241-247.

- [162] F. Osakada, H. Ikeda, M. Mandai, T. Wataya, K. Watanabe, N. Yoshimura, A. Akaike, Y. Sasai, and M. Takahashi, Toward the generation of rod and cone photoreceptors from mouse, monkey and human embryonic stem cells, Nat. Biotechnol., 26 (2008) 215-224.
- [163] H. Klassen and B. Reubinoff, Stem cells in a new light, Nat. Biotechnol., 26 (2008) 187-188.
- [164] M. F. Rath, E. Munoz, S. Ganguly, F. Morin, Q. Shi, D. C. Klein, and M. Moller, Expression of the Otx2 homeobox gene in the developing mammalian brain: embryonic and adult expression in the pineal gland, J. Neurochem., 97 (2006) 556-566.
- [165] T. Akagi, T. Inoue, G. Miyoshi, Y. Bessho, M. Takahashi, J. E. Lee, F. Guillemot, and R. Kageyama, Requirement of multiple basic helix-loop-helix genes for retinal neuronal subtype specification, J. Biol. Chem., 279 (2004) 28492-28498.
- [166] R. T. Yan, W. Ma, L. Liang, and S. Z. Wang, bHLH genes and retinal cell fate specification, Mol. Neurobiol., 32 (2005) 157-171.
- [167] M. J. Ochocinska and P. F. Hitchcock, NeuroD regulates proliferation of photoreceptor progenitors in the retina of the zebrafish, Mech. Dev., 126 (2009) 128-141.
- [168] L. Liang, R. T. Yan, X. Li, M. Chimento, and S. Z. Wang, Reprogramming progeny cells of embryonic RPE to produce photoreceptors: development of advanced photoreceptor traits under the induction of neuroD, Invest Ophthalmol. Vis. Sci., 49 (2008) 4145-4153.
- [169] T. Inoue, B. L. Coles, K. Dorval, R. Bremner, Y. Bessho, R. Kageyama, S. Hino, M. Matsuoka, C. M. Craft, R. R. McInnes, F. Tremblay, G. T. Prusky, and K. D. van der, Maximizing functional photoreceptor differentiation from adult human retinal stem cells, Stem Cells, 28 (2010) 489-500.
- [170] M. Asami, G. Sun, M. Yamaguchi, and M. Kosaka, Multipotent cells from mammalian iris pigment epithelium, Dev. Biol., 304 (2007) 433-446.
- [171] R. Sasaki, S. Aoki, M. Yamato, H. Uchiyama, K. Wada, T. Okano, and H. Ogiuchi, Neurosphere generation from dental pulp of adult rat incisor, Eur. J. Neurosci., 27 (2008) 538-548.
- [172] A. Bez, E. Corsini, D. Curti, M. Biggiogera, A. Colombo, R. F. Nicosia, S. F. Pagano, and E. A. Parati, Neurosphere and neurosphere-forming cells: morphological and ultrastructural characterization, Brain Res., 993 (2003) 18-29.
- [173] F. P. Wachs, S. Couillard-Despres, M. Engelhardt, D. Wilhelm, S. Ploetz, M. Vroemen, J. Kaesbauer, G. Uyanik, J. Klucken, C. Karl, J. Tebbing, C. Svendsen, N. Weidner, H. G. Kuhn, J. Winkler, and L. Aigner, High efficacy of clonal growth and expansion of adult neural stem cells, Lab Invest, 83 (2003) 949-962.

[174] M. G. Ormerod and D. Novo, Flow cytometry: a basic introduction, BPR Publishers, 2008.

- [175] H. Li, M. B. Ferrari, and W. J. Kuenzel, Light-induced reduction of cytoplasmic free calcium in neurons proposed to be encephalic photoreceptors in chick brain, Brain Res. Dev. Brain Res., 153 (2004) 153-161.
- [176] A. Hermann, R. Gastl, S. Liebau, M. O. Popa, J. Fiedler, B. O. Boehm, M. Maisel, H. Lerche, J. Schwarz, R. Brenner, and A. Storch, Efficient generation of neural stem cell-like cells from adult human bone marrow stromal cells, J. Cell Sci., 117 (2004) 4411-4422.
- [177] N. Uchida, D. W. Buck, D. He, M. J. Reitsma, M. Masek, T. V. Phan, A. S. Tsukamoto, F. H. Gage, and I. L. Weissman, Direct isolation of human central nervous system stem cells, Proc. Natl. Acad. Sci. U. S A, 97 (2000) 14720-14725.
- [178] B. A. Reynolds and S. Weiss, Clonal and population analyses demonstrate that an EGF-responsive mammalian embryonic CNS precursor is a stem cell, Dev. Biol., 175 (1996) 1-13.
- [179] L. P. Weiner, Neural stem cells: methods and protocols, Totowa, N.J.: Humana, 2008.
- [180] C. Foroni, R. Galli, B. Cipelletti, A. Caumo, S. Alberti, R. Fiocco, and A. Vescovi, Resilience to transformation and inherent genetic and functional stability of adult neural stem cells ex vivo, Cancer Res., 67 (2007) 3725-3733.
- [181] L. S. Campos, D. P. Leone, J. B. Relvas, C. Brakebusch, R. Fassler, U. Suter, and C. ffrench-Constant, Beta1 integrins activate a MAPK signalling pathway in neural stem cells that contributes to their maintenance, Development, 131 (2004) 3433-3444.
- [182] W. Li, Y. Hayashida, Y. T. Chen, and S. C. Tseng, Niche regulation of corneal epithelial stem cells at the limbus, Cell Res., 17 (2007) 26-36.
- [183] B. A. Reynolds and S. Weiss, Generation of neurons and astrocytes from isolated cells of the adult mammalian central nervous system, Science, 255 (1992) 1707-1710.
- [184] B. Alberts, D. Bray, J. Lewis, M. Raff, K. Roberts, and J. D. Watson, Molecular biology of the cell, New York, NY: Garland Publishing, Inc, 1994.
- [185] K. D. Bunting, ABC transporters as phenotypic markers and functional regulators of stem cells, Stem Cells, 20 (2002) 11-20.
- [186] S. Bhattacharya, A. Das, K. Mallya, and I. Ahmad, Maintenance of retinal stem cells by Abcg2 is regulated by notch signaling, J. Cell Sci., 120 (2007) 2652-2662.
- [187] P. Ellis, B. M. Fagan, S. T. Magness, S. Hutton, O. Taranova, S. Hayashi, A. McMahon, M. Rao, and L. Pevny, SOX2, a persistent marker for multipotential neural stem cells derived from embryonic stem cells, the embryo or the adult, Dev. Neurosci., 26 (2004) 148-165.
- [188] A. A. Avilion, S. K. Nicolis, L. H. Pevny, L. Perez, N. Vivian, and R. Lovell-Badge, Multipotent cell lineages in early mouse development depend on SOX2 function, Genes Dev., 17 (2003) 126-140.

[189] S. C. De, E. Meyer, G. R. Van de Walle, and S. A. Van, Markers of stemness in equine mesenchymal stem cells: a plea for uniformity, Theriogenology, 75 (2011) 1431-1443.

- [190] X. Tu, R. Baffa, S. Luke, M. Prisco, and R. Baserga, Intracellular redistribution of nuclear and nucleolar proteins during differentiation of 32D murine hemopoietic cells, Exp. Cell Res., 288 (2003) 119-130.
- [191] P. A. Zuk, The intracellular distribution of the ES cell totipotent markers OCT4 and Sox2 in adult stem cells differs dramatically according to commercial antibody used, J. Cell Biochem., 106 (2009) 867-877.
- [192] M. I. Koster, S. Kim, A. A. Mills, F. J. DeMayo, and D. R. Roop, p63 is the molecular switch for initiation of an epithelial stratification program, Genes Dev., 18 (2004) 126-131.
- [193] A. B. Firulli and S. J. Conway, Phosphoregulation of Twist1 provides a mechanism of cell fate control, Curr. Med. Chem., 15 (2008) 2641-2647.
- [194] M. Cheung and J. Briscoe, Neural crest development is regulated by the transcription factor Sox9, Development, 130 (2003) 5681-5693.
- [195] R. A. Poche, Y. Furuta, M. C. Chaboissier, A. Schedl, and R. R. Behringer, Sox9 is expressed in mouse multipotent retinal progenitor cells and functions in Muller glial cell development, J. Comp Neurol., 510 (2008) 237-250.
- [196] M. Sosnova, M. Bradl, and J. V. Forrester, CD34+ corneal stromal cells are bone marrow-derived and express hemopoietic stem cell markers, Stem Cells, 23 (2005) 507-515.
- [197] T. Marquardt, R. shery-Padan, N. Andrejewski, R. Scardigli, F. Guillemot, and P. Gruss, Pax6 is required for the multipotent state of retinal progenitor cells, Cell, 105 (2001) 43-55.
- [198] J. M. Wolosin, Cell markers and the side population phenotype in ocular surface epithelial stem cell characterization and isolation, Ocul. Surf., 4 (2006) 10-23.
- [199] H. Xu, D. D. Sta Iglesia, J. L. Kielczewski, D. F. Valenta, M. E. Pease, D. J. Zack, and H. A. Quigley, Characteristics of progenitor cells derived from adult ciliary body in mouse, rat, and human eyes, Invest Ophthalmol. Vis. Sci., 48 (2007) 1674-1682.
- [200] S. D. Schwartz, J. P. Hubschman, G. Heilwell, V. Franco-Cardenas, C. K. Pan, R. M. Ostrick, E. Mickunas, R. Gay, I. Klimanskaya, and R. Lanza, Embryonic stem cell trials for macular degeneration: a preliminary report, Lancet, (2012).
- [201] F. Ciccolini and C. N. Svendsen, Fibroblast growth factor 2 (FGF-2) promotes acquisition of epidermal growth factor (EGF) responsiveness in mouse striatal precursor cells: identification of neural precursors responding to both EGF and FGF-2, J. Neurosci., 18 (1998) 7869-7880.
- [202] R. Kohno, Y. Ikeda, Y. Yonemitsu, T. Hisatomi, M. Yamaguchi, M. Miyazaki, H. Takeshita, T. Ishibashi, and K. Sueishi, Sphere formation of ocular epithelial cells in the ciliary body is a reprogramming system for neural differentiation, Brain Res., 1093 (2006) 54-70.
- [203] P. Y. Lwigale, P. A. Cressy, and M. Bronner-Fraser, Corneal keratocytes retain neural crest progenitor cell properties, Dev. Biol., 288 (2005) 284-293.

[204] V. Pancholi, Multifunctional alpha-enolase: its role in diseases, Cell Mol. Life Sci., 58 (2001) 902-920.

- [205] T. Nakamura, F. Ishikawa, K. H. Sonoda, T. Hisatomi, H. Qiao, J. Yamada, M. Fukata, T. Ishibashi, M. Harada, and S. Kinoshita, Characterization and distribution of bone marrow-derived cells in mouse cornea, Invest Ophthalmol. Vis. Sci., 46 (2005) 497-503.
- [206] M. J. Young, Stem cells in the mammalian eye: a tool for retinal repair, APMIS, 113 (2005) 845-857.
- [207] M. O. Islam, Y. Kanemura, J. Tajria, H. Mori, S. Kobayashi, M. Hara, M. Yamasaki, H. Okano, and J. Miyake, Functional expression of ABCG2 transporter in human neural stem/progenitor cells, Neurosci. Res., 52 (2005) 75-82.
- [208] P. E. Nickerson, T. Myers, D. B. Clarke, and R. L. Chow, Changes in Musashi-1 subcellular localization correlate with cell cycle exit during postnatal retinal development, Exp. Eye Res., 92 (2011) 344-352.
- [209] F. P. Wachs, S. Couillard-Despres, M. Engelhardt, D. Wilhelm, S. Ploetz, M. Vroemen, J. Kaesbauer, G. Uyanik, J. Klucken, C. Karl, J. Tebbing, C. Svendsen, N. Weidner, H. G. Kuhn, J. Winkler, and L. Aigner, High efficacy of clonal growth and expansion of adult neural stem cells, Lab Invest, 83 (2003) 949-962.
- [210] M. C. Moe, R. S. Kolberg, C. Sandberg, E. Vik-Mo, H. Olstorn, M. Varghese, I. A. Langmoen, and B. Nicolaissen, A comparison of epithelial and neural properties in progenitor cells derived from the adult human ciliary body and brain, Exp. Eye Res., 88 (2009) 30-38.
- [211] S. Bhattacharya, A. Das, K. Mallya, and I. Ahmad, Maintenance of retinal stem cells by Abcg2 is regulated by notch signaling, J. Cell Sci., 120 (2007) 2652-2662.
- [212] E. C. Oh, H. Cheng, H. Hao, L. Jia, N. W. Khan, and A. Swaroop, Rod differentiation factor NRL activates the expression of nuclear receptor NR2E3 to suppress the development of cone photoreceptors, Brain Res., 1236 (2008) 16-29.
- [213] S. J. Pittler, Y. Zhang, S. Chen, A. J. Mears, D. J. Zack, Z. Ren, P. K. Swain, S. Yao, A. Swaroop, and J. B. White, Functional analysis of the rod photoreceptor cGMP phosphodiesterase alpha-subunit gene promoter: Nrl and Crx are required for full transcriptional activity, J. Biol. Chem., 279 (2004) 19800-19807.
- [214] A. J. Mears, M. Kondo, P. K. Swain, Y. Takada, R. A. Bush, T. L. Saunders, P. A. Sieving, and A. Swaroop, Nrl is required for rod photoreceptor development, Nat. Genet., 29 (2001) 447-452.
- [215] G. Sun, M. Asami, H. Ohta, J. Kosaka, and M. Kosaka, Retinal stem/progenitor properties of iris pigment epithelial cells, Dev. Biol., 289 (2006) 243-252.
- [216] A. V. Das, J. James, J. Rahnenfuhrer, W. B. Thoreson, S. Bhattacharya, X. Zhao, and I. Ahmad, Retinal properties and potential of the adult mammalian ciliary epithelium stem cells, Vision Res., 45 (2005) 1653-1666.

[217] W. Ma, R. T. Yan, X. Li, and S. Z. Wang, Reprogramming retinal pigment epithelium to differentiate toward retinal neurons with Sox2, Stem Cells, 27 (2009) 1376-1387.

- [218] X. Sun, M. Chen, J. Li, J. Zhuang, Q. Gao, X. Zhong, B. Huang, W. Zhang, L. Huang, and J. Ge, E13.5 retinal progenitors induce mouse bone marrow mesenchymal stromal cells to differentiate into retinal progenitor-like cells, Cytotherapy., 13 (2011) 294-303.
- [219] N. F. Berbari, A. K. O'Connor, C. J. Haycraft, and B. K. Yoder, The primary cilium as a complex signaling center, Curr. Biol., 19 (2009) R526-R535.
- [220] N. Tetreault, M. P. Champagne, and G. Bernier, The LIM homeobox transcription factor Lhx2 is required to specify the retina field and synergistically cooperates with Pax6 for Six6 trans-activation, Dev. Biol., 327 (2009) 541-550.
- [221] D. Jean, G. Bernier, and P. Gruss, Six6 (Optx2) is a novel murine Six3-related homeobox gene that demarcates the presumptive pituitary/hypothalamic axis and the ventral optic stalk, Mech. Dev., 84 (1999) 31-40.
- [222] S. Schmitt, U. Aftab, C. Jiang, S. Redenti, H. Klassen, E. Miljan, J. Sinden, and M. Young, Molecular characterization of human retinal progenitor cells, Invest Ophthalmol. Vis. Sci., 50 (2009) 5901-5908.
- [223] Z. B. Jin, S. Okamoto, F. Osakada, K. Homma, J. Assawachananont, Y. Hirami, T. Iwata, and M. Takahashi, Modeling retinal degeneration using patient-specific induced pluripotent stem cells, PLoS. One., 6 (2011) e17084.
- [224] M. Dorlochter and H. Stieve, The Limulus ventral photoreceptor: light response and the role of calcium in a classic preparation, Prog. Neurobiol., 53 (1997) 451-515.
- [225] S. L. Bruhn and C. L. Cepko, Development of the pattern of photoreceptors in the chick retina, J. Neurosci., 16 (1996) 1430-1439.
- [226] D. G. Luo and K. W. Yau, Rod sensitivity of neonatal mouse and rat, J. Gen. Physiol, 126 (2005) 263-269.
- [227] S. T. Doh, H. Hao, S. C. Loh, T. Patel, H. Y. Tawil, D. K. Chen, A. Pashkova, A. Shen, H. Wang, and L. Cai, Analysis of retinal cell development in chick embryo by immunohistochemistry and in ovo electroporation techniques, BMC. Dev. Biol., 10 (2010) 8.
- [228] J. Akita, M. Takahashi, M. Hojo, A. Nishida, M. Haruta, and Y. Honda, Neuronal differentiation of adult rat hippocampus-derived neural stem cells transplanted into embryonic rat explanted retinas with retinoic acid pretreatment, Brain Res., 954 (2002) 286-293.
- [229] K. Canola, B. Angenieux, M. Tekaya, A. Quiambao, M. I. Naash, F. L. Munier, D. F. Schorderet, and Y. Arsenijevic, Retinal stem cells transplanted into models of late stages of retinitis pigmentosa preferentially adopt a glial or a retinal ganglion cell fate, Invest Ophthalmol. Vis. Sci., 48 (2007) 446-454.
- [230] T. Akagi, M. Haruta, J. Akita, A. Nishida, Y. Honda, and M. Takahashi, Different characteristics of rat retinal progenitor cells from different culture periods, Neurosci. Lett., 341 (2003) 213-216.

[231] G. Pellegrini, L. M. De, and Y. Arsenijevic, Towards therapeutic application of ocular stem cells, Semin. Cell Dev. Biol., 18 (2007) 805-818.

- [232] S. Basti and S. K. Rao, Current status of limbal conjunctival autograft, Curr. Opin. Ophthalmol., 11 (2000) 224-232.
- [233] A. Hendrickson, K. Bumsted-O'Brien, R. Natoli, V. Ramamurthy, D. Possin, and J. Provis, Rod photoreceptor differentiation in fetal and infant human retina, Exp. Eye Res., 87 (2008) 415-426.
- [234] L. D. Carter-Dawson and M. M. LaVail, Rods and cones in the mouse retina. II. Autoradiographic analysis of cell generation using tritiated thymidine, J. Comp Neurol., 188 (1979) 263-272.
- [235] T. Kobayashi, K. Yasuda, and M. Araki, Coordinated regulation of dorsal bone morphogenetic protein 4 and ventral Sonic hedgehog signaling specifies the dorso-ventral polarity in the optic vesicle and governs ocular morphogenesis through fibroblast growth factor 8 upregulation, Dev. Growth Differ., 52 (2010) 351-363.
- [236] L. Zhao, H. Saitsu, X. Sun, K. Shiota, and M. Ishibashi, Sonic hedgehog is involved in formation of the ventral optic cup by limiting Bmp4 expression to the dorsal domain, Mech. Dev., 127 (2010) 62-72.
- [237] M. A. Amato, S. Boy, and M. Perron, Hedgehog signaling in vertebrate eye development: a growing puzzle, Cell Mol. Life Sci., 61 (2004) 899-910.
- [238] Y. Wang, G. D. Dakubo, S. Thurig, C. J. Mazerolle, and V. A. Wallace, Retinal ganglion cell-derived sonic hedgehog locally controls proliferation and the timing of RGC development in the embryonic mouse retina, Development, 132 (2005) 5103-5113.
- [239] M. W. Kelley, J. K. Turner, and T. A. Reh, Retinoic acid promotes differentiation of photoreceptors in vitro, Development, 120 (1994) 2091-2102.
- [240] G. A. Hyatt, E. A. Schmitt, J. M. Fadool, and J. E. Dowling, Retinoic acid alters photoreceptor development in vivo, Proc. Natl. Acad. Sci. U. S. A, 93 (1996) 13298-13303.
- [241] T. Furukawa, E. M. Morrow, T. Li, F. C. Davis, and C. L. Cepko, Retinopathy and attenuated circadian entrainment in Crx-deficient mice, Nat. Genet., 23 (1999) 466-470.
- [242] S. Blackshaw, R. E. Fraioli, T. Furukawa, and C. L. Cepko, Comprehensive analysis of photoreceptor gene expression and the identification of candidate retinal disease genes, Cell, 107 (2001) 579-589.
- [243] H. Xia, Q. Mao, and B. L. Davidson, The HIV Tat protein transduction domain improves the biodistribution of beta-glucuronidase expressed from recombinant viral vectors, Nat. Biotechnol., 19 (2001) 640-644.
- [244] O. Sugiyama, D. S. An, S. P. Kung, B. T. Feeley, S. Gamradt, N. Q. Liu, I. S. Chen, and J. R. Lieberman, Lentivirus-mediated gene transfer induces long-term transgene expression of BMP-2 in vitro and new bone formation in vivo, Mol. Ther., 11 (2005) 390-398.
- [245] C. Delenda, Lentiviral vectors: optimization of packaging, transduction and gene expression, J. Gene Med., 6 Suppl 1 (2004) S125-S138.

[246] F. Mansergh, N. C. Orton, J. P. Vessey, M. R. Lalonde, W. K. Stell, F. Tremblay, S. Barnes, D. E. Rancourt, and N. T. Bech-Hansen, Mutation of the calcium channel gene Cacnalf disrupts calcium signaling, synaptic transmission and cellular organization in mouse retina, Hum. Mol. Genet., 14 (2005) 3035-3046.

- [247] D. Krizaj and D. R. Copenhagen, Calcium regulation in photoreceptors, Front Biosci., 7 (2002) d2023-d2044.
- [248] A. Polans, W. Baehr, and K. Palczewski, Turned on by Ca2+! The physiology and pathology of Ca(2+)-binding proteins in the retina, Trends Neurosci., 19 (1996) 547-554.
- [249] K. Jian, R. Barhoumi, M. L. Ko, and G. Y. Ko, Inhibitory effect of somatostatin-14 on L-type voltage-gated calcium channels in cultured cone photoreceptors requires intracellular calcium, J. Neurophysiol., 102 (2009) 1801-1810.
- [250] J. B. Kim, B. Greber, M. J. Arauzo-Bravo, J. Meyer, K. I. Park, H. Zaehres, and H. R. Scholer, Direct reprogramming of human neural stem cells by OCT4, Nature, 461 (2009) 649-3.
- [251] J. B. Kim, V. Sebastiano, G. Wu, M. J. Arauzo-Bravo, P. Sasse, L. Gentile, K. Ko, D. Ruau, M. Ehrich, D. van den Boom, J. Meyer, K. Hubner, C. Bernemann, C. Ortmeier, M. Zenke, B. K. Fleischmann, H. Zaehres, and H. R. Scholer, Oct4-induced pluripotency in adult neural stem cells, Cell, 136 (2009) 411-419.
- [252] J. B. Kim, H. Zaehres, G. Wu, L. Gentile, K. Ko, V. Sebastiano, M. J. Arauzo-Bravo, D. Ruau, D. W. Han, M. Zenke, and H. R. Scholer, Pluripotent stem cells induced from adult neural stem cells by reprogramming with two factors, Nature, 454 (2008) 646-650.
- [253] T. Furukawa, E. M. Morrow, and C. L. Cepko, Crx, a novel otx-like homeobox gene, shows photoreceptor-specific expression and regulates photoreceptor differentiation, Cell, 91 (1997) 531-541.